

Dissertation zur Erlangung des Doktorgrades
der Fakultät für Chemie und Pharmazie der
Ludwig-Maximilians-Universität München

Genetic analyses of Kindlins in mice

Siegfried Ussar

aus

Graz, Österreich

2008

Erklärung

Diese Dissertation wurde im Sinne von §13 Abs. 3 der Promotionsordnung vom 29. Januar 1998 von Herrn Prof. Dr. Reinhard Fässler betreut.

Ehrenwörtliche Versicherung

Diese Dissertation wurde selbstständig, ohne unerlaubte Hilfe erarbeitet.

München, am 19.09.2008

(Siegfried Ussar)

Dissertation eingereicht am: 22.09.08

- | | |
|--------------|----------------------------|
| 1. Gutachter | Prof. Dr. Reinhard Fässler |
| 2. Gutachter | PD Dr. Klaus-Peter Janssen |

Mündliche Prüfung am: 23.10.2008

Table of Contents

TABLE OF CONTENTS	1
AIM OF THE THESIS	1
LIST OF PUBLICATIONS	2
SUMMARY	3
INTRODUCTION	6
KINDLINS	6
Kindlin gene and protein structure	7
FERM domains	8
PH/PTB superfamily.....	8
The role of UNC-112 in C. elegans	9
Integrins	11
Integrin function in vivo	13
Murine pre- and peri-implantation development	13
The role of integrins during pre- and peri-implantation development	14
Skin	15
The role of integrins in the epidermis.....	16
Intestine.....	17
The role of integrins in the intestine.....	18
Platelets.....	19
The role of integrins in platelets.....	21
Integrin activation (Inside-out signalling).....	22
Talin mediates integrin activation	23
Outside-in Signalling	25
Kindlin function in mammalian cells	26
Kindler Syndrome.....	26
Kindlins in integrin signalling	28
PAPER SUMMARIES	31

Table of Contents

The Kindlins: subcellular localization and expression during murine development.....	31
Kindlin-2 controls bidirectional signalling of integrins.....	32
Integrin-linked kinase: integrin's mysterious partner	33
Kindlin-3 is essential for integrin activation and platelet aggregation.....	34
SILAC-mouse for quantitative proteomics uncovers Kindlin-3 as an essential factor for red blood cell function.....	35
Leukocyte Adhesion Deficiency-III (LAD-III) is caused by mutations in the adhesion protein Kindlin-3, * equal contribution	36
Loss of Kindlin-1 causes skin atrophy and early postnatal ulcerative colitis	37
Colocalization of kindlin-1, kindlin-2 and migfilin at keratinocyte focal contacts and relevance to the pathophysiology of Kindler syndrome.....	38
Expression of truncated kindlin-1 leads to abnormal adhesion and migration of keratinocytes	39
ACKNOWLEDGEMENTS.....	40
CURRICULUM VITAE	41
REFERENCES.....	43
APPENDIX	51

Aim of the thesis

The function of the three Kindlin proteins is unknown. Recently, mutations in the human FERMT1 gene, coding for the Kindlin-1 protein, were shown to cause Kindler Syndrome, a rare autosomal recessive skin blistering disease. In addition to the skin blister phenotype, several other abnormalities have been reported, although a clear genotype to phenotype correlation is not evident. Cell-culture based work on Kindlin-1 and Kindlin-2 demonstrated an important role of these proteins in integrin-mediated cell adhesion and adhesion strengthening by the actin cytoskeleton. No functional data on Kindlin-3 have been reported, although the high homology to the other Kindlins suggests that they share similar functions, at least at integrin adhesion sites.

The overall goal of this thesis was to describe the consequences of loss of each Kindlin protein in mice. Four major aims were defined for addressing these tasks; first, characterisation of the spatial and temporal expression pattern of the three Kindlin mRNAs and proteins. Second, generation of mouse strains deficient for each Kindlin. Third, analyses of their phenotypes and comparison of the Kindlin-1 knockout phenotype in mice with the human Kindler Syndrome. Fourth, identification of the molecular basis for the phenotypes.

List of Publications

This thesis is based on the following publications, which are referred to in the text by their Roman numerals (I-IX):

- I **Ussar S**, Wang HV, Linder S, Fässler R, Moser M (2006) The Kindlins: subcellular localization and expression during murine development. *Exp Cell Res* 312: 3142-3151.
- II Montanez E*, **Ussar S***, Schifferer M, Bösl M, Zent R, Moser M, Fässler R (2008) Kindlin-2 controls bidirectional signaling of integrins. *Genes Dev* 22: 1325-1330. * equal contribution
- III Grashoff C, Thievensen I, Lorenz K, **Ussar S**, and Fässler R (2004) Integrin-linked kinase: integrin's mysterious partner. *Current opinion in cell biology* 16(5), 565-571
- IV Moser M, Nieswandt B, **Ussar S**, Pozgajova M, Fässler R (2008) Kindlin-3 is essential for integrin activation and platelet aggregation. *Nat Med* 14: 325-330.
- V Kruger M*, Moser M*, **Ussar S**, Thievensen I, Lubert C, A, Forner F, Schmidt S, Zanivan S, Fässler R, Mann M, (2008) SILAC mouse for quantitative proteomics uncovers kindlin-3 as an essential factor for red blood cell function. *Cell* 134: 353-364. * equal contribution
- VI. Svensson L*, Howarth K*, McDowall A, Patzak I, Evans R, **Ussar S**, Metin A, Fried M, Tomlinson I, Hogg N, (submitted) Leukocyte Adhesion Deficiency-III (LAD-III) is caused by mutations in the adhesion protein Kindlin-3, * equal contribution
- VII **Ussar S**, Moser M, Widmaier M, Rognoni E, Harrer C, Genzel-Boroviczeny O, Fässler R (submitted) Loss of Kindlin-1 causes skin atrophy and lethal neonatal ulcerative colitis.
- VIII Lai-Cheong JE, **Ussar S**, Arita K, Hart IR, McGrath JA (2008) Colocalization of kindlin-1, kindlin-2, and migfilin at keratinocyte focal adhesion and relevance to the pathophysiology of Kindler syndrome. *J Invest Dermatol* 128: 2156-2165.
- IX Has C, Ludwig RJ, Herz C, Kern JS, **Ussar S**, Ochsendorf FR, Kaufmann R, Schumann H, Kohlhase J, Bruckner-Tuderman L, (2008) C-terminally truncated kindlin-1 leads to abnormal adhesion and migration of keratinocytes. *Br J Dermatol*.

Summary

The Kindlin protein family comprises three members (Kindlin-1-3). The proteins share a common domain architecture consisting of a central FERM domain harbouring a pleckstrin homology domain insertion. Both domains point to a membrane localisation of the Kindlins. Previous *in vitro* studies identified Kindlin-1 and Kindlin-2 as important players in mediating cell substrate adhesion by linking integrins to the actin cytoskeleton. Mutations in the human Kindlin-1 cause a rare inheritable skin blistering disease called Kindler Syndrome.

The first aim of this study was to characterise the expression pattern and subcellular localisation of all three Kindlins during murine development and in adult tissues. This was addressed in **Paper I**. The analysis revealed a differential expression pattern of the three Kindlins. Kindlin-2 is ubiquitously expressed, while Kindlin-1 is predominantly expressed in epithelia and Kindlin-3 exclusively in hematopoietic cells. In addition to its previously characterized localisation in focal contacts, Kindlin-2 also localizes to keratinocyte cell-cell contacts upon differentiation. Finally, the studies revealed that Kindlin-3 localizes to podosomes, which are specialised cell-matrix adhesions of hematopoietic cells.

The second aim was to directly test the function of Kindlins by individually disrupting the Kindlin genes in mice. Therefore three individual constitutive knockout mouse lines were successfully established as described in **Papers II, IV and VII**.

The third aim was to analyse the individual knockout phenotypes, and in particular to compare the phenotype of the Kindlin-1 knockout to the Kindler Syndrome. As expected from the different expression patterns the phenotypes of the Kindlin knockout mice were diverse. Kindlin-2 is the only Kindlin expressed already in embryonic stem (ES) cells. Disruption of the Kindlin-2 gene results in lethality around embryonic day (E) 5.5-6.5. *In vitro* studies with embryoid bodies (EBs) demonstrated that loss of Kindlin-2 abrogates integrin activation (inside-out signalling) leading to detachment of primitive endoderm and epiblast from the basement membrane (BM) and finally to the deterioration of the EBs (**Paper II**). The study also identified Kindlin-2 as an important regulator of integrin outside-in signalling. This was shown as Mn²⁺ treated Kindlin-2 deficient primitive endoderm cells were unable to spread and to recruit integrin linked kinase (ILK) into focal adhesions (FAs). A general overview about the function of ILK its association with other proteins and its role during development is reviewed in **Paper III**.

Kindlin-3 deficient mice were born although a few displayed embryonic lethality due to severe bleedings. The newborn mice died within one week after birth due to severe haemorrhages and anaemia (**Papers IV and V**). In **Paper IV** we showed that Kindlin-3 deficient platelets are unable to activate integrins resulting in an inability of them to adhere to injured vessel walls and to form thrombi.

Summary

Apart from this platelet defect, these mice develop a severe anaemia, which was analyzed with stable isotope labelling of the entire mouse proteome. These studies revealed that Kindlin-3 deficient erythrocytes have structural defects caused by an almost complete absence of ankyrin-1, band 4.1, adducin-2, and dematin from their membrane fractions. Thus, Kindlin-3 is an important structural element for the membrane cytoskeleton of erythrocytes (**Paper V**).

Importantly, we could identify mutated Kindlin-3 to cause Leukocyte Adhesion Deficiency-III (LAD-III) syndrome. LAD-III is characterised by an inability of leukocyte $\beta 2$ integrin to become activated and patients (**Paper VI**).

Deletion of Kindlin-1 resulted in early postnatal lethality due to a severe ulcerative colitis (UC) triggered by shear stress-induced detachment of the colonic epithelium (**Paper VII**). The epithelial detachment was caused by an integrin activation defect. Interestingly, although co-expressed in colonic epithelial cells, Kindlin-2 was unable to compensate for loss of Kindlin-1 due to its localisation to cell-cell contacts. Additional analysis of the murine skin showed no signs of epidermolysis but a progressive skin atrophy which is also seen in Kindler Syndrome patients (**Paper VII**). Thus this study showed that complete loss of Kindlin-1 results in severe intestinal complications and some but not all described skin symptoms. Recent data from patients demonstrate that complete loss of Kindlin-1 can result in UC preceding epidermolysis in humans. Thus, these data showed that Kindlin-1^{-/-} mice model the most severe form of Kindler Syndrome.

In primary human keratinocytes Kindlin-1 and Kindlin-2 can form a ternary complex with Migfilin, a LIM domain containing protein (**Paper VIII**), although neither Kindlin-2 nor Migfilin localisation was depending on the presence of Kindlin-1. We identified Kindler Syndrome patients that, in addition to reduced Kindlin-1 levels, had also reduced Kindlin-2 and Migfilin immunostaining, suggesting that abnormal levels of Kindlin-1 associated proteins may lead and/or contribute to Kindler Syndrome. Furthermore, we identified a novel mutation in the FERMT1 gene, which affects splicing of exon 13 and gives rise to a severe form of Kindler Syndrome (**Paper IX**).

The fourth aim addressed the molecular mechanism underlying the Kindlin defects. The studies revealed that Kindlins share a common binding site at integrins cytoplasmic domains. Kindlins bind the membrane distal NxxY motif within the cytoplasmic domain of $\beta 1$ and $\beta 3$ integrins. In addition these studies demonstrated for the first time that Talin requires integrin bound Kindlins to trigger integrin activation (**Papers II, IV and VII**).

In summary, Kindlin proteins are essential triggers of integrin affinity. The individual phenotypes of Kindlin deficient mice reflect the spatial and temporal expression pattern of these proteins, rather than different functions. Our studies underlined the important role of

Summary

Talin in integrin activation. However, we introduced the Kindlin proteins as essential elements in this process. The exact mechanism of how Kindlins assist Talin in integrin activation and the identification of additional functions will be challenging tasks for future studies.

Introduction

Kindlins

The Kindlin family of proteins consists of three members (Kindlin-1, -2 and -3) in mice and men. They share an evolutionary conserved gene and protein structure. Kindlin-2, formerly named Mig-2 (mitogen inducible gene 2/PLEKHC1) was the first described family member. It was discovered in a differential cDNA library screen for mitogen induced genes [1]. More recently, two other family members have been described; URP1 (Unc-112 related protein 1; Kindlin-1) and URP2 (Kindlin-3) [2]. Blast searches identified one Kindlin orthologue (Uncoordinated protein 112 (UNC-112)) in *C.elegans* and two (fermitin-1 and -2) in *Drosophila*.

Kindlin proteins have a common domain composition but there are some differences on the DNA and protein level. A phylogenetic tree illustrates the relationship between the three proteins in comparison to the *C. elegans* orthologue UNC-112. As shown in figure 1, Kindlin-1 and Kindlin-2 are slightly closer related to each other than to Kindlin-3. However, despite some areas of variability especially at the N-terminus and within the FERM (Band 4.1, ezrin, radixin, moesin) domain at the border between the F2 and F3 subdomain, the amino acid sequence is highly conserved (see figure 2).

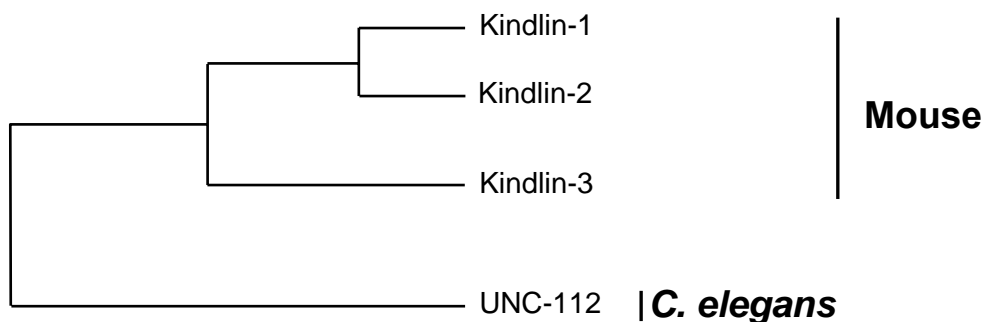


Figure 1: A phylogenetic tree of Kindlins.

In comparison to other FERM domain containing proteins, the Kindlin FERM domain has been found to share closest homology with the FERM domain of Talin. Talin is a large (~250kDa) cytoskeletal protein with an important role in the regulation of integrins, a family of heterodimeric transmembrane receptors important for binding to extracellular matrix components (ECM). Both Talin and integrins will be discussed in more detail below.

Introduction

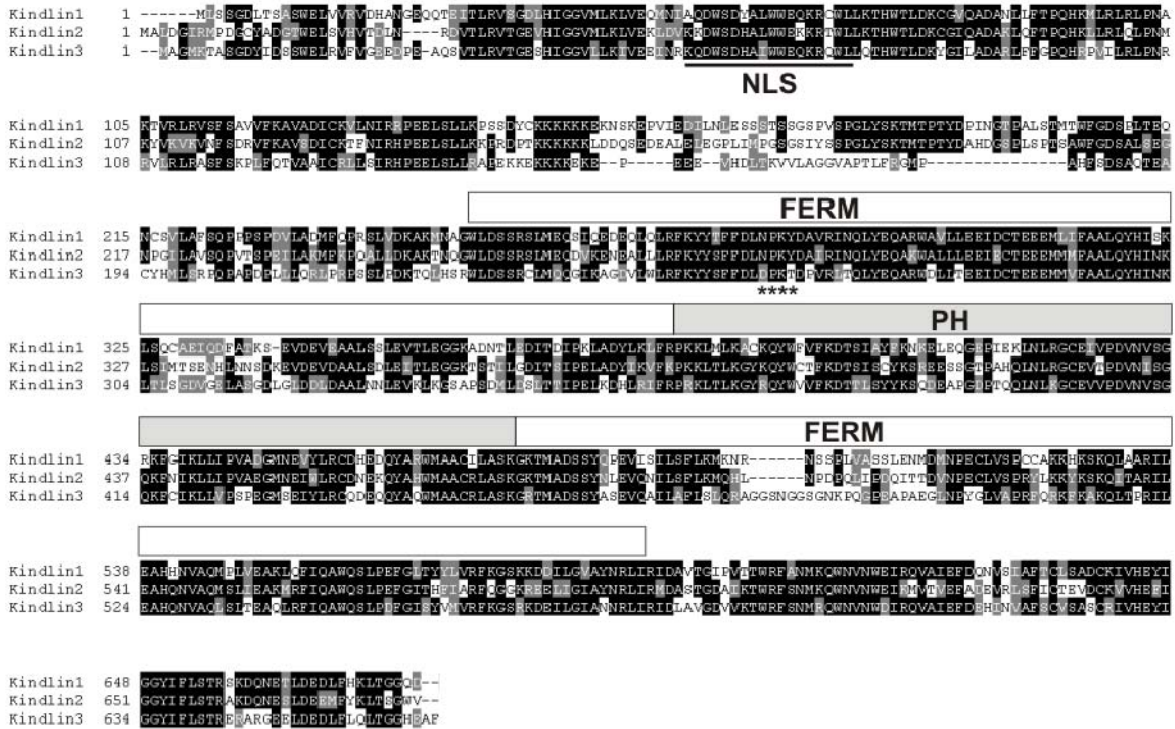


Figure 2: Murine Kindlin protein alignment. NLS; nuclear localisation signal. ** indicates a NPXY motif in Kindlin-1 and Kindlin-2. PH; pleckstrin homology domain.**

Kindlin gene and protein structure

Analysis of the exon/intron organization of the genes and the protein domains revealed a common structure, indicating that the three Kindlins recently separated in evolution. The genes consist of fifteen exons with the translation start codon in exon 2. Murine Kindlin proteins (1-3) have a length of 677, 680 and 665 amino acids, respectively. They are composed of a central FERM domain whose F2 subdomain contains a pleckstrin homology (PH) domain (see figure 3) [2]. In addition, Kindlin-2 has a nuclear localisation signal in the N-terminus of the protein that is neither present in Kindlin-1 nor in Kindlin-3.

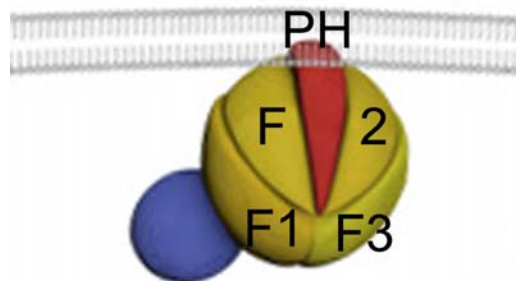


Figure 3: Kindlin protein structure; F1, F2 and F3 are the subdomains of the FERM domain and PH is indicating the pleckstrin homology domain.

FERM domains

FERM domain-containing proteins (81 in mice; <http://smart.embl-heidelberg.de>) constitute a heterogeneous family of membrane proteins that function as membrane-cytoskeleton linkers [3]. The FERM domain itself is around 200-300 amino acids (in Talin [4] and Band 4.1 [5], respectively) long. It was initially identified in Band 4.1 from erythrocyte ghosts [5]. Diverse studies on FERM domain containing proteins like Band 4.1, Merlin, protein phosphatases and Talin, unravelled an important role of this domain in membrane localising proteins [3]. Furthermore, Ezrin, Radixin, Moesin (ERM proteins) [6,7,8,9,10,11] and Talin [4] have been shown to mediate the linkage of transmembrane receptors with the actin cytoskeleton.

FERM domains are divided into three subdomains, F1-F3. The first subdomain has a ubiquitin fold, the second an α -helix bundle structure, and the third subdomain was classified as a pleckstrin homology (PH)-like or phospho tyrosine binding (PTB) domain, which belongs to the PH domain superfold family [12,13,14]. ERM proteins and Talin use the PTB domain for binding adhesion molecules. Although they share a similar function, the sequence homology can be variable with only 24% homology between ERM proteins and Talin.

PH/PTB superfamily

The PH/PTB domain superfold family is characterised by a common core fold, where two nearly orthogonal β sheets form a β sandwich with an α -helix capping off at one closed corner [14,15].

PTB domains are found in around 50 proteins in mice and man (<http://smart.embl-heidelberg.de>). This domain was initially identified in the Src homology 2 domain adaptor protein Shc, to mediate the binding of Shc to an NPXpY motif in activated receptor tyrosine kinases, such as the epidermal growth factor (EGF) receptor [16]. Interestingly, this recognition motif differs fundamentally from those of SH2 domains. In contrast to SH2 domains, the amino acids N-terminally to the tyrosine define the specificity of the PTB domains. In addition, several other PTB domain containing proteins including Talin [17] or ICAP1 α [18] either bind with the same or higher affinity to an unphosphorylated NPXY motif, indicating that the majority of PTB domains do not specifically interact with phosphorylated tyrosine residues.

PH domains are also short (~120 amino acids) modules with a common fold. They consist of very diverse sequences and are present in around 250 human proteins (<http://smart.embl-heidelberg.de>). Although they share a common core fold, PH domains have a variety of binding abilities [19]. Known ligands include structurally diverse proteins, phosphoinositides, and inositol polyphosphates/pyrophosphates [20].

The main function of PH domains is to bind membrane phosphoinositides [21,22]. There are three potential phosphatidylinositol (PtdIns) phosphorylation sites; PtdIns(3), PtdIns(4) and

Introduction

PtdIns(5) that refer to the position of the phosphate group on the D-myoinositol ring. These three sites can be phosphorylated in each combination resulting in mono-, bi-, and tri-phosphorylated PtdIns in a synergism of different kinases like phosphoinositide 3-kinase (PI3K) and lipid phosphatases such as phosphatase and tensin homolog (PTEN) [15]. The bulk cellular levels of phosphoinositides are typically relatively low with <1% of total phospholipids [23] and the different phosphoinositides show distinct subcellular localisations. PtdIns(4)P, PtdIns(4,5)P₂ (present at significant steady state levels), PtdIns(3,4,5)P₃ and PtdIns(3,4)P₂ (after receptor stimulation) can be found at the plasma membrane. In addition, PtdIns(4)P and PtdIns(4,5) are also found at the Golgi. PtdIns(3)P is mainly present at the endosome and in the nucleus, and PtdIns(3,5) is involved in vacuolar sorting. The spatial and temporal localisation of PtdIns(5)P is poorly understood, but a nuclear localisation has been suggested [15]. Thus, the specificity of a PH domain can be important for the subcellular localisation and targeting of the host protein.

The role of *UNC-112* in *C. elegans*

First functional data on Kindlin proteins came from the *C. elegans* orthologue UNC-112. The name UNC-112 comes from a disorganized body wall muscle leading to paralysis in adult worms and uncoordinated movement in homozygous animals for the r367 allele of *unc-112* [24].

C. elegans has four muscle cell quadrants separated from the epidermis via a BM, which is composed of ECM such as Perlecan/UNC-52. The BM is essential for the development of M-lines and dense bodies (see figure 4). Due to space limitations in the eggshell the embryo has to fold back upon itself twice during embryonic development, resulting in the formation of the two- and threefold stages of embryogenesis [25].

Introduction

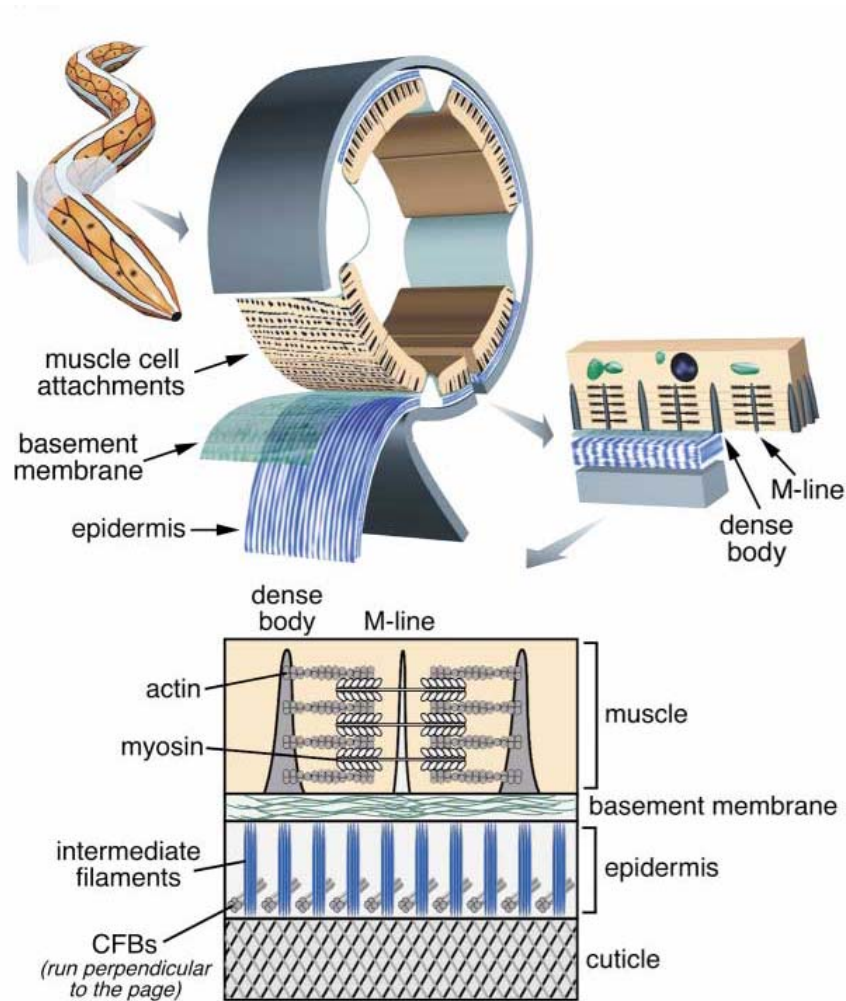


Figure 4: Localization and arrangement of dense bodies and M-lines. Scheme shows the localization and arrangement of dense bodies and M-lines in *C. elegans* body wall muscle and fibrous organelles in the epidermis [26].

Therefore, embryonic movement starts before the twofold stage [26]. Force transduction within the muscle is accomplished through anchorage of actin and myosin filaments to the muscle cell membrane via linkage to PAT2/ α integrin and PAT3/ β integrin heterodimers. During sarcomere assembly, actin (thin bundles) and myosin (thick filaments) link to the cell body through dense bodies and M-lines, respectively (see figure 4).

Interestingly, the *unc-112* r367 phenotype can be suppressed by null mutations in a novel protein called *dim-1* with unknown function [27]. However, null mutants of *unc-112* show a much more severe phenotype compared to the r367 allele and display a paralyzed, arrested elongation at twofold stage (PAT) phenotype. A PAT phenotype indicates that the missing gene products are essential for the formation of a functional embryonic body wall muscle [28,29]. The *unc-112* phenotype belongs like the *unc-52* (perlecan), *pat-2* (α integrin) and *pat-3* (β integrin) phenotypes to the most severe variant of PAT phenotypes [28]. Rogalski and co-workers could show that GFP-tagged UNC-112 localises with PAT-3 to the basal cell

Introduction

membrane in regions of contact with adjacent muscle cells, and to dense bodies and M-lines. They demonstrated that in UNC-112 deficient worms PAT-3/ β integrin is localised to the plasma membrane but cannot be properly organised in dense bodies and M-lines. Deletion of UNC-112 did not alter localisation of UNC-52 or the PAT-3 association of DEB-1 (vinculin) [29].

Conversely, it was shown that UNC-112 recruitment to the plasma membrane is dependent on PAT-3 and PAT-4 (ILK). The PAT-4 mammalian orthologue ILK has been reported to be an important mediator of integrin signalling and actin organisation [30,31]. Moreover, the proper localisation of PAT-4 itself seems also to be depending on UNC-112. This dependence may be achieved by direct interaction, as both proteins interact with each other in a yeast two hybrid assay. A more detailed analysis revealed that the first 31 amino acids of UNC-112 bind to a region in the pseudokinase domain of PAT-4, partly overlapping with the binding site of PAT-6/parvin [32,33].

These data position UNC-112/Kindlin as an important regulator of integrin clustering and integrin linkage to the actin cytoskeleton. The observations were further corroborated by RNAi studies in post-embryonic stages, where depletion of UNC-112 resulted in sterility due to defective ovulation and in migration defects of the distal tip cells that form the gonads. The sterility was caused by an inability of the mature oocytes to enter the spermatheca, which in turn was due to a greatly reduced contractility of the gonad sheath [34]. Thus, UNC-112 is an important regulator of actin mediated cell contractility. More recently, UIG-1 (UNC-112 interacting guanine nucleotide exchange factor-1) was identified to bind to UNC-112 and to co-localise with UNC-112 at dense bodies. The consequences of this binding remain to be elucidated but the findings raise the possibility that UNC-112 additionally functions as a signalling scaffold [35].

Taken together, these first functional data on UNC-112/Kindlin confirmed the functional predictions based on the domain architecture. UNC-112 could be defined as an important regulator of integrin function.

Integrins

Integrins are heterodimeric surface receptors consisting of an α and a β subunit [36]. They mediate the connection between extracellular matrix components or cellular counter receptors and the actin cytoskeleton or intermediate filaments, which led to the name "integrin" [37]. This functional property allows them to regulate cell migration, proliferation, survival and polarity [38]. With increasing complexity of the organism the number of integrin receptors is raising. In *C. elegans* the integrin family consists of two members, which result from the combination of two α integrin subunits (PAT-2 and INA-1 [39]) and one β integrin subunit (PAT-3). The *Drosophila melanogaster* genome codes for five integrins composed

Introduction

out of five α and one β subunits [40]. In mammals the combination of 18 α and 8 β subunits gives rise to at least 24 distinct integrins. The globular head domains of the α and β subunit form the ligand binding domain. Accordingly, the ligand specificity depends on both subunits. Among this large family the twelve $\beta 1$ integrins are the largest subclass (see figure 5).

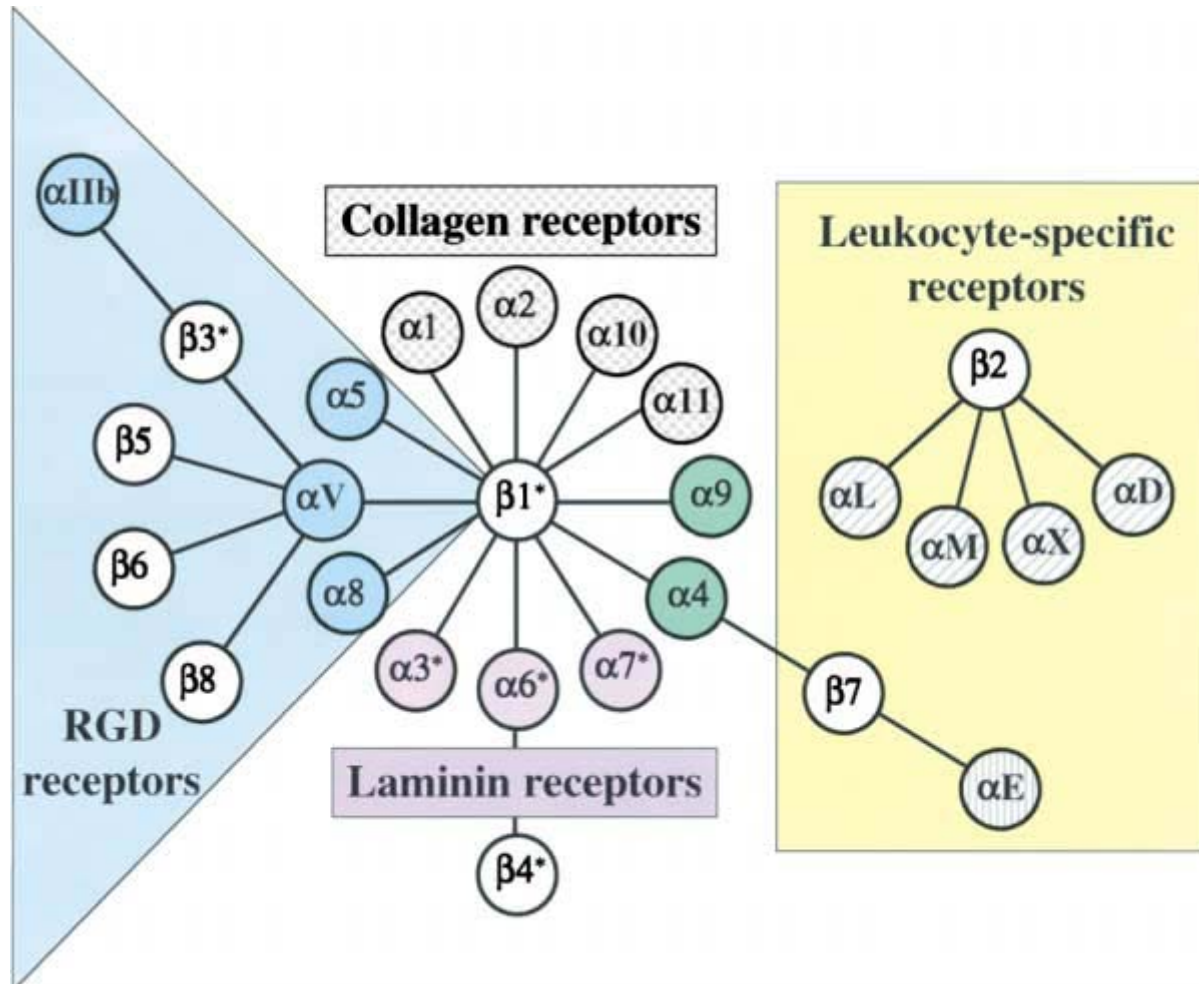


Figure 5: The mammalian integrin family. Integrins are heterodimers composed of an α and a β subunit. The figure depicts the mammalian subunits and their $\alpha\beta$ associations. The heterodimers can be grouped in several subfamilies based on evolutionary relationships (colouring of subunits), ligand specificity and, in the case of $\beta 2$ and $\beta 7$ integrins, restricted expression on white blood cells. α subunits with gray hatching or stippling have inserted I/A domains. Such α subunits are restricted to chordates, as are $\alpha 4$ and $\alpha 9$ (green) and subunits $\beta 2$ - $\beta 8$. In contrast, α subunits with specificity for laminins (purple) or RGD (blue) are found throughout the metazoa and are clearly ancient. Asterisks denote alternatively spliced cytoplasmic domains. [36].

Integrins can be grouped into five classes; (i) RGD peptide recognizing integrins that bind molecules like fibronectin, vitronectin and others through an RGD motif; (ii) Laminin receptors; (iii) collagen receptors; (iv) leukocyte specific receptors that bind Ig-superfamily cell-surface counter-receptors such as VCAM-1 and mediate heterotypic cell-cell adhesion and (v) two related integrins ($\alpha 4\beta 1$ and $\alpha 9\beta 1$) that recognise both ECM proteins such as fibronectin and Ig-superfamily counter-receptors [36,41]. All integrins, with the exception of $\alpha 6\beta 4$ integrin, which is connected to intermediate filaments, link to the actin cytoskeleton. In

Introduction

addition, the $\alpha6\beta4$ integrin differs from all the others with a much larger cytoplasmic domain consisting of 1072 amino acids.

Integrin function in vivo

Integrins have multiple functions, which are reflected by the diversity of phenotypes observed in mice lacking individual α or β subunits (see figure 6). This diversity originates from the different spatial and temporal expression pattern and the ligand binding specificity of individual integrins. There is an overwhelming literature on the *in vivo* function of the individual integrin subunits reviewed in [36,42]. Thus, only selected information will be provided here. An overview about the function of integrins during pre- and peri-implantation development, in skin, the intestine and platelets, is important to better understand the consequences of loss of Kindlin-1-3. Furthermore the focus will be on $\beta1$ and $\beta3$ integrins, which have been shown in this thesis to associate with Kindlins [43,44].

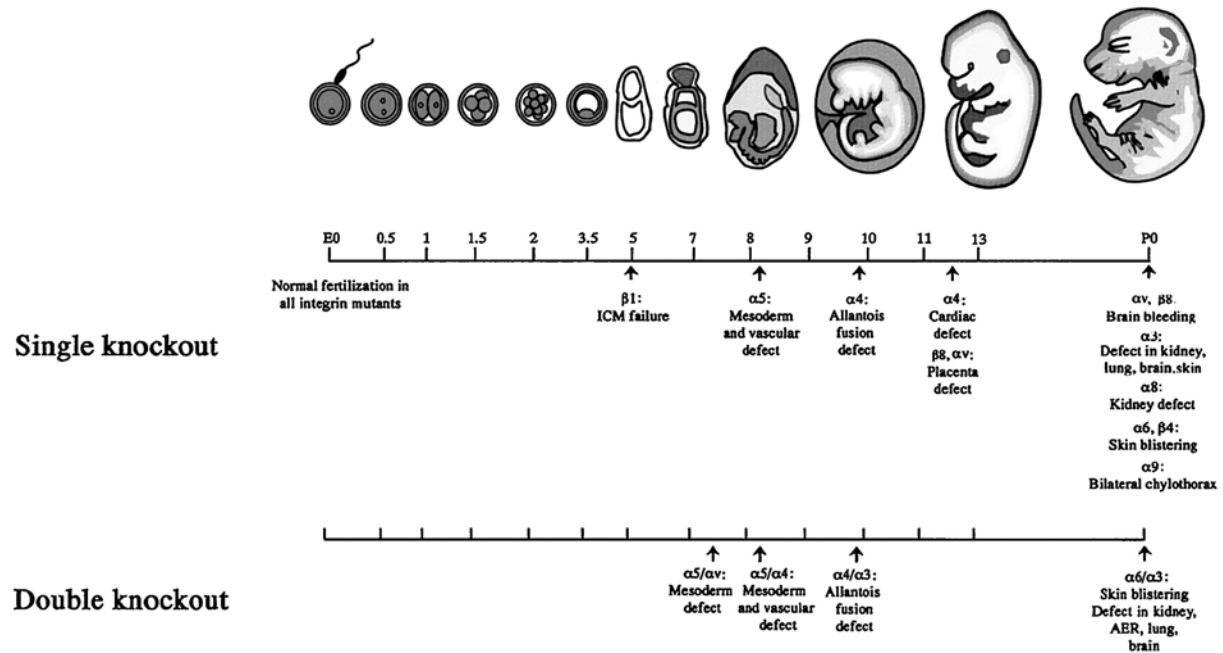


Figure 6: Phenotypes of integrin knockout mice during development. Diagram shows the embryonic and perinatal lethal phenotypes of single and double integrin-null mutant mice. The earliest lethal phenotype is observed in $\beta1$ -deficient mice at E5.5. Studies of double $\alpha5/\alpha v$ -null and $\alpha3/\alpha6$ -null mice revealed a redundant and/or compensatory function for $\alpha5/\alpha v$ during early mouse development and for $\alpha3/\alpha6$ in several organs and tissues including brain, and lung [42].

Murine pre- and peri-implantation development

The pre-implantation development of mammals encompasses the period from fertilization to implantation. It is characterized by three distinct phases: (i) fertilization and followed by cell divisions; (ii) the establishment of cell polarity and compaction into a morula, (iii) lineage differentiation in blastocysts and implantation (figure 7) [45,46]. In mice the blastocyst develops around day E3.5 and is composed of three cell types, the outer terminally

Introduction

differentiated epithelial trophoblast, the primitive endoderm covering the inner cell mass. The trophoblast mediates the first contact with the luminal epithelium of the uterus while the inner cell mass gives rise to the embryo proper. The primitive endoderm differentiates from the inner cell mass and further differentiates into visceral and parietal endoderm. Both cell types are separated via a BM from the inner cell mass and trophoblast, respectively. After implantation inner cell mass cells adjacent to the BM differentiate into epiblast while the remaining inner cell mass cells undergo apoptosis, which leads to cavitation and formation of the pro-amniotic cavity.

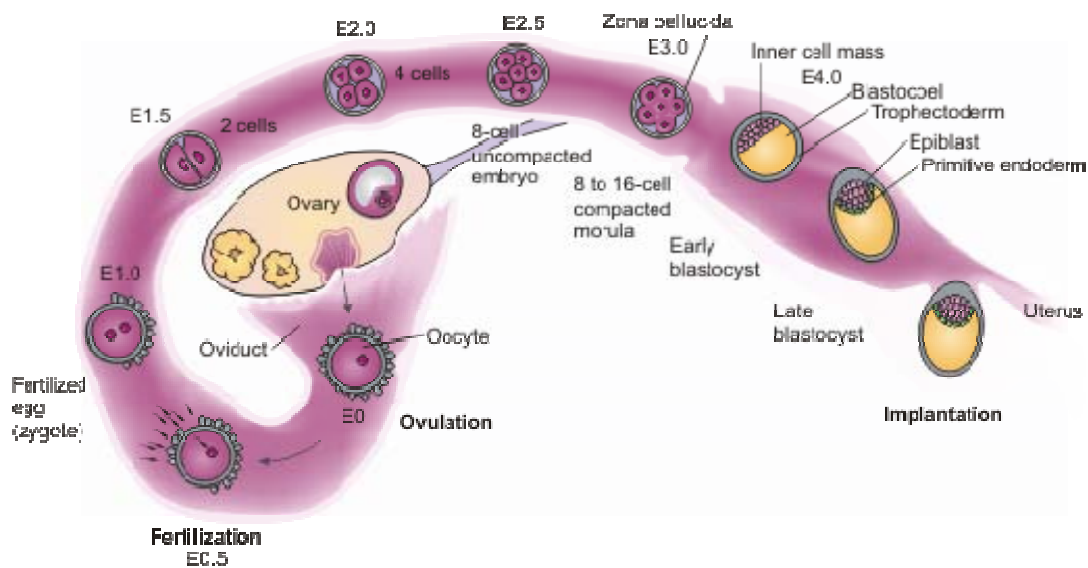


Figure 7: Pre-implantation development in mice. After fertilization in the oviduct the embryo proliferates and forms the morula. At this stage the embryo enters the uterine lumen and further develops into a blastocyst. The blastocyst is characterised by a cavity (blastocoel) and two different cell types, the inner cell mass and the trophoblast, which will give rise to the trophoblast cells. In order to implant the blastocyst has to hatch from the outer shell called zona pellucida and further differentiate to form the epiblast and the primitive endoderm. At this stage the trophoblast attaches to the uterine lining to initiate the implantation [45].

To facilitate the analysis of these embryonic stages an *in vitro* model, termed embryoid bodies (EBs), has been established. EBs are ES cell aggregates, which mimic endoderm and epiblast differentiation. The development of this *in vitro* system is limited partially due to the fact that no trophoblast is formed. This is also responsible for peripheral aggregates of the parietal endoderm [47,48].

The role of integrins during pre- and peri-implantation development

Several *in vitro* studies suggested a role of integrins in the interaction of the blastocyst with the luminal epithelium [49,50]. It has been shown that especially $\alpha\beta3$ and $\alpha\beta5$ integrins are expressed on the apical pole of the luminal epithelium [51] but also on the epithelial surface of blastocysts [52,53]. Furthermore, studies using arginine-glycine-aspartic acid (RGD)

Introduction

blocking peptides or blocking antibodies against $\alpha v\beta 3$ suggested that implantation in the mouse can be significantly reduced with these tools [54].

In contrast to these studies, neither single knockouts of integrin subunits nor a combination of knockouts of different α subunits [42] led to a defect during pre-implantation so far. This could either be the result of residual maternal mRNA, although unlikely [55], or a compensation by other integrins. Therefore, a double knockout of αv and $\beta 1$ integrin could help to clarify whether integrins are important during pre-implantation (see figure 5).

Deletion of the $\beta 1$ integrin affects the largest number of integrin receptors. Thus, it is not surprising that constitutive deletion of $\beta 1$ integrin leads to the most severe phenotype with lethality at the peri-implantation stage at around E5.5 [56,57]. *In vitro* analysis with $\beta 1$ integrin-deficient EBs revealed that the mutant endoderm is unable to secrete sufficient laminin $\alpha 1$ chains and thus fail to deposit a BM, to differentiate an epiblast and to cavitate [58]. Laminin $\alpha 1$ is required to form a functional heterotrimeric laminin [59], which in turn is a prerequisite for the formation of a BM [47]. Reconstitution of $\beta 1$ integrin deficient EBs with laminin-111 permitted BM formation and epiblast differentiation although detachment of the outer endodermal layer was still present [60]. The important role of $\beta 1$ integrin was further highlighted by the analysis of chimeric $\beta 1$ integrin deficient mice, showing impaired recruitment of haematopoietic progenitor cells into the foetal liver and no homing of adult haematopoietic stem cells into the bone marrow [61,62] despite normal differentiation *in vitro* and *in vivo* [42].

Skin

The skin is a complex organ consisting of more than 20 cell types. Its main functions are protection from water loss, temperature change, radiation, trauma and infections [63]. The skin is composed of three different layers. The outermost layer consists of a squamous stratified epithelial layer (epidermis). The dermis is separated from the epidermis via a BM and is mainly consisting of ECM secreting fibroblasts of mesodermal origin. The subcutis is the third layer where the adipocytes reside.

The epidermis itself consists of several layers of keratinocytes (see figure 8) that provide a physical barrier to the outside of the body. The basal keratinocytes face on their basal side the BM and contain the proliferative cell pool within the epidermis.

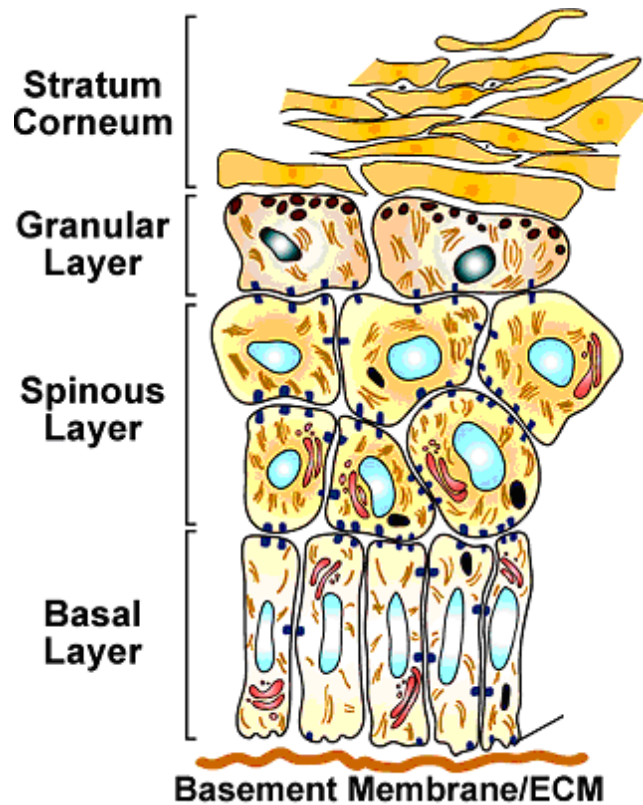


Figure 8: The epidermal architecture is shown in this schematic, illustrating the basement membrane at the base, the proliferative basal layer, and the three differentiation stages: spinous layer, granular layer, and outermost stratum corneum. [64].

During differentiation/stratification keratinocytes move upwards, withdraw from the cell cycle, downregulate their integrin expression and finally de-nucleate. Thereby these cells give rise to the spinous and granular layers and finally to the production of dead corneocytes of the stratum corneum that eventually shed from the epidermal surface [65].

The role of integrins in the epidermis

The major integrins expressed in normal epidermis are the $\alpha 6\beta 4$ and $\alpha 3\beta 1$ integrin that bind laminins and $\alpha 2\beta 1$ which is a collagen binding integrin [66]. Integrin expression is restricted to the basal keratinocytes (figure 8).

Genetic deletion of either the $\alpha 6$ or the $\beta 4$ integrin in mice results in loss of hemidesmosomes and severe keratinocyte de-adhesion from the BM [67,68,69] leading to a severe early postnatal lethal skin blistering phenotype. Similarly, mutations in the human $\beta 4$ integrin cause a recessive skin blistering disease termed junctional epidermolysis bullosa (JEB), that is also observed upon mutation of the main ligand laminin-332 [70].

The early lethality of $\beta 1$ integrin-deficient mice required the establishment of a conditional knockout allele for the $\beta 1$ integrin. Keratinocyte specific disruption of the $\beta 1$ integrin gene during early embryonic development results in a stronger phenotype than observed in $\alpha 3$ integrin-null mice, although $\alpha 3\beta 1$ was believed to be the predominant keratinocyte $\beta 1$

Introduction

containing integrin [71,72]. The phenotype is characterised by reduced cell proliferation, extensive skin blistering, altered BM assembly and a failure of hair follicle keratinocytes to remodel the BM and invaginate into the dermis [65]. This indicates that other $\beta 1$ integrin containing receptors such as $\alpha 2\beta 1$ integrin have important functions in skin homeostasis as well. Later skin-specific $\beta 1$ integrin deletion, around birth, results in hair-loss, epidermolysis and a reduced proliferation rate of basal keratinocytes. The role of other integrins is less clear. $\alpha v\beta 6$ integrin, for example, is expressed upon injury or inflammation and known to bind TGF- $\beta 1$ in its latent form. Deletion of the $\beta 6$ integrin subunit does not alter wound healing, but leads to a local reduction of activated TGF- $\beta 1$ [73,74].

Intestine

The intestine, composed of the small intestine, the caecum and the colon, is part of the gastrointestinal tract that in addition includes the pharynx, oesophagus and stomach. Developmentally, the pharynx, oesophagus and stomach are formed from the foregut, while the small intestine, the caecum and the colon arise from the midgut and hindgut, respectively [75]. The intestinal epithelium like the epithelium in the skin provides a barrier to the outside of the body [76].

In mice, the gut epithelium can be first identified at E7.5 as a single layer of proliferative, endodermal cells, followed by the formation of a pseudostratified epithelium within the next days [77]. While the oesophagus is lined by a stratified epithelium, parts of the stomach and the whole intestine (small intestine and colon) are covered by a single epithelial cell layer. The surface of the small intestine is increased by numerous evaginations (villi) and invaginations (crypts). In contrast, the colon lacks villi and the crypts are thus connected to a flat surface epithelium (see figure 9).

The villi in the small intestine increase the surface of the small intestine to maximise nutrient and water resorption. The main function of the colon is the thickening of the stool, making a large surface dispensable. Thus the intestinal epithelium has a bi-functional role; on one side it has to function as a barrier to a massive bacterial load, but on the other side it has to permit passage of nutrients and water into the body.

Introduction

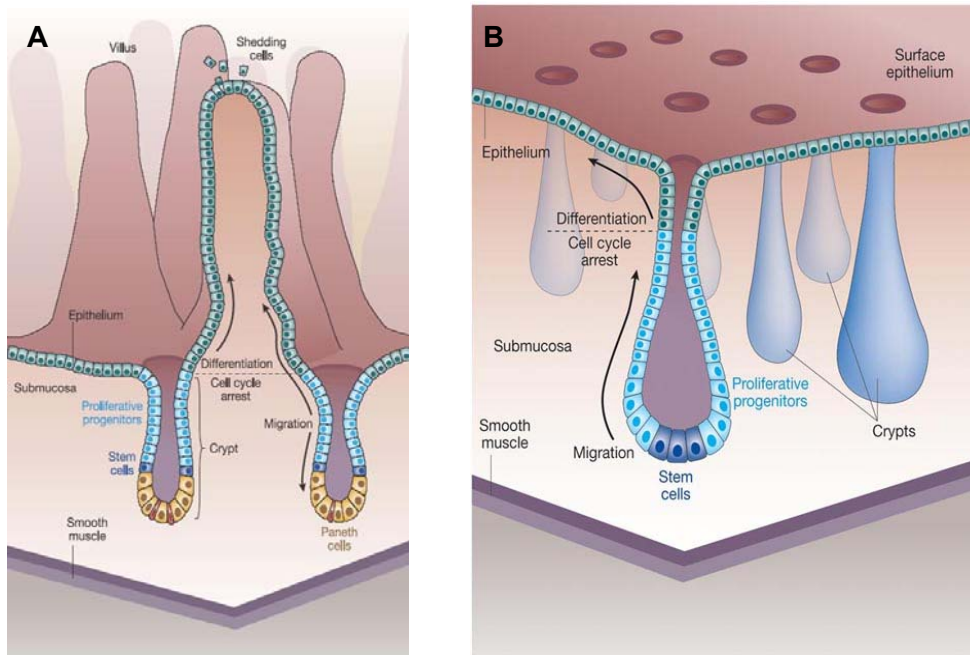


Figure 9: Intestinal architecture. (A) The small intestine is characterised by large villi surrounded by stem cell containing crypts. The stem cells (dark blue) reside above the Paneth cells (yellow). The stem cells give rise to progenitor cells that further proliferate and occupy the remainder of the crypt. Differentiated cells (green) move upwards and populate the villus. (B) The colon lacks villi and instead has a flat surface epithelium. The putative stem cells (dark blue) reside at the crypt bottom and the progenitor cells occupy two-thirds of the crypt. The differentiated cells (green) populate the remainder of the crypt and the flat surface epithelium [78].

In order to achieve this multiple functions the intestinal epithelium differentiates into different specialised cell types: goblet cells, enterocytes, entero-endocrine cells and Paneth cells. While the goblet cells, enterocytes and entero-endocrine cells populate the villi the Paneth cells reside at the bottom of the crypts. The cells migrate within three days upwards from the crypts to the villus tips where they finally undergo apoptosis and are shed into the intestinal lumen [76,79,80]. Within the crypts there is a clearly defined positioning of the stem cells. While the stem cells are positioned at the crypt mid in the small intestine [81] and descending colon [82] they can be found in the crypt base of the ascending colon [83]. The stem cells slowly proliferate and give rise to progenitor cells that then further differentiate. Therefore, the intestine is an excellent tissue to investigate processes such as stem cell function, host defence, differentiation, cell migration and apoptosis.

The role of integrins in the intestine

The vast majority of studies on the function of intestinal integrins were performed in cell culture. Several studies, however, investigated the expression pattern of different integrins along the crypt villus axis, primarily in humans.

These studies revealed expression of $\beta 1$, $\beta 4$, $\alpha 2$ integrins predominantly in the crypts and $\alpha 3$ integrin on the villi. $\alpha 6$ and αv integrins expression is uniformly distributed from the crypts to

Introduction

the villi tips, whereas $\alpha 5$ and $\alpha 7$ integrin show a very restricted expression pattern. $\alpha 5$ integrin is only found at the crypt base and $\alpha 7$ integrin at the interface between the crypt and the villus. $\alpha 6\beta 4$ integrins cluster into keratin linked hemidesmosomes that can be found in a regressing gradient from the crypts to the villi. In contrast to basal keratinocytes, intestinal epithelial cells lack major hemidesmosomal proteins like BP230 and BP180 and thus form so called type II hemidesmosomes [84]. In addition intestinal hemidesmosomes have a distinct role in mediating cell adhesion in comparison to the skin. This is best illustrated as mice lacking the intracellular domain of the $\beta 4$ integrin develop severe epidermolysis but no intestinal epithelial detachment. However IECs show a severe proliferation defect due to an altered cell cycle control [85].

Initial data on ECM proteins showed a differential expression pattern of collagen IV isoforms [86,87], laminin 111, laminin 211 [88,89,90] and laminin-332 [91]. Laminin 111 is present in the villus while laminin 211 in crypts. Laminin-332, initially believed to be solely present in the BM of stratified epithelia, is expressed in an increasing gradient from the upper crypt to the villus tip [91]. These data suggested a relation between the integrin expression, the BM composition and the differentiation state of the intestinal epithelium [92].

A detailed genetic analysis of the intestinal epithelium was limited due to the lack of specific Cre lines. The recent establishment of a Cre line using the villin promoter that is specifically activated in the intestinal epithelium [93], allowed the conditional deletion of genes in the intestine. The intestinal epithelial specific deletion of the $\beta 1$ integrin with this villin-Cre strain did not result in altered epithelial adhesion, but in crypt expansion due to increased proliferation which was linked to reduced hedgehog expression [94].

These data indicated that intestinal integrins have an important role in tuning stem cell and progenitor cell proliferation and differentiation. The absence of adhesion defects, especially in $\beta 1$ deficient mice, suggests that αv containing integrins (see figure 5) might compensate. Deletion of individual α integrin subunits might provide further insights into the role of integrins in intestinal epithelial cell migration proliferation and differentiation.

Platelets

Platelets mediate primary haemostasis and are small anuclear cell fragments that arise from megakaryocyte cytoplasmic extensions called proplatelets (see figure 10). They are sheared from their transendothelial stems by flowing blood. [95,96]. Megakaryocytes are large polyploid cells of at least 16N in rodents and men that reside in the bone marrow of adults [97,98]. Polyploidy is achieved by endomitosis [97] and is required to produce enough templates for the high rate of transcription and translation. The production of secretory granules, like α - and dense granules, is a prerequisite for thrombopoiesis.

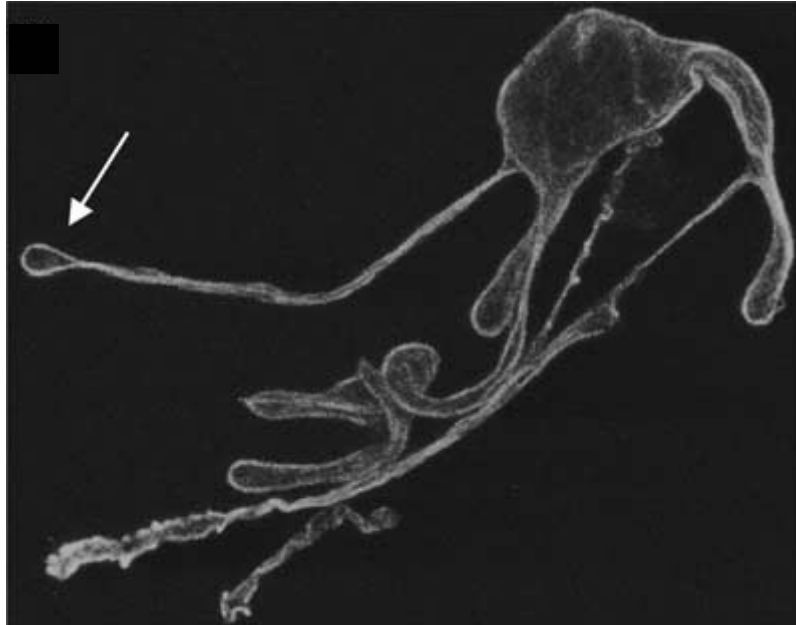


Figure 10: Formation of proplatelets. Shown is a cultured murine megakaryocyte stained for β tubulin. Long pseudopodia end with proplatelets (arrow) [95].

Secretory granules originate from the Golgi complex [99] and acquire their content by a combination of synthesis, endo- and pinocytosis [100,101]. Several critical components of platelet function are incorporated into α - and dense granules, like P-selectin, α IIb β 3 integrin, van Willebrand Factor (vWF) and granulophysin, respectively [99].

The physiologic function of platelets is to seal injured blood vessels. This process has to be tightly controlled as abnormal platelet activation can lead to pathological thrombus formation causing myocardial infarction or stroke.

Therefore, a tightly regulated signalling cascade is initiated once a platelet encounters an injury in the blood vessel wall (see figure 11). The first step in this haemostatic cascade is the interaction of platelets with the ECM. At sites of high shear stress, like in small arteries and arterioles, the initial tethering is mediated by the platelet receptor glycoprotein (GP)Ib and vWF bound to BM collagens [102]. This interaction has a very high off rate and is not able to mediate stable adhesion. Therefore in a next step an interaction between collagen and the immunoglobulin superfamily receptor GPVI forms. The low affinity interaction is not sufficient for stable platelet adhesion. However, it leads to a signalling cascade in platelets resulting in the activation of integrins enabling them to bind their ligands. Furthermore, GPVI binding triggers the release of secondary mediators ADP and thromboxane A2 (TXA2) from granules, which together with thrombin activates heterotrimeric G protein coupled receptors leading to full platelet activation. These cells are characterised by shape change, secretion due to degranulation and aggregation upon integrin activation [96,103].

Introduction

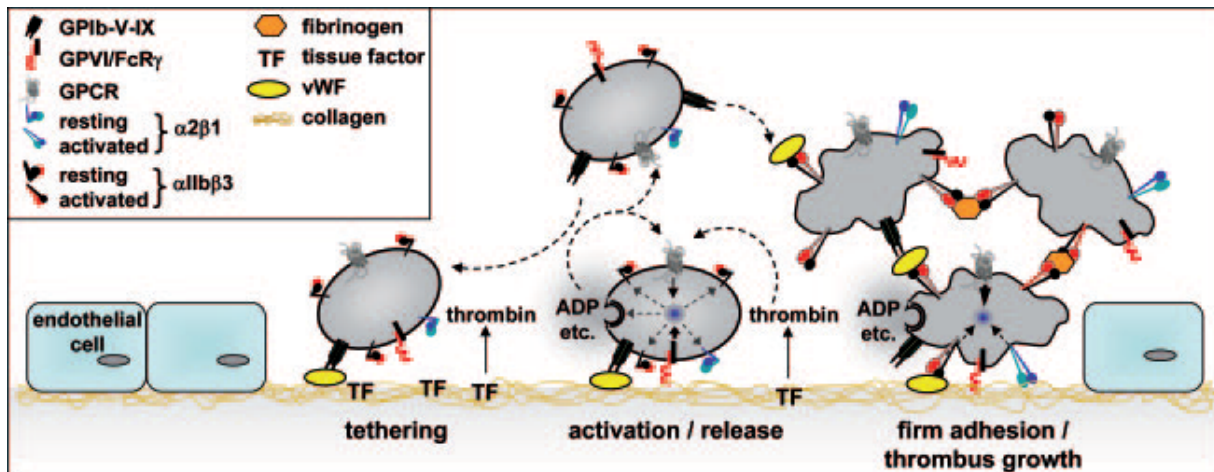


Figure 11: Schematic of platelet adhesion and aggregation on the ECM. Initial platelet contact is mediated via a GPIb/ vWF interaction. This results in platelet tethering and GPVI/ collagen interactions. The binding of GPVI to collagen induces integrin activation and release of ADP and TXA2. In parallel, tissue factor (TF) induces thrombin formation which also leads to platelet activation. [96]

The role of integrins in platelets

Platelets express five different integrin receptors namely, $\alpha 2\beta 1$, $\alpha 5\beta 1$, $\alpha 6\beta 1$, $\alpha \text{IIb}\beta 3$ and $\alpha \text{v}\beta 3$ integrin. Initially it was believed that $\alpha 2\beta 1$ integrin is the main platelet collagen receptor mediating firm adhesion. Studies in $\alpha 2$ and $\beta 1$ integrin deficient mice, however, showed no major haemostatic defect. These data revealed that $\alpha 2\beta 1$ integrin only supports adhesion to fibrillar collagen whereas the main collagen adhesion molecule is GPVI [104,105,106]. GPVI mediates only low affinity adhesion, thus it is believed that other receptors, most notably $\alpha \text{IIb}\beta 3$ integrin, mediate shear resistant attachment to the ECM [96,102].

$\alpha \text{IIb}\beta 3$ integrin binds an RGD sequence (see figure 5) present in proteins such as fibrinogen, its cleavage product fibrin, vWF, fibronectin, thrombospondin and vitronectin. Among those ligands fibrinogen is especially important as it has two binding sites for the $\alpha \text{IIb}\beta 3$ integrin. Thus, it can serve as a bridge to connect two platelets and thus mediates their aggregation.

$\alpha \text{IIb}\beta 3$ integrin is the most abundant glycoprotein on the platelet surface [107], and lack or dysfunction of $\alpha \text{IIb}\beta 3$ integrin results in Glanzmann thrombasthenia in humans [108]. This inheritable disorder is characterised by a failure of platelets to aggregate. The severity of the observed bleeding defects varies among patients [109]. Similarly mice lacking the $\beta 3$ integrin subunit have absent platelet aggregation, reduced clot retraction and greatly reduced fibrinogen uptake into platelets [110]. The role of the other integrins present in platelets is less well described. Recent reports suggest, that these integrins might modulate platelet response by the nature of the exposed ECM, as the laminin binding $\alpha 6\beta 1$ integrin for instance enhances platelet spreading through GPVI [111].

Introduction

Taken together integrins have a variety of different functions. They primarily mediate a connection between the extracellular environment and the cellular cytoskeleton. Thereby they provide a mechanical link but also provide a signalling platform sensing the cellular surrounding. The essential role of integrins in cellular adhesion is underlined by (i) the severe most often lethal phenotypes upon deletion of key integrin subunits or (ii) the expression of compensating integrins to overcome the potential loss of one integrin subunit.

Integrin activation (Inside-out signalling)

Regulating the affinity of individual integrins for their ligands is an additional regulatory step to modulate the function of integrins. This becomes most apparent when looking at platelets. Constitutive activation of $\alpha\text{IIb}\beta\text{3}$ integrin would be incompatible with life. Platelets would bind their major ligand fibrinogen, present at high levels in the plasma and aggregate leading to instant thrombosis. A theoretical possibility to circumvent this would be the intracellular storage of these receptors and the transport to the cell surface upon stimulation. This is indeed partially the case as $\alpha\text{IIb}\beta\text{3}$ integrin is stored in α -granules that fuse with the plasma membrane upon GPVI signalling. However, the high amounts of $\alpha\text{IIb}\beta\text{3}$ integrin on the surface of resting platelets suggest an additional regulatory step.

Structural analysis of the extracellular domain of $\alpha\text{v}\beta\text{3}$ integrin [112,113,114] revealed a bended, v-shape conformation unable to bind immobilized ligands like fibronectin or vitronectin (see figure 12A). Upon treatment with Mn^{2+} , a known activator of integrins [115], or RGD peptide binding, $\alpha\text{v}\beta\text{3}$ extracellular domains undergo a dramatic global change in conformation and converted to an extended form (see figure 12B and C) [114]. These and other studies led to the conclusion that integrins exist in an inactive (low affinity, bended) and an active (high affinity, extended) conformation [116].

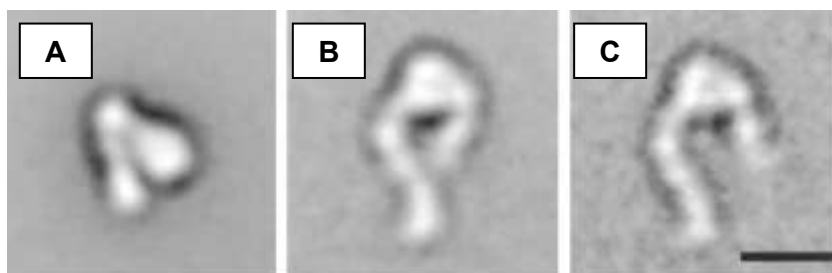


Figure 12: 2D Projections of negatively stained $\alpha\text{v}\beta\text{3}$ integrin electron micrographs. (A) $\alpha\text{v}\beta\text{3}$ integrin in the presence of Ca^{2+} showing a bended inactive conformation (B & C) show extended $\alpha\text{v}\beta\text{3}$ integrins with an open headpiece purified in the presence of (B) Mn^{2+} or (C) Ca^{2+} and cyclo-RGDfV. Black bar indicates 100 Å. Modified from [114].

In a process called inside-out signalling, intracellular signalling pathways lead to changes in the intracellular domains of integrins rendering the extracellular domain competent for ligand binding [117]. Extensive studies showed that the short cytoplasmic tails of the α and β

Introduction

integrin subunit can interact with each other to regulate integrin activity [36]. Studies on α IIb β 3 integrin showed that the α IIb cytoplasmic domain acts as negative regulator of activation and that deletion of it results in a constitutively active integrin [118,119]. The same effect could be observed upon mutation of the membrane-proximal segment in the β 3 integrin, destroying a salt bridge between R995 of α IIb and D723 of β 3 integrin [120,121]. It was shown that the separation of the two integrin tails leads to conformational changes characterized by the described switchblade-like opening of the bended inactive into the extended active integrin [122]. Therefore changes in the intracellular binding of proteins to the β integrin cytoplasmic tail translate into structural changes in the extracellular part of the heterodimer resulting in a high affinity fold.

Talin mediates integrin activation

Talin-1 (mostly referred to as Talin) is a large cytoplasmic adaptor protein (~250kDa) [4] with a FERM domain located at the N-terminus or head region. It was shown that Talin is essential for integrin activation. It binds via a PTB domain encoded in the FERM domain to an NPLY (amino acids 744-747) motif of β 3 integrin [17,123,124,125].

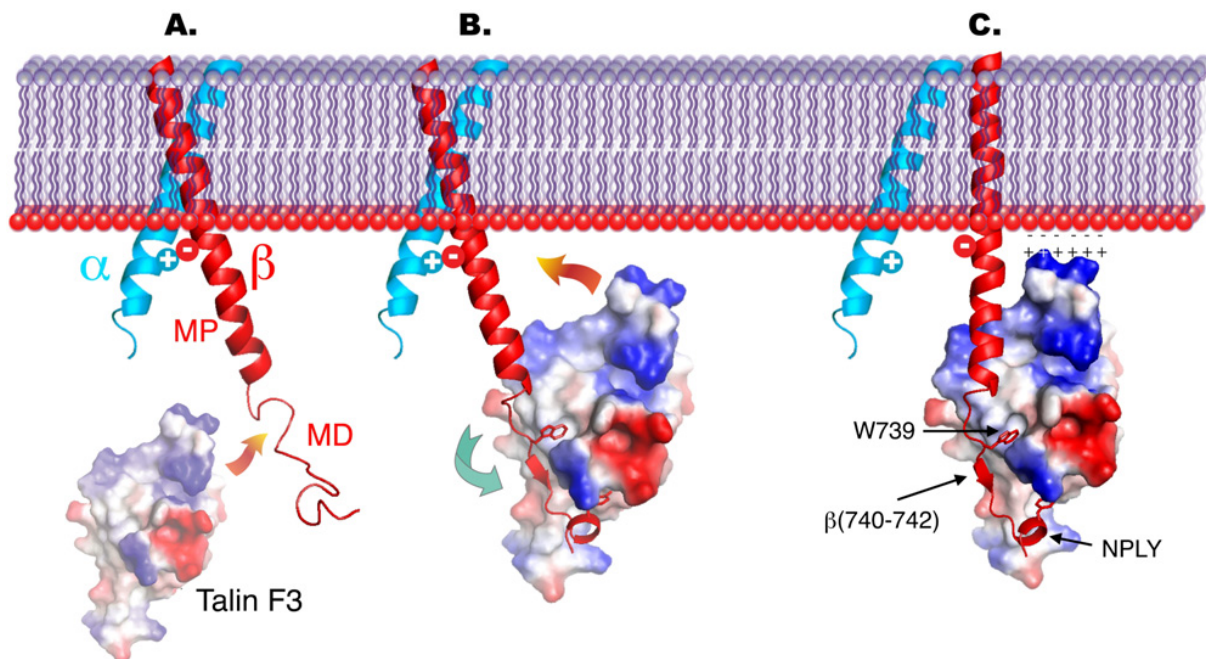


Figure 13: Structural model of Talin induced integrin activation (A) $\alpha\beta$ integrin heterodimer connected via a salt bridge. The talin F3 domain is shown as surface representation and coloured by charge. (B) The Talin F3 domain binds to the membrane distal (MD) part of the β 3-integrin tail (in red). This results in a higher order of the β 3 integrin cytoplasmic tail but the $\alpha\beta$ interaction remains intact. (C) The Talin F3 domain additionally interacts with a membrane proximal (MP) region of the β 3 integrin cytoplasmic tail. This induces the destabilization of the $\alpha\beta$ integrin saltbridge and the stabilization of the helical structure of the MP region. Furthermore the Talin F3 domain can electrostatically interact with acidic lipid head groups in the plasma membrane. These changes result in the separation of the integrin tails and integrin activation. [125]

Introduction

Structural analysis of the $\beta 3$ integrin and Talin head interaction showed that the initial PTB-NPLY interaction does not result in separation of the integrin tails but enables Talin binding to more membrane proximal regions within the $\beta 3$ tail [125] leading to separation of the integrin tails [123,124,126] (see figure 13). Recently it has been shown, that the F3 subdomain of the FERM domain, encoding the PTB domain, is sufficient to promote $\beta 3$ integrin activation. Interestingly additional elements in the F1 domain are required to promote $\beta 1$ integrin activation [127]. This indicates certain differences between the individual integrin heterodimers with regards to their activation mechanisms. The essential role of Talin in integrin activation is underlined by the severe adhesion and aggregation defects of Talin-1 deficient platelets that mimic loss of $\beta 3$ integrin [128].

Apart from Talin-1 a second gene, Talin-2 has been identified, but it is not very well characterized. This is mainly due to the lack of Talin-1 or -2 specific antibodies and the very restricted expression pattern of Talin-2 [129]. However it is currently believed that Talin-2 compensates during early embryonic development for the loss of Talin-1. This could explain the relatively late embryonic lethality of Talin-1 deficient mice around E8.5-9.5 [130]. In addition a mutational screen within the $\beta 3$ integrin cytoplasmic tail identified a Y759A mutation in the membrane distal NxxY motif also to inhibit integrin activation, despite normal Talin binding. This suggests that additional proteins are involved in Talin mediated integrin activation [131].

Nevertheless, binding of Talin or the Talin head to the β integrin cytoplasmic tail induces integrin activation. Thus this binding event has to be tightly regulated either at the level of Talin or integrins [132,133]. At the level of integrins post-translational modifications of cytoplasmic tails could alter Talin binding. Indeed, Src family kinases phosphorylate β integrin cytoplasmic tail NPXY motifs [134,135] which inhibits the Talin PTB/NPXY interaction [136,137,138]. Whether this phosphorylation plays a role *in vivo* has to be elucidated. Mice harbouring tyrosine to phenylalanine mutations of both NxxY motifs of the $\beta 1$ integrin did not show any abnormalities while tyrosine to alanine mutations resembled a null phenotype [139]. The specific effects of Talin phosphorylation on its function are not known [132]. However, Talin is known to form a homodimer [140], while other FERM domain containing proteins exhibit an autoinhibitory intramolecular binding [141]. This creates the possibility that the integrin binding site is masked by an intra- or intermolecular interaction. In addition phosphatidylinositol 4,5-bisphosphate promotes Talin binding to integrin $\beta 1$ tails associated with a conformational change in Talin exposing the integrin binding site [142]. Finally, calpain-mediated cleavage of Talin was shown to release the Talin head from the rod domain that binds the $\beta 3$ integrin cytoplasmic tail with a six-fold higher affinity than full length Talin [124,143]. Thus the Talin-integrin interaction is tightly regulated in order to prevent unintentional integrin activation.

Outside-in Signalling

Activation of integrins permits ligand binding. This information is transmitted from the extracellular domain to the cytoplasm in a process called outside-in signalling. Diverse signalling events are subsequently initiated regulating processes like cytoskeletal strengthening, migration but also cell proliferation and apoptosis. The processes that regulate the number and spatial organisation of integrin-ligand bonds are best characterised for adhesion strengthening [116].

Cell matrix adhesions can be divided into four groups; immature focal complexes, mature FAs, fibrillar adhesions and podosomes [144]. Focal complexes are ~100nm dot-like matrix adhesions at membrane protrusions that either disassemble or further mature. They give rise to larger more elongated FAs that are best distinguished from focal complexes by their anchorage to actin stress fibres. Fibrillar adhesions are a special form of FAs that are mainly composed of $\alpha 5\beta 1$ integrins and are thought to be important for the parallel orientation of fibronectin fibres along the actin stress fibres [145]. Finally, podosomes are specialised adhesion structures of monocyte derived cells with a circular structure and an actin core [146].

Despite its role in integrin activation, Talin is a central element in the initial steps of focal complex formation. Talin has two integrin binding sites. The PTB site within the Talin head domain, which is crucial for integrin activation, and a lower affinity binding site in the Talin rod [147]. These two sites and a potential dimerisation site within the Talin rod mediate initial integrin clustering. In addition to its integrin binding ability Talin has three actin and vinculin binding sites in its rod domain [148]. Vinculin binding to Talin and its recruitment to focal complexes is dependent on its activation by PIP_2 . Local production of PIP_2 is accomplished by Talin mediated recruitment of $\text{PIP}K1\gamma$ [149]. Therefore the proper recruitment of these proteins can be seen as minimal requirement for the formation of focal complexes, the linkage to the actin cytoskeleton and their maturation into FAs.

In addition to these proteins a multitude of different signalling and structural proteins are recruited to focal adhesions that regulate cell adhesion, migration but also proliferation and apoptosis [38]. The multitude of signalling events concentrated at FAs is maybe best described by the fact that staining with anti-phospho tyrosine antibodies nicely stains FAs. In addition to Talin, more than 20 proteins are able to bind the cytoplasmic domain of integrins and thus are part of focal contacts. The vast majority of these proteins interact with different β integrin cytoplasmic tails rather than with the even shorter cytoplasmic tails of α integrin subunits. The diverse list of proteins includes actin-binding proteins, enzymes, adaptor proteins, transcriptional co-activators and others of unknown function [150]. Due to the short length of the cytoplasmic tail the *in vivo* relevance and co-occurrence of these interactions

Introduction

has to be addressed in future studies as not all of these proteins can bind one cytoplasmic tail simultaneously.

Kindlin function in mammalian cells

In comparison to integrins, relatively little is known about the role of Kindlin proteins in mammalian cells. Kindlins were shown to be differentially expressed in lung and colon carcinomas. Kindlin-1 was identified to be overexpressed in colon and lung cancers, while Kindlin-2 was overexpressed in breast cancer [2]. Kindlin-3 is overexpressed in B-cell malignancies [151]. The functional consequences of this deregulated Kindlin expression remain to be elucidated. In addition to these data, mutations in the FERMT1 (C20ORF42, KIND1) gene, encoding for Kindlin-1, uncovered the genetic cause for Kindler Syndrome [152,153], a very rare skin blistering disease.

Kindler Syndrome

The Kindler Syndrome was first described by Theresia Kindler (1890-1975) in 1954 [154]. She described a 14 year old girl showing a combination of epidermolysis bullosa hereditaria and poikiloderma congenitale [155].

The clinical overlap with dystrophic epidermolysis bullosa [70] and hereditary acrokeratotic poikiloderma (Weary Syndrome) [156] makes the diagnosis of Kindler Syndrome still difficult [157]. This could explain the very low number (slightly above 100) of cases reported up to now worldwide.



Figure 14: Characteristic clinical presentation of Kindler Syndrome. This patient showed poikiloderma on the face, neck and hands and ulceration is present on the lower lip [158].

Introduction

The characteristic features of this disease are acral blistering in infancy and childhood, progressive poikiloderma, skin atrophy, photosensitivity [159] and periodontal inflammation [160] (see figure 14). Furthermore, a predisposition to squamous cell carcinomas, already at very young age, has also been reported [159]. Besides the predisposition to squamous cell carcinomas and a potential secondary infection Kindler Syndrome per se does not reduce the life expectancy of patients.

If present, blister formation occurs close or at the dermal/epidermal junction, separated by the BM (seen figure 15). In contrast to dystrophic epidermolysis bullosa, Kindler Syndrome shows multiple planes of split within the basal keratinocytes and/or in the lamina lucida, as well as extensive reduplication of the lamina densa [161,162,163]. In addition, skin biopsies frequently show hyperkeratosis, epidermal atrophy, hyper- and hypo-pigmentation and telangiectasiae [164]. The clinical course heavily depends on the age of the patient. A large heterogeneity in the appearance and also disappearance of symptoms is characteristic for this disease.

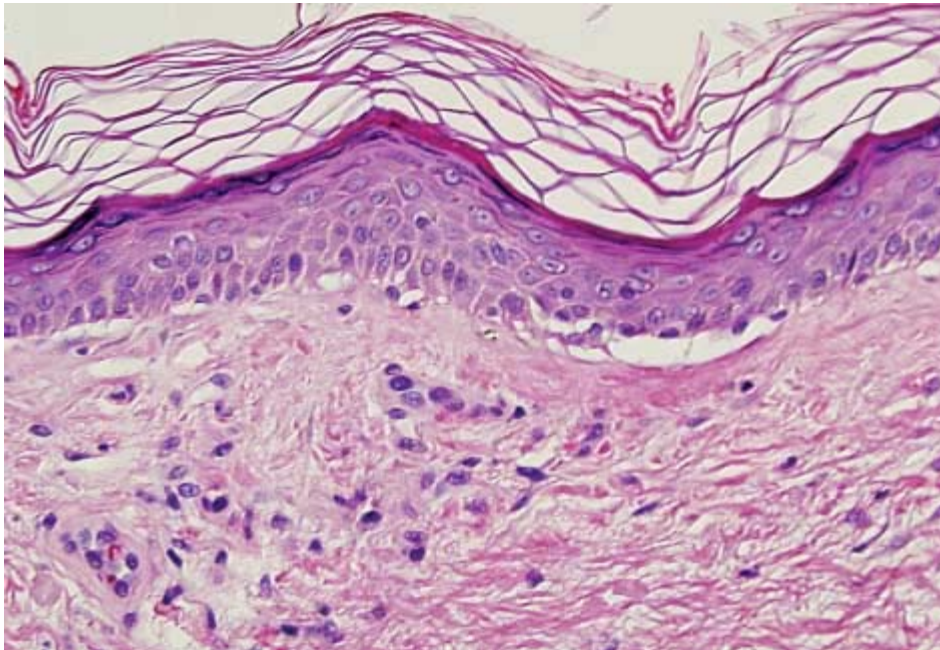


Figure 15: H&E staining of a sun exposed skin biopsy taken from a seven year old Kindler Syndrome patient. The picture shows vacuolar alteration of the basal keratinocytes and early cleft formation. In addition, sparse lymphocytic dermal infiltrate can be observed. [165].

Initially mutations or abnormal deposition of the extracellular matrix component collagen VII have been hypothesised as cause of Kindler Syndrome [166] but could be excluded by linkage and mutation studies [161,167]. Alternatively, it has been proposed that Kindler Syndrome is primarily an apoptotic skin disorder [168], which could not be confirmed in more recent reports [169].

Finally, the identification of mutations in the human FERMT1 gene coding for Kindlin-1 as cause of Kindler Syndrome, advanced the understanding and diagnostics of this disease

Introduction

[152,153]. Using DNA sequencing and specific antibodies raised against the C-terminus of human Kindlin-1 it is now possible to diagnose Kindler Syndrome. Currently more than 30 mutations in the FERMT1 gene have been identified. Interestingly, however, it was not possible to correlate the severity of this disease or the occurrence of specific symptoms with a specific mutations in the Kindlin-1 gene [160]. Very recently, three cases revealed a correlation between N-terminal mutations in Kindlin-1 and the appearance of UC [170,171,172], indicating that Kindlin-1 could have an important role in other epithelia, too. The identification of Kindlin-1 as part of the integrin actin connection allowed the conclusion that Kindler Syndrome is the first skin blistering disease caused by detachment of the actin cytoskeleton from the basal cell membrane. Nevertheless, it is unknown to which extend the perturbed actin linkage contributes to the symptoms of Kindler Syndrome. Certainly, the loss of this mechanical linkage can explain the skin blistering observed, but it already fails to explain why the patients loose this feature when they become older. In addition, many other prominent features like the poikiloderma cannot be explained by an altered actin linkage, suggesting additional functions of Kindlin-1 in keratinocytes and maybe also melanocytes.

Kindlins in integrin signalling

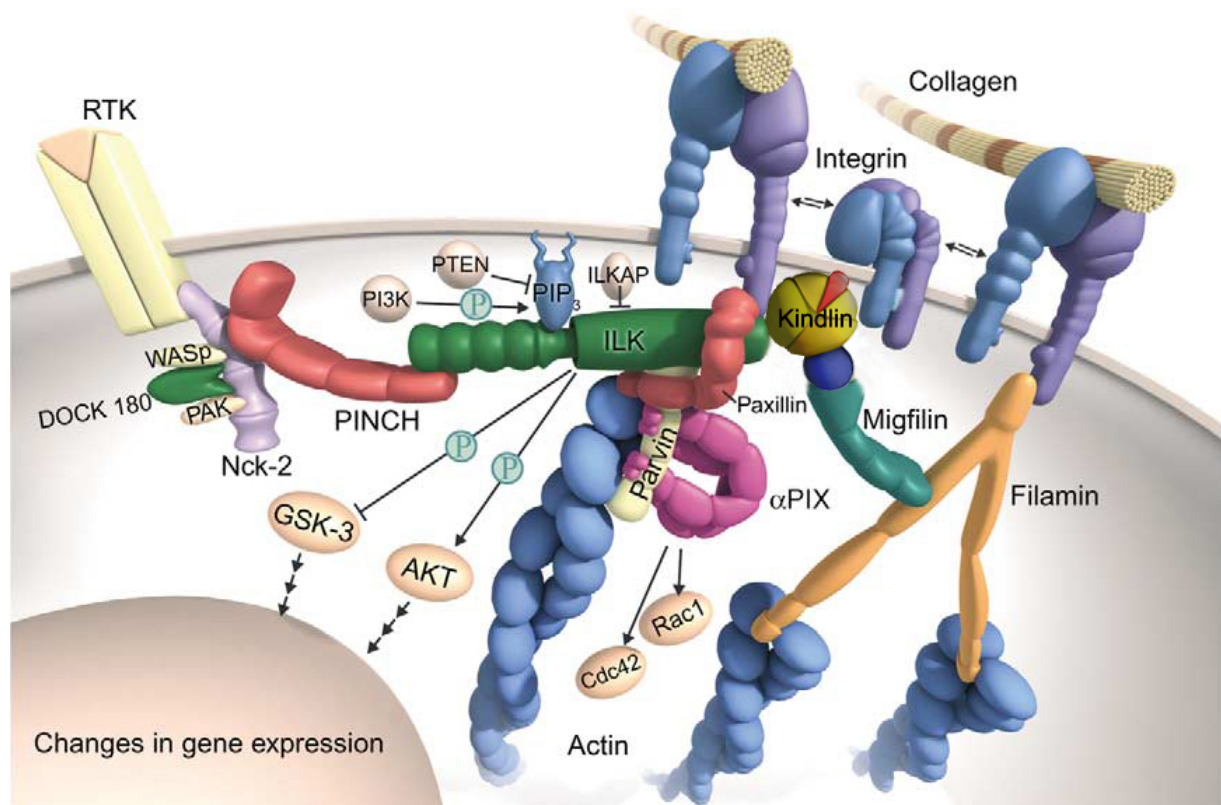


Figure 16: Kindlin interaction partners. Kindlin-1 has been shown to interact with $\beta 1$ and $\beta 3$ integrin cytoplasmic tails. Kindlin-2 interacts with ILK and Migfilin. Migfilin in addition interacts with Filamins, providing a linkage to the actin cytoskeleton. Kindlin and actin interaction via ILK is mediated via binding of ILK to parvins. (modified from [30])

Introduction

The first member of the Kindlin family that was functionally characterised was Kindlin-2. Tu and co-workers showed that Kindlin-2 localises to FAs, where it binds a LIM domain-containing adaptor protein, called Migfilin [173] (see figure 16). This is of special interest as Migfilin was shown to interact with Filamin A and B, which in turn are important in the assembly of the actin cytoskeleton [174,175]. Thereby the Kindlin-2/Migfilin/Filamin complex provides a novel link from the integrins to the actin cytoskeleton. Similar like UNC-112, Kindlin-2 has been suggested to bind ILK, which provides an additional link via Paxillin and/or Parvin to the actin cytoskeleton [30,122]. RNAi-mediated depletion of Kindlin-2 in HeLa and C2C12 cells resulted in impaired cell spreading and an altered organisation of the actin cytoskeleton. Unlike in *C. elegans*, these cells were still able to cluster integrins into FA and to recruit FA components like paxillin [173]. More recently it has been reported that Kindlin-2 can interact via its PTB domain in the F3 subdomain of the FERM domain with the cytoplasmic tails of $\beta 1$ and $\beta 3$ integrins. The exact interaction site within the β integrin was not determined. However, the authors excluded that Kindlin-2 binds to the same site as Talin, which contains a highly homologous FERM domain [44]. Furthermore *Shi et al.* could show that overexpression of EGFP-Kindlin-2 but not of a mutant form, unable to bind to β integrin cytoplasmic tails, leads to an increased activation of $\beta 3$ integrins. In addition, overexpression of Kindlin-2 leads to increased cytoskeletal strengthening and a higher number of FAs [44]. In line with these observations, Kindlin-1 has been shown to interact with the cytoplasmic tails of $\beta 1$ and $\beta 3$ integrins too [43]. Interestingly, it was shown to bind the same NPXY motif within $\beta 1$ and $\beta 3$ integrin cytoplasmic tails as Talin does. Despite the identical binding sites overexpression of Kindlin-1 did not increase activation of $\beta 3$ integrin [176]. Thus, there are conflicting findings in the literature regarding the mode of action of Kindlin-1 and Kindlin-2. This reflects either differences between these two proteins or different experimental handlings. Nevertheless, depletion of Kindlin-1 using RNAi impairs cell spreading of keratinocytes [43,176]. Furthermore, Kindlin-1 but not Kindlin-2 is transcriptionally upregulated upon TGF- β treatment and translocates from FAs to so called “membrane ruffles” [43].

Thus Kindlin-1 and Kindlin-2, although they share a common protein structure and are both components of cell matrix adhesions, seem to fulfil non redundant functions within FAs and to function in different cellular compartments when released from FAs. This notion is further supported by a recent report that described a nuclear localisation of Kindlin-2 in normal and neoplastic smooth muscle cells of the myometrium [177]. Although a potential function of Kindlin-2 within the nucleus is purely speculative, the Kindlin-2 binding partner Migfilin has also been shown to translocate to the nucleus and to function as a transcriptional co-activator with CSX/NKX2-5 in cardiac differentiation [178]. This suggests that Kindlin-2 together with Migfilin might act as a co-regulator of transcription. The important role of

Introduction

Kindlin-2 has been further highlighted by a mouse line harbouring a gene trap insertion in the Kindlin-2 gene. Homozygous mice for this insertion were reported to die before E 7.5 [179]. Very little is known about the function of Kindlin-3. One report showed that overexpression of Kindlin-3 suppresses NF- κ B activity via inhibition of nuclear translocation, which in turn leads to apoptosis [180]. Conversely, depleting Kindlin-3 using RNAi activates the NF- κ B pathway and attenuates TNF- α induced apoptosis [180].

Paper Summaries

The Kindlins: subcellular localization and expression during murine development.

Ussar S, Wang HV, Linder S, Fässler R, Moser M

In this publication we show the murine expression pattern and subcellular localisation of all three Kindlin proteins. We show that Kindlin-1 is predominantly expressed in epithelia of different organs with highest expression in the intestinal epithelium. Kindlin-3 has a very restricted expression pattern and is exclusively found in the haematopoietic system. During embryonic development Kindlin-3 mRNA and protein was predominantly detected in the foetal liver, where the haematopoietic stem cells, B-cells and megakaryocytes, from which platelets arise, reside. In contrast to Kindlin-1 and -3, Kindlin-2 was widely expressed, already from the earliest embryonic stage (E7.5) investigated on, with highest expression in skeletal and smooth muscle. Using EGFP-tagged cDNA constructs we could show that Kindlin-1 and Kindlin-2 localize to cell-matrix adhesions, while Kindlin-3 is unable to do so in non-haematopoietic cells. Kindlin-3 localises to specialized matrix adhesion sites, called podosomes, in cells like macrophages or dendritic cells. Additionally we could show that Kindlin-2 translocates to cell-cell contacts upon differentiation of keratinocytes.

Taken together we could show that (i) Kindlins are expressed already from very early embryonic development on, (ii) there is expression of at least one Kindlin in every cell type, while epithelia express both Kindlin-1 and Kindlin-2 and (iii) Kindlins are part of integrin containing cell-matrix adhesion sites and in case of Kindlin-2 additionally of cell-cell contacts.

Kindlin-2 controls bidirectional signalling of integrins

Montanez E*, Ussar S*, Schifferer M, Bosl M, Zent R, Moser M, Fässler R

*** equal contribution**

This publication identifies Kindlin-2 as an important regulator of integrin function. Mice deficient for Kindlin-2 die at the peri-implantation stage at around E5.5-6.5. ES cells, derived from these mice show severe adhesion defects and a lack of integrin activation in comparison to wild-type ES cells, expressing Kindlin-2 but no other Kindlin. We show that Kindlin-2 directly interacts with the membrane distal NXXY motif in $\beta 1$ and $\beta 3$ integrins via its PTB domain. In addition we can show that Kindlin-2 acts synergistically with Talin on integrin activation as overexpression of Kindlin-2 and Talin significantly increases integrin activation in comparison to Talin overexpression alone. To understand the embryonic lethality of Kindlin-2 deficient mice we used EBs. EBs deficient for Kindlin-2 showed (i) severe adhesion defects of the outermost cell layer (endoderm) and the epiblast to the underlying abnormally appearing BM, (ii) a delay in cavitation and (iii) an increased unorganized apoptosis. Isolated endoderm cells from Kindlin-2 deficient EBs showed an inability of adhere and spread, while treatment of these cells with Mn^{2+} , that forces integrins in an active conformation uncoupled from intracellular signals, restored the ability of the cells to adhere. However Kindlin-2 deficient Mn^{2+} treated cells were still unable to spread due to an inability to recruit necessary proteins like ILK and thus to form mature FAs. These data showed that despite the function of Kindlin-2 in integrin activation, it is a crucial regulator of signal transduction upon ligand binding of integrins (outside-in signalling).

In summary we show that Kindlin-2 is an important element of both integrin inside-out and outside-in signalling and that deficiency of Kindlin-2 results in very early embryonic lethality.

Integrin-linked kinase: integrin's mysterious partner

Grashoff C, Thievessen I, Lorenz K, **Ussar S**, and Fässler R

Here we review the functional properties of Integrin Linked Kinase (ILK). The review addresses the cell biological properties and the function of ILK *in vivo*. ILK is recruited to integrin adhesion as a ternary complex together with PINCH and parvin family members through other interaction partners like paxillin and Kindlins.

ILK has two proposed functions. First, it is a central binding platform to regulate the actin cytoskeleton. This is evidenced by defective cell spreading, FA formation, cell adhesion and ECM assembly, upon loss of ILK. Second, ILK has been shown to regulate cell proliferation which has been proposed to rely on its putative serine/ threonine kinase activity to phosphorylate GSK3 β and PKB/Akt.

ILK deficiency causes embryonic lethality in *C. elegans* and peri-implantation lethality in mice, but none of the observed phenotypes could be attributed to its kinase activity. Additionally conditional ILK deletion in chondrocytes also did not result in altered GSK3 β or PKB/Akt phosphorylation.

Taken together, ILK is an important regulator of actin organisation during development and in adult tissue, its kinase activity, however, remains controversial.

Kindlin-3 is essential for integrin activation and platelet aggregation.

Moser M, Nieswandt B, **Ussar S**, Pozgajova M, Fässler R

This publication identifies Kindlin-3 as an important regulator of platelet function. We demonstrate that Kindlin-3 deficient mice develop bleedings already during embryonic development which causes lethality early after birth. Analysis of platelets derived from Kindlin-3 deficient foetal liver chimeras show an inability of these platelets to activate $\alpha\text{IIb}\beta\text{3}$ integrin, therefore fail to bind fibrinogen, causing an inability to form thrombi. We show that Kindlin-3 directly interacts with the membrane distal NXXY and a TT motif of β1 and β3 integrins via its PTB domain. Using a macrophage cell line we could demonstrate that overexpression of Kindlin-3 increases the ability of these cells to bind an RGD motif containing fibronectin fragment, due to an increase in active integrins. This increased integrin activity, however, was dependent on the ability of Kindlin-3 to interact with the β integrin subunit, as a mutant form, unable to bind integrins, did not lead to increased fibronectin binding. In addition we could demonstrate that Kindlin-3 does not solely play a role in integrin activation (inside-out signalling) but also in signal transduction upon integrin ligand interaction (outside-in signalling). Therefore integrins on Kindlin-3 deficient platelets were activated using Mn^{2+} and allowed to adhere and spread on fibrinogen. Kindlin-3 deficient platelets were able to adhere to fibrinogen upon Mn^{2+} treatment, but did not spread and form lamellipodia, indicating that Kindlin-3 has an additional role in outside-in signalling.

In summary we conclude, that Kindlin-3 is an important regulator of integrin affinity in haematopoietic cells, especially platelets.

SILAC-mouse for quantitative proteomics uncovers Kindlin-3 as an essential factor for red blood cell function

Kruger M*, Moser M*, **Ussar S**, Thievensen I, Lubber C, A, Forner F, Schmidt S, Zanivan S, Fässler R, Mann M

*equal contribution

This publication describes the establishment of stable isotope labelling by amino acids in cell culture (SILAC) applied to whole mice. Using a special diet, in which normal $^{12}\text{C}_6$ -lysine (light) was replaced with $^{13}\text{C}_6$ -lysine (heavy), we were able to breed mice that were completely labelled with the heavy amino acid. This allowed the quantitative analysis of whole proteomes by mass-spectrometry. Labelling of mice with this diet had no effect on weight, fertility or litter size. Combination of this method with mouse genetics enabled us to show that platelets deficient for $\beta 1$ integrin had comparable proteomes with the exception of $\beta 1$ and its dimerisation partners, $\alpha 2$ and $\alpha 6$ integrin. In a second approach we analyzed β -parvin deficient hearts and could show that β -parvin deficiency is compensated by upregulation of α -parvin. Analysis of Kindlin-3 deficient erythrocytes revealed a severe anaemia, caused by structural alterations of erythrocytes. SILAC labelling of mice was applied to discover that Kindlin-3 deficient erythrocytes had an almost complete absence of ankyrin-1, band 4.1, adducin-2, and dematin in their membrane fractions, while other membrane skeleton proteins like α/β spectrin and band-3 were not changed.

In summary we could show that mice can be completely labelled with $^{13}\text{C}_6$ -lysine allowing a quantitative proteome comparison. This method was used to show that Kindlin-3 deficiency in erythrocytes affects their shape and contributes to their severe anaemia.

Leukocyte Adhesion Deficiency-III (LAD-III) is caused by mutations in the adhesion protein Kindlin-3, * equal contribution

Svensson L*, Howarth K*, McDowall A, Patzak I, Evans R, **Ussar S**, Metin A, Fried M, Tomlinson I, Hogg N
*equal contribution

Here we describe that mutations in the human Kindlin-3 cause LAD-III. Previously mutations in the Rap1-GEF, CalDAG-GEF1, have been described to cause LAD-III. Indeed, homozygosity mapping of two Turkish patients revealed a previously described C/A base exchange in the *CalDAG-GEF1* gene (chr11:64.25-64.27Mb) but no mutation could be found in a Maltese patient. The CalDAG-GEF1 mutation was previously described to alter splicing of exon 15 to exon 16. Interestingly, real time PCR did not reveal any statistically significant changes in CalDAG-GEF1 expression. Furthermore, expression of wild type CalDAG-GEF1 could not rescue the adhesion and migration defects of EBV transformed B-cells derived from those patients on ICAM-1 and fibronectin.

The FERMT3 (Kindlin-3) gene is located in close proximity (chr11:63.73-63.76Mb) to the *CalDAG-GEF1* gene and the described phenotype of LAD-III patients shows high similarities to Kindlin-3^{-/-} mice. Therefore the FERMT3 gene was sequenced and an R509X stop mutation in the two Turkish patients and an A>G change at the splice acceptor site of exon 14 in the Maltese patient were found. In addition to the altered amino-acid sequence, these mutations diminished mRNA stability.

Unlike the rescue experiments with wild type CalDAG-GEF1, expression of wild type Kindlin-3 fully rescued the adhesion and migration defects of EBV transformed B-cells from those patients.

In summary we could show that mutations in the human Kindlin-3 gene result in a severe leukocyte adhesion deficiency syndrome due to an inability of $\beta 1$, $\beta 3$ and also $\beta 2$ integrins to become activated and bind their ligands.

Loss of Kindlin-1 causes skin atrophy and early postnatal ulcerative colitis

Ussar S, Moser M, Widmaier M, Rognoni E, Harrer C, Genzel-Boroviczeny O, Fässler R

Here we show that loss of Kindlin-1, known to be mutated in the human skin blistering disease Kindler Syndrome, in mice leads to some skin features of Kindler Syndrome, but predominantly to a lethal early postnatal UC. Analysis of the neonatal skin revealed a severe epidermal atrophy due to an almost abolished proliferation of basal keratinocytes. The reduction in the proliferation was progressive as at birth proliferation rates were normal but declined during the following days. No epidermolysis could be observed even after application of mild stress. Interestingly, however, keratinocytes isolated from these mice showed adhesion and spreading defects. This suggests that either the composition of the BM or the lower turnover of adhesion structures prevents epidermolysis *in vivo*.

Using a detailed histological and immunochemical analysis of the murine intestine we could identify the colostrum to cause epithelial rupture and subsequently, upon loss of the intestinal barrier, a severe inflammation that shows all signs of an UC in men. Importantly, a previous publication reported a neonatal case of Kindler Syndrome that developed an UC prior to the development of skin symptoms. This finding allowed us to conclude that the murine phenotype indeed reflects the human presentation of a complete loss of Kindlin-1. Furthermore, we could identify impaired integrin activation to cause the shear induced epithelial detachment. We could show that direct Kindlin-1 and β integrin interaction is important for Talin mediated integrin activation. We provide evidence that Kindlin-1 interacts via its PTB domain with the membrane distal NXXY motif of $\beta 1$ and $\beta 3$ integrins. We demonstrate that Talin, previously believed to be solely sufficient to promote integrin activation, needs at least one Kindlin protein to activate integrins. Interestingly Kindlin-1 and Kindlin-2 could compensate for this function in integrin activation *in vitro* but not *in vivo* due to a sequestration of Kindlin-2 to cell-cell contacts in epithelia of the skin and intestine.

In summary, we could identify null mutations in the FERMT1 gene as the cause for a severe neonatal UC in mice and man that is triggered by defective integrin activation in the intestinal epithelium.

Colocalization of kindlin-1, kindlin-2 and migfilin at keratinocyte focal contacts and relevance to the pathophysiology of Kindler syndrome

Lai-Cheong JE, **Ussar S**, Arita K, Hart IR, McGrath JA

In this publication we show that Kindlin-1 co-localises and complexes with Kindlin-2 and Migfilin at focal contact sites of human keratinocytes. Depletion of Kindlin-1 using RNAi did not result in altered levels or in a mislocalisation of Kindlin-2 or Migfilin. Skin biopsies taken from different Kindler Syndrome patients, however, revealed that several cases showed reduced immunolabeling of Kindlin-2 and Migfilin that seemed to correlate with the level of reduction of Kindlin-1 labelling. Interestingly not all Kindler Syndrome patients showed an absence of Kindlin-1 staining, although confirmed mutations in the FERMT1 gene. This is of special interest as immunostaining for Kindlin-1 is used as a diagnostic marker for Kindler Syndrome. Our data, however suggest that not all Kindler Syndrome patients necessarily need to have reduced staining intensity and that gene sequencing should be applied to exclude or confirm the diagnosis of Kindler Syndrome. Furthermore we could identify and describe the first potential Kindlin-1 interaction partners. To test whether these interactions are direct and which function these interactions fulfil will be interesting tasks.

Taken together we could identify Kindler Syndrome patients that show normal Kindlin-1 protein expression or despite a reduction in Kindlin-1 immunoreactivity also a reduction in Kindlin-2 and Migfilin.

Expression of truncated kindlin-1 leads to abnormal adhesion and migration of keratinocytes

Has C, Ludwig RJ, Herz C, Kern JS, **Ussar S**, Ochsendorf FR, Kaufmann R, Schumann H, Kohlhase J, Bruckner-Tuderman L

This case report describes a 27 year old Kindler Syndrome patient that showed a homozygous splice site mutation at the first position of intron 13 c.1718+1G>A. The patient presented a severe form of Kindler Syndrome with skin blistering, skin atrophy, poikiloderma and fragility of the oral mucosa, diarrhoea and anal bleeding. Protein and mRNA analysis revealed that both protein and mRNA were present. The described mutation however resulted in a truncated Kindlin-1 protein, lacking the terminal part of the FERM domain, essential for Kindlin and β integrin interaction. Atrophic skin areas showed a reduction of proliferating keratinocytes. *In vitro* analysis of keratinocytes derived from the patient revealed, in line with previous reports from other Kindler Syndrome patient derived keratinocytes, deficits in proliferation and adhesion to fibronectin and laminin-332. In addition altered cell morphology and deficits in an *in vitro* wound closure assay could be observed. Taken together we could add an additional mutation affecting splicing of exon 13 to the known list of 31 mutations within the FERMT1 gene that results in all classical symptoms of Kindler Syndrome.

Acknowledgements

I would like to express my sincere gratitude to the people that helped me during the time of my thesis.

First I would like to thank my mentor Prof. Reinhard Fässler, as his door was always open when I needed support and discussion but he also gave me the freedom to develop my own ideas and concepts. This experience will certainly be an essential part for my further career in science.

I would like to thank, PD Dr. Klaus-Peter Janssen, with whom I had very fruitful discussions and who agreed to be the second referee of my thesis and Prof. Dr. Christian Wahl, Prof. Dr. Martin Biel, Prof. Dr. Karl-Peter Hopfner and Prof. Dr. Angelika Vollmar, the members of my thesis committee for taking the time to review my work.

I also had the pleasure to have very nice and productive collaborations with Prof. Ralf Paus, Prof. Roy Zent, Prof. John McGrath and Dr. Joey Lai-Cheong, Dr. Marcus Krüger, Prof. Lena Bruckner-Tuderman, and Prof. Nancy Hogg and the members of their labs.

I am very happy that I could share my time in the lab with a number of outstanding scientists and very good friends. Among those I would like to especially say thanks to Anika, Hao-Wen, Martina, Sara, Claudia and Ralf with whom I had great discussions and a lot of fun in- and outside of the lab.

I also would like to thank Dr. Markus Moser for his help very nice discussions and Dr. Walther Göhring who provided the “infrastructure” of my thesis.

My thesis certainly would not have been possible without these persons.

However I would never have come that far without the incredible effort and big trust of my parents that always supported me in my dreams and gave and give me the feeling of being able to reach the stars. Although the stars might be still far away, my loved wife Julia brings light to my life. She makes my get up in the morning, but also come home at night. I could not imagine a life without her.

Curriculum Vitae

SIEGFRIED USSAR

Personal details

Date and place of birth 24.12.1979 in Graz, Austria

Nationality Austrian

Private address Baaderstr. 55, 80469 Munich, Germany,

E-mail ussar@biochem.mpg.de

Education

2004 – 2008 **Max Planck Institute of Biochemistry**, Martinsried, Germany
PhD thesis
Mentor: Dr. Reinhard Fässler
Project: Genetic analyses of Kindlins in mice

2003-2004 **Boehringer Ingelheim Austria**, Vienna, Austria
Master thesis
Mentor: Dr. Tilman Voss
Project: Roles of MEK1 and MEK2 in cell proliferation

1999-2003 **University of Vienna**, Vienna, Austria
Graduate studies (MSc) of Genetics

Publications

1. Svensson L*, Howarth K*, McDowall A, Patzak I, Evans R, **Ussar S**, Metin A, Fried M, Tomlinson I, Hogg N, (submitted) Leukocyte Adhesion Deficiency-III (LAD-III) is caused by mutations in the adhesion protein Kindlin-3, * equal contribution
2. **Ussar S**, Moser M, Widmaier M, Rognoni E, Harrer C, Genzel-Boroviczeny O, Fässler R (submitted) Loss of Kindlin-1 causes skin atrophy and lethal neonatal ulcerative colitis.
3. Krüger M*, Moser M*, **Ussar S**, Thievensen I, Luber CA, Forner F, Schmidt S, Zanivan S, Fassler R, Mann M (2008) SILAC mouse for quantitative proteomics uncovers kindlin-3 as an essential factor for red blood cell function. *Cell* 134: 353-364. * equal contribution
4. Has C, Ludwig RJ, Herz C, Kern JS, **Ussar S**, Ochsendorf FR, Kaufmann R, Schumann H, Kohlhase J, Bruckner-Tuderman L (2008) C-terminally truncated kindlin-1 leads to abnormal adhesion and migration of keratinocytes. *Br J Dermatol*.
5. Lai-Cheong JE, **Ussar S**, Arita K, Hart IR, McGrath JA (2008) Colocalization of kindlin-1, kindlin-2, and migfilin at keratinocyte focal adhesion and relevance to the pathophysiology of Kindler syndrome. *J Invest Dermatol* 128: 2156-2165.
6. Montanez E*, **Ussar S***, Schifferer M, Bosl M, Zent R, Moser M, Fässler R (2008) Kindlin-2 controls bidirectional signaling of integrins. *Genes Dev* 22: 1325-1330. * **equal contribution**
7. Moser M, Nieswandt B, **Ussar S**, Pozgajova M, Fässler R (2008) Kindlin-3 is essential for integrin activation and platelet aggregation. *Nat Med* 14: 325-330.
8. **Ussar S**, Wang HV, Linder S, Fässler R, Moser M (2006) The Kindlins: subcellular localization and expression during murine development. *Exp Cell Res* 312: 3142-3151.
9. Grashoff C, Thievensen I, Lorenz K, **Ussar S**, and Fässler R (2004) Integrin-linked kinase: integrin's mysterious partner. *Current opinion in cell biology* 16(5), 565-571
10. **Ussar S**, and Voss T, MEK1 and MEK2, different regulators of the G1/S transition., (2004) *The Journal of biological chemistry* 279(42), 43861-43869

References

1. Wick M, Burger C, Brusselbach S, Lucibello FC, Muller R (1994) Identification of serum-inducible genes: different patterns of gene regulation during G0-->S and G1-->S progression. *J Cell Sci* 107 (Pt 1): 227-239.
2. Weinstein EJ, Bourner M, Head R, Zakeri H, Bauer C, et al. (2003) URP1: a member of a novel family of PH and FERM domain-containing membrane-associated proteins is significantly over-expressed in lung and colon carcinomas. *Biochim Biophys Acta* 1637: 207-216.
3. Chishti AH, Kim AC, Marfatia SM, Lutchman M, Hanspal M, et al. (1998) The FERM domain: a unique module involved in the linkage of cytoplasmic proteins to the membrane. *Trends Biochem Sci* 23: 281-282.
4. Rees DJ, Ades SE, Singer SJ, Hynes RO (1990) Sequence and domain structure of talin. *Nature* 347: 685-689.
5. Leto TL, Marchesi VT (1984) A structural model of human erythrocyte protein 4.1. *J Biol Chem* 259: 4603-4608.
6. Arpin M, Algrain M, Louvard D (1994) Membrane-actin microfilament connections: an increasing diversity of players related to band 4.1. *Curr Opin Cell Biol* 6: 136-141.
7. Bretscher A, Reczek D, Berryman M (1997) Ezrin: a protein requiring conformational activation to link microfilaments to the plasma membrane in the assembly of cell surface structures. *J Cell Sci* 110 (Pt 24): 3011-3018.
8. Serrador JM, Alonso-Lebrero JL, del Pozo MA, Furthmayr H, Schwartz-Albiez R, et al. (1997) Moesin interacts with the cytoplasmic region of intercellular adhesion molecule-3 and is redistributed to the uropod of T lymphocytes during cell polarization. *J Cell Biol* 138: 1409-1423.
9. Tsukita S, Oishi K, Sato N, Sagara J, Kawai A, et al. (1994) ERM family members as molecular linkers between the cell surface glycoprotein CD44 and actin-based cytoskeletons. *J Cell Biol* 126: 391-401.
10. Tsukita S, Yonemura S (1997) ERM (ezrin/radixin/moesin) family: from cytoskeleton to signal transduction. *Curr Opin Cell Biol* 9: 70-75.
11. Yonemura S, Hirao M, Doi Y, Takahashi N, Kondo T, et al. (1998) Ezrin/radixin/moesin (ERM) proteins bind to a positively charged amino acid cluster in the juxta-membrane cytoplasmic domain of CD44, CD43, and ICAM-2. *J Cell Biol* 140: 885-895.
12. Hamada K, Shimizu T, Matsui T, Tsukita S, Hakoshima T (2000) Structural basis of the membrane-targeting and unmasking mechanisms of the radixin FERM domain. *Embo J* 19: 4449-4462.
13. Hamada K, Shimizu T, Yonemura S, Tsukita S, Tsukita S, et al. (2003) Structural basis of adhesion-molecule recognition by ERM proteins revealed by the crystal structure of the radixin-ICAM-2 complex. *Embo J* 22: 502-514.
14. Schlessinger J, Lemmon MA (2003) SH2 and PTB domains in tyrosine kinase signaling. *Sci STKE* 2003: RE12.
15. DiNitto JP, Lambright DG (2006) Membrane and juxtamembrane targeting by PH and PTB domains. *Biochim Biophys Acta* 1761: 850-867.
16. Blaikie P, Immanuel D, Wu J, Li N, Yajnik V, et al. (1994) A region in Shc distinct from the SH2 domain can bind tyrosine-phosphorylated growth factor receptors. *J Biol Chem* 269: 32031-32034.
17. Garcia-Alvarez B, de Pereda JM, Calderwood DA, Ulmer TS, Critchley D, et al. (2003) Structural determinants of integrin recognition by talin. *Mol Cell* 11: 49-58.
18. Chang DD, Hoang BQ, Liu J, Springer TA (2002) Molecular basis for interaction between Icap1 alpha PTB domain and beta 1 integrin. *J Biol Chem* 277: 8140-8145.
19. Lemmon MA (2004) Pleckstrin homology domains: not just for phosphoinositides. *Biochem Soc Trans* 32: 707-711.
20. Lemmon MA, Ferguson KM (2001) Molecular determinants in pleckstrin homology domains that allow specific recognition of phosphoinositides. *Biochem Soc Trans* 29: 377-384.

References

21. Lemmon MA, Ferguson KM (2000) Signal-dependent membrane targeting by pleckstrin homology (PH) domains. *Biochem J* 350 Pt 1: 1-18.
22. Lemmon MA (2005) Pleckstrin homology domains: two halves make a hole? *Cell* 120: 574-576.
23. Vanhaesebroeck B, Leever SJ, Ahmadi K, Timms J, Katso R, et al. (2001) Synthesis and function of 3-phosphorylated inositol lipids. *Annu Rev Biochem* 70: 535-602.
24. Bejsovec A, Eide D, Anderson P (1984) Genetic techniques for analysis of nematode muscle. *Molecular Biology of the Cytoskeleton*: 267-273.
25. Schaller MD (2000) UNC112. A new regulator of cell-extracellular matrix adhesions? *J Cell Biol* 150: F9-F11.
26. Cox EA, Hardin J (2004) Sticky worms: adhesion complexes in *C. elegans*. *J Cell Sci* 117: 1885-1897.
27. Rogalski TM, Gilbert MM, Devenport D, Norman KR, Moerman DG (2003) DIM-1, a novel immunoglobulin superfamily protein in *Caenorhabditis elegans*, is necessary for maintaining bodywall muscle integrity. *Genetics* 163: 905-915.
28. Williams BD, Waterston RH (1994) Genes critical for muscle development and function in *Caenorhabditis elegans* identified through lethal mutations. *J Cell Biol* 124: 475-490.
29. Rogalski TM, Mullen GP, Gilbert MM, Williams BD, Moerman DG (2000) The UNC-112 gene in *Caenorhabditis elegans* encodes a novel component of cell-matrix adhesion structures required for integrin localization in the muscle cell membrane. *J Cell Biol* 150: 253-264.
30. Grashoff C, Thievensen I, Lorenz K, Ussar S, Fassler R (2004) Integrin-linked kinase: integrin's mysterious partner. *Curr Opin Cell Biol* 16: 565-571.
31. Legate KR, Montanez E, Kudlacek O, Fassler R (2006) ILK, PINCH and parvin: the tIPP of integrin signalling. *Nat Rev Mol Cell Biol* 7: 20-31.
32. Mackinnon AC, Qadota H, Norman KR, Moerman DG, Williams BD (2002) *C. elegans* PAT-4/ILK functions as an adaptor protein within integrin adhesion complexes. *Curr Biol* 12: 787-797.
33. Lin X, Qadota H, Moerman DG, Williams BD (2003) *C. elegans* PAT-6/actopaxin plays a critical role in the assembly of integrin adhesion complexes in vivo. *Curr Biol* 13: 922-932.
34. Xu X, Rongali SC, Miles JP, Lee KD, Lee M (2006) pat-4/ILK and unc-112/Mig-2 are required for gonad function in *Caenorhabditis elegans*. *Exp Cell Res* 312: 1475-1483.
35. Hikita T, Qadota H, Tsuboi D, Taya S, Moerman DG, et al. (2005) Identification of a novel Cdc42 GEF that is localized to the PAT-3-mediated adhesive structure. *Biochem Biophys Res Commun* 335: 139-145.
36. Hynes RO (2002) Integrins: bidirectional, allosteric signaling machines. *Cell* 110: 673-687.
37. Hynes RO, Schwarzbauer JE, Tamkun JW (1987) Isolation and analysis of cDNA and genomic clones of fibronectin and its receptor. *Methods Enzymol* 144: 447-463.
38. Brakebusch C, Bouvard D, Stanchi F, Sakai T, Fassler R (2002) Integrins in invasive growth. *J Clin Invest* 109: 999-1006.
39. Baum PD, Garriga G (1997) Neuronal migrations and axon fasciculation are disrupted in *ina-1* integrin mutants. *Neuron* 19: 51-62.
40. Takada Y, Ye X, Simon S (2007) The integrins. *Genome Biol* 8: 215.
41. Plow EF, Haas TA, Zhang L, Loftus J, Smith JW (2000) Ligand binding to integrins. *J Biol Chem* 275: 21785-21788.
42. Bouvard D, Brakebusch C, Gustafsson E, Aszodi A, Bengtsson T, et al. (2001) Functional consequences of integrin gene mutations in mice. *Circ Res* 89: 211-223.
43. Kloeker S, Major MB, Calderwood DA, Ginsberg MH, Jones DA, et al. (2004) The Kindler syndrome protein is regulated by transforming growth factor-beta and involved in integrin-mediated adhesion. *J Biol Chem* 279: 6824-6833.
44. Shi X, Ma YQ, Tu Y, Chen K, Wu S, et al. (2007) The MIG-2/integrin interaction strengthens cell-matrix adhesion and modulates cell motility. *J Biol Chem* 282: 20455-20466.
45. Wang H, Dey SK (2006) Roadmap to embryo implantation: clues from mouse models. *Nat Rev Genet* 7: 185-199.
46. Carson DD, Bagchi I, Dey SK, Enders AC, Fazleabas AT, et al. (2000) Embryo implantation. *Dev Biol* 223: 217-237.
47. Li S, Edgar D, Fassler R, Wadsworth W, Yurchenco PD (2003) The role of laminin in embryonic cell polarization and tissue organization. *Dev Cell* 4: 613-624.

References

48. Montanez E, Piwko-Czuchra A, Bauer M, Li S, Yurchenco P, et al. (2007) Analysis of integrin functions in peri-implantation embryos, hematopoietic system, and skin. *Methods Enzymol* 426: 239-289.
49. Bronson RA, Fusi FM (1996) Integrins and human reproduction. *Mol Hum Reprod* 2: 153-168.
50. Sueoka K, Shiokawa S, Miyazaki T, Kuji N, Tanaka M, et al. (1997) Integrins and reproductive physiology: expression and modulation in fertilization, embryogenesis, and implantation. *Fertil Steril* 67: 799-811.
51. Aplin JD, Spanswick C, Behzad F, Kimber SJ, Vicovac L (1996) Integrins beta 5, beta 3 and alpha v are apically distributed in endometrial epithelium. *Mol Hum Reprod* 2: 527-534.
52. Campbell S, Swann HR, Seif MW, Kimber SJ, Aplin JD (1995) Cell adhesion molecules on the oocyte and preimplantation human embryo. *Hum Reprod* 10: 1571-1578.
53. Sutherland AE, Calarco PG, Damsky CH (1993) Developmental regulation of integrin expression at the time of implantation in the mouse embryo. *Development* 119: 1175-1186.
54. Illera MJ, Cullinan E, Gui Y, Yuan L, Beyler SA, et al. (2000) Blockade of the alpha(v)beta(3) integrin adversely affects implantation in the mouse. *Biol Reprod* 62: 1285-1290.
55. Nothias JY, Majumder S, Kaneko KJ, DePamphilis ML (1995) Regulation of gene expression at the beginning of mammalian development. *J Biol Chem* 270: 22077-22080.
56. Fassler R, Meyer M (1995) Consequences of lack of beta 1 integrin gene expression in mice. *Genes Dev* 9: 1896-1908.
57. Stephens LE, Sutherland AE, Klimanskaya IV, Andrieux A, Meneses J, et al. (1995) Deletion of beta 1 integrins in mice results in inner cell mass failure and peri-implantation lethality. *Genes Dev* 9: 1883-1895.
58. Aumailley M, Pesch M, Tunggal L, Gail F, Fassler R (2000) Altered synthesis of laminin 1 and absence of basement membrane component deposition in (beta)1 integrin-deficient embryoid bodies. *J Cell Sci* 113 Pt 2: 259-268.
59. Yurchenco PD, Quan Y, Colognato H, Mathus T, Harrison D, et al. (1997) The alpha chain of laminin-1 is independently secreted and drives secretion of its beta- and gamma-chain partners. *Proc Natl Acad Sci U S A* 94: 10189-10194.
60. Li S, Harrison D, Carbonetto S, Fassler R, Smyth N, et al. (2002) Matrix assembly, regulation, and survival functions of laminin and its receptors in embryonic stem cell differentiation. *J Cell Biol* 157: 1279-1290.
61. Hirsch E, Iglesias A, Potocnik AJ, Hartmann U, Fassler R (1996) Impaired migration but not differentiation of haematopoietic stem cells in the absence of beta1 integrins. *Nature* 380: 171-175.
62. Potocnik AJ, Brakebusch C, Fassler R (2000) Fetal and adult hematopoietic stem cells require beta1 integrin function for colonizing fetal liver, spleen, and bone marrow. *Immunity* 12: 653-663.
63. Blanpain C, Fuchs E (2006) Epidermal stem cells of the skin. *Annu Rev Cell Dev Biol* 22: 339-373.
64. Fuchs E (2008) Skin stem cells: rising to the surface. *J Cell Biol* 180: 273-284.
65. Raghavan S, Bauer C, Mundschaug G, Li Q, Fuchs E (2000) Conditional ablation of beta1 integrin in skin. Severe defects in epidermal proliferation, basement membrane formation, and hair follicle invagination. *J Cell Biol* 150: 1149-1160.
66. Watt FM, Hertle MD (1994) Keratinocyte Integrins. *The Keratinocyte Handbook*: 153-164.
67. Dowling J, Yu QC, Fuchs E (1996) Beta4 integrin is required for hemidesmosome formation, cell adhesion and cell survival. *J Cell Biol* 134: 559-572.
68. Georges-Labouesse E, Messaddeq N, Yehia G, Cadalbert L, Dierich A, et al. (1996) Absence of integrin alpha 6 leads to epidermolysis bullosa and neonatal death in mice. *Nat Genet* 13: 370-373.
69. van der Neut R, Krimpenfort P, Calafat J, Niessen CM, Sonnenberg A (1996) Epithelial detachment due to absence of hemidesmosomes in integrin beta 4 null mice. *Nat Genet* 13: 366-369.
70. Aumailley M, Has C, Tunggal L, Bruckner-Tuderman L (2006) Molecular basis of inherited skin-blistering disorders, and therapeutic implications. *Expert Rev Mol Med* 8: 1-21.

References

71. DiPersio CM, Hodivala-Dilke KM, Jaenisch R, Kreidberg JA, Hynes RO (1997) alpha3beta1 Integrin is required for normal development of the epidermal basement membrane. *J Cell Biol* 137: 729-742.
72. Kreidberg JA, Donovan MJ, Goldstein SL, Rennke H, Shepherd K, et al. (1996) Alpha 3 beta 1 integrin has a crucial role in kidney and lung organogenesis. *Development* 122: 3537-3547.
73. Huang XZ, Wu JF, Cass D, Erle DJ, Corry D, et al. (1996) Inactivation of the integrin beta 6 subunit gene reveals a role of epithelial integrins in regulating inflammation in the lung and skin. *J Cell Biol* 133: 921-928.
74. Munger JS, Huang X, Kawakatsu H, Griffiths MJ, Dalton SL, et al. (1999) The integrin alpha v beta 6 binds and activates latent TGF beta 1: a mechanism for regulating pulmonary inflammation and fibrosis. *Cell* 96: 319-328.
75. de Santa Barbara P, van den Brink GR, Roberts DJ (2003) Development and differentiation of the intestinal epithelium. *Cell Mol Life Sci* 60: 1322-1332.
76. Karam SM (1999) Lineage commitment and maturation of epithelial cells in the gut. *Front Biosci* 4: D286-298.
77. Maunoury R, Robine S, Pringault E, Leonard N, Gaillard JA, et al. (1992) Developmental regulation of villin gene expression in the epithelial cell lineages of mouse digestive and urogenital tracts. *Development* 115: 717-728.
78. Reya T, Clevers H (2005) Wnt signalling in stem cells and cancer. *Nature* 434: 843-850.
79. Potten CS, Booth C, Pritchard DM (1997) The intestinal epithelial stem cell: the mucosal governor. *Int J Exp Pathol* 78: 219-243.
80. Heath JP (1996) Epithelial cell migration in the intestine. *Cell Biol Int* 20: 139-146.
81. Cheng H, Leblond CP (1974) Origin, differentiation and renewal of the four main epithelial cell types in the mouse small intestine. I. Columnar cell. *Am J Anat* 141: 461-479.
82. Chang WW, Leblond CP (1971) Renewal of the epithelium in the descending colon of the mouse. I. Presence of three cell populations: vacuolated-columnar, mucous and argentaffin. *Am J Anat* 131: 73-99.
83. Sato M, Ahnen DJ (1992) Regional variability of colonocyte growth and differentiation in the rat. *Anat Rec* 233: 409-414.
84. Fontao L, Stutzmann J, Gendry P, Launay JF (1999) Regulation of the type II hemidesmosomal plaque assembly in intestinal epithelial cells. *Exp Cell Res* 250: 298-312.
85. Murgia C, Blaikie P, Kim N, Dans M, Petrie HT, et al. (1998) Cell cycle and adhesion defects in mice carrying a targeted deletion of the integrin beta4 cytoplasmic domain. *Embo J* 17: 3940-3951.
86. Beaulieu JF, Vachon PH, Herring-Gillam FE, Simoneau A, Perreault N, et al. (1994) Expression of the alpha-5(IV) collagen chain in the fetal human small intestine. *Gastroenterology* 107: 957-967.
87. Simoneau A, Herring-Gillam FE, Vachon PH, Perreault N, Basora N, et al. (1998) Identification, distribution, and tissular origin of the alpha5(IV) and alpha6(IV) collagen chains in the developing human intestine. *Dev Dyn* 212: 437-447.
88. Beaulieu JF, Vachon PH (1994) Reciprocal expression of laminin A-chain isoforms along the crypt-villus axis in the human small intestine. *Gastroenterology* 106: 829-839.
89. Simon-Assmann P, Duclos B, Orian-Rousseau V, Arnold C, Mathelin C, et al. (1994) Differential expression of laminin isoforms and alpha 6-beta 4 integrin subunits in the developing human and mouse intestine. *Dev Dyn* 201: 71-85.
90. Perreault N, Vachon PH, Beaulieu JF (1995) Appearance and distribution of laminin A chain isoforms and integrin alpha 2, alpha 3, alpha 6, beta 1, and beta 4 subunits in the developing human small intestinal mucosa. *Anat Rec* 242: 242-250.
91. Orian-Rousseau V, Aberdam D, Fontao L, Chevalier L, Meneguzzi G, et al. (1996) Developmental expression of laminin-5 and HD1 in the intestine: epithelial to mesenchymal shift for the laminin gamma-2 chain subunit deposition. *Dev Dyn* 206: 12-23.
92. Beaulieu JF (1999) Integrins and human intestinal cell functions. *Front Biosci* 4: D310-321.
93. Madison BB, Dunbar L, Qiao XT, Braunstein K, Braunstein E, et al. (2002) Cis elements of the villin gene control expression in restricted domains of the vertical (crypt) and horizontal (duodenum, cecum) axes of the intestine. *J Biol Chem* 277: 33275-33283.

References

94. Jones RG, Li X, Gray PD, Kuang J, Clayton F, et al. (2006) Conditional deletion of beta1 integrins in the intestinal epithelium causes a loss of Hedgehog expression, intestinal hyperplasia, and early postnatal lethality. *J Cell Biol* 175: 505-514.
95. Italiano JE, Jr., Shivdasani RA (2003) Megakaryocytes and beyond: the birth of platelets. *J Thromb Haemost* 1: 1174-1182.
96. Varga-Szabo D, Pleines I, Nieswandt B (2008) Cell adhesion mechanisms in platelets. *Arterioscler Thromb Vasc Biol* 28: 403-412.
97. Therman E, Sarto GE, Stubblefield PA (1983) Endomitosis: a reappraisal. *Hum Genet* 63: 13-18.
98. Odell TT, Jr., Jackson CW, Friday TJ (1970) Megakaryocytopoiesis in rats with special reference to polyploidy. *Blood* 35: 775-782.
99. Youssefian T, Cramer EM (2000) Megakaryocyte dense granule components are sorted in multivesicular bodies. *Blood* 95: 4004-4007.
100. Handagama PJ, George JN, Shuman MA, McEver RP, Bainton DF (1987) Incorporation of a circulating protein into megakaryocyte and platelet granules. *Proc Natl Acad Sci U S A* 84: 861-865.
101. Collier BS, Seligsohn U, West SM, Scudder LE, Norton KJ (1991) Platelet fibrinogen and vitronectin in Glanzmann thrombasthenia: evidence consistent with specific roles for glycoprotein IIb/IIIa and alpha v beta 3 integrins in platelet protein trafficking. *Blood* 78: 2603-2610.
102. Savage B, Almus-Jacobs F, Ruggeri ZM (1998) Specific synergy of multiple substrate-receptor interactions in platelet thrombus formation under flow. *Cell* 94: 657-666.
103. Offermanns S (2000) The role of heterotrimeric G proteins in platelet activation. *Biol Chem* 381: 389-396.
104. Nieswandt B, Brakebusch C, Bergmeier W, Schulte V, Bouvard D, et al. (2001) Glycoprotein VI but not alpha2beta1 integrin is essential for platelet interaction with collagen. *Embo J* 20: 2120-2130.
105. Holtkotter O, Nieswandt B, Smyth N, Muller W, Hafner M, et al. (2002) Integrin alpha 2-deficient mice develop normally, are fertile, but display partially defective platelet interaction with collagen. *J Biol Chem* 277: 10789-10794.
106. Chen J, Diacovo TG, Grenache DG, Santoro SA, Zutter MM (2002) The alpha(2) integrin subunit-deficient mouse: a multifaceted phenotype including defects of branching morphogenesis and hemostasis. *Am J Pathol* 161: 337-344.
107. Shattil SJ, Kashiwagi H, Pampori N (1998) Integrin signaling: the platelet paradigm. *Blood* 91: 2645-2657.
108. Chen YP, Djaffar I, Pidad D, Steiner B, Cieutat AM, et al. (1992) Ser-752-->Pro mutation in the cytoplasmic domain of integrin beta 3 subunit and defective activation of platelet integrin alpha IIb beta 3 (glycoprotein IIb-IIIa) in a variant of Glanzmann thrombasthenia. *Proc Natl Acad Sci U S A* 89: 10169-10173.
109. Nurden AT (2006) Glanzmann thrombasthenia. *Orphanet J Rare Dis* 1: 10.
110. Hodivala-Dilke KM, McHugh KP, Tsakiris DA, Rayburn H, Crowley D, et al. (1999) Beta3-integrin-deficient mice are a model for Glanzmann thrombasthenia showing placental defects and reduced survival. *J Clin Invest* 103: 229-238.
111. Inoue O, Suzuki-Inoue K, McCarty OJ, Moroi M, Ruggeri ZM, et al. (2006) Laminin stimulates spreading of platelets through integrin alpha6beta1-dependent activation of GPVI. *Blood* 107: 1405-1412.
112. Xiong LY, Xu JS, Hong FX, Chen MC (2002) [Effects of salinity stress on cytosolic calcium in *Stevia rebaudiana* Bertoni cells]. *Shi Yan Sheng Wu Xue Bao* 35: 151-154.
113. Xiong JP, Stehle T, Zhang R, Joachimiak A, Frech M, et al. (2002) Crystal structure of the extracellular segment of integrin alpha Vbeta3 in complex with an Arg-Gly-Asp ligand. *Science* 296: 151-155.
114. Takagi J, Petre BM, Walz T, Springer TA (2002) Global conformational rearrangements in integrin extracellular domains in outside-in and inside-out signaling. *Cell* 110: 599-511.
115. Humphries MJ, McEwan PA, Barton SJ, Buckley PA, Bella J, et al. (2003) Integrin structure: heady advances in ligand binding, but activation still makes the knees wobble. *Trends Biochem Sci* 28: 313-320.

References

116. Carman CV, Springer TA (2003) Integrin avidity regulation: are changes in affinity and conformation underemphasized? *Curr Opin Cell Biol* 15: 547-556.
117. Shimaoka M, Takagi J, Springer TA (2002) Conformational regulation of integrin structure and function. *Annu Rev Biophys Biomol Struct* 31: 485-516.
118. O'Toole TE, Mandelman D, Forsyth J, Shattil SJ, Plow EF, et al. (1991) Modulation of the affinity of integrin alpha IIb beta 3 (GPIIb-IIIa) by the cytoplasmic domain of alpha IIb. *Science* 254: 845-847.
119. O'Toole TE, Katagiri Y, Faull RJ, Peter K, Tamura R, et al. (1994) Integrin cytoplasmic domains mediate inside-out signal transduction. *J Cell Biol* 124: 1047-1059.
120. Hughes PE, O'Toole TE, Ylanne J, Shattil SJ, Ginsberg MH (1995) The conserved membrane-proximal region of an integrin cytoplasmic domain specifies ligand binding affinity. *J Biol Chem* 270: 12411-12417.
121. Hughes PE, Diaz-Gonzalez F, Leong L, Wu C, McDonald JA, et al. (1996) Breaking the integrin hinge. A defined structural constraint regulates integrin signaling. *J Biol Chem* 271: 6571-6574.
122. Brakebusch C, Fassler R (2003) The integrin-actin connection, an eternal love affair. *Embo J* 22: 2324-2333.
123. Calderwood DA, Zent R, Grant R, Rees DJ, Hynes RO, et al. (1999) The Talin head domain binds to integrin beta subunit cytoplasmic tails and regulates integrin activation. *J Biol Chem* 274: 28071-28074.
124. Calderwood DA, Yan B, de Pereda JM, Alvarez BG, Fujioka Y, et al. (2002) The phosphotyrosine binding-like domain of talin activates integrins. *J Biol Chem* 277: 21749-21758.
125. Wegener KL, Partridge AW, Han J, Pickford AR, Liddington RC, et al. (2007) Structural basis of integrin activation by talin. *Cell* 128: 171-182.
126. Vinogradova O, Velyvis A, Velyviene A, Hu B, Haas T, et al. (2002) A structural mechanism of integrin alpha(IIb)beta(3) "inside-out" activation as regulated by its cytoplasmic face. *Cell* 110: 587-597.
127. Bouaouina M, Lad Y, Calderwood DA (2008) The N-terminal Domains of Talin Cooperate with the Phosphotyrosine Binding-like Domain to Activate {beta}1 and {beta}3 Integrins. *J Biol Chem* 283: 6118-6125.
128. Nieswandt B, Moser M, Pleines I, Varga-Szabo D, Monkley S, et al. (2007) Loss of talin1 in platelets abrogates integrin activation, platelet aggregation, and thrombus formation in vitro and in vivo. *J Exp Med* 204: 3113-3118.
129. Monkley SJ, Pritchard CA, Critchley DR (2001) Analysis of the mammalian talin2 gene TLN2. *Biochem Biophys Res Commun* 286: 880-885.
130. Monkley SJ, Zhou XH, Kinston SJ, Giblett SM, Hemmings L, et al. (2000) Disruption of the talin gene arrests mouse development at the gastrulation stage. *Dev Dyn* 219: 560-574.
131. Xi X, Bodnar RJ, Li Z, Lam SC, Du X (2003) Critical roles for the COOH-terminal NITY and RGT sequences of the integrin beta3 cytoplasmic domain in inside-out and outside-in signaling. *J Cell Biol* 162: 329-339.
132. Ratnikov BI, Partridge AW, Ginsberg MH (2005) Integrin activation by talin. *J Thromb Haemost* 3: 1783-1790.
133. Calderwood DA (2004) Talin controls integrin activation. *Biochem Soc Trans* 32: 434-437.
134. Datta A, Huber F, Boettiger D (2002) Phosphorylation of beta3 integrin controls ligand binding strength. *J Biol Chem* 277: 3943-3949.
135. Wennerberg K, Armulik A, Sakai T, Karlsson M, Fassler R, et al. (2000) The cytoplasmic tyrosines of integrin subunit beta1 are involved in focal adhesion kinase activation. *Mol Cell Biol* 20: 5758-5765.
136. Ling K, Doughman RL, Iyer VV, Firestone AJ, Bairstow SF, et al. (2003) Tyrosine phosphorylation of type Igamma phosphatidylinositol phosphate kinase by Src regulates an integrin-talin switch. *J Cell Biol* 163: 1339-1349.
137. Tapley P, Horwitz A, Buck C, Duggan K, Rohrschneider L (1989) Integrins isolated from Rous sarcoma virus-transformed chicken embryo fibroblasts. *Oncogene* 4: 325-333.

References

138. Oxley CL, Anthis NJ, Lowe ED, Vakonakis I, Campbell ID, et al. (2008) An Integrin Phosphorylation Switch: THE EFFECT OF β 3 INTEGRIN TAIL PHOSPHORYLATION ON DOK1 AND TALIN BINDING. *J Biol Chem* 283: 5420-5426.
139. Czuchra A, Meyer H, Legate KR, Brakebusch C, Fassler R (2006) Genetic analysis of beta1 integrin "activation motifs" in mice. *J Cell Biol* 174: 889-899.
140. Goldmann WH, Bremer A, Haner M, Aebi U, Isenberg G (1994) Native talin is a dumbbell-shaped homodimer when it interacts with actin. *J Struct Biol* 112: 3-10.
141. Pearson MA, Reczek D, Bretscher A, Karplus PA (2000) Structure of the ERM protein moesin reveals the FERM domain fold masked by an extended actin binding tail domain. *Cell* 101: 259-270.
142. Martel V, Racaud-Sultan C, Dupe S, Marie C, Paulhe F, et al. (2001) Conformation, localization, and integrin binding of talin depend on its interaction with phosphoinositides. *J Biol Chem* 276: 21217-21227.
143. Yan B, Calderwood DA, Yaspan B, Ginsberg MH (2001) Calpain cleavage promotes talin binding to the beta 3 integrin cytoplasmic domain. *J Biol Chem* 276: 28164-28170.
144. Wiesner S, Legate KR, Fassler R (2005) Integrin-actin interactions. *Cell Mol Life Sci* 62: 1081-1099.
145. Zamir E, Katz M, Posen Y, Erez N, Yamada KM, et al. (2000) Dynamics and segregation of cell-matrix adhesions in cultured fibroblasts. *Nat Cell Biol* 2: 191-196.
146. Linder S, Aepfelbacher M (2003) Podosomes: adhesion hot-spots of invasive cells. *Trends Cell Biol* 13: 376-385.
147. Xing B, Jedsadayanmata A, Lam SC (2001) Localization of an integrin binding site to the C terminus of talin. *J Biol Chem* 276: 44373-44378.
148. Hemmings L, Rees DJ, Ohanian V, Bolton SJ, Gilmore AP, et al. (1996) Talin contains three actin-binding sites each of which is adjacent to a vinculin-binding site. *J Cell Sci* 109 (Pt 11): 2715-2726.
149. Gilmore AP, Burridge K (1996) Regulation of vinculin binding to talin and actin by phosphatidyl-inositol-4-5-bisphosphate. *Nature* 381: 531-535.
150. Liu S, Calderwood DA, Ginsberg MH (2000) Integrin cytoplasmic domain-binding proteins. *J Cell Sci* 113 (Pt 20): 3563-3571.
151. Boyd RS, Adam PJ, Patel S, Loader JA, Berry J, et al. (2003) Proteomic analysis of the cell-surface membrane in chronic lymphocytic leukemia: identification of two novel proteins, BCNP1 and MIG2B. *Leukemia* 17: 1605-1612.
152. Jobard F, Bouadjar B, Caux F, Hadj-Rabia S, Has C, et al. (2003) Identification of mutations in a new gene encoding a FERM family protein with a pleckstrin homology domain in Kindler syndrome. *Hum Mol Genet* 12: 925-935.
153. Siegel DH, Ashton GH, Penagos HG, Lee JV, Feiler HS, et al. (2003) Loss of kindlin-1, a human homolog of the *Caenorhabditis elegans* actin-extracellular-matrix linker protein UNC-112, causes Kindler syndrome. *Am J Hum Genet* 73: 174-187.
154. Kindler T (1954) Congenital poikiloderma with traumatic bulla formation and progressive cutaneous atrophy. *Br J Dermatol* 66: 104-111.
155. White SJ, McLean WH (2005) Kindler surprise: mutations in a novel actin-associated protein cause Kindler syndrome. *J Dermatol Sci* 38: 169-175.
156. Weary PE, Manley WF, Jr., Graham GF (1971) Hereditary acrokeratotic poikiloderma. *Arch Dermatol* 103: 409-422.
157. Forman AB, Prendiville JS, Esterly NB, Hebert AA, Duvic M, et al. (1989) Kindler syndrome: report of two cases and review of the literature. *Pediatr Dermatol* 6: 91-101.
158. Martignago BC, Lai-Cheong JE, Liu L, McGrath JA, Cestari TF (2007) Recurrent KIND1 (C20orf42) gene mutation, c.676insC, in a Brazilian pedigree with Kindler syndrome. *Br J Dermatol* 157: 1281-1284.
159. Arita K, Wessagowit V, Inamadar AC, Palit A, Fassihi H, et al. (2007) Unusual molecular findings in Kindler syndrome. *Br J Dermatol* 157: 1252-1256.
160. Lai-Cheong JE, Liu L, Sethuraman G, Kumar R, Sharma VK, et al. (2007) Five new homozygous mutations in the KIND1 gene in Kindler syndrome. *J Invest Dermatol* 127: 2268-2270.

References

161. Shimizu H, Sato M, Ban M, Kitajima Y, Ishizaki S, et al. (1997) Immunohistochemical, ultrastructural, and molecular features of Kindler syndrome distinguish it from dystrophic epidermolysis bullosa. *Arch Dermatol* 133: 1111-1117.
162. Hovnanian A, Blanchet-Bardon C, de Prost Y (1989) Poikiloderma of Theresa Kindler: report of a case with ultrastructural study, and review of the literature. *Pediatr Dermatol* 6: 82-90.
163. Patrizi A, Pauluzzi P, Neri I, Trevisan G, De Giorgi LB, et al. (1996) Kindler syndrome: report of a case with ultrastructural study and review of the literature. *Pediatr Dermatol* 13: 397-402.
164. Ashton GH (2004) Kindler syndrome. *Clin Exp Dermatol* 29: 116-121.
165. Burch JM, Fassihi H, Jones CA, Mengshol SC, Fitzpatrick JE, et al. (2006) Kindler syndrome: a new mutation and new diagnostic possibilities. *Arch Dermatol* 142: 620-624.
166. Wiebe CB, Larjava HS (1999) Abnormal deposition of type VII collagen in Kindler syndrome. *Arch Dermatol Res* 291: 6-13.
167. Yasukawa K, Sato-Matsumura KC, McMillan J, Tsuchiya K, Shimizu H (2002) Exclusion of COL7A1 mutation in Kindler syndrome. *J Am Acad Dermatol* 46: 447-450.
168. Lanschuetzer CM, Muss WH, Emberger M, Pohla-Gubo G, Klausegger A, et al. (2003) Characteristic immunohistochemical and ultrastructural findings indicate that Kindler's syndrome is an apoptotic skin disorder. *J Cutan Pathol* 30: 553-560.
169. Herz C, Aumailley M, Schulte C, Schlotzer-Schrehardt U, Bruckner-Tuderman L, et al. (2006) Kindlin-1 is a phosphoprotein involved in regulation of polarity, proliferation, and motility of epidermal keratinocytes. *J Biol Chem* 281: 36082-36090.
170. Kern J, Herz C, Haan E, Moore D, Nottelmann S, et al. (2007) Chronic colitis due to an epithelial barrier defect: the role of kindlin-1 isoforms. *J Pathol*.
171. Sadler E, Klausegger A, Muss W, Deinsberger U, Pohla-Gubo G, et al. (2006) Novel KIND1 gene mutation in Kindler syndrome with severe gastrointestinal tract involvement. *Arch Dermatol* 142: 1619-1624.
172. Freeman EB, Kogelmeier J, Martinez AE, Mellerio JE, Haynes L, et al. (2008) Gastrointestinal complications of epidermolysis bullosa in children. *Br J Dermatol* 158: 1308-1314.
173. Tu Y, Wu S, Shi X, Chen K, Wu C (2003) Migfilin and Mig-2 link focal adhesions to filamin and the actin cytoskeleton and function in cell shape modulation. *Cell* 113: 37-47.
174. Stossel TP, Condeelis J, Cooley L, Hartwig JH, Noegel A, et al. (2001) Filamins as integrators of cell mechanics and signalling. *Nat Rev Mol Cell Biol* 2: 138-145.
175. van der Flier A, Sonnenberg A (2001) Structural and functional aspects of filamins. *Biochim Biophys Acta* 1538: 99-117.
176. Calderwood DA (2004) Integrin activation. *J Cell Sci* 117: 657-666.
177. Kato K, Shiozawa T, Mitsushita J, Toda A, Horiuchi A, et al. (2004) Expression of the mitogen-inducible gene-2 (mig-2) is elevated in human uterine leiomyomas but not in leiomyosarcomas. *Hum Pathol* 35: 55-60.
178. Akazawa H, Kudoh S, Mochizuki N, Takekoshi N, Takano H, et al. (2004) A novel LIM protein Cal promotes cardiac differentiation by association with CSX/NKX2-5. *J Cell Biol* 164: 395-405.
179. Dowling JJ, Gibbs E, Russell M, Goldman D, Minarcik J, et al. (2008) Kindlin-2 is an essential component of intercalated discs and is required for vertebrate cardiac structure and function. *Circ Res* 102: 423-431.
180. Wang L, Deng W, Shi T, Ma D (2008) URP2SF, a FERM and PH domain containing protein, regulates NF-kappaB and apoptosis. *Biochem Biophys Res Commun* 368: 899-906.

Appendix

In the following, papers I to IX are reprinted.

Paper I

available at www.sciencedirect.comwww.elsevier.com/locate/yexcr

Research Article

The Kindlins: Subcellular localization and expression during murine development

Siegfried Ussar^a, Hao-Ven Wang^a, Stefan Linder^b, Reinhard Fässler^a, Markus Moser^{a,*}

^aMax-Planck-Institute of Biochemistry, Department of Molecular Medicine, D-82152 Martinsried, Germany

^bInstitut für Prophylaxe und Epidemiologie der Kreislauferkrankheiten, Ludwig-Maximilians-Universität, 80336 Munich, Germany

ARTICLE INFORMATION

Article Chronology:

Received 28 March 2006

Revised version received

6 June 2006

Accepted 13 June 2006

Available online 29 June 2006

Keywords:

Kindler Syndrome

Integrins

Cell-cell adhesion

Cell-matrix adhesion

ABSTRACT

The three Kindlins are a novel family of focal adhesion proteins. The Kindlin-1 (URP1) gene is mutated in Kindler syndrome, the first skin blistering disease affecting actin attachment in basal keratinocytes. Kindlin-2 (Mig-2), the best studied member of this family, binds ILK and Migfilin, which links Kindlin-2 to the actin cytoskeleton. Kindlin-3 is expressed in hematopoietic cells. Here we describe the genomic organization, gene expression and subcellular localization of murine Kindlins-1 to -3. In situ hybridizations showed that Kindlin-1 is preferentially expressed in epithelia, and Kindlin-2 in striated and smooth muscle cells. Kindlins-1 and -2 are both expressed in the epidermis. While both localize to integrin-mediated adhesion sites in cultured keratinocytes Kindlin-2, but not Kindlin-1, colocalizes with E-cadherin to cell-cell contacts in differentiated keratinocytes. Using a Kindlin-3-specific antiserum and an EGFP-tagged Kindlin-3 construct, we could show that Kindlin-3 is present in the F-actin surrounding ring structure of podosomes, which are specialized adhesion structures of hematopoietic cells.

© 2006 Elsevier Inc. All rights reserved.

Introduction

The Kindlin gene family is named after the gene mutated in Kindler syndrome, an autosomal recessive genodermatosis in humans [1]. Kindlin-1 is a member of a new family of focal adhesion (FA) proteins. The family consists of three members in mice and men. The Kindlin proteins are composed of a centrally located FERM (Band 4.1/Ezrin/Radixin/Moesin) domain interrupted by a pleckstrin homology (PH) domain. The first member of this family was identified in a differential cDNA library screen as mitogen inducible gene-2 (Mig2 now termed Kindlin-2) [2]. The two other genes were initially named Unc-112 Related Protein 1 (URP1 now termed Kindlin-1) and URP2 (now termed Kindlin-3), due to their homology to the *Caenorhabditis elegans* gene *unc-112* [3]. Siegel et al. [5]

proposed to name the three different genes Kindlin-1 (URP1), Kindlin-2 (Mig2) and Kindlin-3 (URP2/Mig2B [4]), which we will also do throughout this article.

Kindlin-1 and Kindlin-2 have been shown to play an essential role in integrin-mediated adhesion and spreading. Both proteins localize to FAs and loss of either leads to delayed cell spreading in different cell lines [6,7]. These studies also showed that Kindlin-1 can interact with the cytoplasmic tails of $\beta 1$ and $\beta 3$ integrins and Kindlin-2 with the integrin-linked kinase (ILK). Binding partners for Kindlin-3 are not known. The ability of Kindlin-2 to bind Migfilin, a LIM domain containing protein capable of binding Filamin, revealed a novel linkage between integrins and the actin cytoskeleton [7]. Whether Kindlin-1 also binds Migfilin has not been investigated yet, although the high homology

* Corresponding author.

E-mail address: moser@biochem.mpg.de (M. Moser).

between Kindlin-1 and Kindlin-2 makes such a binding activity very likely [8].

Genetic studies have so far been performed in humans and *C. elegans*. Null mutations of the Kindlin orthologue Unc-112 in nematodes are embryonic lethal due to a paralyzed arrested elongation at twofold (PAT) phenotype. Unc-112 localizes together with PAT3/ β -integrin and PAT4/ILK to dense bodies and M-lines at muscle attachment sites, which link the muscle to the body wall. Loss of Unc-112 impairs cell–matrix adhesion and integrin function resulting in muscle detachment from the body wall and severe paralysis [9].

Loss of Kindlin-1 in humans gives rise to Kindler syndrome. Kindler syndrome patients show different skin pathologies that undergo changes during the patients' lifetime. The syndrome is characterized by skin atrophy and trauma-induced skin blisters at early life. During infancy, the blistering becomes less and instead photosensitivity and progressive poikiloderma develops. In addition, there are indications that Kindler Syndrome patients may be prone to squamous cell carcinoma development [10]. Kindler Syndrome is the first skin blistering disease resulting from defects in actin cytoskeleton anchorage to cell matrix adhesion sites [5,11,12,13]. However, the molecular mechanism leading to the multiple defects of Kindler Syndrome is only poorly understood and simple actin anchorage insufficiencies cannot completely explain the phenotype.

Several reports describe a transcriptional misregulation of Kindlins in various types of cancer. Kindlin-1 is overexpressed in lung and colon carcinomas, whereas Kindlins-2 and -3 were unchanged or even reduced [3]. Kindlin-2 expression has been shown to be elevated in leiomyomas and greatly decreased in leiomyosarcomas [14]. Interestingly, an almost exclusive nuclear staining of Kindlin-2 was observed in both tumors, suggesting additional functions of Kindlin-2. This observation is of note since Migfilin has been shown function in the nucleus as transcriptional coactivator during cardiomyocyte differentiation in mice [15]. Finally, increased expression of Kindlin-3 has been reported in different kinds of B cell lymphomas [4]. However, the molecular role of Kindlin proteins during tumor formation is so far completely unclear.

In the present paper, we report the expression of the three Kindlins during murine development and in adult tissues and characterize their subcellular localization in different cell types.

Materials and methods

Northern blotting

Total RNA was extracted with Trizol (Invitrogen) following the manufacturer's protocol. Total RNA (8 μ g) was separated on a denaturing agarose gel and transferred to Hybond N+ membranes (Amersham). The following primers were used to amplify the Kindlin probes:

Kindlin-1 forward: TCTGAGGTTGACGAGGTAG (Exon 6);
Kindlin-1 reverse: ACTTCATTCATACCATCAGC (Exon 9);
Kindlin-2 forward: CTAGATGACCAGTCTGAAGACG (Exon 4);
Kindlin-2 reverse: TGAATCGGAGCAGCAAGGCC (Exon 6);

Kindlin-3 forward: GAGAAGGAGCCTGAAGAGGAG (Exon 4);
Kindlin-3 reverse: TAAATCGCAGCCAAAGCACATC (Exon 6).

The amplified probes were radiolabeled using the Redi-Prime II random prime labeling kit (Amersham). Membranes were hybridized overnight at 65°C in Church buffer, washed and exposed for 1–8 days at –80°C with Kodak Biomax MS screens (Kodak).

RT-PCR

Total RNA (1 μ g) was used for first strand cDNA synthesis according to the protocol of the manufacturer using Super-Script III polymerase (Invitrogen) and random hexamer primers. Specific cDNA fragments were amplified using the following primers:

Kindlin-1 forward: CTACACCTTCTTTGACTTG;
Kindlin-1 reverse: AGGGATGTCAGTTATGTC.
Kindlin-2 forward: GTACCGAAGTAGACTGCAAGG;
Kindlin-2 reverse: CATACGGCATATCAAGTAGGC.
Kindlin-3 forward: AGCTGTCTCTGCTGCGTGCTC;
Kindlin-3 reverse: ATACCTTGCTGCATGAGGCAC.

Radioactive in situ hybridization

³³P-UTP-labeled sense and antisense riboprobes were generated by in vitro transcription from linearized vectors containing Kindlins-1/-2/-3-specific cDNA fragments (see Northern Blotting). Paraffin sections from mouse embryos at different embryonic stages were dewaxed, rehydrated and hybridized as previously described [16].

Antibody production and affinity purification

A Kindlin-3-specific peptide (EPEEEVHDLTKVVLA; aa 156–170) was coupled to Imject Maleimide Activated mCKLH (Pierce) and used to immunize rabbits. The antiserum was subsequently affinity purified using a commercial kit (SulfoLink Kit, Pierce Biotechnology Inc., Rockford, IL, USA). High affinity antibodies were eluted from the column using 100 mM Glycine buffer, pH 2.7 and then dialyzed against phosphate-buffered saline (PBS).

Western blotting

Both cells and tissues from adult C57BL/6 mice were homogenized in lysis buffer (1% Triton X-100, 50 mM Tris–Cl pH 7.4, 300 mM NaCl, 5 mM EDTA and protease inhibitors (Roche)). Equal amounts of total protein (about 20 μ g) per lane were separated on a 10% polyacrylamide gel and transferred to PVDF membranes (Millipore). Kindlin-3 (1:1000), tubulin (1:5000), GAPDH antibodies (1:5000; Chemicon) were used together with the appropriate secondary antibody (1:50000 in 5% bovine serum albumin (BSA); Biorad).

Constructs

All Kindlin cDNAs were cloned into the pEGFP-C1 vector (Clontech). A partial Kindlin-1 cDNA was obtained from Image

clone 3157716. The missing N-terminal part was amplified from epidermal cDNA by PCR using CAGGTCGAC-CATCTGCCTGGGCCACAATG as forward primer and CAAGT-CAAAGAAGGTGTAG as reverse primer. Kindlin-2 full-length cDNA was obtained from Image clone 3596509. Kindlin-3 was cloned by amplifying a 558 bp fragment from the N-terminus (CAGGTCGACATGGCGGTATGAAGACAG; AGAA-GTGTGCTGGCATGC) containing the start codon combined with the residual nucleotides from the Image clone 4187161. Final expression constructs were confirmed by sequencing.

Immunostaining

Paraffin sections were dewaxed, rehydrated and endogenous peroxidase was blocked by incubating the slides for 20 min in 2.5 ml H₂O₂/75 ml methanol. Blocking was performed for 1 h in PBS supplemented with 10% goat serum and 1% BSA. Subsequently, the Kindlin-3 antibody (1:500) was incubated at 4°C over night. Sections were incubated with a 1:200 dilution of biotinylated anti-rabbit secondary antibody for one hour and transferred to ABC solution (Vector Laboratories) for an additional 30 min. Secondary antibody was detected with diaminobenzidine (DAB). Counterstaining of the sections was performed with methylene green and sections were mounted with Entellan.

Immunohistochemistry

Cells were grown on fibronectin (5 µg/ml, Calbiochem) coated glass cover slips, fixed with PBS supplemented with 4% paraformaldehyde (PFA) and 3% sucrose, permeabilized with 0.25% Triton X-100 in PBS for 10 min, blocked in PBS containing 3% BSA and 5% goat serum for 1 h. Cells were immunostained for paxillin (monoclonal antibodies, BD Transduction), α -actinin (monoclonal antibodies, Sigma), vinculin (monoclonal antibodies, Sigma) and TRITC-labeled phalloidin (1:500; Sigma) to visualize F-actin. Alexa647 and Cy3-conjugated secondary antibodies were purchased from Molecular Probes. Stained cells were mounted in Elvanol and pictures were taken with a Leica DMRA2 microscope and a Hamamatsu camera.

Transfections

Immortalized wild-type mouse embryonic fibroblasts, mouse keratinocytes, primary cardiomyocytes and dendritic cells were transfected with the EGFP-Kindlin-1, EGFP-Kindlin-2 and EGFP-Kindlin-3 cDNA constructs using Lipofectamine 2000 (Invitrogen) following the manufacturer's instructions.

Cell culture

Primary wild-type macrophages and dendritic cells were derived from bone marrow of 5-day-old mice and cultured on bacterial petri dishes for 7 days in DMEM, supplemented with glutamine, 10% FCS, Pen/Strep (all Invitrogen), M-CSF (to derive macrophages) or GM-CSF (to generate dendritic cells). Both cytokines were derived from a hybridoma supernatant. The supernatant was used in a 1:10 dilution.

Immortalized newborn mouse keratinocytes were maintained in MEM supplemented with 5 µg/ml insulin (Sigma),

10 ng/ml EGF (Roche), 10 µg/ml transferrin (Sigma), 10 µM phosphoethanolamine (Sigma), 10 µM ethanolamine, 0.36 µg/ml hydrocortisone (Calbiochem), glutamine (Invitrogen), Pen/Strep (Invitrogen), 45 µM CaCl₂ and 8% chelated FCS. For differentiation keratinocytes were cultured in growth medium containing 1 mM CaCl₂ over night. Immortalized mouse embryonic kidney fibroblasts were maintained in DMEM supplemented with 10% FCS.

Isolation and culture of neonatal mouse cardiomyocytes

Cardiomyocytes were isolated from hearts of P1 newborn mice by treatment with 0.4 mg/ml collagenase II (Worthington, Freehold, NJ) and 1 mg/ml pancreatin (Sigma) in ADS buffer (116 mM NaCl, 0.8 mM NaH₂PO₄, 1 g/l glucose, 5.4 mM KCl, 0.8 mM MgSO₄ and 20 mM 2,3-butanedione monoxime in 20 mM HEPES, pH 7.35) for 10 min at 37°C. Fresh enzyme solution (0.3 ml/heart) was added and tissue was incubated for 8 min. The supernatant containing dispersed cardiac cells was transferred to a new tube containing 1 ml FCS (per heart) and centrifuged at low speed (80×g, 6 min), resuspended in 2 ml FCS and kept at 37°C. The remaining tissue fragments were incubated with fresh enzyme solution (0.3 ml/heart) as above for additional 5 times. Cell suspensions were pooled and centrifuged at low speed (80×g, 6 min) and resuspended in 4 ml ADS buffer.

Cells were grown on glass coverslips coated with fibronectin (10 µg/ml) at a cell density of 3.0×10⁵ cells/35-mm culture dish in plating medium (67% DMEM, 17% M199 medium, 10% horse serum, 5% FCS, 1% Pen/Strep and 4 mM glutamine). Cells were incubated at 37°C in a 5% CO₂ humidified incubator. The next day the plating medium was replaced with maintenance medium (75% DMEM, 23.5% M199 medium, 0.5% horse serum, 1% Pen/Strep, 4 mM glutamine and 0.1 mM phenylephrine).

MAC sorting of primary T and B cells

A whole spleen from an adult C57BL/6 mouse was strained to obtain a single cell suspension. 3×10⁷ cells were incubated in 300 µl PBS with 3 µl FITC conjugated B220 (PharMingen) and CD3 (eBioscience) antibodies for 10 min at 4°C. Cells were washed with PBS and incubated with 30 µl anti-FITC MACS-beads (Miltenyi Biotec) for 10 min, washed with PBS, isolated in a magnetic field and eluted from beads, following the manufacturer's recommendations.

Results and discussion

Genomic organization of the murine Kindlin gene family

All three murine Kindlin genes were identified in a genomic search of the Ensembl database using the human Kindlin cDNAs. The chromosomal localization of the three human and murine Kindlin genes is shown in Table 1. The human as well as the murine Kindlin genes are composed of 15 exons with the translation start site in exon 2. The murine Kindlin-1 gene spans 38.5 kb resulting in a transcript of approximately 4.6 kb. The murine Kindlin-2 gene has a length of 70 kb and gives rise

Table 1 – Genomic localization of the human and murine Kindlin genes

	Mouse	Human
Kindlin-1	2F2	20p12.3
Kindlin-2	14B	14q22.1
Kindlin-3	19A	11q13.1

to a 3.2 kb transcript. Kindlin-3 represents the smallest gene with 19.8 kb encoding a 2.5 kb mRNA.

Kindlin protein structure

Translation of the murine cDNAs results in proteins of 637 aa (Kindlin-1), 680 aa (Kindlin-2) and 655 aa (Kindlin-3), respectively. A sequence alignment between the three murine Kindlin proteins revealed that Kindlins-1 and -2 are most closely related, sharing 60% identity and 74% similarity, while Kindlin-3 is more distantly related sharing 53% identity and 69% similarity to Kindlin-1 and 49% identity and 67% similarity to Kindlin-2.

Kindlin proteins have a unique domain architecture. They are composed of a centrally located FERM domain interrupted

by a PH domain [6]. FERM domains are found in a number of proteins linking the membrane to the cytoskeleton [17]. Among these proteins, the FERM domain of talin is most homologous to the Kindlin FERM domains. In vitro assays have shown an interaction between Kindlin-1 and the cytoplasmic tails of $\beta 1$ and $\beta 3$ integrins [6]. Therefore, it has been proposed that Kindlins bind to $\beta 1$ and $\beta 3$ integrins with a similar mechanism as it has been described for talin [18,19].

The second common domain within Kindlins is the PH domain. Although PH domains are known to mediate binding to phosphatidylinositol phosphates [20], the function and specificity of this domain have not been further characterized in Kindlin proteins.

A nuclear localization signal (NLS), amino acids 55–72, is exclusively present in Kindlin-2 only. In accordance with this finding, nuclear localization of Kindlin-2 has been reported in leiomyosarcomas and leiomyomas. Furthermore, the Kindlin-2 interacting protein Migfilin can localize to the nucleus. There it functions as a coactivator for the CSX/NKX2-5 transcription factor to promote cardiomyocyte differentiation [14].

Taken together, Kindlin proteins are typical adaptor proteins with two domains known to mediate membrane association. However, both the molecular regulation of

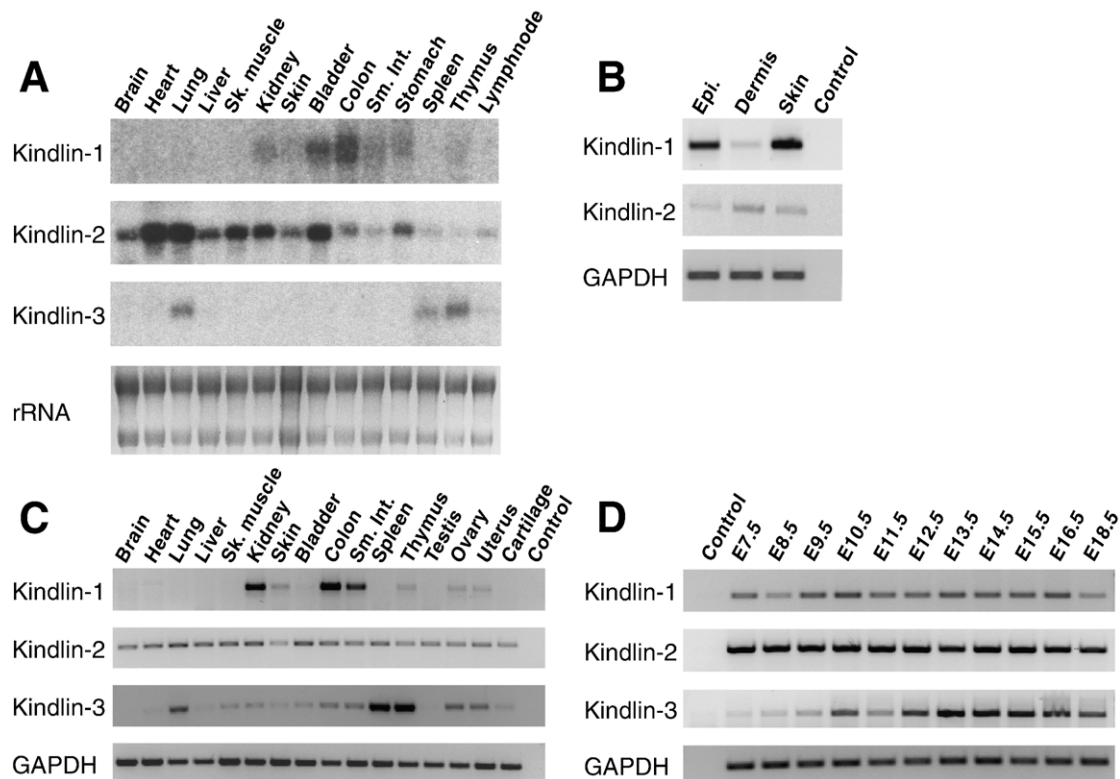


Fig. 1 – Expression pattern of Kindlins-1/-2/-3. (A) Northern blot from different tissues. Total RNA was extracted from organs of 2-week-old C57BL/6 mice. Staining of ribosomal RNA with ethidium bromide was used to control loading. **(B)** Skin from adult C57BL/6 mice was separated into epidermis and dermis by trypsin digestion and total RNA was reverse transcribed to detect differential expression of Kindlin-1 and Kindlin-2 in epidermis, dermis and whole skin. **(C)** Total RNA from 2-week-old C57BL/6 mice was reverse transcribed into cDNA and expression of the three Kindlins was checked by RT-PCR. GAPDH was used as loading control. **(D)** Total RNA was extracted from total embryos at different embryonic stages. RT-PCR was performed for all three Kindlins with cDNA derived from the total RNA. GAPDH was used to show equal loading. Sk. muscle: skeletal muscle; Sm. Int.: small intestine; Epi: epidermis.

Kindlin proteins and the specific binding of certain interactors to individual Kindlin proteins are only poorly understood.

Expression patterns of murine Kindlin-1 to -3 in adult tissues and during embryonic development

The tissue distribution of the murine Kindlin genes was analyzed by multiple tissue Northern blots and RT-PCR of total RNA from 2-week-old mice using specific cDNA fragments and primer pairs (Fig. 1A). The specificity of the cDNA probes was confirmed in a Southern blot containing all three murine Kindlin cDNAs (data not shown).

Kindlin-1 transcripts were detected in bladder and colon and at lower expression levels in kidney, skin, small intestine, stomach and thymus with Northern blot assays. RT-PCR revealed additional weak Kindlin-1 expression in ovary and uterus. Recently, a larger splice variant of Kindlin-1 was detected in human intestine [5]. This isoform is generated by including intron 7 into the coding sequence and was recently found in a thymus cDNA (AK_030947). This alternative splicing event gives rise to a 5.2 kb transcript, a premature translation stop, and a short protein isoform of 352 amino acids. Using primer pairs located in exon 6 and intron 7 we could detect the long transcript in kidney, colon and small intestine (data not shown). The existence of this isoform became also apparent in our Northern blots, which revealed a second, approximately 5.2 kb large transcript in colon and small intestine (Fig. 2A). Since no antibody against the N-terminus of Kindlin-1 is currently available, it remains to be seen whether this transcript is translated and if so, which function this short Kindlin-1 protein might fulfil.

Since there is a strong interest in a detailed expression analysis of Kindlin-1 in skin, we separated epidermis from dermis. RT-PCR analysis indicated strong expression of

Kindlin-1 in the epidermis, and much weaker expression in the dermis (Fig. 1B). Whether the dermal expression is indeed derived from dermal cells or alternatively from hair follicle keratinocytes is unclear. Interestingly, Kindlin-2 is inversely expressed, with higher expression levels in the dermis than in the epidermis (Fig. 1B). This finding is particularly interesting, since Kindlin-2 seems not to compensate for the loss of Kindlin-1 in Kindler Syndrome. Whether this is due to the distinct expression in different cell layers of the skin or because of differences in the subcellular localization of both proteins within the keratinocytes needs to be addressed in the future.

Northern blot and RT-PCR analyses confirmed Kindlin-2 expression in all tissues analyzed. The levels differed between tissues and were high in heart, lung, skeletal muscle, kidney, bladder and stomach. In contrast to the broad expression pattern of Kindlin-2, Kindlin-3 showed a restricted expression pattern with signals in lung, spleen, thymus and very low in lymph nodes (Fig. 1A). RT-PCR confirmed a strong Kindlin-3 expression in hematopoietic tissues and much lower in other tissues, which may be due to contamination of these tissues by blood cells (Fig. 1C).

Expression of Kindlin genes during embryonic development was tested by RT-PCR from RNA samples derived from E7.5 to 18.5 embryos. All Kindlin genes are expressed throughout the analyzed time points, although Kindlin-3 expression was low at E7.5 and increases until E13.5 (Fig. 1D).

To determine the distribution of the Kindlin mRNAs during mouse development, we performed radioactive in situ hybridizations on mouse embryo sections from different developmental stages.

The same probes that were used for Northern blot experiments were subcloned into pBluescript to derive sense and antisense transcripts. As expected from the RT-PCR and

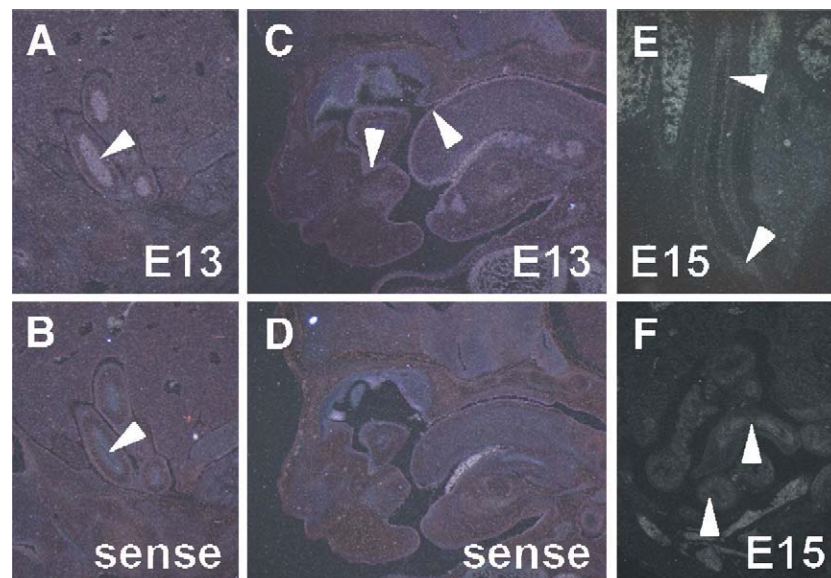


Fig. 2 – Radioactive in situ hybridizations on E13 and E15 mouse embryo sections reveal Kindlin-1 expression in the developing gut epithelium (arrowhead in panel A) and epithelium of the oral cavity and tongue at E13 (arrowheads in panel C). Consecutive sections hybridized with the sense probe indicate signal specificity (B, D). At E15, Kindlin-1 expression is found in the oesophageal epithelium (E) and gut epithelium (F).

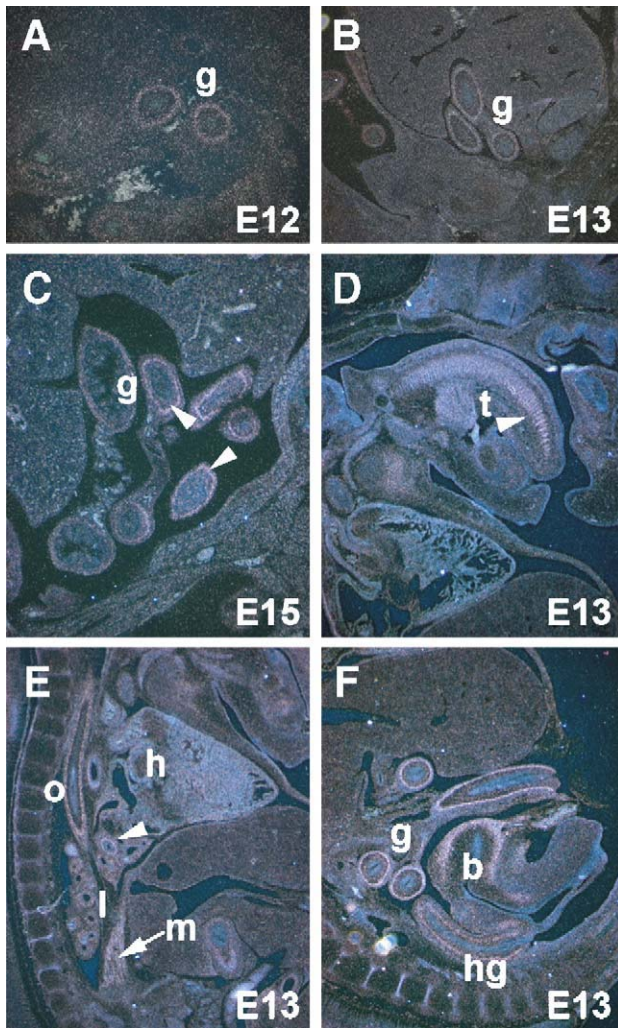


Fig. 3 – In situ hybridizations reveal Kindlin-2 expression in all three muscle types. Kindlin-2 is expressed in the smooth muscle layer of the developing gut at E12 (A), E13 (B) and E15 (C). In addition, Kindlin-2 expression is found in the smooth muscle layers surrounding the oesophagus (E), large vessels (arrowhead in panel E), around the bronchial epithelium of the lung (E), in the bladder and hindgut (both F). Expression in skeletal muscle is seen in the tongue and the diaphragm (D,E). A weaker signal is detected in cardiac muscle (E). b, bladder; g, gut; h, heart; hg, hindgut; l, lung; m, skeletal muscle; o, oesophagus; t, tongue.

Northern blot analyses, Kindlin-1 expression was hardly detected in the embryo. Weak signals could be detected in the epithelium of the gut from E12.5 onwards, as well as in the oral epithelium and oesophagus. Control hybridizations with the sense probe revealed no signal in these organs (Fig. 2). All attempts to detect Kindlin-1 in other embryonic or adult tissues were unsuccessful.

In contrast, Kindlin-2 expression was seen in many organs with strongest expression in the not sooth but smooth muscle cell layer of a number of organs including the developing gut, bladder, oesophagus and blood vessels (Fig. 3). Strong expression was also found in striated muscle such as tongue and

heart. In agreement with Northern blot and RT-PCR data, Kindlin-3 expression was restricted to hematopoietic organs such as the fetal liver and thymus. Interestingly, between E12.5 and E16.5 Kindlin-3 signals were detectable throughout the whole liver with strong signals in large multinucleated cells that most likely represent megakaryocytes (Figs. 4A–F). Weak staining was detected in the thymus (Figs. 4G, H). Based on the restricted expression of Kindlin-3 in adult hematopoietic tissues, the uniform signal in the embryonic liver was likely derived from lymphoid progenitor cells rather than from hepatocytes. In line with this notion, neither Northern blot nor RT-PCR revealed Kindlin-3 expression in adult liver (Figs. 1A and C).

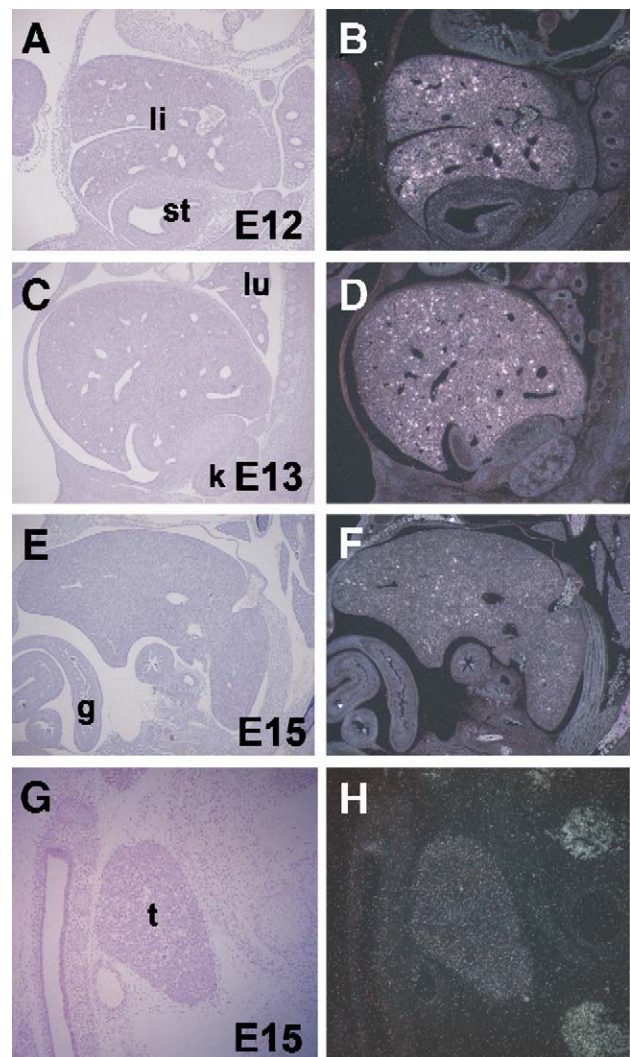


Fig. 4 – In situ hybridizations on sagittal sections of murine embryos at E12 (A, B), E13 (C, D), and E15 (E–H). Panels A, C, E, and G show brightfield views of panels B, D, F, and H, respectively. Kindlin-3 expression is mainly restricted to the developing liver with particularly strong signals in large multinucleated cells, most likely representing megakaryocytes (A–F). (G,H) Kindlin-3 is also expressed in thymus at E15. g, gut; k, kidney; li, liver; lu, lung; st, stomach; t, thymus.

Altogether these data indicate that Kindlin-1 expression is confined to epithelial cells of the skin and gut, Kindlin-2 expression is broad with high expression in striated and smooth muscle cells and Kindlin-3 expression is restricted to hematopoietic tissues.

Kindlin-3 is expressed in different hematopoietic cell types and is localized to podosomes

To date, the Kindlin-3 protein has not been investigated in any study. Therefore we generated a rabbit polyclonal antiserum against Kindlin-3 (see Materials and methods). The affinity purified antibody reacted with an approximately 100 kDa protein from mouse embryonic fibroblasts transfected with EGFP-tagged murine Kindlin-3 cDNA. As a control, cell lysates from fibroblasts transfected with EGFP-Kindlin-1 or -2 constructs showed no crossreactivity with the Kindlin-3 antibody (Fig. 5A). The anti-Kindlin-3 antibody was then used to immunoblot lysates derived from multiple organs of adult C57BL/6 mice. In accordance with the RNA data Kindlin-3 protein could be detected in spleen, thymus, lymph node and lung (Fig. 5B).

Due to this very broad expression pattern of Kindlin-3 within hematopoietic tissues, we addressed the expression in different hematopoietic cell types. Western Blots from MACS sorted T and B cells and in vitro differentiated macrophages, immature and mature dendritic cells were performed. Interestingly, Kindlin-3 was expressed in all these hematopoietic cell types at similar levels and seems not to be restricted to a specific hematopoietic lineage (Fig. 5C). Since Northern blot and RT-PCR analyses revealed weak expression of Kindlins-1 and -2 in spleen and thymus, we investigated expression of both genes in different hematopoietic cell types by RT-PCR. Interestingly, both Kindlins-1 and -2 are expressed in T cells and very weak in B cells (Fig. 5D).

Furthermore, the anti-Kindlin-3 antibody was used for immunohistochemical stainings of mouse embryo sections. The Kindlin-3 protein was observed in the developing liver with particularly high signals in megakaryocytes (Fig. 5E), confirming our in situ hybridization data (Figs. 4A-F).

To investigate the subcellular localization of Kindlin-3, we first overexpressed EGFP-tagged Kindlin-3 in murine fibroblasts. Unexpectedly, we could not observe any specific localization to FA but rather a diffuse cytoplasmic staining

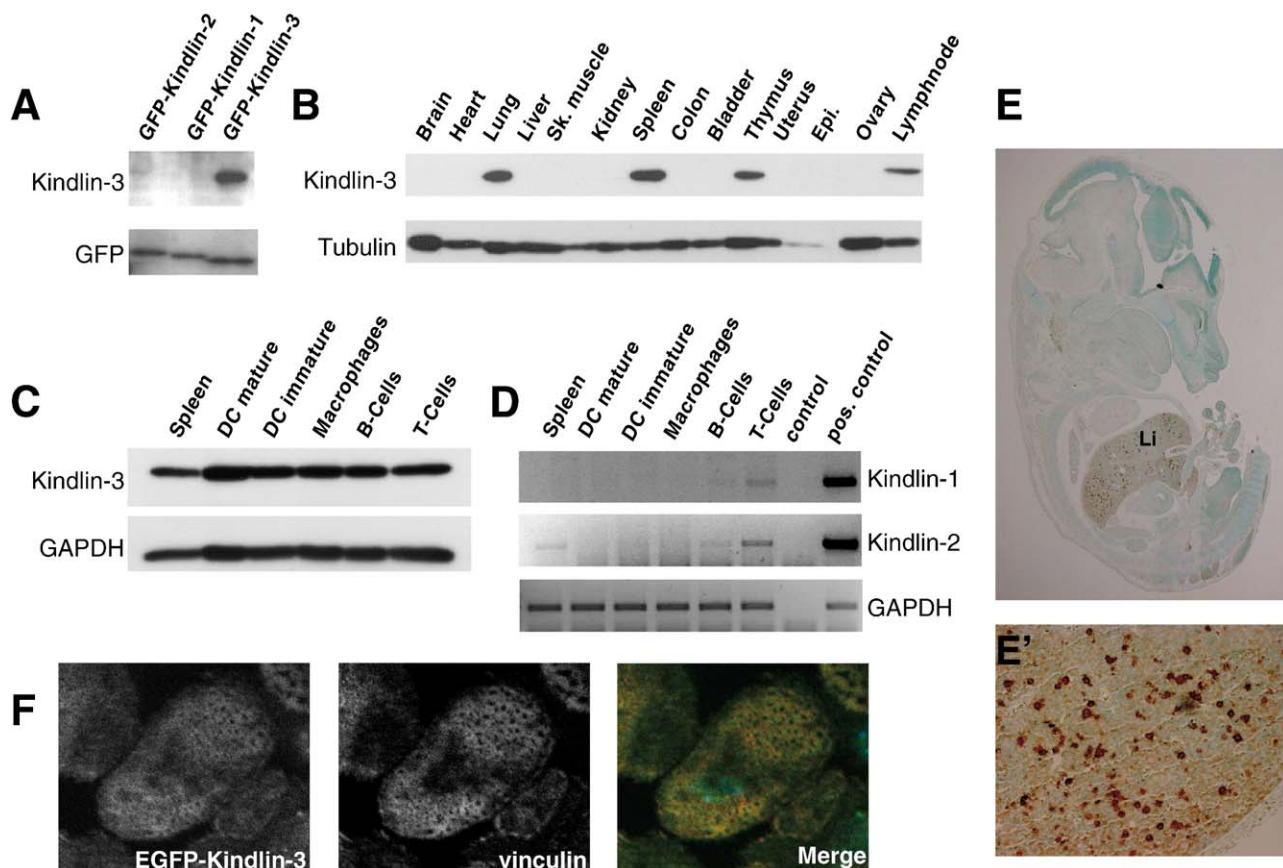


Fig. 5 – Hematopoietic expression pattern and typical subcellular localization of Kindlin-3. (A) Western blot of NIH3T3 cells transfected with EGFP-Kindlins-1/-2/-3 with the Kindlin-3 antibody. A GFP antibody was used to control loading. (B) Western blot of different mouse tissues from adult C57BL/6 probed with the Kindlin-3 antibody. Tubulin was used to control loading. (C) Western blot for Kindlin-3 from different hematopoietic cell types (DC: dendritic cells). GAPDH was used to control loading. (D) RT-PCR for Kindlin-1 and Kindlin-2 from different hematopoietic cell types. GAPDH was used to control loading. (E) Immunostaining of E14.5 embryo sections with Kindlin-3 antibody (Li: liver). (E') Higher magnification of the liver. (F) EGFP-Kindlin-3 colocalizes with vinculin in podosomes of cultured dendritic cells.

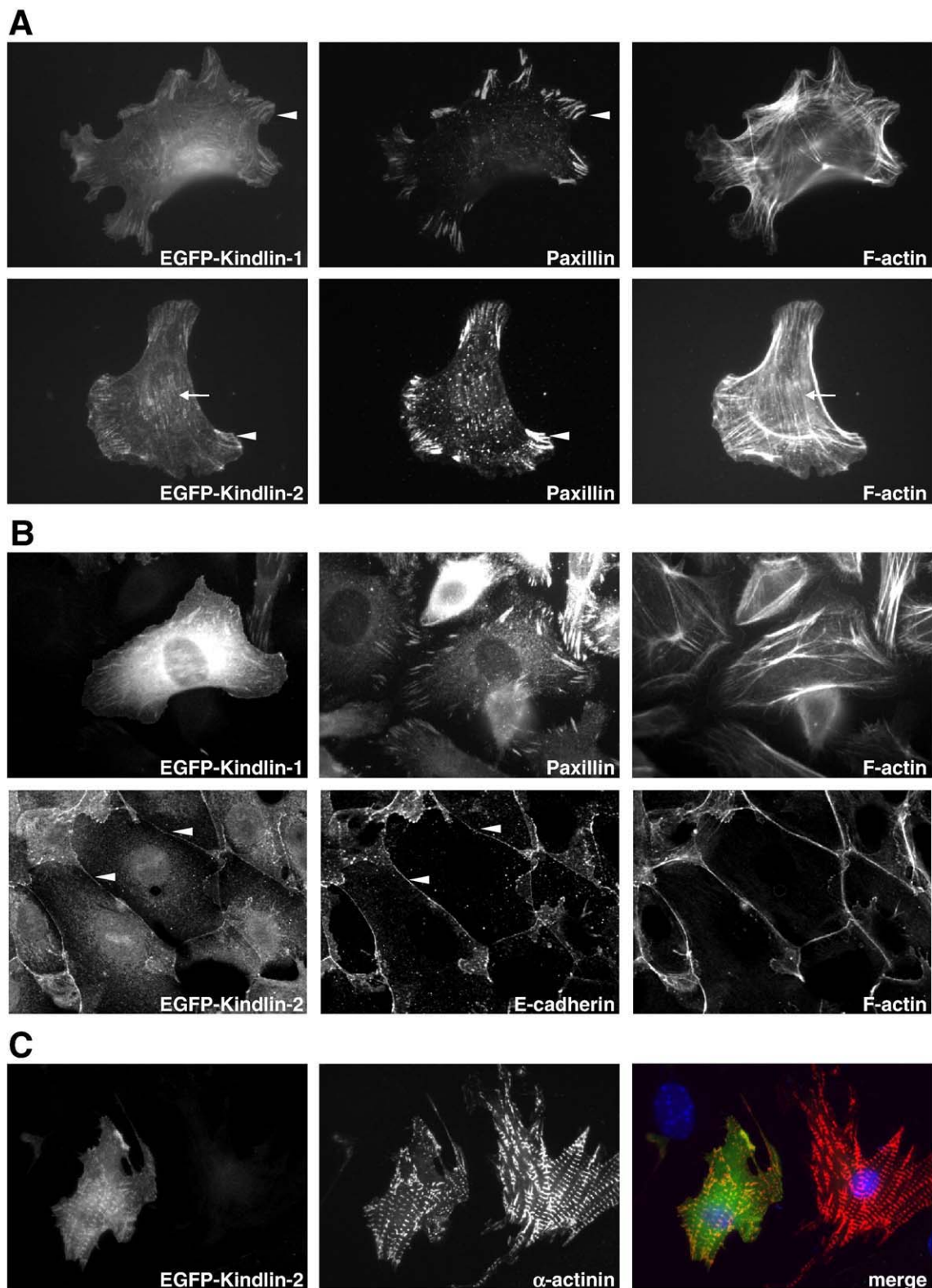


Fig. 6 – Subcellular localization of Kindlin-1 and Kindlin-2. **(A)** Mouse embryonic fibroblasts (MEFs) were seeded onto fibronectin and transiently transfected with EGFP-Kindlin-1 and EGFP-Kindlin-2, respectively. 24 h after transfection cells were costained for paxillin and F-actin. Arrowheads indicate focal adhesion sites. Arrows indicate colocalization with F-actin. **(B)** Spontaneously immortalized mouse keratinocytes were transiently transfected with EGFP-Kindlin-1. Cells were costained for paxillin and F-actin. EGFP-Kindlin-2 transfected cells were differentiated with 1 mM CaCl₂ overnight, and costained for E-cadherin and F-actin. Arrowheads show colocalization of EGFP-Kindlin-2 and E-cadherin at cell-cell contacts. **(C)** Primary mouse cardiomyocytes were transfected with EGFP-Kindlin-2 and after fixation costained with α -actinin.

(data not shown). This indicates that either Kindlin-3 differs in its localization from the other two family members or cannot compete with the endogenous Kindlin-2 for FA recruitment in these cells. Kindlin-1 and Kindlin-3 expression could not be detected in these cells by RT-PCR (data not shown). Therefore, we used immunofluorescence stainings of *in vitro* differentiated macrophages and dendritic cells. In contrast to fibroblasts or epithelial cells, hematopoietic cells do not form classical FA. Instead, they form podosomes, adhesion structures characterized by a core of F-actin and actin-associated proteins surrounded by a ring consisting of plaque proteins such as talin or vinculin (reviewed in [21] and [22]). Coimmunofluorescence stainings with phalloidin revealed that Kindlin-3 colocalizes to podosomes (data not shown). Therefore, a more detailed analysis of Kindlin-3 localization within podosomes was performed. Transfection of immature dendritic cells with EGFP-Kindlin-3 and subsequent staining for vinculin (Fig. 5F) and talin (data not shown) revealed Kindlin-3 localization to the actin surrounding ring of podosomes. Altogether these data show that Kindlin-3 is present in hematopoietic adhesion complexes and expressed in multiple hematopoietic cell lineages.

Kindlins-1 and -2 localize to different cell adhesion sites

Previous studies have localized human Kindlin-1 and Kindlin-2 to FAs. Using EGFP-tagged cDNA constructs transiently transfected into mouse embryonic fibroblasts, we tested the localization of murine Kindlins. Transfection of neither Kindlin constructs nor the EGFP control affected cell morphology during cell spreading when compared to untransfected cells (data not shown).

Kindlin-1 colocalized with paxillin to focal complexes and FAs (Fig. 6A). A similar staining pattern was also observed for Kindlin-2 suggesting that Kindlins-1 and -2 are recruited to newly formed focal contacts, and hence may play an important role during the assembly of the cell–matrix adhesion complex. In addition to the integrin-containing adhesion structures, Kindlin-2 also localized to actin stress fibers. Altogether these data indicate that all three Kindlin proteins localize to specific cell–matrix adhesion sites *in vitro*.

Our *in situ* hybridizations suggested a preferential expression of Kindlin-1 in epithelial cells and Kindlin-2 in striated and smooth muscle cells *in vivo*. Therefore we investigated the localization of Kindlins-1 and -2 in immortalized mouse keratinocytes and of Kindlin-2 in addition in primary cardiomyocytes.

Keratinocytes transfected with EGFP-Kindlin-1 revealed fluorescent labeling of paxillin-positive FAs and phalloidin-positive actin stress fibers (Fig. 6B). A similar staining pattern could be observed for Kindlin-2 (data not shown). However, cells transfected with EGFP-Kindlin-1 often revealed a strong perinuclear and a weak filamentous signal that failed to colocalize with F-actin. Whether these signals are a consequence of Kindlin-1 overexpression or indeed represent an additional subcellular localization of Kindlin-1 outside of FAs remains to be addressed. Furthermore, we investigated the localization of Kindlins-1 and -2 in calcium differentiated keratinocytes. Surprisingly, we could not observe localization of EGFP-Kindlin-1 to cell–cell contacts, as previously assumed [8] (data not shown). In contrast, EGFP-Kindlin-2 colocalized

with E-cadherin to cell–cell contacts (Fig. 6B). This result is the first indication that Kindlins-1 and -2 can localize to different subcellular compartments. It could explain why Kindlin-2 cannot compensate for Kindlin-1 loss in Kindler Syndrome. Unfortunately, no Kindlin-1 or -2-specific antibodies are available, which would be required to investigate the subcellular localization *in vivo*.

To test the localization of Kindlin-2 in muscle cells, we isolated primary cardiomyocytes from newborn mice and transfected them with EGFP-tagged Kindlin-2. Kindlin-2 colocalized with α -actinin to Z-discs of cardiomyocytes (Fig. 6C). This observation implies that Kindlin-2 like UNC-112 plays an important role in the organization of cell–matrix adhesion sites in muscle cells.

In summary, our analyses revealed that all three Kindlins are expressed during early development, but expression of each isoform is restricted to certain tissues and cell types. This is most evident for Kindlin-3, which is exclusively expressed in cells of hematopoietic origin. The expression pattern of Kindlins-1 and -2 show a partial overlap, although with a preference for Kindlin-1 expression in epithelial cells of the skin and the gastrointestinal tract and Kindlin-2 in striated and smooth muscle cells. Kindlins-1 and -2-specific antibodies will be important tools to investigate their subcellular localization in more detail *in vivo*. This is medically relevant, since our analyses demonstrate that Kindlin-2 is expressed in the epidermis but can apparently not compensate for the loss of Kindlin-1 expression in Kindler syndrome patients. This observation is in line with our *in vitro* data indicating that in contrast to Kindlin-1, Kindlin-2 localizes to cell–cell contacts of differentiated keratinocytes and might therefore be less involved in the cell–matrix adhesion of keratinocytes. Identification of novel Kindlin binding partners will be one important aim to understand the cellular functions of Kindlin proteins. Additionally, Kindlin-deficient mice could give important insights into the function of this gene family during development and disease.

Acknowledgments

We thank Melanie Ried for excellent technical assistance, Michael Sixt, Kyle Legate, Julia Schlehe and Tim Lämmermann for helpful suggestions and critical reading of the manuscript. Peter C. Weber and Jürgen Heesemann for the continuous support and Barbara Böhlig for expert technical assistance.

The work was supported by the DFG, the Max-Planck-Society and the Fonds der Chemischen Industrie to R.F.

REFERENCES

- [1] F. Jobard, B. Bouadjar, F. Caux, S. Hadj-Rabia, C. Has, F. Matsuda, J. Weissenbach, M. Lathrop, J.F. Prud'homme, J. Fischer, Identification of mutations in a new gene encoding a FERM family protein with a pleckstrin homology domain in Kindler syndrome, *Hum. Mol. Genet.* 12 (2003) 925–935.
- [2] M. Wick, C. Burger, S. Brusselbach, F.C. Lucibello, R. Muller, Identification of serum-inducible genes: different patterns of

- gene regulation during G0→S and G1→S progression, *J. Cell Sci.* 107 (1994) 227–239.
- [3] E.J. Weinstein, M. Bourner, R. Head, H. Zakeri, C. Bauer, R. Mazarella, URP1: a member of a novel family of PH and FERM domain-containing membrane-associated proteins is significantly over-expressed in lung and colon carcinomas, *Biochim. Biophys. Acta* 1637 (2003) 207–216.
- [4] R.S. Boyd, P.J. Adam, S. Patel, J.A. Loader, J. Berry, N.T. Redpath, H.R. Poyser, G.C. Fletcher, N.A. Burgess, A.C. Stamps, L. Hudson, P. Smith, M. Griffiths, T.G. Willis, E.L. Karran, D.G. Oscier, D. Catovsky, J.A. Terrett, M.J. Dyer, Proteomic analysis of the cell-surface membrane in chronic lymphocytic leukemia: identification of two novel proteins, BCNP1 and MIG2B, *Leukemia* 17 (2003) 1605–1612.
- [5] D.H. Siegel, G.H. Ashton, H.G. Penagos, J.V. Lee, H.S. Feiler, K.C. Wilhelmsen, A.P. South, F.J. Smith, A.R. Prescott, V. Wessagowit, N. Oyama, M. Akiyama, D. Al Aboud, K. Al Aboud, A. Al Githami, K. Al Hawsawi, A. Al Ismaily, R. Al-Suwaid, D.J. Atherton, R. Caputo, J.D. Fine, I.J. Frieden, E. Fuchs, R.M. Haber, T. Harada, Y. Kitajima, S.B. Mallory, H. Ogawa, S. Sahin, H. Shimizu, Y. Suga, G. Tadani, K. Tsuchiya, C.B. Wiebe, F. Wojnarowska, A.B. Zaghloul, T. Hamada, R. Mallipeddi, R.A. Eady, W.H. McLean, J.A. McGrath, E.H. Epstein, Loss of kindlin-1, a human homolog of the *Caenorhabditis elegans* actin-extracellular-matrix linker protein UNC-112, causes Kindler syndrome, *Am. J. Hum. Genet.* 73 (2003) 174–187.
- [6] S. Kloeker, M.B. Major, D.A. Calderwood, M.H. Ginsberg, D.A. Jones, M.C. Beckerle, The Kindler syndrome protein is regulated by transforming growth factor-beta and involved in integrin-mediated adhesion, *J. Biol. Chem.* 279 (2004) 6824–6833.
- [7] Y. Tu, S. Wu, X. Shi, K. Chen, C. Wu, Migfilin and Mig-2 link focal adhesions to filamin and the actin cytoskeleton and function in cell shape modulation, *Cell* 113 (2003) 37–47.
- [8] V. Gkretsi, Y. Zhang, Y. Tu, K. Chen, D.B. Stolz, Y. Yang, S.C. Watkins, C. Wu, Physical and functional association of migfilin with cell–cell adhesions, *J. Cell Sci.* 118 (2005) 697–710.
- [9] T.M. Rogalski, G.P. Mullen, M.M. Gilbert, B.D. Williams, D.G. Moerman, The UNC-112 gene in *Caenorhabditis elegans* encodes a novel component of cell–matrix adhesion structures required for integrin localization in the muscle cell membrane, *J. Cell Biol.* 150 (2000) 253–264.
- [10] M. Lotem, M. Raben, R. Zeltser, M. Landau, M. Sela, M. Wygoda, Z.A. Tochner, Kindler syndrome complicated by squamous cell carcinoma of the hard palate: successful treatment with high-dose radiation therapy and granulocyte-macrophage colony-stimulating factor, *Br. J. Dermatol.* 144 (2001) 1284–1286.
- [11] T. Kindler, Congenital poikiloderma with traumatic bulla formation and progressive cutaneous atrophy, *Br. J. Dermatol.* 66 (1954) 104–111.
- [12] G.H. Ashton, W.H. McLean, A.P. South, N. Oyama, F.J. Smith, R. Al-Suwaid, A. Al-Ismaïly, D.J. Atherton, C.A. Harwood, I.M. Leigh, C. Moss, B. Didona, G. Zambruno, A. Patrizi, R.A. Eady, J.A. McGrath, Recurrent mutations in kindlin-1, a novel keratinocyte focal contact protein, in the autosomal recessive skin fragility and photosensitivity disorder, Kindler syndrome, *J. Invest. Dermatol.* 122 (2004) 78–83.
- [13] S.J. White, W.H. McLean, Kindler surprise: mutations in a novel actin-associated protein cause Kindler syndrome, *J. Dermatol. Sci.* 38 (2005) 169–175.
- [14] K. Kato, T. Shiozawa, J. Mitsushita, A. Toda, A. Horiuchi, T. Nikaïdo, S. Fujii, I. Konishi, Expression of the mitogen-inducible gene-2 (mig-2) is elevated in human uterine leiomyomas but not in leiomyosarcomas, *Hum. Pathol.* 35 (2004) 55–60.
- [15] H. Akazawa, S. Kudoh, N. Mochizuki, N. Takekoshi, H. Takano, T. Nagai, I. Komuro, A novel LIM protein Cal promotes cardiac differentiation by association with CSX/NKX2-5, *J. Cell Biol.* 164 (2004) 395–405.
- [16] M. Moser, A. Imhof, A. Pscherer, R. Bauer, W. Amselgruber, F. Sinowatz, F. Hofstadter, R. Schule, R. Buettner, Cloning and characterization of a second AP-2 transcription factor: AP-2 beta, *Development* 121 (1995) 2779–2788.
- [17] A.H. Chishti, A.C. Kim, S.M. Marfatia, M. Lutchman, M. Hanspal, H. Jindal, S.C. Liu, P.S. Low, G.A. Rouleau, N. Mohandas, J.A. Chasis, J.G. Conboy, P. Gascard, Y. Takakuwa, S.C. Huang, E.J. Benz Jr., A. Bretscher, R.G. Fehon, J.F. Gusella, V. Ramesh, F. Solomon, V.T. Marchesi, S. Tsukita, S. Tsukita, M. Arpin, D. Louvard, N.K. Tonks, J.M. Anderson, A.S. Fanning, P.J. Bryant, D.F. Woods, K.B. Hoover, The FERM domain: a unique module involved in the linkage of cytoplasmic proteins to the membrane, *Trends Biochem. Sci.* 23 (1998) 281–282.
- [18] D.A. Calderwood, B. Yan, J.M. de Pereda, B.G. Alvarez, Y. Fujioka, R.C. Liddington, M.H. Ginsberg, The phosphotyrosine binding-like domain of talin activates integrins, *J. Biol. Chem.* 277 (2002) 21749–21758.
- [19] B. Garcia-Alvarez, J.M. de Pereda, D.A. Calderwood, T.S. Ulmer, D. Critchley, I.D. Campbell, M.H. Ginsberg, R.C. Liddington, Structural determinants of integrin recognition by talin, *Mol. Cell.* 11 (2003) 49–58.
- [20] M.A. Lemmon, K.M. Ferguson, Signal-dependent membrane targeting by pleckstrin homology (PH) domains, *Biochem. J.* 350 (2000) 1–18.
- [21] S. Linder, P. Kopp, Podosomes at a glance, *J. Cell Sci.* 118 (2005) 2079–2082.
- [22] S. Linder, M. Aepfelbacher, Podosomes: adhesion hot-spots of invasive cells, *Trends Cell Biol.* 13 (2003) 376–385.

Paper II

RESEARCH COMMUNICATION

Kindlin-2 controls bidirectional signaling of integrins

Eloi Montanez,^{1,3} Siegfried Ussar,^{1,3}
Martina Schifferer,¹ Michael Bösl,¹ Roy Zent,²
Markus Moser,¹ and Reinhard Fässler^{1,4}

¹Department of Molecular Medicine, Max Planck Institute of Biochemistry, 82152 Martinsried, Germany; ²Division of Nephrology, Department of Medicine, Vanderbilt Medical Center and Veterans Affairs Hospital, Nashville, Tennessee 37232, USA

Control of integrin activation is required for cell adhesion and ligand-induced signaling. Here we report that loss of the focal adhesion protein Kindlin-2 in mice results in peri-implantation lethality caused by severe detachment of the endoderm and epiblast from the basement membrane. We found that Kindlin-2-deficient cells were unable to activate their integrins and that Kindlin-2 is required for talin-induced integrin activation. Furthermore, we demonstrate that Kindlin-2 is required for integrin outside-in signaling to enable firm adhesion and spreading. Our findings provide evidence that Kindlin-2 is a novel and essential element of bidirectional integrin signaling.

Supplemental material is available at <http://www.genesdev.org>.

Received January 3, 2008; revised version accepted March 10, 2008.

The establishment and maintenance of cell–extracellular matrix (ECM) and cell–cell interactions are essential for the development of multicellular organisms. These interactions are mediated via membrane-associated proteins that firmly bind to ECM proteins or cell counter-receptors. The integrins, consisting of at least 24 members, represent the largest and most important family of cell–ECM receptors in vertebrates (Hynes 2002). Integrins are heterodimeric glycoproteins composed of α and β subunits. Each subunit consists of a large extracellular domain, a transmembrane domain, and a short cytoplasmic domain. Integrins are bidirectional signaling molecules. They regulate their affinity for ligand (integrin activation) by direct interactions of the β -subunit cytoplasmic tails with the cytoskeletal protein talin (inside-out signaling) (Calderwood et al. 1999, 2002; Wegener et al. 2007). Following ligand binding, integrins transduce signals into cells (outside-in signaling) by recruiting signaling and adaptor proteins to the cytoplasmic tails of the α and/or β subunits, which results in actin reorgani-

zation and modulation of various intracellular signaling pathways (Hynes 2002).

Kindlins are a novel family of adaptor proteins that are recruited to integrin-containing adhesion sites, termed focal adhesions (FAs) (Rogalski et al. 2000; Tu et al. 2003; Weinstein et al. 2003; Ussar et al. 2006). The Kindlin family consists of three members, termed Kindlin-1/Unc-112-Related Protein 1 (URP1), which is expressed in epithelial cells; Kindlin-2/Mig-2, which is ubiquitously expressed; and Kindlin-3/URP2, whose expression is restricted to hematopoietic cells. The structural hallmark of Kindlins is a FERM (Band 4.1/Ezrin/Radixin/Moesin) domain that was shown to associate with the β 1-integrin subunit cytoplasmic tails (Kloeker et al. 2004; Shi et al. 2007).

Kindlin-1 is the founding member of the Kindlin family. Mutations in the *Kindlin-1* gene lead to Kindler syndrome in humans, which is characterized by skin blistering (Jobard et al. 2003; Siegel et al. 2003). The defect in Kindler patients suggested a role of Kindlin-1 in integrin–ECM adhesion in vivo. This assumption has been corroborated further in siRNA-mediated depletion studies of Kindlins in different cell lines and genetic analyses of the Kindlin-2 ortholog in *Caenorhabditis elegans*. Knockdown experiments in mammalian cells showed that Kindlin-1 and Kindlin-2 are essential for integrin-mediated cell–ECM adhesion and spreading (Tu et al. 2003; Kloeker et al. 2004). Absent expression of UNC-112, the nematode ortholog of the mammalian Kindlins, gives rise to a PAT (paralyzed, arrested elongation at twofold) phenotype. The embryonic lethality of UNC-112 mutants is caused by an abrogated integrin function leading to pronounced muscle cell rounding and detachment. An identical phenotype is also observed in nematodes lacking the expression of PAT-3/ β integrin or PAT-4/ILK and, consistent with this observation, UNC-112/Kindlin was shown to be required for the proper spatial localization of PAT-3/ β integrin and PAT-4/ILK to cell–ECM adhesion sites (Rogalski et al. 2000; Mackinnon et al. 2002).

To address the role of Kindlin-2 in vivo, we generated mice, embryonic stem cells (ESCs), and embryoid bodies (EBs) lacking Kindlin-2 expression. We found that Kindlin-2 is required for integrin activation. The consequences of impaired integrin activation in Kindlin-2-deficient mice are severe endoderm and epiblast detachments, which arrest development at the peri-implantation stage.

Results and Discussion

Loss of Kindlin-2 leads to peri-implantation lethality and impaired integrin activation

To investigate Kindlin-2 function, we disrupted the *Kindlin-2* gene in mice (Supplemental Fig. 1). Mice with a heterozygous Kindlin-2-null mutation (*Kindlin-2*^{+/-}) were viable and normal (data not shown). Among 166 newborn offspring from *Kindlin-2*^{+/-} intercrosses, 67% were *Kindlin-2*^{+/-} and 33% were wild type. Timed mating of *Kindlin-2*^{+/-} intercrosses revealed that *Kindlin-2*^{+/-} embryos were missing at embryonic day 7.5 (E7.5), and histology of implantation chambers at E6.5 showed that 74% of the embryos were normally developed (presumptive wild type or *Kindlin-2*^{+/-}) and 26% were severely

[*Keywords*: Integrin activation; Kindlin-2; adhesion; mouse development; embryonic stem cells]

³These authors contributed equally to this work.

⁴Corresponding author.

E-MAIL faessler@biochem.mpg.de; FAX 49-89-8578-2422.

Article is online at <http://www.genesdev.org/cgi/doi/10.1101/gad.469408>.

Montanez et al.

misshapen or already partially resorbed (putative Kindlin-2^{-/-}) (Fig. 1A). These results suggest that ablation of Kindlin-2 leads to lethality at the peri-implantation stage.

To analyze the function of Kindlin-2 in vitro, we established wild-type and Kindlin-2^{-/-} ESCs. While Kindlin-2^{-/-} ESCs were readily obtained and showed a normal proliferation rate, their colonies barely adhered to the feeder layer and were less compact than wild-type ESC colonies (Fig. 1B). Western blot analysis revealed that Kindlin-2 is the only Kindlin expressed in ESCs and its expression was lost in Kindlin-2^{-/-} ESCs (Fig. 1C; data not shown). To test whether the poor adhesion of Kindlin-2^{-/-} ESC colonies to the feeder layer is caused by impaired adhesion to ECM proteins deposited by feeder cells, we performed adhesion assays on defined ECM

substrates. They revealed that wild-type ESCs readily adhered to laminin-111 (LN111), laminin-332 (LN332), or fibronectin (FN), while Kindlin-2^{-/-} ESCs showed strongly reduced adhesion to these substrates (Fig. 1D).

To exclude impaired integrin expression as the reason for the severe adhesion defects of Kindlin-2^{-/-} ESCs, the expression levels of major ESC integrins were determined by flow cytometry and were found to be similar to wild-type ESCs (Fig. 1E). Next we tested whether diminished integrin-binding affinity (activation) is responsible for the adhesion defect. To this end, we compared the binding of a fluorescently labeled FN fragment containing the central cell-binding domain for α v and α 5 β 1 integrins (FNIII7-10) to wild-type and Kindlin-2^{-/-} ESCs. Interestingly, the binding of FNIII7-10 to Kindlin-2^{-/-} ESCs was strongly reduced when compared with wild-type ESCs (Fig. 1F). The antibody 9EG7, which specifically recognizes activated mouse β 1 integrins, also failed to bind Kindlin-2^{-/-} ESCs (Fig. 1G). When cellular activation of integrins was bypassed by the addition of MnCl₂, a powerful activator of integrins (Chen et al. 2003), wild-type as well as Kindlin-2^{-/-} ESCs bound significant amounts of FNIII7-10 fragment (Fig. 1F). Collectively, these findings show that loss of Kindlin-2 prevents integrin activation.

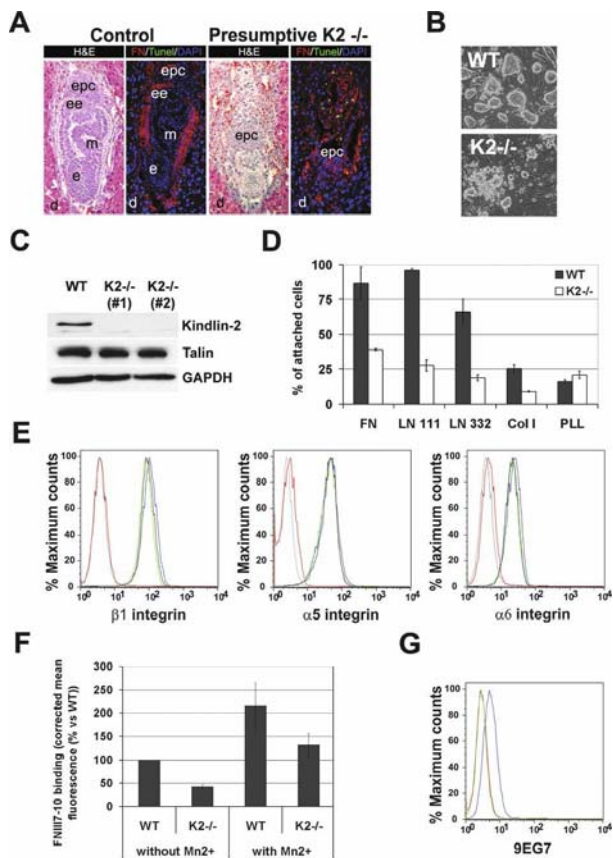


Figure 1. Peri-implantation lethality and impaired integrin activation in ESCs in the absence of Kindlin-2 expression. (A) Hematoxylin and eosin staining of an E6.5 control and presumptive Kindlin-2^{-/-} implantation chamber. TUNEL staining (green) and FN staining (red) show apoptosis and disturbed matrix deposition in Kindlin-2^{-/-} embryos. Nuclei are counterstained with DAPI (blue). (B) Bright-field pictures of wild-type and Kindlin-2^{-/-} ESCs lines seeded on feeder cells. (C) Western Blot for Kindlin-2 and talin in wild-type and two independent Kindlin-2^{-/-} ESCs lines. (D) Adhesion assay of wild-type and Kindlin-2^{-/-} ESCs on different ECM substrates. (E) Integrin surface expression of wild-type (blue), Kindlin-2^{-/-} (light and dark green), and β 1-integrin^{-/-} (red) ESC lines. A background control is shown in gray. (F) Binding of FNIII7-10 to wild-type and Kindlin-2^{-/-} ESCs in the presence and absence of MnCl₂. (G) 9EG7 binding on wild-type (blue) and Kindlin-2^{-/-} (green) ESC lines. A background control is shown in red. (d) Decidua; (epc) ectoplacental cone; (ee) extraembryonic ectoderm; (e) ectoderm; (m) mesoderm.

Kindlin-2-integrin interaction enhances talin-mediated integrin activation

It is currently believed that talin binding to β -integrin tails is necessary and sufficient to trigger the activation of integrins (Calderwood et al. 1999, 2002; Wegener et al. 2007). Talin levels, however, were not decreased in Kindlin-2^{-/-} ESCs (Fig. 1C), indicating that Kindlin-2 does not control integrin activation by regulating talin levels. To test whether Kindlin-2 controls integrin activation by binding to the β tails, we performed pull-down assays with GST-tagged β 1- and β 3-integrin cytoplasmic tails. We found that Kindlin-2 in wild-type ESC lysates bound the β 1- and β 3-integrin tails. Moreover, substitutions of the tyrosine (Y) to alanine (A) in the proximal NPxY motifs of the β 1 and β 3 tails (β 1Y788A; β 3Y747A), known to abrogate talin binding (Calderwood et al. 2002), did not diminish Kindlin-2 association. However, mutation of the distal NxxY motifs (β 1Y800A; β 3Y759A), which is known to be dispensable for talin binding but required for integrin activation (Xi et al. 2003), completely abolished the interaction with Kindlin-2 (Fig. 2A). To test whether the interaction between β -integrin tails and Kindlin-2 is direct, pull-down assays were performed with purified GST-tagged Kindlin-2 phosphotyrosine-binding (PTB) domain and recombinant His-tagged β 1-integrin cytoplasmic tail. They demonstrated that the Kindlin-2 PTB domain was able to interact with β 1-integrin cytoplasmic tails and that this interaction was eliminated by mutating the PTB domain (QW614/615AA) of Kindlin-2 (Fig. 2B). Together, these results indicate that, despite the sequence similarities between the FERM domains of talin and Kindlin-2, these proteins bind distinct sites within the β 1- and β 3-integrin tails.

Since Kindlin-2 can directly bind β 1- and β 3-integrin tails and is essential for ESC adhesion and binding to ECM substrates, we hypothesized that a potential role of Kindlin-2 could be to regulate integrin affinity for ligands. To confirm this hypothesis, we overexpressed Kindlin-2 in CHO cells engineered to express the inactive form of the

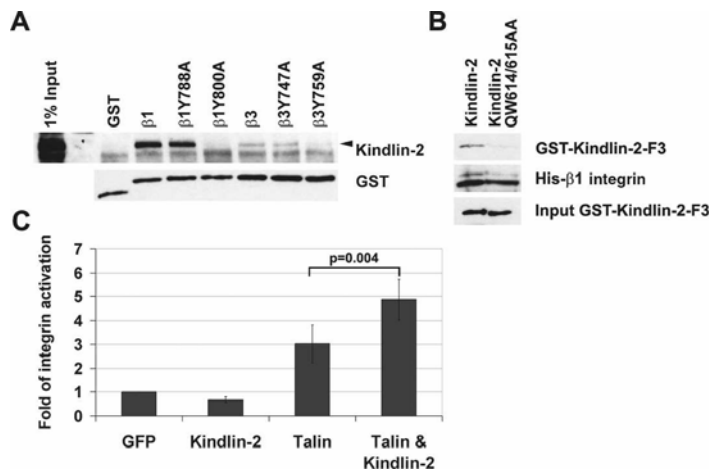


Figure 2. Kindlin-2 interacts with integrin tails and is required for integrin activation. (A) GST pull-down assay from ESC lysates with wild-type and mutant GST-tagged $\beta 1$ - and $\beta 3$ -integrin cytoplasmic tails. (B) Pull-down assays with the recombinant GST-tagged wild-type and mutant (QW614/615AA) PTB domain of Kindlin-2 and the recombinant His-tagged $\beta 1$ -integrin cytoplasmic tail. (C) $\alpha \text{IIb}\beta 3$ -integrin activation in CHO cells transfected with EGFP, EGFP-Kindlin-2, EGFP-Talin head, and EGFP-Kindlin-2 together with the Talin head.

human platelet integrin $\alpha \text{IIb}\beta 3$ (O'Toole et al. 1994). As shown previously, overexpression of the talin FERM domain is sufficient to activate the $\alpha \text{IIb}\beta 3$ integrin (Fig. 2C; Calderwood et al. 2002). Interestingly, overexpression of Kindlin-2 did not significantly change integrin activation when compared with EGFP-transfected cells. However, expression of the talin FERM domain together with Kindlin-2 resulted in a synergistic effect on $\alpha \text{IIb}\beta 3$ -integrin activation. These results clearly demonstrate that Kindlin-2 acts in concert with talin to trigger the activation of $\beta 3$ integrins.

Kindlin-2^{-/-} EBs show severe endoderm and epiblast detachments

To investigate whether the peri-implantation defect of Kindlin-2^{-/-} embryos is caused by an integrin activation defect, we generated EBs from wild-type and Kindlin-2^{-/-} ESCs (Li et al. 2003; Montanez et al. 2007). When wild-type and Kindlin-2^{-/-} ESCs were cultured in suspension for 2–4 d, they developed into simple EBs consisting of an outer layer of primitive endoderm cells and a core of undifferentiated ESCs. By day 4–6 in suspension, wild-type EBs developed into cystic EBs consisting of an outer layer of cubical-shaped endoderm cells, an inner layer of columnar pseudostratified epithelial cells (called epiblast or primitive ectoderm), a thin and continuous basement membrane (BM) between epiblast and endoderm, and a central cavity (Fig. 3A–C). Immunostaining with 9EG7 antibody revealed that endoderm and epiblast cells expressed activated integrins adjacent to their BM (Fig. 3D). In contrast, Kindlin-2^{-/-} EBs were severely abnormal. About half of Kindlin-2^{-/-} simple EBs did not develop further and degenerated. They consisted of a compact aggregate of ESCs covered by a discontinuous, spotted BM and detached endoderm. Despite evidence of scattered apoptotic cells, they lacked discernible cavities. This phenotype is similar to that

described in $\beta 1$ -integrin^{-/-} EBs, which arrested their development at the same stage of differentiation, showing defects in LN- $\alpha 1$ secretion and impaired cavitation (Aumailley et al. 2000; Li et al. 2002). The remaining half of the Kindlin-2^{-/-} EBs formed an epiblast layer with poorly developed cavities and BMs and varying degrees of endoderm and epiblast detachment (Fig. 3A–C). The absence of 9EG7 staining at the basal sites of endoderm and epiblast cells indicates that $\beta 1$ integrins of Kindlin-2^{-/-} EBs were expressed in an inactive conformation (Fig. 3D). The abnormal BM contained all major proteins including LN- $\alpha 1$ (Supplemental Fig. 2A,B), suggesting that loss of Kindlin-2 does not impair expression and secretion of BM proteins. We reported previously that Kindlin-2 colocalizes with E-cadherin at cell–cell junctions (Ussar et al. 2006). Interestingly, however, Kindlin-2^{-/-} EBs showed a normal E-cadherin distribution and developed normal cell–cell junctions (Supplemental Fig. 3; data not shown), indicating that they are not required for the establishment of cell junctional complexes in EBs. Together, these findings show that loss of Kindlin-2 expression impairs the activity of integrins in developing EBs, resulting in severe cell–ECM adhesion defects, abnormal BM de-

positions, abnormal cavity formation, and impaired cell survival.

Kindlin-2 is required for actin polarization, cell spreading, and ILK localization into FAs

In endoderm and epiblast cells from wild-type EBs, F-actin predominantly accumulated at E-cadherin-positive adherens junctions to form the characteristic apical F-actin belt. In contrast, BM-attached endoderm and epiblast cells of Kindlin-2^{-/-} EBs showed in addition to the apical F-actin belt a prominent F-actin accumulation at

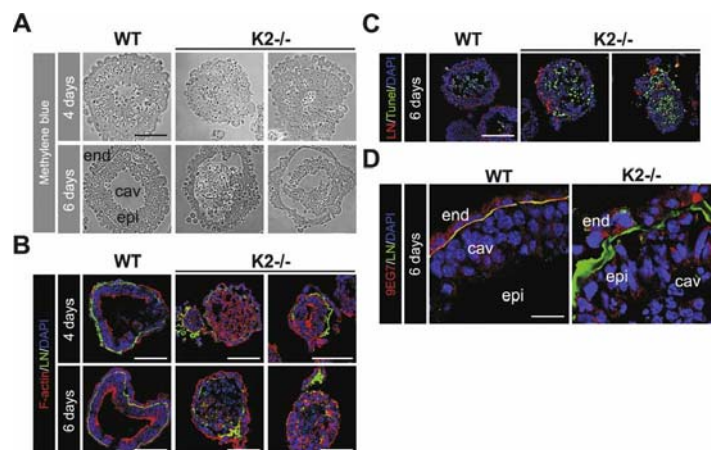


Figure 3. Kindlin-2 EBs show endoderm and epiblast detachment and diminished integrin activation. (A) Micrographs of methylene blue-stained sections of 4- and 6-d-old wild-type and Kindlin-2^{-/-} EBs. (B) Cryosections of wild-type and Kindlin-2^{-/-} EBs were stained with an antibody specific for LN- $\alpha 1$ chain (green) and fluorescently labeled phalloidin to visualize F-actin (red). Nuclei are counterstained with DAPI (blue). (C) TUNEL staining (green), LN- $\alpha 1$ chain (red), and nuclei (blue) of 6-d-old wild-type and Kindlin-2^{-/-} EBs. (D) Six-day-old wild-type and Kindlin-2^{-/-} EBs stained with LN- $\alpha 1$ chain (green) and 9EG7 (red) antibodies. Nuclei are counterstained with DAPI (blue). (epi) Epiblast; (end) endoderm.

Montanez et al.

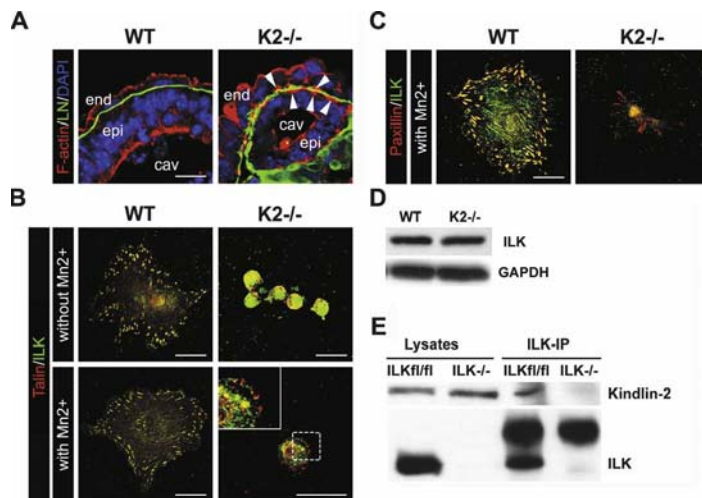


Figure 4. Impaired cell spreading of Kindlin-2^{-/-} endoderm cells. (A) Cryosections of 6-d-old wild-type and Kindlin-2^{-/-} EBs stained with LN- α 1 chain antibody (green) and fluorescently labeled phalloidin to visualize F-actin (red). Nuclei are counterstained with DAPI (blue). (B) Immunofluorescence staining for talin (red) and ILK (green) of wild-type and Kindlin-2^{-/-} endoderm cells seeded of FN in the presence or absence of MnCl₂. (C) Immunofluorescence staining for paxillin (red) and ILK (green) of wild-type and Kindlin-2^{-/-} endoderm cells seeded of FN in the presence of MnCl₂. (D) Western blot analysis of ILK in wild-type and Kindlin-2^{-/-} endoderm cells. (E) Coimmunoprecipitation of ILK and Kindlin-2 from ILK^{fl/fl} and ILK^{-/-} fibroblasts.

their basal sites, indicating that loss of Kindlin-2 affects F-actin polarization (Fig. 4A). To determine the mechanism by which Kindlin-2 depletion affects actin reorganization, we isolated endoderm cells from wild-type and Kindlin-2^{-/-} EBs and plated them on FN. Endoderm cells from wild-type EBs readily adhered to FN, spread, and formed multiple FAs. In contrast, loss of Kindlin-2 expression abrogated adhesion and spreading to FN (Fig. 4B). To determine if this difference in the phenotype was only due to lack of integrin activation, the Kindlin-2^{-/-} endoderm cells were treated with MnCl₂ (Cluzel et al. 2005) and then plated on FN for 3 h. Under these conditions, Kindlin-2^{-/-} cells developed only a few FA-like structures containing talin and paxillin and were still incapable of spreading (Fig. 4B). In nematodes, the ortholog of Kindlin called Unc-112 was shown to bind and recruit ILK to integrin adhesion sites (Mackinnon et al. 2002). ILK forms a complex together with the adaptor proteins PINCH and parvin that regulates cell spreading and actin cytoskeleton organization (Legate et al. 2006). Interestingly, ILK was either absent from the FA-like structures in Kindlin-2^{-/-} cells (Fig. 4C) or did not properly colocalize with other FA proteins (Fig. 4B). Western blot analysis revealed normal ILK levels in Kindlin-2^{-/-} endoderm cells, and immunoprecipitation assays with lysates from fibroblasts showed that Kindlin-2 interacts with ILK (Fig. 4D,E). These results indicate that Kindlin-2 is dispensable for ILK stability but required for ILK localization into integrin-containing adhesion sites. This observation together with the impaired FA formation and spreading suggest that Kindlin-2 is required for integrin inside-out as well as for integrin outside-in signaling.

The results of our study show that Kindlin-2 is a novel and essential component for integrin inside-out and outside-in signaling, and its absence results in a peri-implantation lethality in mice. We found that loss of Kindlin-2 severely impairs activation of β 1 and β 3 integrins and that, following Mn²⁺ treatment Kindlin-2^{-/-} endo-

derm cells fail to form multiple FAs and were incapable of spreading.

Bidirectional integrin signaling requires interactions between the cytoplasmic domains of the integrins and intracellular signaling molecules. It is currently believed that the interaction between the membrane-proximal NPxY motif of the integrin β cytoplasmic domain and talin is necessary and sufficient for integrin activation (Calderwood et al. 2002). Using conditional gene ablation, it was shown recently that talin is indeed essential for integrin activation in vivo (Nieswandt et al. 2007; Petrich et al. 2007). In contrast to the previous assumptions, however, our findings indicate that talin is not sufficient for triggering the activation of integrins, at least in ESCs, primitive endoderm, and epiblast, which clearly require Kindlin-2 for this process. In line with this observation, loss of Kindlin-3 was also found to compromise integrin activation on platelets, rendering

them incapable of binding integrin ligands such as fibrinogen or collagen despite the expression of normal levels of talin (Moser et al. 2008). Future studies are now needed to investigate whether all cell types require Kindlins for integrin activation; whether the entire Kindlin family, including Kindlin-1, can trigger integrin activation; and to what extent the different Kindlins can compensate each other.

Interestingly, it has been shown previously that the membrane-distal NxxY motif of the β 3-integrin cytoplasmic domain is required for bidirectional integrin signaling, although the binding partner for the distal NxxY motif remained elusive (Xi et al. 2003). In our pull-down studies, we found that Kindlin-2 bound specifically the membrane-distal NxxY motif since the substitution of Y759 to an A residue eliminated the interaction of Kindlin-2 with the integrin tail. Therefore, we propose that Kindlin-2 mediates integrin activation (1) through a direct interaction of the PTB site in the F3 subdomain of Kindlin-2 and the distal NxxY motif of the β 1- and β 3-integrin cytoplasmic domains, and (2) in cooperation with talin, which binds the proximal NPxY motif of integrin tails. The close proximity of the two NPxY motifs raises questions about the hierarchy of their binding to the β -integrin tails and the specific roles of Kindlin-2 and talin in integrin activation. Future studies examining how and at which step of integrin activation Kindlin-2 and talin cooperate will be instrumental to our understanding of how these receptors become activated. Finally, we also found that elimination of Kindlin-2 also prevents the formation of multiple FAs, recruitment of ILK to integrin adhesion sites, and cell spreading. Hence, Kindlin-2 also seems to be involved in integrin outside-in signaling. A similar double function has been assigned to talin, since thrombin treatment of talin-deficient platelets failed to trigger their spreading on immobilized fibrinogen (Nieswandt et al. 2007). In analogy to talin, Kindlin-2 fulfills an important requirement of a bidirec-

tional signaling relay for integrins: Upon integrin activation and cell adhesion, Kindlin-2 remains in focal complexes and FAs (Ussar et al. 2006) and is thus optimally positioned to transduce signals from the integrin tail to downstream effectors.

Materials and methods

Generation of Kindlin-2-deficient mice

A 417-base-pair fragment was amplified from mouse genomic DNA using the primers (fwd) TTCTTCAGGGTGTAGCTACTGG and (rev) CACCCCTAGAAAGACAGAAATAG, and was used to screen a PAC (phage artificial chromosome) library (BACPAC Resource Center) and as an external probe for ESC genotyping. The PAC clone 638-M21 Mouse PAC (RPC121) was used to generate the Kindlin-2 knockout construct. To abolish Kindlin-2 gene function, an IRES- β -galactosidase cassette followed by a PGK neomycin resistance cassette was inserted into exon 2.

Antibodies and TUNEL staining

The following antibodies were used: rat antibody against $\beta 1$ integrin, clone MB1.2 (Chemicon); rat antibody against $\beta 1$ integrin, 9E7 epitope (BD Bioscience); mouse antibody against talin (Sigma); rabbit antibody against LN- $\alpha 1$ chain (a gift from Rupert Timpl); rat antibody against LN- $\alpha 1$ chain (Chemicon); rabbit antibody against GAPDH (Calbiochem); rabbit antibody against ILK (Cell Signaling Technology); mouse antibody against paxillin (Transduction Laboratories); Cy3- and FITC-conjugated antibodies specific for mouse IgG, rabbit IgG, and rat IgG (Jackson Immunochemicals Laboratories, Inc.) were used as secondary antibodies. TRITC-conjugated phalloidin was used to detect F-actin (Molecular Probes). A Kindlin-2-specific polyclonal antibody was produced in rabbits (Ussar et al. 2006).

Apoptosis in embryos and EB sections was analyzed with the In situ Cell Death Detection Kit, POD (TUNEL technology; Roche).

ESC adhesion assay

ESCs were trypsinized and plated on cell tissue culture dishes for 30 min to remove the feeder cells. ESCs were then plated onto 96-well plates coated with FN, LN, or collagen IV at 1×10^5 cells per well. After 45 min of incubation, cells were lysed in a substrate buffer (7.5 mM NPAG [Sigma], 0.1 M Na citrate at pH 5, 0.5% Triton X-100) overnight at 37°C. Stop buffer (50 mM glycine at pH 10.4, 5 mM EDTA) was added and OD 405 was recorded.

FNIII7-10 binding and flow cytometry

FNIII7-10 binding and flow cytometry assays were performed as described previously (Czuchra et al. 2006). The human FNIII7-10 fragment was subcloned into pET15b plasmid (Invitrogen), expressed and purified from *Escherichia coli*, and directly labeled with Alexa Fluor 647 carboxylic acid via a succinimidyl ester (Invitrogen).

Generation of EBs and isolation of endoderm cells

EBs from wild-type and Kindlin-2^{-/-} ESCs were generated as described (Montanez et al. 2007). To isolate endoderm cells, wild-type and Kindlin-2^{-/-} EBs were collected in a 15-mL conical tube and shaken, and the EBs were allowed to settle down by gravity for 10 min at room temperature. The supernatant containing the detached endoderm cells was carefully aspirated and transferred into a fresh 15-mL conical tube. The process was repeated two times to ensure complete removal of EBs. The resulting suspension with endoderm cells was transferred into a FN-coated (10 μ g/mL) tissue culture dish.

SDS-PAGE and immunoblotting

Cells were lysed in lysis buffer (in 150 mM NaCl, 50 mM Tris at pH 7.4, 1 mM EDTA, 1% Triton X-100 supplemented with protein inhibitors [Roche] and phosphatase inhibitors [Sigma]), homogenized in sample buffer, and boiled for 5 min. Cell lysates were resolved by SDS-PAGE gels. Proteins were then electrophoretically transferred from gels onto nitrocellulose membranes, followed by incubation with antibodies. For antibody detection, a blotting ECL detection kit (Millipore Corporation) was used.

GST pull-downs

The $\beta 1A$ - and $\beta 3$ -integrin cytoplasmic domains and their mutant forms were expressed as GST fusion proteins in BL21 cells. ESCs were lysed in lysis buffer (50 mM Tris at pH 7.4, 150 mM NaCl, 1 mM EDTA, 1% Triton X-100 and proteinase [Roche] and phosphatase inhibitors [Sigma]). Six-hundred micrograms of lysate were incubated overnight with 5 μ g of the indicated GST constructs. The complexes were precipitated with GST beads, subsequently washed and resuspended in LDS Sample buffer (Invitrogen), and used for SDS-PAGE.

For direct protein-protein interaction assay, recombinant GST-tagged Kindlin-2-F3 domain (GST-K2F3) and a mutated form (QW614/615AA) were expressed in BL21 cells. His-tagged $\beta 1$ -integrin cytoplasmic tails were expressed in BL21 cells upon 1 mM IPTG induction and purified under denaturing conditions. Five micrograms of GST-K2F3 or QW614/615AA were incubated with His-tagged $\beta 1$ -integrin cytoplasmic tails bound to Ni²⁺-coated beads for 2 h in buffer D (50 mM NaCl, 10 mM PIPES, 150 mM sucrose, 0.1% Triton X-100 at pH 6.8, containing protease inhibitor cocktails [Roche]). After washing in buffer D, bound proteins were analyzed by SDS-PAGE and Western blotting.

$\alpha 1 \beta 3$ -integrin activation assay

CHO cells stably expressing human $\alpha 1 \beta 3$ integrin were transiently transfected with 2 μ g of the indicated EGFP-tagged cDNAs using Lipofectamine 2000 following the manufacturer's instructions. Double-transfected cells were transfected with 2 μ g of each plasmid. Twenty-four hours after transfection, cells were trypsinized and incubated with the mouse monoclonal antibody PAC-1 (BD) in Tyrode's buffer (pH 7.35) for 40 min at room temperature. Cells were washed and stained with a secondary anti-mouse IgM Alexa 647-labeled antibody (Invitrogen) for 20 min on ice. PAC-1 binding was measured with a FACSCalibur (BD), gating for living cells, using propidium iodide exclusion. Data evaluation was performed with the FlowJo software. Statistical analysis was performed with five independent experiments using the *t*-test.

Coimmunoprecipitation

ILK^{+/+} and ILK^{-/-} fibroblast cells were lysed in lysis buffer, and 1 mg of each cell lysate was incubated with an anti-ILK mouse monoclonal antibody (BD Bioscience) for 1 h on ice. Bound protein complexes were bound to protein A beads (Sigma) for 1 h, subsequently washed in lysis buffer containing 0.1% Triton X-100, resuspended in LDS sample buffer (Invitrogen), and used for SDS-PAGE.

Histological analysis, immunostaining, and electron microscopy

Immunohistochemistry of embryos and immunofluorescence studies of EBs were performed as described previously (Montanez et al. 2007).

Acknowledgments

We thank Dr. Gerhard Wanner for EM analysis, Mrs. Simone Bach for expert technical assistance, and Drs. Kyle Legate and Sara Wickström for critically reading the manuscript. Roy Zent is supported by a Merit Award from the Department of Veterans Affairs and RO1 DK69921 and P01 DK65123. The work was supported by the BMBF (01GM0301), Austrian Science Foundation (SFB021), and the Max Planck Society.

References

- Aumailley, M., Pesch, M., Tunggal, L., Gail, F., and Fässler, R. 2000. Altered synthesis of laminin 1 and absence of basement membrane component deposition in $\beta 1$ integrin-deficient embryoid bodies. *J. Cell Sci.* **113**: 259–268.
- Calderwood, D.A., Zent, R., Grant, R., Rees, D.J., Hynes, R.O., and Ginsberg, M.H. 1999. The Talin head domain binds to integrin β subunit cytoplasmic tails and regulates integrin activation. *J. Biol. Chem.* **274**: 28071–28074.
- Calderwood, D.A., Yan, B., de Pereda, J.M., Alvarez, B.G., Fujioka, Y., Liddington, R.C., and Ginsberg, M.H. 2002. The phosphotyrosine binding-like domain of talin activates integrins. *J. Biol. Chem.* **277**: 21749–21758.
- Chen, J., Salas, A., and Springer, T.A. 2003. Bistable regulation of integrin adhesiveness by a bipolar metal ion cluster. *Nat. Struct. Biol.* **10**: 995–1001.

Montanez et al.

- Cluzel, C., Saltel, F., Lussi, J., Paulhe, F., Imhof, B.A., and Wehrle-Haller, B. 2005. The mechanisms and dynamics of $\alpha\text{v}\beta\text{3}$ integrin clustering in living cells. *J. Cell Biol.* **171**: 383–392.
- Czuchra, A., Meyer, H., Legate, K.R., Brakebusch, C., and Fässler, R. 2006. Genetic analysis of β1 integrin 'activation motifs' in mice. *J. Cell Biol.* **174**: 889–899.
- Hynes, R.O. 2002. Integrins: Bidirectional, allosteric signaling machines. *Cell* **110**: 673–687.
- Jobard, F., Bouadjar, B., Caux, F., Hadj-Rabia, S., Has, C., Matsuda, F., Weissenbach, J., Lathrop, M., Prud'homme, J.F., and Fischer, J. 2003. Identification of mutations in a new gene encoding a FERM family protein with a pleckstrin homology domain in Kindler syndrome. *Hum. Mol. Genet.* **15**: 925–935.
- Kloeker, S., Major, M.B., Calderwood, D.A., Ginsberg, M.H., Jones, D.A., and Beckerle, M.C. 2004. The Kindler syndrome protein is regulated by transforming growth factor- β and involved in integrin-mediated adhesion. *J. Biol. Chem.* **279**: 6824–6833.
- Legate, K.R., Montañez, E., Kudlacek, O., and Fässler, R. 2006. ILK, PINCH and parvin: The tIPP of integrin signalling. *Nat. Rev. Mol. Cell Biol.* **7**: 20–31.
- Li, S., Harrison, D., Carbonetto, S., Fassler, R., Smyth, N., Edgar, D., and Yurchenco, P.D. 2002. Matrix assembly, regulation, and survival functions of laminin and its receptors in embryonic stem cell differentiation. *J. Cell Biol.* **157**: 1279–1290.
- Li, S., Edgar, D., Fässler, R., Wadsworth, W., and Yurchenco, P.D. 2003. The role of laminin in embryonic cell polarization and tissue organization. *Dev. Cell* **4**: 613–624.
- Mackinnon, A.C., Qadota, H., Norman, K.R., Moerman, D.G., and Williams, B.D. 2002. *C. elegans* PAT-4/ILK functions as an adaptor protein within integrin adhesion complexes. *Curr. Biol.* **12**: 787–797.
- Montanez, E., Piwko-Czuchra, A., Bauer, M., Li, S., Yurchenco, P.D., and Fässler, R. 2007. Analysis of integrin functions in peri-implantation embryos, hematopoietic system, and skin. *Methods Enzymol.* **426**: 239–289.
- Moser, M., Nieswandt, B., Ussar, S., Pozgajova, M., and Fässler, R. 2008. Kindlin-3 is essential for integrin activation and platelet aggregation. *Nat. Med.* **14**: 325–330.
- Nieswandt, B., Moser, M., Pleines, I., Varga-Szabo, D., Monkley, S., Critchley, D., and Fässler, R. 2007. Loss of talin1 in platelets abrogates integrin activation, platelet aggregation, and thrombus formation in vitro and in vivo. *J. Exp. Med.* **204**: 3113–3118.
- O'Toole, T.E., Katagiri, Y., Faull, R.J., Peter, K., Tamura, R., Quaranta, V., Loftus, J.C., Shattil, S.J., and Ginsberg, M.H. 1994. Integrin cytoplasmic domains mediate inside-out signal transduction. *J. Cell Biol.* **124**: 1047–1059.
- Petrich, B.G., Marchese, P., Ruggeri, Z.M., Spiess, S., Weichert, R.A., Ye, F., Tiedt, R., Skoda, R.C., Monkley, S.J., Critchley, D.R., et al. 2007. Talin is required for integrin-mediated platelet function in hemostasis and thrombosis. *J. Exp. Med.* **204**: 3103–3111.
- Rogalski, T.M., Mullen, G.P., Gilbert, M.M., Williams, B.D., and Moerman, D.G. 2000. The UNC-112 gene in *Caenorhabditis elegans* encodes a novel component of cell-matrix adhesion structures required for integrin localization in the muscle cell membrane. *J. Cell Biol.* **150**: 253–264.
- Siegel, D.H., Ashton, G.H., Penagos, H.G., Lee, J.V., Feiler, H.S., Wilhelmsen, K.C., South, A.P., Smith, F.J., Prescott, A.R., Wesagowit, V., et al. 2003. Loss of kindlin-1, a human homolog of the *Caenorhabditis elegans* actin-extracellular-matrix linker protein UNC-112, causes Kindler syndrome. *Am. J. Hum. Genet.* **73**: 174–187.
- Shi, X., Ma, Y.Q., Tu, Y., Chen, K., Wu, S., Fukuda, K., Qin, J., Plow, E.F., and Wu, C. 2007. The MIG-2/integrin interaction strengthens cell-matrix adhesion and modulates cell motility. *J. Biol. Chem.* **282**: 20455–20466.
- Tu, Y., Wu, S., Shi, X., Chen, K., and Wu, C. 2003. Migfilin and Mig-2 link focal adhesions to filamin and the actin cytoskeleton and function in cell shape modulation. *Cell* **113**: 37–47.
- Ussar, S., Wang, H.V., Linder, S., Fässler, R., and Moser, M. 2006. The Kindlins: Subcellular localization and expression during murine development. *Exp. Cell Res.* **312**: 42–51.
- Wegener, K.L., Partridge, A.W., Han, J., Pickford, A.R., Liddington, R.C., Ginsberg, M.H., and Campbell, I.D. 2007. Structural basis of integrin activation by talin. *Cell* **128**: 171–182.
- Weinstein, E.J., Bourner, M., Head, R., Zakeri, H., Bauer, C., and Mazzarella, R. 2003. URP1: A member of a novel family of PH and FERM domain-containing membrane-associated proteins is significantly overexpressed in lung and colon carcinomas. *Biochim. Biophys. Acta* **1637**: 207–216.
- Xi, X., Bodnar, R.J., Li, Z., Lam, S.C., and Du, X. 2003. Critical roles for the COOH-terminal NITY and RGT sequences of the integrin β3 cytoplasmic domain in inside-out and outside-in signaling. *J. Cell Biol.* **162**: 329–339.

Paper III

Integrin-linked kinase: integrin's mysterious partner

Carsten Grashoff, Ingo Thievessen, Katrin Lorenz, Siegfried Ussar and Reinhard Fässler¹

Integrin-mediated cell adhesion regulates a vast number of biological processes including migration, survival and proliferation of cells. It is therefore not surprising that defects in integrin function are often rate-limiting for development and profoundly affect the progression of several diseases. The functions of integrins are mediated through the recruitment of cytoplasmic plaque proteins. One of these is integrin-linked kinase, which connects integrins to the actin cytoskeleton and transduces signals through integrins to the extracellular matrix and from integrins to various subcellular compartments.

Addresses

Department of Molecular Medicine, Max Planck Institute of Biochemistry, Am Klopferspitz 18, 82152 Martinsried, Germany
¹e-mail: Faessler@biochem.mpg.de

Current Opinion in Cell Biology 2004, **16**:565–571

This review comes from a themed issue on
Cell-to-cell contact and extracellular matrix
Edited by Kathleen Green and Fiona Watt

Available online 21st July 2004

0955-0674/\$ – see front matter

© 2004 Elsevier Ltd. All rights reserved.

DOI 10.1016/j.ceb.2004.07.004

Abbreviations

αPIX	PAK-interactive exchange factor-α
BM	basement membrane
CH	calponin homology
CPI-17	protein-kinase-C-dependent phosphatase inhibitor of 17 kDa
Dock180	180-kDa protein downstream of CRK
EB	embryoid body
ECM	extracellular matrix
EMT	epithelial-to-mesenchymal transition
FA	focal adhesions
GSK-3	glycogen synthase kinase 3
ILK	integrin-linked kinase
ILKAP	ILK-associated phosphatase
Mig-2	mitogen inducible gene-2
MLC	myosin light chain
PAK	p21-activated serine/threonine kinase
PDK	3-phosphoinositide-dependent kinase
PH	pleckstrin homology
PHI-1	phosphatase holoenzyme inhibitor 1
PI3K	phosphatidylinositol-3-kinase
PINCH	particularly interesting new cysteine-histidine-rich protein
PIP3	phosphoinositol trisphosphate
PTEN	protein tyrosine phosphatase and tensin homolog

Introduction

Cell adhesion is mediated by multiprotein complexes composed of adhesion receptors, extracellular matrix

(ECM) proteins and cytoplasmic plaque proteins. The cell adhesion receptors determine the specificity of the cell–cell or the cell–ECM interaction and recruit cytoplasmic plaque proteins to the cell adhesion site. The cytoplasmic plaque proteins transduce signals initiated by the adhesion receptor, link the adhesion receptors to the cytoskeleton and regulate the functional properties of the adhesion receptors themselves.

Integrins are a large family of adhesion receptors comprising >20 members that mediate highly dynamic cell–cell and cell–ECM interactions. The association and the release of integrin–ligand interactions are achieved by the ability of integrins to adopt different conformations. The active conformation is triggered by intracellular signals and cytoskeleton assembly and results in ligand binding, integrin clustering and recruitment of cytoplasmic plaque proteins into integrin attachment sites called focal adhesions (FAs) [1,2]. One protein that plays a central role in integrin activation and signaling is integrin-linked kinase (ILK) [3]. ILK is composed of three structurally distinct domains: three ankyrin repeats near the N terminus (a fourth ankyrin repeat was identified in human ILK but lacks well-conserved residues), a short linker sequence, and a kinase domain at the C terminus. The linker domain, together with sequences from the N terminus of the kinase domain, shares some similarities with pleckstrin homology (PH) domains (Figure 1).

In the present review we will discuss the functional properties of ILK, which are governed by ILK's interaction partners and kinase activity. The first part of this review summarizes biochemical and cell biological studies of ILK and the second part deals with *in vivo* experiments from invertebrates and mice.

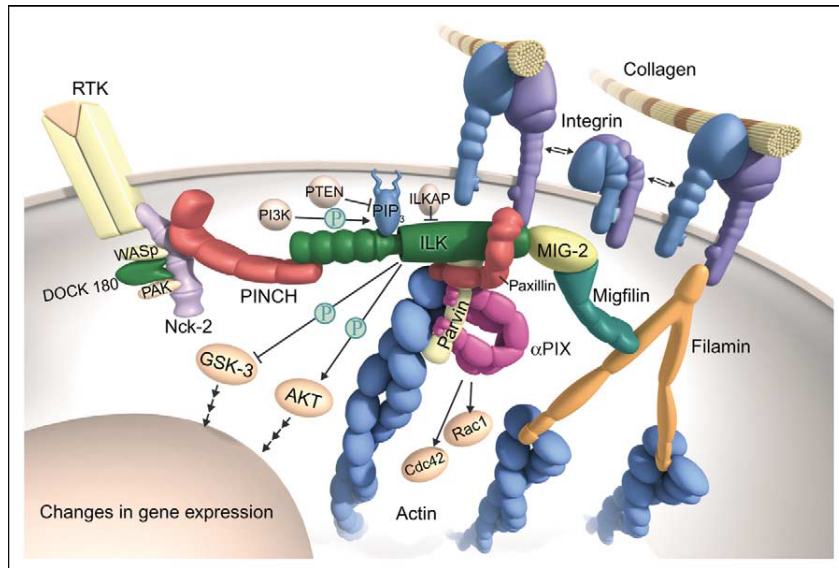
Cell biology and biochemistry of ILK

Overexpression of ILK as well as loss or reduction of ILK expression in cells profoundly affects their morphology and function. The most striking changes are impaired cell spreading, abnormal cell adhesion to and assembly of ECM proteins, delayed formation of FAs and altered cell proliferation [3–6,7**]. How can these defects be explained? Important hints have come from the identification of ILK binding partners (Table 1), from their mode of interaction with ILK and from the identification of substrates for the ILK kinase domain (Table 2).

ILK – a platform for actin regulatory proteins

Almost all adaptor proteins that bind either directly or indirectly to ILK regulate the actin cytoskeleton and

Figure 1



ILK binds Pinch and parvin and this ternary complex subsequently locates to the plasma membrane through the interaction with the cytoplasmic domain of activated $\beta 1$ and $\beta 3$ integrin subunits as well as unknown FAs component(s). Binding to phospholipids results in the activation of the kinase function of ILK, which in turn leads to the phosphorylation of GSK3 β and PKB/Akt. Finally, ILK can recruit several adaptor proteins, which are able to regulate actin dynamics or actin attachment to FAs. The molecules presented in Figure 1 are not drawn to scale. AKT, protein kinase B/Akt; RTK, receptor tyrosine kinase; WASP, Wiskott-Aldrich syndrome protein.

hence could be responsible for the shape change and FA dysfunction associated with altered ILK expression (Figure 1). Pinch (“particularly interesting new cysteine-histidine-rich protein”) was the first interactor to be identified [8]. Pinch-2, a Pinch homologue, was subsequently identified in mice and humans [9,10]. They are both composed of five LIM domains and a nuclear localization signal (NLS) at the C terminus. The first LIM domain binds the first ankyrin repeat of ILK. The interaction has been well-characterized using structural [11], biochemical and cell biological approaches [8,9]. The fourth LIM domain of Pinch-1 was shown to bind

with very low affinity to the SH2/SH3 adaptor protein Nck2, which in turn interacts with growth factor receptors and recruits a large number of proteins, including actin modulators such as Dock180 (180-kDa protein downstream of CRK) and the p21-activated serine/threonine kinase (PAK) [8,12,13]. Whether Pinch-1 interacts with Nck2 *in vivo* is not clear. Since mice and cells lacking Nck2 are normal [14] but mice lacking Pinch-1 die during implantation (F Stanchi and R Fässler, unpublished) this interaction has not seem to be crucial for Pinch-1 function. It has been shown that Pinch-2 can translocate into the nucleus [9]. Its role there, however, is unclear.

Table 1

ILK interacting proteins, the location of their binding site on ILK and the method(s) used to confirm their interaction.

Interactor	Domain	Detection	Reference
$\beta 1$ integrin	C terminus	Y2H/IP	[3]
$\beta 3$ integrin	C terminus	IP	[3,61]
ILKAP	N terminus	Y2H/IP	[62]
Mig-2/Kindlin-2	C terminus	Y2H	[21**]
α -parvin	C terminus	Y2H/IP	[18]
β -parvin	C terminus	Y2H/IP	[19]
paxillin	C terminus	IP	[15]
Pinch-1	N terminus	Y2H/IP/CC	[8,11]
Pinch-2	N terminus	IP	[9]
PIP3	PH	—	[26]

CC, co-crystallization; IP, co-immunoprecipitation; Y2H, yeast-two-hybrid assay

Table 2

Putative targets of the ILK kinase activity and the amino acid residue(s) phosphorylated by ILK.

Target	Phosphorylation site	Reference
ILK	(Ser343)	[35,40]
$\beta 1$ integrin	(Ser785)	[3]
$\beta 3$ integrin	—	[61]
β -parvin	—	[19]
GSK-3 β	(Ser9)	[26,62]
PKB/Akt	(Ser473)	[26]
MLC-20	(Thr18/Ser19)	[42]
MYPT-1	(Thr695, Thr495/Thr709)	[43,44]
CPI-17	(Thr38)	[45]
PHI-1	(Thr57)	[45]

MYPT1, myosin phosphatase target subunit isoform 1.

A search for paxillin binding proteins showed that the kinase domain of ILK contains sequences resembling a paxillin binding subdomain (PBS) motif, which firmly binds paxillin [15]. The ILK–paxillin interaction is necessary but not sufficient to recruit ILK into FAs, where the complex may modulate the function of other paxillin binding proteins such as vinculin, α -actinin, talin and FAK.

Several laboratories have simultaneously shown that parvins, a new family of F-actin binding proteins, bind the kinase domain of ILK [16–19]. The parvins comprise three members (α -parvin or actopaxin or CH-ILK binding protein; β -parvin or affixin; and γ -parvin) and are composed of two calponin homology (CH) domains that bind ILK, paxillin and F-actin. β -parvin was shown to interact with the guanine nucleotide exchange factor α -PIX (PAK-interactive exchange factor- α), which may activate Rac1 and Cdc42 [20]. Parvins are found in FAs and apparently do not colocalize to stress fibers [16,17]. An important future task will be to map the binding sites of ILK, paxillin and F-actin on the CH domains and to test whether their binding occurs simultaneously or is mutually exclusive.

A recent paper identified an additional ILK binding partner in *Caenorhabditis elegans*, termed UNC-112 [21**]. UNC-112 contains a FERM domain [22] and is important for the recruitment of the ILK orthologue, Pat-4, to muscle attachment sites. The mammalian orthologue of UNC-112, Mig-2/Kindlin-2, was shown to bind the LIM-domain-containing adaptor protein migfilin, which in turn binds filamin [23*]. It will be interesting to see whether Mig-2/Kindlin-2 also binds ILK in mammalian cells and whether this interaction modulates the function of filamin, which is mutated in a variety of human diseases.

ILK, Pinch and parvin — a ternary complex required for stability and focal adhesion localization

The association of ILK, Pinch and parvin into a ternary protein complex happens before their recruitment into FAs [24*] and serves at least two purposes: it stabilizes the individual proteins and targets the individual components into FAs [24*,25*]. Loss of ILK expression in cells leads to the degradation of Pinch and parvin and, conversely, loss of Pinch expression diminishes ILK and parvin levels [25*]. The degradation can be prevented either by inhibiting the proteasome [25*] or by expressing short N-terminal fragments of ILK (the ankyrin repeats) in ILK-deficient cells (C Grashoff, R Fässler, unpublished data) or Pinch (the first LIM domain) in Pinch-deficient cells (F Stanchi, R Fässler, unpublished data). Their recruitment into FAs, however, cannot be rescued with these fragments. These results support the notion that ILK and Pinch must have binding partner(s) that facilitate FA targeting. Possible candidates for ILK targeting partners are integrins, paxillin and Mig-2/Kindlin-2. It has been

shown that nematodes lacking β integrin fail to localize ILK to cell attachment sites [21**]. Mammalian cells may have a similar requirement for β integrin to localize ILK, but this has not been shown yet with cell lines lacking either β 1 or β 3 or both integrin subunits. Paxillin binds ILK via its N-terminal leucine-rich motifs and targets to FAs via the C-terminal LIM domains. Mutation in the paxillin binding site of ILK prevents ILK/Pinch/parvin recruitment to FAs [15]. Mig-2/Kindlin-2 could also play a role since the worm orthologue UNC-112 is essential for localization of Pat-4/ILK to integrin-containing attachment sites [21**]. No candidate binding partners are currently known that could promote recruitment of Pinch into FAs.

The dependence of ILK, Pinch and parvin stability on the formation of a ternary complex has implications for the interpretation of overexpression experiments. Accumulation of ILK in the cytoplasm of ILK-overexpressing cells may cause a partial depletion of Pinch and parvin from FAs, resulting in an impaired FA function. This could explain why cells either lacking [7**] or overexpressing ILK [3] have similar phenotypes: they both show a rounded morphology and have decreased adhesive properties.

The kinase activity of ILK

Despite the sequence differences between the ILK kinase domain and other protein kinases (important residues in the activation loop of the kinase are not conserved) the similarity was immediately recognized and investigated [3]. Initial studies showed that GST-tagged ILK purified from bacteria or mammalian cells could phosphorylate serine and threonine residues in peptides representing the β 1 integrin tail, and model substrates such as myelin basic protein [3].

ILK kinase activity took center stage when it was suggested to be directly associated with cell proliferation, tumor growth and metastasis [4,26–29]. On the one hand, overexpression of ILK in cells results in anchorage-independent cell cycle progression [5] and epithelial-to-mesenchymal transition (EMT) of non-tumorigenic as well as tumorigenic epithelial cells [4,29]. Inhibition of ILK kinase activity, on the other hand, suppresses cell growth in culture as well as growth of human colon carcinoma cells in SCID mice [30]. Several lines of experimental evidence suggest that these phenotypes are largely attributed to enhanced ILK kinase activity and phosphorylation of GSK3 β and PKB/Akt [26], two key enzymes involved in a diverse array of cell functions including cell proliferation, survival and insulin responses [31,32]. ILK-dependent phosphorylation of GSK3 β in epithelial cells downregulates GSK3 β kinase activity [26]. This in turn is associated with reduced E-cadherin expression, enhanced AP1 activity and increased β -catenin–Lef/Tcf activity [4,33], which induces the expression

of cell-cycle-promoting genes such as cyclins and c-myc [5,34]. The reduced E-cadherin expression could be due to a direct effect of the β -catenin-Lef/Tcf complex on E-cadherin gene expression [4]. Alternatively, ILK can reduce E-cadherin levels indirectly by triggering snail expression, which in turn represses E-cadherin gene expression [30].

Full activation of PKB/Akt requires PIP3-dependent phosphorylation of two residues: Thr308 and Ser473 [32]. Whereas PDK-1 (3-phosphoinositide-dependent kinase 1) phosphorylates Thr308, ILK has been identified as 'PDK-2', which phosphorylates Ser473 via a direct interaction at the plasma membrane [26,35]. Besides possessing a kinase activity, ILK fulfils other requirements of a PDK2, including PIP3 binding and regulation of its activity by PI3K (phosphatidylinositol-3-kinase) or PTEN (protein tyrosine phosphatase and tensin homolog) [26,27]. However, some doubts about ILK's kinase activity arose when it was reported that it has no Ser473 phosphorylation activity [36,37^{*}]. These doubts were reinforced by genetic studies in invertebrates and mice that demonstrated normal Ser473 phosphorylation in the absence of ILK [7^{**},21^{**},38]. Loss-of-function mutations of ILK in worms and flies show no defects that can be explained by impaired PKB/Akt activity, but develop severe muscle defects that are fully rescued when different kinase-dead versions of ILK are expressed [21^{**},38]. Similarly, fibroblasts with or without the ILK gene phosphorylate Ser473 to a similar extent following insulin or PDGF stimulation [7^{**}], and neither chondrocytes nor keratinocytes change their steady-state Ser473 phosphorylation after ILK gene ablation *in vivo* [39] (T Sakai and R Fässler, unpublished). These findings convincingly demonstrate that ILK — even if it has Ser473 phosphorylation activity — is not the only PDK2. These findings, however, do not exclude the possibility that ILK mediates the phosphorylation of PKB/Akt and other target proteins in an indirect manner, for example by recruiting a kinase or inhibiting a phosphatase [37^{*},40]. Support for such a notion also comes from gene ablation experiments. Monocytes lacking ILK expression show reduced Ser473 phosphorylation [41^{*}]. Similarly, ILK-null fibroblasts, which respond normally to insulin treatment, fail to maintain Ser473 phosphorylation levels to the same extent as normal cells upon PDGF treatment [7^{**}]. Furthermore, they display a slightly reduced steady state level of Ser473 phosphorylation under normal culture conditions (T Sakai and R Fässler, unpublished).

Other targets of the ILK kinase activity (Table 2) are β -parvin [19], the regulatory myosin light chain (MLC) [42], and MLC phosphatase [43,44] and its regulators CPI-17 (protein-kinase-C-dependent phosphatase inhibitor of 17 kDa) and PHI-1 (phosphatase holoenzyme inhibitor 1) [45]. The significance of their phosphorylation, however, is not clear.

Since ILK regulates so many essential cellular functions it is important to settle the debate on ILK's kinase activity. Solving the structure of the ILK kinase domain will be very informative, as will the analysis of mice carrying 'kinase-dead' versions of the ILK gene and the identification of PDK2(s). In addition to these new experimental approaches, new reagents to probe ILK's function will be useful. The E359K mutation in ILK, for example, was originally found to lack kinase activity and was therefore used in many studies as a 'kinase-dead' version of ILK. It turns out, however, that the mutation does not affect kinase activity but rather impairs paxillin binding and FA targeting [46^{*}]. Furthermore, a polyclonal anti-ILK antiserum that recognizes a 59 kDa band of unknown origin instead of the 52 kDa sized ILK has been used in a large number of studies and could potentially have given misleading results [3,6,47].

Studies of ILK/Pinch/parvin in invertebrates and mice

The attachment sites of the body wall muscle to the hypodermis of *C. elegans* are called dense bodies and resemble FA-like structures. They contain β -pat-3 integrin (the only β integrin subunit in *C. elegans*), pat-4/ILK, UNC-97/Pinch, pat-6/parvin and UNC-112/Mig-2 and loss-of-function alleles of these proteins lead to severe adhesion defects manifesting as muscle detachment and embryonic lethality [21^{**},22,48,49^{*}]. The loss-of-function studies also reveal that β -pat-3 integrin is required to recruit ILK to the plasma membrane [21^{**}] and that integrins are partially mislocalized in the absence of pat-4/ILK [21^{**}] or UNC-112/Mig-2/Kindlin-2 [22]. A recent report showed that the Zn²⁺-finger-containing transcription factor UNC-98 can bind UNC-97/Pinch and is also required for muscle attachment to the body wall [50^{*}]. UNC-98 shuttles between dense bodies and the nucleus where it binds DNA and probably regulates gene transcription. So far an ortholog of the UNC-98 gene has not been identified in flies or mammals.

Drosophila melanogaster has a similar requirement for β PS integrins, ILK and Pinch in muscle cell attachment [38,51^{**}]. Interestingly, loss of β PS integrin function in flies leads to detachment of ECM from the cell membrane, while loss of ILK function leads to detachment of F-actin from the plasma membrane, indicating an important role for ILK in actin stabilization at integrin attachment sites [38]. The severe muscle defect in worms or flies lacking ILK can be fully rescued by the expression of different kinase-dead ILK transgenes, supporting the idea that ILK functions as an important adaptor protein, independent of its kinase activity [21^{**},38].

The loss of ILK expression in mice leads to peri-implantation lethality similar to what is seen upon loss of β 1 integrin expression [7^{**},52]. The cause of the developmental arrest was studied in embryoid bodies (EBs)

[7^{••},53,54]; these studies showed that $\beta 1$ -integrin-mutant EBs are unable to deposit a basement membrane (BM), while ILK-null EBs produce a BM but fail to polarize the epiblast (a primitive tissue that will give rise to all three germ layers). Since addition of laminin to $\beta 1$ -integrin-null EBs rescues the BM assembly phenotype and allows epiblast development it is likely that $\beta 1$ integrin and ILK function independently during the peri-implantation period [54].

Conditional loss of ILK in chondrocytes leads to skeletal growth retardations characterized by abnormal chondrocyte shape and decreased proliferation *in vivo* [39,55], and diminished chondrocyte spreading on ECM and reduced stress fiber formation *in vitro* [39]. Similar, albeit more severe, defects are also observed in mice with a chondrocyte-specific deletion of the $\beta 1$ integrin gene [56], indicating that $\beta 1$ integrins and ILK are both required for normal chondrocyte function. The mechanism leading to reduced chondrocyte proliferation in the absence of ILK expression is not understood; altered phosphorylation of PKB/Akt or GSK-3 β was excluded [39]. A conditional deletion or reduction of ILK gene expression in macrophages, on the other hand, results in a strong inhibition of the PKB/Akt-Ser473 phosphorylation associated with apoptosis [41[•]], indicating that ILK kinase activity might differ depending on the cell type.

Overexpression of ILK in mammary glands of transgenic mice leads to tumor formation [29]. Similarly, pharmacological inhibition of ILK in prostate carcinoma cells causes them to proliferate much less rapidly *in vivo* [57^{••}]. These findings can principally be explained by the oncogenic activities of ILK (activation of PKB/Akt, inhibition of GSK-3 β , and stimulation of AP-1, NF- κ B and β -catenin–Lef/Tcf transcription factors) and its ability to promote tumor angiogenesis. ILK promotes blood vessel invasion into tumors in two ways: ILK induces HIF1 α -dependent VEGF expression in tumor cells, which in turn regulates endothelial cell migration and proliferation in an ILK kinase-dependent manner [57^{••}]. The importance of ILK for tumor pathology is underscored by the fact that a large number of malignant tumors display increased ILK levels and kinase activity [58], and in some tumor types ILK levels correlate with tumor grade [59,60].

Outlook

ILK has many interesting functional facets and work in both invertebrates and mice has revealed an essential role for ILK in development. There is a general consensus that ILK plays a central role in the reorganization of the F-actin cytoskeleton and its attachment to FAs. The role of ILK as a kinase is more controversial. Since a large number of ILK functions rely on kinase activity, including EMT, proliferation and VEGF expression, this controversy should urgently be settled. This can be assisted

by solving the structure of the ILK kinase domain, using continued genetic approaches or the well-defined antibodies that have become available over the past few years. As has already been done in flies and worms, it should be tested in mice whether point mutations in the kinase domain of ILK impair the function of the molecule.

An important future task will be to identify the signals that trigger assembly of the ILK/Pinch/parvin complex, to identify the proteins that recruit the core complex into FAs, and to establish how the core complex modulates integrin functions and regulates actin dynamics. The availability of cell lines and mice that lack ILK and the progress in proteomics and live cell imaging should together help to dissect these mechanisms and to clarify ILK's role in integrin-mediated cell adhesion.

Acknowledgements

We thank Drs. Kyle Legate, Cord Brakebusch and Haiyan Chu for discussion, comments and critical reading of the manuscript. The integrin/ILK work is supported by the DFG (SFB413), the Fonds der Chemischen Industrie and the Max Planck Society.

References and recommended reading

Papers of particular interest, published within the annual period of review, have been highlighted as:

- of special interest
- of outstanding interest

1. Hynes RO: **Integrins: bidirectional, allosteric signaling machines.** *Cell* 2002, **110**:673-687.
2. Brakebusch C, Fässler R: **The integrin-actin connection, an eternal love affair.** *EMBO J* 2003, **22**:2324-2333.
3. Hannigan GE, Leung-Hagsteejin C, Fitz-Gibbon L, Coppolino MG, Radeva G, Filmus J, Bell JC, Dedhar S: **Regulation of cell adhesion and anchorage-dependent growth by a new $\beta 1$ -integrin-linked protein kinase.** *Nature* 1996, **379**:91-96.
4. Novak A, Hsu SC, Leung-Hagsteejin C, Radeva G, Papkoff J, Montesano R, Roskelley C, Grosschedl R, Dedhar S: **Cell adhesion and the integrin-linked kinase regulate the LEF-1 and β -catenin signaling pathways.** *Proc Natl Acad Sci USA* 1998, **95**:4374-4379.
5. Radeva G, Petrocelli T, Behrend E, Leung-Hagsteejin C, Filmus J, Slingerland J, Dedhar S: **Overexpression of the integrin-linked kinase promotes anchorage-independent cell cycle progression.** *J Biol Chem* 1997, **272**:13937-13944.
6. Wu C, Keightley SY, Leung-Hagsteejin C, Radeva G, Coppolino M, Goicoechea S, McDonald JA, Dedhar S: **Integrin-linked protein kinase regulates fibronectin matrix assembly, E-cadherin expression, and tumorigenicity.** *J Biol Chem* 1998, **273**:528-536.
7. Sakai T, Li S, Docheva D, Grashoff C, Sakai K, Kostka G, Braun A, Pfeifer A, Yurchenco PD, Fässler R: **Integrin-linked kinase (ILK) is required for polarizing the epiblast, cell adhesion, and controlling actin accumulation.** *Genes Dev* 2003, **17**:926-940.
This paper analyzes the role of ILK during mouse development and in fibroblast cells. It demonstrates that ILK is required for F-actin reorganization, epiblast polarity and cavitation. Fibroblasts lacking ILK expression display reduced adhesion, spreading, F-actin distribution and proliferation but normal GSK3 β and PKB/Akt phosphorylation.
8. Tu Y, Li F, Goicoechea S, Wu C: **The LIM-only protein PINCH directly interacts with integrin-linked kinase and is recruited to integrin-rich sites in spreading cells.** *Mol Cell Biol* 1999, **19**:2425-2434.
9. Zhang Y, Chen K, Guo L, Wu C: **Characterization of PINCH-2, a new focal adhesion protein that regulates the PINCH-1-ILK**

- interaction, cell spreading, and migration. *J Biol Chem* 2002, **277**:38328-38338.
10. Braun A, Bordoy R, Stanchi F, Moser M, Kostka G, Ehler E, Brandau O, Fässler R: **PINCH-2 is a new five LIM domain protein, homologous to PINCH and localized to focal adhesions.** *Exp Cell Res* 2003, **284**:239-250.
 11. Velyvis A, Yang Y, Wu C, Qin J: **Solution structure of the focal adhesion adaptor PINCH LIM1 domain and characterization of its interaction with the integrin-linked kinase ankyrin repeat domain.** *J Biol Chem* 2001, **276**:4932-4939.
 12. Tu Y, Li F, Wu C: **Nck-2, a novel Src homology2/3-containing adaptor protein that interacts with the LIM-only protein PINCH and components of growth factor receptor kinase-signaling pathways.** *Mol Biol Cell* 1998, **9**:3367-3382.
 13. Velyvis A, Vaynberg J, Yang Y, Vinogradova O, Zhang Y, Wu C, Qin J: **Structural and functional insights into PINCH LIM4 domain-mediated integrin signaling.** *Nat Struct Biol* 2003, **10**:558-564.
 14. Blatt F, Aippersbach E, Gelkop S, Strasser GA, Nash P, Tafuri A, Gertler FB, Pawson T: **The murine Nck SH2/SH3 adaptors are important for the development of mesoderm-derived embryonic structures and for regulating the cellular actin network.** *Mol Cell Biol* 2003, **23**:4586-4597.
 15. Nikolopoulos SN, Turner CE: **Integrin-linked kinase (ILK) binding to paxillin LD1 motif regulates ILK localization to focal adhesions.** *J Biol Chem* 2001, **276**:23499-23505.
 16. Nikolopoulos SN, Turner CE: **Actopaxin, a new focal adhesion protein that binds paxillin LD motifs and actin and regulates cell adhesion.** *J Cell Biol* 2000, **151**:1435-1448.
 17. Olski TM, Noegel AA, Korenbaum E: **Parvin, a 42 kDa focal adhesion protein, related to the α -actinin superfamily.** *J Cell Sci* 2001, **114**:525-538.
 18. Tu Y, Huang Y, Zhang Y, Hua Y, Wu C: **A new focal adhesion protein that interacts with integrin-linked kinase and regulates cell adhesion and spreading.** *J Cell Biol* 2001, **153**:585-598.
 19. Yamaji S, Suzuki A, Sugiyama Y, Koide Y, Yoshida M, Kanamori H, Mohri H, Ohno S, Ishigatsubo Y: **A novel integrin-linked kinase-binding protein, affixin, is involved in the early stage of cell-substrate interaction.** *J Cell Biol* 2001, **153**:1251-1264.
 20. Rosenberger G, Jantke I, Gal A, Kutsche K: **Interaction of α PIX (ARHGEF6) with β -parvin (PARVB) suggests an involvement of α PIX in integrin-mediated signaling.** *Hum Mol Genet* 2003, **12**:155-167.
 21. Mackinnon AC, Qadota H, Norman KR, Moerman DG, Williams BD: **C.elegans PAT-4/ILK functions as an adaptor protein within integrin adhesion complexes.** *Curr Biol* 2002, **12**:787-797.
- Loss of PAT-4/ILK leads to muscle detachment. Genetic studies place PAT-4/ILK downstream of b-PAT-3/intgerin and upstream of UNC-97/ Pinch.
22. Rogalski TM, Mullen GP, Gilbert MM, Williams BD, Moerman DG: **The UNC-112 gene in *Caenorhabditis elegans* encodes a novel component of cell-matrix adhesion structures required for integrin localization in the muscle cell membrane.** *J Cell Biol* 2000, **150**:253-264.
 23. Tu Y, Wu S, Shi X, Chen K, Wu C: **Migfilin and Mig-2 link focal adhesions to filamin and the actin cytoskeleton and function in cell shape modulation.** *Cell* 2003, **113**:37-47.
- This paper describes a new ILK adaptor protein termed migfilin, which links Mig-2/ILK to filamin. Knockdown of migfilin leads to altered cell shape, reduced migration and abnormal F-actin distribution. These defects resemble the phenotype of ILK-deficient cells.
24. Zhang Y, Chen K, Tu Y, Velyvis A, Yang Y, Qin J, Wu C: **Assembly of the PINCH-ILK-CH-ILKBP complex precedes and is essential for localization of each component to cell-matrix adhesion sites.** *J Cell Sci* 2002, **115**:4777-4786.
- This paper shows that ILK/Pinch/parvin have formed a ternary complex already prior to recruitment into FAs.
25. Fukuda T, Chen K, Shi X, Wu C: **PINCH-1 is an obligate partner of integrin-linked kinase (ILK) functioning in cell shape modulation, motility, and survival.** *J Biol Chem* 2003, **278**:51324-51333.
- Knockdown experiments show that Pinch and ILK are obligate partners and if not associated will be degraded by the proteasome.
26. Delcommenne M, Tan C, Gray V, Rue L, Woodgett J, Dedhar S: **Phosphoinositide-3-OH kinase-dependent regulation of glycogen synthase kinase 3 and protein kinase B/AKT by the integrin-linked kinase.** *Proc Natl Acad Sci USA* 1998, **95**:11211-11216.
 27. Persad S, Attwell S, Gray V, Delcommenne M, Troussard A, Sanghera J, Dedhar S: **Inhibition of integrin-linked kinase (ILK) suppresses activation of protein kinase B/Akt and induces cell cycle arrest and apoptosis of PTEN-mutant prostate cancer cells.** *Proc Natl Acad Sci USA* 2000, **97**:3207-3212.
 28. Attwell S, Roskelley C, Dedhar S: **The integrin-linked kinase (ILK) suppresses anoikis.** *Oncogene* 2000, **19**:3811-3815.
 29. White DE, Cardiff RD, Dedhar S, Muller WJ: **Mammary epithelial-specific expression of the integrin-linked kinase (ILK) results in the induction of mammary gland hyperplasias and tumors in transgenic mice.** *Oncogene* 2001, **20**:7064-7072.
 30. Tan C, Costello P, Sanghera J, Dominguez D, Baulida J, de Herreros AG, Dedhar S: **Inhibition of integrin linked kinase (ILK) suppresses β -catenin-Lef/Tcf-dependent transcription and expression of the E-cadherin repressor, snail, in APC^{-/-} human colon carcinoma cells.** *Oncogene* 2001, **20**:133-140.
 31. Cohen P, Frame S: **The renaissance of GSK3.** *Nat Rev Mol Cell Biol* 2001, **2**:769-776.
 32. Lawlor MA, Alessi DR: **PKB/Akt: a key mediator of cell proliferation, survival and insulin responses?** *J Cell Sci* 2001, **114**:2903-2910.
 33. Troussard AA, Tan C, Yoganathan TN, Dedhar S: **Cell-extracellular matrix interactions stimulate the AP-1 transcription factor in an integrin-linked kinase- and glycogen synthase kinase 3-dependent manner.** *Mol Cell Biol* 1999, **19**:7420-7427.
 34. Novak A, Dedhar S: **Signaling through β -catenin and Lef/Tcf.** *Cell Mol Life Sci* 1999, **56**:523-537.
 35. Persad S, Attwell S, Gray V, Mawji N, Deng JT, Leung D, Yan J, Sanghera J, Walsh MP, Dedhar S: **Regulation of protein kinase B/Akt-serine 473 phosphorylation by integrin-linked kinase: critical roles for kinase activity and amino acids arginine 211 and serine 343.** *J Biol Chem* 2001, **276**:27462-27469.
 36. Balendran A, Casamayor A, Deak M, Paterson A, Gaffney P, Currie R, Downes CP, Alessi DR: **PDK1 acquires PDK2 activity in the presence of a synthetic peptide derived from the carboxyl terminus of PRK2.** *Curr Biol* 1999, **9**:393-404.
 37. Hill MM, Feng J, Hemmings BA: **Identification of a plasma membrane Raft-associated PKB Ser473 kinase activity that is distinct from ILK and PDK1.** *Curr Biol* 2002, **12**:1251-1255.
- This paper shows that ILK is part of a protein complex with PKB/Akt Ser473 activity. Interestingly, however, the kinase activity is distinct from ILK.
38. Zervas CG, Gregory SL, Brown NH: **Drosophila integrin-linked kinase is required at sites of integrin adhesion to link the cytoskeleton to the plasma membrane.** *J Cell Biol* 2001, **152**:1007-1018.
 39. Grashoff C, Aszodi A, Sakai T, Hunziker EB, Fässler R: **Integrin-linked kinase regulates chondrocyte shape and proliferation.** *EMBO Rep* 2003, **4**:432-438.
 40. Lynch DK, Ellis CA, Edwards PA, Hiles ID: **Integrin-linked kinase regulates phosphorylation of serine 473 of protein kinase B by an indirect mechanism.** *Oncogene* 1999, **18**:8024-8032.
 41. Troussard AA, Mawji NM, Ong C, Mui A, St-Arnaud R, Dedhar S: **Conditional knock-out of integrin-linked kinase demonstrates an essential role in protein kinase B/Akt activation.** *J Biol Chem* 2003, **278**:22374-22378.
- Conditional deletion of ILK in monocytes/macrophages results in reduced phosphorylation of Ser473 of PKB/Akt, indicating that the Ser473 activity of ILK may occur in a cell-type-dependent manner.

42. Deng JT, Van Lierop JE, Sutherland C, Walsh MP: **Ca²⁺-independent smooth muscle contraction. A novel function for integrin-linked kinase.** *J Biol Chem* 2001, **276**:16365-16373.
43. Kiss E, Muranyi A, Csontos C, Gergely P, Ito M, Hartshorne DJ, Erdodi F: **Integrin-linked kinase phosphorylates the myosin phosphatase target subunit at the inhibitory site in platelet cytoskeleton.** *Biochem J* 2002, **365**:79-87.
44. Muranyi A, MacDonald JA, Deng JT, Wilson DP, Haystead TA, Walsh MP, Erdodi F, Kiss E, Wu Y, Hartshorne DJ: **Phosphorylation of the myosin phosphatase target subunit by integrin-linked kinase.** *Biochem J* 2002, **366**:211-216.
45. Deng JT, Sutherland C, Brautigam DL, Eto M, Walsh MP: **Phosphorylation of the myosin phosphatase inhibitors, CPI-17 and PHI-1, by integrin-linked kinase.** *Biochem J* 2002, **367**:517-524.
46. Nikolopoulos SN, Turner CE: **Molecular dissection of actopaxin-integrin-linked kinase-paxillin interactions and their role in subcellular localization.** *J Biol Chem* 2002, **277**:1568-1575.
 This report identifies a paxillin binding site in the ILK kinase domain. The interaction of ILK with paxillin is essential for the recruitment of ILK into FAs. Furthermore, the paper provides evidence that the E359K mutation in ILK affects paxillin binding but not the kinase activity.
47. Ahmed N, Oliva K, Rice GE, Quinn MA: **Cell-free 59 kDa immunoreactive integrin-linked kinase: a novel marker for ovarian carcinoma.** *Clin Cancer Res* 2004, **10**:2415-2420.
48. Hobert O, Moerman DG, Clark KA, Beckerle MC, Ruvkun G: **A conserved LIM protein that affects muscular adherens junction integrity and mechanosensory function in *Caenorhabditis elegans*.** *J Cell Biol* 1999, **144**:45-57.
49. Lin X, Qadota H, Moerman DG, Williams BD: ***C. elegans* PAT-6/actopaxin plays a critical role in the assembly of integrin adhesion complexes in vivo.** *Curr Biol* 2003, **13**:922-932.
 A phenotype analysis of PAT-6/parvin-deficient nematodes. Genetic experiments place PAT-6/parvin downstream of PAT-4/ILK and UNC97/Pinch.
50. Mercer KB, Flaherty DB, Miller RK, Qadota H, Tinley TL, Moerman DG, Benian GM: ***Caenorhabditis elegans* UNC-98, a C2H2 Zn finger protein, is a novel partner of UNC-97/PINCH in muscle adhesion complexes.** *Mol Biol Cell* 2003, **14**:2492-2507.
 A Zn²⁺ finger protein called UNC-98 shuttles between FAs and nucleus and interacts with UNC-97/Pinch in dense bodies. The nuclear function of UNC-98 is unknown.
51. Clark KA, McGrail M, Beckerle MC: **Analysis of PINCH function in *Drosophila* demonstrates its requirement in integrin-dependent cellular processes.** *Development* 2003, **130**:2611-2621.
 Analysis of Pinch-deficient flies demonstrates muscle detachment and wing blisters. Pinch localization to muscle attachment sites is integrin-dependent, whereas ILK localization to integrin attachment sites is not Pinch-dependent. This indicates that in *Drosophila*, ILK and Pinch are not obligate binding partners.
52. Fässler R, Meyer M: **Consequences of lack of $\beta 1$ integrin gene expression in mice.** *Genes Dev* 1995, **9**:1896-1908.
53. Aumailley M, Pesch M, Tunggal L, Gaill F, Fässler R: **Altered synthesis of laminin 1 and absence of basement membrane component deposition in $\beta 1$ integrin-deficient embryoid bodies.** *J Cell Sci* 2000, **113**:259-268.
54. Li S, Harrison D, Carbonetto S, Fässler R, Smyth N, Edgar D, Yurchenco PD: **Matrix assembly, regulation, and survival functions of laminin and its receptors in embryonic stem cell differentiation.** *J Cell Biol* 2002, **157**:1279-1290.
55. Terpstra L, Prud'homme J, Arabian A, Takeda S, Karsenty G, Dedhar S, St-Arnaud R: **Reduced chondrocyte proliferation and chondrodysplasia in mice lacking the integrin-linked kinase in chondrocytes.** *J Cell Biol* 2003, **162**:139-148.
56. Aszodi A, Hunziker EB, Brakebusch C, Fässler R: **$\beta 1$ integrins regulate chondrocyte rotation, G1 progression, and cytokinesis.** *Genes Dev* 2003, **17**:2465-2479.
57. Tan C, Cruet-Hennequart S, Troussard A, Fazli L, Costello P, Sutton K, Wheeler J, Gleave M, Sanghera J, Dedhar S: **Regulation of tumor angiogenesis by integrin-linked kinase (ILK).** *Cancer Cell* 2004, **5**:79-90.
 This paper demonstrates a dual role for ILK in tumor growth. ILK in tumor cells promotes VEGF release leading to the recruitment of endothelial cells, and ILK in endothelial cells supports their migration and proliferation in a PKB/Akt-dependent manner.
58. Marotta A, Parhar K, Owen D, Dedhar S, Salh B: **Characterisation of integrin-linked kinase signalling in sporadic human colon cancer.** *Br J Cancer* 2003, **88**:1755-1762.
59. Graff JR, Deddens JA, Konicek BW, Colligan BM, Hurst BM, Carter HW, Carter JH: **Integrin-linked kinase expression increases with prostate tumor grade.** *Clin Cancer Res* 2001, **7**:1987-1991.
60. Dai DL, Makretsov N, Campos EI, Huang C, Zhou Y, Huntsman D, Martinka M, Li G: **Increased expression of integrin-linked kinase is correlated with melanoma progression and poor patient survival.** *Clin Cancer Res* 2003, **9**:4409-4414.
61. Pasquet JM, Noury M, Nurden AT: **Evidence that the platelet integrin $\alpha IIb\beta 3$ is regulated by the integrin-linked kinase, ILK, in a PI3-kinase dependent pathway.** *Thromb Haemost* 2002, **88**:115-122.
62. Leung-Hagesteijn C, Mahendra A, Naruszewicz I, Hannigan GE: **Modulation of integrin signal transduction by ILKAP, a protein phosphatase 2C associating with the integrin-linked kinase ILK1.** *EMBO J* 2001, **20**:2160-2170.

Paper IV

Kindlin-3 is essential for integrin activation and platelet aggregation

Markus Moser¹, Bernhard Nieswandt^{2,3}, Siegfried Ussar¹, Miroslava Pozgajova² & Reinhard Fässler¹

Integrin-mediated platelet adhesion and aggregation are essential for sealing injured blood vessels and preventing blood loss, and excessive platelet aggregation can initiate arterial thrombosis, causing heart attacks and stroke¹. To ensure that platelets aggregate only at injury sites, integrins on circulating platelets exist in a low-affinity state and shift to a high-affinity state (in a process known as integrin activation or priming) after contacting a wounded vessel². The shift is mediated through binding of the cytoskeletal protein Talin to the β subunit cytoplasmic tail^{3–5}. Here we show that platelets lacking the adhesion plaque protein Kindlin-3 cannot activate integrins despite normal Talin expression. As a direct consequence, Kindlin-3 deficiency results in severe bleeding and resistance to arterial thrombosis. Mechanistically, Kindlin-3 can directly bind to regions of β -integrin tails distinct from those of Talin and trigger integrin activation. We have therefore identified Kindlin-3 as a novel and essential element for platelet integrin activation in hemostasis and thrombosis.

Cellular control of integrin activation is essential for virtually all cells, including platelets, which seal injured blood vessels and stop bleeding. At sites of injury, the platelet receptors GPIb and GPVI bind to von Willebrand factor (vWF) and collagen, respectively^{1–3}, which together with locally produced thrombin trigger activation of integrin $\alpha_{IIb}\beta_3$ and the release of soluble platelet agonists including ADP and thromboxane A2 (TxA2). Activated $\alpha_{IIb}\beta_3$ integrins bind fibrinogen, vWF and fibronectin, thus allowing firm platelet adhesion and platelet aggregation. The central role of integrin activation in platelet adhesion and aggregation sparked the search for critical integrin tail-binding proteins that control integrin affinity for ligands. Irrespective of the platelet-activating stimulus and signaling pathways, Talin binding to the β -integrin tails was shown to be the final common step in $\alpha_{IIb}\beta_3$ integrin activation and ligand binding^{4,6,7}. Talin, a major cytoskeletal protein at integrin adhesion sites, consists of a large C-terminal rod-like domain and an N-terminal FERM (protein 4.1, ezrin, radixin, moesin) domain with three subdomains: F1, F2 and F3 (ref. 8). The phosphotyrosine-binding (PTB) subdomain in the F3 domain sequentially binds to two distinct regions in the β cytoplasmic tails and is sufficient for integrin activation *in vitro*^{8,9}.

In addition to Talin, other FERM domain-containing proteins, including the Kindlins, interact with integrin β tails¹⁰. The Kindlin protein family consist of three members (Kindlin-1, Kindlin-2 and Kindlin-3), all of which localize to integrin adhesion sites^{11–13}. In contrast to the widely expressed Kindlin-1 and Kindlin-2, Kindlin-3 is restricted to hematopoietic cells and is particularly abundant in megakaryocytes and platelets¹². The structural hallmark of Kindlins is a FERM domain whose F2 subdomain is split by a pleckstrin homology (PH) domain. In a comparison of FERM-domain proteins, the F3 subdomains of Kindlins have been found to share highest homology with the F3 domain of Talin¹⁰.

To address the function of Kindlin-3 *in vivo*, we disrupted the *Kind3* (also called *Fermt3*) gene in mice (Supplementary Fig. 1 online). Mice heterozygous for the Kindlin-3-null mutation (*Kind3*^{+/-}) were normal, whereas mice lacking Kindlin-3 (*Kind3*^{-/-}; Fig. 1a) died within a week of birth and showed a pronounced osteopetrosis (unpublished data) and severe hemorrhages in the gastrointestinal tract, skin, brain and bladder, which were already apparent during development (Fig. 1b and data not shown). To test whether the severe bleeding of Kindlin-3-deficient mice was due to impaired platelet production and/or function, we generated fetal liver cell chimeras by transferring either *Kind3*^{-/-} or wild-type fetal liver cells into lethally irradiated wild-type recipient mice. Tail-bleed assays revealed that *Kind3*^{-/-} chimeras suffer from a pronounced hemostatic defect like that of Kindlin-3-deficient mice. After the tail-tip cut, bleeding in control mice arrested within 10 min (mean of 5.4 ± 4.3 min), whereas *Kind3*^{-/-} chimeras bled for longer than 15 min, suggesting severe platelet dysfunction (Fig. 1c).

Kind3^{-/-} chimeras showed platelet counts similar to those of wild-type chimeras (Fig. 1d), ruling out an essential role for Kindlin-3 in platelet formation. Analysis of glycoprotein abundance on platelets revealed elevated levels of the vWF receptor complex GPIb-IX in Kindlin-3-deficient as compared to wild-type platelets, whereas levels of other glycoproteins, including GPVI, CD9, and β_1 and β_3 integrins, were reduced (Supplementary Table 1 online). Thus Kindlin-3 has an apparent yet undefined role in the expression of several glycoproteins. However, the reduced expression of integrin $\alpha_{IIb}\beta_3$ does not account for the hemostasis defect, as mice carrying a heterozygous null mutation in the β_3 integrin express even less $\alpha_{IIb}\beta_3$ integrin on their platelets (50% of wild-type) without developing a bleeding defect¹⁴.

¹Department of Molecular Medicine, Max Planck Institute of Biochemistry, Am Klopferspitz 18, 82152 Martinsried, Germany. ²University of Würzburg, Rudolf Virchow Center, Deutsche Forschungsgemeinschaft Research Center for Experimental Biomedicine, Zinklesweg 10, 97080 Würzburg, Germany. ³Institute of Clinical Biochemistry and Pathobiochemistry, Josef-Schneider-Str. 2, 97078 Würzburg, Germany. Correspondence should be addressed to R.F. (faessler@biochem.mpg.de).

Received 11 October 2007; accepted 4 January 2008; published online 17 February 2008; doi:10.1038/nm1722

LETTERS

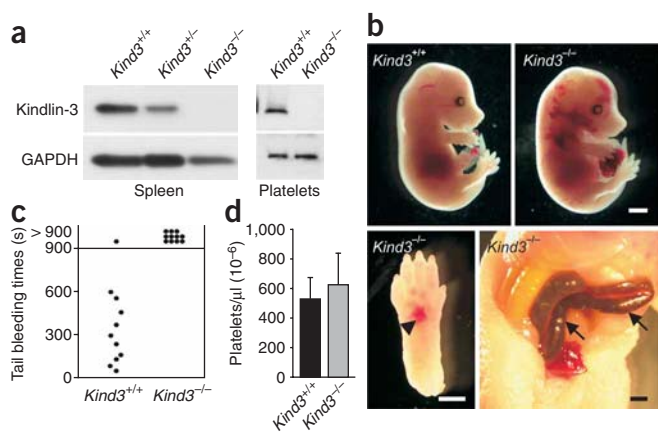


Figure 1 Kindlin-3-deficient animals show severe hemorrhages. (a) Western blot analyses from spleen and platelet lysates of wild-type (*Kind3*^{+/+}), heterozygous (*Kind3*^{+/-}) and Kindlin-3-deficient (*Kind3*^{-/-}) mice. (b) E15.5 embryos reveal severe bleeding. Postnatally, *Kind3*^{-/-} mice show skin (arrowhead) and intestinal (arrows) bleeding. All scale bars, 1 mm. (c) Tail-bleeding times in wild-type and *Kind3*^{-/-} mice. (d) Peripheral platelet counts in wild-type and *Kind3*^{-/-} chimeras.

To determine the mechanism of the platelet defect, we performed *ex vivo* platelet aggregation studies. Wild-type platelets aggregated in response to ADP, the TxA2 analog U46619, thrombin, collagen and the GPVI-activating collagen-related peptide (CRP), whereas none of the agonists induced aggregation of *Kind3*^{-/-} platelets (Fig. 2a). Notably, all agonists induced a comparable activation-dependent change from discoid to spherical shape in control and *Kind3*^{-/-} platelets, which can be seen in aggregometry as a short decrease in light transmission following the addition of agonists. This suggests a selective defect in $\alpha_{IIb}\beta_3$ -dependent aggregation rather than a general impairment of signaling pathways in *Kind3*^{-/-} platelets.

To test whether activation of $\alpha_{IIb}\beta_3$ integrin is indeed abrogated in *Kind3*^{-/-} platelets, we determined their ability to bind fibrinogen using flow cytometry. Wild-type platelets showed robust fibrinogen

binding in response to ADP, ADP plus U46619 and CRP, whereas *Kind3*^{-/-} platelets failed to bind fibrinogen upon agonist treatment (Fig. 2b). The antibody JON/A-PE, which specifically detects the activated form of mouse $\alpha_{IIb}\beta_3$ integrin¹⁴, likewise did not bind stimulated *Kind3*^{-/-} platelets (Fig. 2c). When cellular activation of $\alpha_{IIb}\beta_3$ integrin was bypassed by the addition of MnCl₂, comparable fibrinogen binding to *Kind3*^{-/-} and wild-type platelets occurred (Fig. 2b). Together, these findings indicate that loss of Kindlin-3 expression prevents energy-dependent conformational rearrangements required for integrin- $\alpha_{IIb}\beta_3$ activation.

Resting platelets store P-selectin in α -granules, which fuse with the plasma membrane during agonist-induced platelet activation¹. Both CRP and thrombin induced P-selectin translocation on wild-type and *Kind3*^{-/-} platelets, although a significant reduction was consistently observed at intermediate concentrations of thrombin ($P < 0.001$; Fig. 2d). As expected, the weak agonist ADP did not induce P-selectin surface expression in wild-type and *Kind3*^{-/-} platelets. Thus, although loss of Kindlin-3 specifically disables integrin activation, it still permits agonist-induced P-selectin translocation.

Integrin- $\alpha_{IIb}\beta_3$ is also involved in adhesion to immobilized ligands, including collagen-bound vWF, where it acts in concert with the collagen-binding $\alpha_2\beta_1$ integrin^{2,15}. We analyzed the ability of *Kind3*^{-/-} platelets to interact with fibrous collagen in a whole-blood perfusion

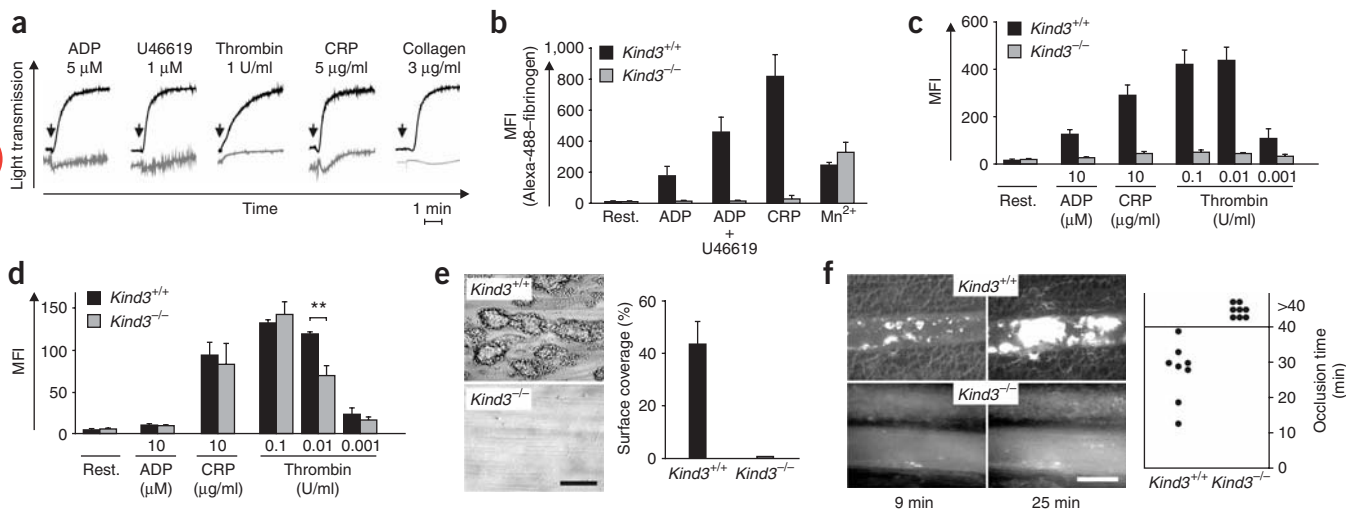


Figure 2 Impaired platelet function in *Kind3*^{-/-} mice. (a) Platelet aggregation assay reveals impaired aggregation of *Kind3*^{-/-} platelets (gray lines) in response to ADP, U46619, thrombin, CRP and collagen when compared with control platelets (black lines). Arrows denote addition of agonist. (b) Wild-type (*Kind3*^{+/+}) platelets (black bars), but not *Kind3*^{-/-} platelets (gray bars), bind fibrinogen in response to ADP (10 μ M), ADP (10 μ M) plus U46619 (3 μ M) or CRP (10 μ g/ml). Treatment with MnCl₂ (Mn²⁺; 3 mM) triggers comparable binding. Resting (rest.) platelets were used as a control. (c, d) *Kind3*^{-/-} platelets (gray bars) show a complete block in activation of integrin- $\alpha_{IIb}\beta_3$ after stimulation with ADP (10 μ M), CRP (10 μ g/ml) and different concentrations (0.001–0.1 U/ml) of thrombin (c), whereas platelet degranulation measured by the surface expression of P-selectin is largely intact after the same treatments (d). Wild-type platelets (black bars) were used as a control. At the intermediate thrombin concentration, moderately but significantly reduced degranulation was observed with mutant platelets (** $P < 0.01$). MFI, mean fluorescence intensity. (e) *Kind3*^{-/-} platelets in whole blood failed to form thrombi when perfused over a collagen-coated (0.25 mg/ml) surface at a wall shear rate of 1,000 s⁻¹. Scale bar, 30 μ m. (f) Mesenteric arterioles were injured with FeCl₃, and adhesion and thrombus formation of fluorescently labeled platelets were monitored by *in vivo* video microscopy. Representative images (left) and time to vessel occlusion (right) are shown. Each symbol represents one individual. Scale bar, 30 μ m.

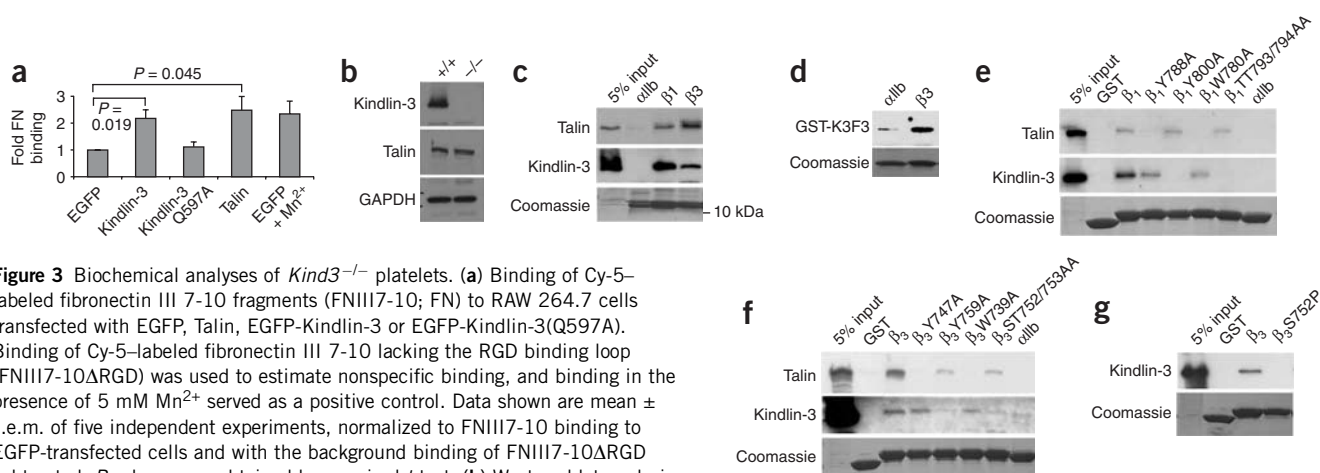


Figure 3 Biochemical analyses of *Kind3*^{-/-} platelets. **(a)** Binding of Cy-5-labeled fibronectin III 7-10 fragments (FNIII7-10; FN) to RAW 264.7 cells transfected with EGFP, Talin, EGFP-Kindlin-3 or EGFP-Kindlin-3(Q597A). Binding of Cy-5-labeled fibronectin III 7-10 lacking the RGD binding loop (FNIII7-10ΔRGD) was used to estimate nonspecific binding, and binding in the presence of 5 mM Mn²⁺ served as a positive control. Data shown are mean ± s.e.m. of five independent experiments, normalized to FNIII7-10 binding to EGFP-transfected cells and with the background binding of FNIII7-10ΔRGD subtracted. *P* values were obtained by unpaired *t*-test. **(b)** Western blot analysis of lysates from wild-type (+/+) control and *Kind3*^{-/-} (-/-) platelets. **(c)** Pull-down experiment with His-tagged αIIb, β₁ and β₃ integrin tails incubated with 100 μg platelet lysate. **(d)** Protein-protein interaction assay of recombinant GST-Kindlin-3 F3 domain (GST-K3F3) incubated with His-tagged αIIb and β₃ integrin tails reveals direct binding between the F3 domain of Kindlin-3 and the β₃ tail. GST pull-down experiments were performed with recombinant GST-β₁A (wild-type), GST-β₁Y788A, GST-β₁Y800A, GST-β₁W780A and GST-β₁TT793/794AA (**e**); with GST-β₃ (wild-type), GST-β₃Y747A, GST-β₃Y759A, GST-β₃W739A and GST-β₃ST752/753AA (**f**); and with GST-β₃ (wild-type) and GST-β₃S752A (**g**) integrin cytoplasmic domains after incubation with 100 μg platelet lysate. GST protein and GST-αIIb were used as controls. 5% of the platelet lysate used for the pull-down experiment is shown as input control. Bound Talin and Kindlin-3 proteins were detected by western blotting. Coomassie blue staining showed that equal amount of GST fusion proteins were used. Shown are results from pull-down assays representative of a minimum of seven experiments.

assay. Under high- (1,000 s⁻¹, **Fig. 2e**) or low-shear (150 s⁻¹, data not shown) flow conditions, wild-type platelets adhered to the collagen fibers and rapidly built stable three-dimensional aggregates (**Fig. 2e**). In contrast, *Kind3*^{-/-} platelets never established stable adhesions and either detached immediately or translocated along the fibers for a few seconds, resulting in virtually no platelets attaching to the collagen-coated surface at the end of the 4-min perfusion time (**Fig. 2e**). Furthermore, agonist-stimulated *Kind3*^{-/-} platelets failed to bind the monoclonal anti-β₁ integrin antibody 9EG7, which specifically recognizes the activated form of β₁ integrins¹⁶, and also failed to adhere to soluble, pepsin-digested collagen type I under static conditions (**Supplementary Fig. 2** online), a process known to be mediated exclusively by α₂β₁ integrins¹⁷. Together these findings indicate that *Kind3*^{-/-} platelets can establish initial contacts with vWF/collagen via GPIIb and probably GPVI, but are unable to adhere firmly as a result of defective activation of α_{IIb}β₃ and α₂β₁ integrins.

As platelet aggregation may lead to pathological occlusive thrombus formation, we examined whether lack of Kindlin-3 is protective against ischemia and infarction after mesenteric arteriole injury. This injury was induced by ferric chloride and assessed by *in vivo* fluorescence microscopy. Five minutes after injury, numerous platelets adhered firmly to the denuded vessel wall in control chimeras (5,380 ± 2,465/mm²); after approximately 10 min, the first thrombi were observed; and after 18–39 min, the vessels were occluded (mean occlusion time: 27.6 ± 8.1 min; **Fig. 2f**). In contrast, a few *Kind3*^{-/-} platelets transiently (<5 s) attached to the injured vessel wall, but virtually none adhered firmly throughout the 40-min observation period (50 ± 24 / mm²). Furthermore, no thrombi formed in the injured vessels of *Kind3*^{-/-} chimeras, and blood flow was maintained in all vessels tested (**Fig. 2f**). These results confirm the *ex vivo* results and underscore the pivotal function of Kindlin-3 in integrin-mediated platelet adhesion to injured vessels *in vivo*.

The requirement for Kindlin-3 to trigger agonist-induced integrin activation on platelets, integrin-mediated platelet adhesion and thrombus formation suggests that it may be a downstream target of

cellular signaling pathways that activate integrins. To test whether Kindlin-3 is able to activate integrins, we overexpressed Kindlin-3 in integrin-α_{IIb}β₃-overexpressing CHO cells. In these cells Kindlin-3 was unable to trigger integrin activation, likely because the hematopoietic Kindlin-3 is not recruited to integrin containing focal adhesions¹³. Kindlin-3 overexpression in the mouse macrophage cell line RAW 264.7 (RAW), however, yielded a 2.2-fold increase in binding of the Cy5-labeled fibronectin repeat 7-10 (FN7-10), which harbors the integrin-binding RGD motif (**Fig. 3a**). Enhanced green fluorescent protein (EGFP)-transfected RAW cells showed virtually no increase in FN7-10 binding as compared to untransfected cells, whereas Talin overexpression and treatment with Mn²⁺ induced a 2.5-fold increase. Notably, overexpression of a Kindlin-3 variant with a point mutation in the PTB-like domain (Q597A), which in Talin (R358) reduces binding to β tails⁴, did not trigger FN7-10 binding. These data indicate that Kindlin-3 is capable of activating FN binding integrins and that this activity requires an intact PTB-like domain.

How does Kindlin-3 activate integrins? As reduced Talin expression did not account for the defect (**Fig. 3b**), we investigated whether the FERM domain of Kindlin-3, which is similar to that of Talin, might play a direct role in integrin activation. As previously shown, recombinant Talin bound wild-type β₁ and β₃ integrin tails, and this binding was significantly reduced when alanine mutations were introduced into the membrane-proximal tryptophan residue or NPXY motif (β₃W739A, β₃Y747A, β₁W780A and β₁Y788A)¹⁸. Kindlin-3 was also able to interact with the wild-type β₁ and β₃ integrin tails (**Fig. 3c**), in the presence and absence of Talin1 (**Supplementary Fig. 3** online), and the F3 subdomain of Kindlin-3 was sufficient for this interaction and this interaction occurred in a direct manner (**Fig. 3d**). However, specific point mutations within the β₁ and β₃ integrin cytoplasmic tails revealed that the binding properties of Kindlin-3 were different from those of Talin, as the former still bound to β₃W739A, β₃Y747A, β₁W780A and β₁Y788A tails, although less efficiently than to wild-type tails (**Fig. 3e,f**). Mutations to the membrane distal NxxY motif of the β₁ and β₃ tails (β₁Y800A, β₃Y759A) and the β₁TT793/794AA and

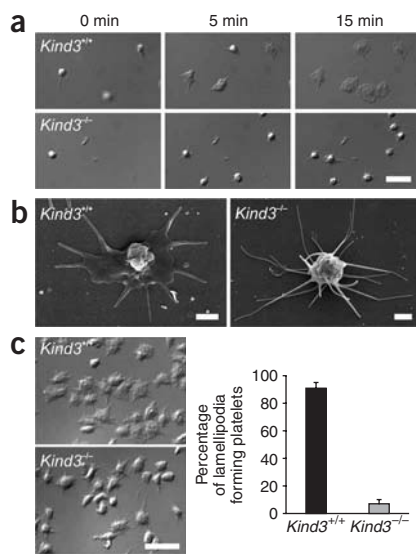


Figure 4 Defective adhesion and spreading of *Kind3*^{-/-} platelets. (a) Washed wild-type and *Kind3*^{-/-} platelets were stimulated with 0.01 U/ml thrombin and then allowed to adhere to immobilized fibrinogen for 15 min. Scale bar, 5 μ m. (b) Scanning electron microscopy of wild-type and *Kind3*^{-/-} platelets after thrombin stimulation and adhesion to fibrinogen for 30 min. Scale bars, 1 μ m. (c) Washed platelets were allowed to adhere to immobilized fibrinogen in the presence of 3 mM Mn²⁺ for 30 min. Left, representative DIC images. Scale bar, 5 μ m. Right, number of lamellipodia-forming platelets (% of adherent platelets; mean \pm s.d. of four experiments per group).

β_3 ST752/753AA, however, abolished Kindlin-3 but not Talin binding (Fig. 3e,f). Moreover, the β_3 S752P mutation found in a subset of individuals with Glanzmann's thrombasthenia also abolished Kindlin-3 binding¹⁹ (Fig. 3g). These data indicate that Talin primarily requires membrane-proximal residues for binding, whereas Kindlin-3 requires membrane-distal residues for binding to the β_1 and β_3 tails.

Ligand-occupied integrins transduce signals that lead to the activation of Src family kinases, resulting in cell spreading (outside-in signaling). We tested the role of Kindlin-3 in outside-in signaling by analyzing the adhesion of washed control and *Kind3*^{-/-} platelets to fibrinogen under static conditions. As mouse platelets, in contrast to human platelets, do not spread well on immobilized fibrinogen without cellular activation²⁰, we performed the experiments in the presence of 0.01 U/ml thrombin, with and without added Mn²⁺. Comparable adhesion of control and *Kind3*^{-/-} platelets to the fibrinogen matrix occurred, confirming a previous observation that integrin- $\alpha_{IIb}\beta_3$ activation is not required for static adhesion of platelets to fibrinogen²¹. However, whereas control platelets readily formed lamellipodia and spread within 10–15 min, *Kind3*^{-/-} platelets only formed filopodia, with occasional transient small lamellipodia, and completely failed to spread for up to 45 min (Fig. 4a,b). We obtained similar results when we carried out adhesion in the presence of Mn²⁺ (Fig. 4c). Thus, Kindlin-3 is also required for integrin $\alpha_{IIb}\beta_3$ -dependent outside-in signaling.

Our study demonstrates that Kindlin-3 is essential for platelet integrin activation and subsequent integrin outside-in signaling. Furthermore, we found that Kindlin-3 regulates activation of both β_3 ($\alpha_{IIb}\beta_3$) and β_1 ($\alpha_2\beta_1$) integrins, suggesting that Kindlin-3, like Talin, is a general regulator of integrin activation. We propose that this regulatory mechanism is mediated through a direct interaction

between the PTB site of the F3 domain in Kindlin-3 and the integrin β_3 and β_1 tails, including their distal NxxY motifs. Because Talin binding requires an intact proximal NPxY motif, our findings raise questions regarding the roles of Kindlin-3 and Talin in integrin activation and the hierarchy of their binding to the integrin β tails. Future studies on the structure of the Kindlin-3–integrin complex are required to examine the relative roles of Kindlin-3 and Talin interactions with integrin tails so as to fully understand how these receptors become activated. Finally, we show that elimination of Kindlin-3 prevents the formation of pathological thrombi. As Kindlin-3 is selectively expressed in cells of hematopoietic origin, it may serve as a potential target for the design of therapeutics aimed at specifically disrupting integrin activation in platelets.

METHODS

Inactivation of the Kindlin-3 gene. A BAC clone containing the *Kind3* (*Fermt3*) gene was isolated and used to generate the targeting construct containing an *IRES-lacZ-neo* cassette between exons 3 and 6. The targeting vector was electroporated into R1 ES cells, and targeted ES-cell clones were identified by southern blotting and injected into host blastocysts to generate germline chimeras.

Generation of fetal liver cell chimeras. Fetal liver cells from E15 wild-type and *Kind3*^{-/-} embryos were obtained by pushing the liver through a cell strainer (Falcon). 4×10^6 cells were injected into the tail vein of lethally irradiated (10 Gy) recipient C57BL/6 mice. At 3–4 weeks after transfer, platelets were isolated from whole blood collected from the retro-orbital plexus.

Western blot analysis. Platelet lysates were subjected to a 5–15% gradient SDS-PAGE. After blotting, PVDF membranes were probed with anti-Kindlin-3 (ref. 12), anti-Talin (Sigma) and anti-GAPDH (Chemicon).

GST fusion protein pull-down assays. The β_1A and β_3 integrin cytoplasmic domains and their mutant forms (GST- β_1 Y788A, GST- β_1 Y800A, GST- β_1 W780A and GST- β_1 TT793/794AA; GST- β_3 Y747A, GST- β_3 Y759A, GST- β_3 W739A, GST- β_3 ST752/753AA and GST- β_3 S752A) were expressed as GST-fusion proteins in BL21 cells upon induction with 1 mM IPTG. Bacteria were washed and lysed in buffer A (150 mM NaCl, 1 mM EDTA, 10 mM Tris, pH 8) containing 100 μ g/ml lysozyme for 15 min on ice and then sonicated. After dialysis against buffer B (100 mM NaCl, 50 mM Tris pH 7.5, 1% NP-40, 10% glycerol, 2 mM MgCl₂), GST-fusion proteins were bound to glutathione-Sepharose beads (Novagen), eluted in 50 mM Tris, pH 8, 20 mM glutathione, and dialyzed against buffer C (20 mM Tris pH 7.5, 20% glycerol, 100 mM KCl, 0.2 mM EDTA, 2 mM DTT, 10 mM β -glycerophosphate).

For GST pull-down experiments, GST fusion proteins were bound to glutathione-Sepharose beads for 1 h at room temperature ($\sim 20^\circ\text{C}$) in buffer A. Fresh platelet lysates were incubated with GST or GST-integrin cytoplasmic-domain fusion proteins for 4 h or overnight at 4°C . The glutathione-Sepharose beads were washed four times with buffer A containing 1% Triton X-100 and 10 mM EDTA. Bound proteins were eluted from the beads by boiling in Laemmli buffer (2% SDS, 10% glycerol, 5% 2-mercaptoethanol, 0.002% bromophenol blue, 62.5 mM Tris-HCl, pH 6.8) after separation by a SDS-PAGE and western blotting.

For direct protein-protein interaction assay, recombinant Kindlin-3 F3 domain, spanning amino acids 550–665 (GST-K3F3), was expressed in BL21 cells as described above. Histidine (His)-tagged integrin cytoplasmic tails were expressed in BL21 bacteria upon induction with 1 mM IPTG and purified under denaturing conditions. Ten micrograms of GST-K3F3 was incubated with His-tagged α_{IIb} and β_3 integrin cytoplasmic tails bound to Ni²⁺-coated beads for 2 h in buffer D (50 mM NaCl, 10 mM PIPES, 150 mM sucrose, 0.1% Triton X-100, pH 6.8) containing phosphatase and protease inhibitor cocktails (Sigma, Roche). After being washed in buffer D, bound proteins were analyzed by SDS-PAGE and western blotting. Loading of Ni²⁺-coated beads with the recombinant integrin tails was assessed by Coomassie Blue staining.

Fibronectin binding assay. RAW 264.7 cells were electroporated with 4 μg of the indicated DNAs using a Macrophage Kit from the Amaxa system. Twenty-four hours after transfection, cells were trypsinized, washed in FACS Tris-buffer (24 mM Tris-HCl, pH 7.4, 137 mM NaCl and 2.7 mM KCl) and incubated for 40 min with 0.3 μM Cy5-labeled recombinant fibronectin III 7-10 fragment or FNIII 7-10 Δ RGD fragment²². As a positive control, EGFP-transfected cells were incubated with 5 mM Mn^{2+} . After washing, the amount of cell-bound fibronectin fragment was measured with a FACSCalibur (Becton Dickinson). Dead cells were excluded from FACS analysis by addition of 2.5 $\mu\text{g}/\text{ml}$ propidium iodide and gating for living (propidium iodide negative) and EGFP-positive cells.

Chemicals. The anesthetic drugs xylazine (Rompun) and ketamine (Imalgene 1000) were purchased from Bayer and Merial, respectively. High-molecular-weight heparin and human fibrinogen and ADP were from Sigma and collagen was from Kollagenreagent Horm, Nycomed. Monoclonal antibodies conjugated to either fluorescein isothiocyanate (FITC) or phycoerythrin (PE) were from Emfret Analytics. Alexa-Fluor-488-labeled fibrinogen was from Molecular Probes.

Aggregometry. To determine platelet aggregation, light transmission was measured using washed platelets ($2 \times 10^8/\text{ml}$) in the presence of 70 $\mu\text{g}/\text{ml}$ human fibrinogen. Transmission was recorded on a Fibrintimer 4 channel aggregometer (APACT Laborgeräte und Analysensysteme) over 10 min and was expressed as arbitrary units with transmission through buffer defined as 100% transmission.

Flow cytometry. Heparinized whole blood was diluted 1:20 with modified Tyrode's-HEPES buffer (134 mM NaCl, 0.34 mM Na_2HPO_4 , 2.9 mM KCl, 12 mM NaHCO_3 , 20 mM HEPES, pH 7.0) containing 5 mM glucose, 0.35% bovine serum albumin (BSA) and 1 mM CaCl_2 . For assessment of glycoprotein expression and platelet count, blood samples were incubated with appropriate fluorophore-conjugated monoclonal antibodies for 15 min at room temperature and directly analyzed on a FACSCalibur (Becton Dickinson). Activation studies were performed with blood samples washed twice with modified Tyrode's-HEPES buffer, which then were activated with the indicated agonists or 3 mM MnCl_2 for 15 min, stained with fluorophore-labeled antibodies for 15 min at room temperature and directly analyzed.

Adhesion under flow conditions. Rectangular coverslips (24 \times 60 mm) were coated with 0.25 mg/ml fibrillar type I collagen (Nycomed) for 1 h at 37 $^\circ\text{C}$ and blocked with 1% BSA. Perfusion of heparinized whole blood was performed as described¹⁵. Briefly, transparent flow chambers with a slit depth of 50 μm , equipped with the collagen-coated coverslips, were rinsed with HEPES buffer, pH 7.45, and connected to a syringe filled with the anticoagulated blood. Perfusion was carried out at room temperature using a pulse-free pump at low (150 s^{-1}) and high shear stress ($1,000 \text{ s}^{-1}$). During perfusion, microscopic phase-contrast images were recorded in real time. Thereafter, the chambers were rinsed by a 10-min perfusion with HEPES buffer, pH 7.45, at the same shear stress, and phase-contrast pictures were recorded from at least five different microscopic fields ($63\times$ objectives). Image analysis was performed off-line using Metamorph software (Visitron). Thrombus formation results are expressed as the mean percentage of total area covered by thrombi.

Analysis of bleeding time. Mice were anesthetized and a 3-mm segment of the tail tip was cut off with a scalpel. Tail bleeding was monitored by gently absorbing the bead of blood with a filter paper without contacting the wound site. When no blood was observed on the paper after 15-s intervals, bleeding was determined to have ceased. The experiment was stopped after 15 min.

Intravital microscopy of thrombus formation in FeCl_3 injured mesenteric arterioles. Mice 4–5 weeks old were anesthetized, and the mesentery was gently exteriorized through a midline abdominal incision. Arterioles (35–60- μm diameter) were visualized with a Zeiss Axiovert 200 inverted microscope ($10\times$) equipped with a 100-W HBO fluorescent lamp source and a CoolSNAP-EZ camera (Visitron). Digital images were recorded and analyzed off-line using Metavue software (Visitron). Injury was induced by topical application of a 3-mm² filter paper tip saturated with FeCl_3 (20%) for 10 s.

Adhesion and aggregation of fluorescently labeled platelets in arterioles were monitored for 40 min or until complete occlusion occurred (blood flow stopped for >1 min).

Platelet spreading. Cover slips were coated overnight with 1 mg/ml human fibrinogen and then blocked for 1 h with 1% BSA in PBS. Washed platelets of wild-type or *Kind3*^{-/-} mice were resuspended at a concentration of 0.5×10^6 platelets/ μl and then further diluted 1:10 in Tyrode's-HEPES buffer. Shortly before platelets were seeded on the fibrinogen-coated coverslip, they were activated with 0.01 U/ml thrombin. Platelets were allowed to spread for 30 min and analyzed by differential interference contrast (DIC) microscopy. In parallel, platelets were fixed in 2.5% glutaraldehyde in Tyrode's-HEPES buffer and processed for scanning electron microscopy as previously described²³. In another set of experiments, washed platelets were allowed to adhere to fibrinogen in the presence of 3 mM Mn^{2+} without thrombin stimulation and analyzed as above.

Note: Supplementary information is available on the Nature Medicine website.

ACKNOWLEDGMENTS

We thank D. Calderwood (Yale University) and I. Campbell (Oxford University) for recombinant integrin tails and integrin tail expression vectors and help with pull-down assays, G. Wanner for imaging of platelets by scanning electron microscopy, M. Sixt and M. Boesl for mouse manipulation experiments, and R. Zent, A. Pozzi, M. Humphries and M. Schwartz for critical reading of the manuscript. This work was supported by the Deutsche Forschungsgemeinschaft and the Max Planck Society.

AUTHOR CONTRIBUTIONS

M.M. and R.F. designed and supervised research. M.M., B.N. and R.F. wrote the manuscript. M.M., B.N., S.U. and M.P. performed experiments. All authors discussed the results and commented on the manuscript.

Published online at <http://www.nature.com/naturemedicine>

Reprints and permissions information is available online at <http://npg.nature.com/reprintsandpermissions>

- Ruggeri, Z.M. Platelets in atherothrombosis. *Nat. Med.* **8**, 1227–1234 (2002).
- Savage, B., Almus-Jacobs, F. & Ruggeri, Z.M. Specific synergy of multiple substrate-receptor interactions in platelet thrombus formation under flow. *Cell* **94**, 657–666 (1998).
- Nieswandt, B. & Watson, S.P. Platelet-collagen interaction: is GPVI the central receptor? *Blood* **102**, 449–461 (2003).
- Tadokoro, S. *et al.* Talin binding to integrin β tails: a final common step in integrin activation. *Science* **302**, 103–106 (2003).
- Critchley, D.R. Cytoskeletal protein talin and vinculin in integrin-mediated adhesion. *Biochem. Soc. Trans.* **32**, 831–836 (2004).
- Nieswandt, B. *et al.* Loss of talin1 in platelets abrogates integrin activation, platelet aggregation, and thrombus formation in vitro and in vivo. *J. Exp. Med.* (in the press).
- Calderwood, D.A. *et al.* The phosphotyrosine binding-like domain of talin activates integrins. *J. Biol. Chem.* **277**, 21749–21758 (2002).
- Calderwood, D.A. *et al.* The talin head domain binds to integrin β subunit cytoplasmic tails and regulates integrin activation. *J. Biol. Chem.* **274**, 28071–28074 (1999).
- Wegener, K.L. *et al.* Structural basis of integrin activation by talin. *Cell* **128**, 171–182 (2007).
- Kloeker, S. *et al.* The Kindler syndrome protein is regulated by transforming growth factor- β and involved in integrin-mediated adhesion. *J. Biol. Chem.* **279**, 6824–6833 (2004).
- Tu, Y., Wu, S., Shi, X., Chen, K. & Wu, C. Migfilin and Mig-2 link focal adhesions to filamin and the actin cytoskeleton and function in cell shape modulation. *Cell* **113**, 37–47 (2003).
- Ussar, S., Wang, H.V., Linder, S., Fässler, R. & Moser, M. The Kindlins: subcellular localization and expression during murine development. *Exp. Cell Res.* **312**, 3142–3151 (2006).
- Weinstein, E.J. *et al.* URP1: a member of a novel family of PH and FERM domain-containing membrane-associated proteins is significantly over-expressed in lung and colon carcinomas. *Biochim. Biophys. Acta* **1637**, 207–216 (2003).
- Hodivala-Dilke, K.M. *et al.* $\beta 3$ -integrin-deficient mice are a model for Glanzmann thrombasthenia showing placental defects and reduced survival. *J. Clin. Invest.* **103**, 229–238 (1999).
- Nieswandt, B. *et al.* Glycoprotein VI but not $\alpha 2\beta 1$ integrin is essential for platelet interaction with collagen. *EMBO J.* **20**, 2120–2130 (2001).
- Lenter, M. *et al.* A monoclonal antibody against an activation epitope on mouse integrin chain $\beta 1$ blocks adhesion of lymphocytes to the endothelial integrin $\alpha 6\beta 1$. *Proc. Natl. Acad. Sci. USA* **90**, 9051–9055 (1993).
- Holtkotter, O. *et al.* Integrin $\alpha 2$ -deficient mice develop normally, are fertile, but display partially defective platelet interaction with collagen. *J. Biol. Chem.* **277**, 10789–10794 (2002).

LETTERS

18. Pfaff, M., Liu, S., Erle, D.J. & Ginsberg, M.H. Integrin β cytoplasmic domains differentially bind to cytoskeletal proteins. *J. Biol. Chem.* **273**, 6104–6109 (1998).
19. Chen, Y.P. *et al.* Ser-752→Pro mutation in the cytoplasmic domain of integrin $\beta 3$ subunit and defective activation of platelet integrin $\alpha IIb\beta 3$ (glycoprotein IIb-IIIa) in a variant of Glanzmann thrombasthenia. *Proc. Natl. Acad. Sci. USA* **89**, 10169–10173 (1992).
20. McCarty, O.J. *et al.* Rac1 is essential for platelet lamellipodia formation and aggregate stability under flow. *J. Biol. Chem.* **280**, 39474–39484 (2005).
21. Savage, B., Shattil, S.J. & Ruggeri, Z.M. Modulation of platelet function through adhesion receptors. A dual role for glycoprotein IIb-IIIa (integrin $\alpha IIb\beta 3$) mediated by fibrinogen and glycoprotein Ib-von Willebrand factor. *J. Biol. Chem.* **267**, 11300–11306 (1992).
22. Takahashi, S. *et al.* The RGD motif in fibronectin is essential for development but dispensable for fibril assembly. *J. Cell Biol.* **178**, 167–178 (2007).
23. Fässler, R. *et al.* Lack of $\beta 1$ integrin gene in embryonic stem cells affects morphology, adhesion, and migration but not integration into the inner cell mass of blastocysts. *J. Cell Biol.* **128**, 979–988 (1995).

Paper V

SILAC Mouse for Quantitative Proteomics Uncovers Kindlin-3 as an Essential Factor for Red Blood Cell Function

Marcus Krüger,^{1,3} Markus Moser,^{2,3} Siegfried Ussar,² Ingo Thievensen,² Christian A. Luber,¹ Francesca Forner,¹ Sarah Schmidt,² Sara Zanivan,¹ Reinhard Fässler,^{2,*} and Matthias Mann^{1,*}

¹Department of Proteomics and Signal Transduction

²Department of Molecular Medicine

Max-Planck-Institute for Biochemistry, 82152 Martinsried, Germany

³These authors contributed equally to this work

*Correspondence: faessler@biochem.mpg.de (R.F.), mmann@biochem.mpg.de (M.M.)

DOI 10.1016/j.cell.2008.05.033

SUMMARY

Stable isotope labeling by amino acids in cell culture (SILAC) has become a versatile tool for quantitative, mass spectrometry (MS)-based proteomics. Here, we completely label mice with a diet containing either the natural or the ¹³C₆-substituted version of lysine. Mice were labeled over four generations with the heavy diet, and development, growth, and behavior were not affected. MS analysis of incorporation levels allowed for the determination of incorporation rates of proteins from blood cells and organs. The F2 generation was completely labeled in all organs tested. SILAC analysis from various organs lacking expression of $\beta 1$ integrin, β -Parvin, or the integrin tail-binding protein Kindlin-3 confirmed their absence and disclosed a structural defect of the red blood cell membrane skeleton in Kindlin-3-deficient erythrocytes. The SILAC-mouse approach is a versatile tool by which to quantitatively compare proteomes from knockout mice and thereby determine protein functions under complex in vivo conditions.

INTRODUCTION

The administration of radioactive or stable isotope tracers to animals is a well established technique by which to investigate the rate of protein synthesis and protein degradation. (Wolfe and Chinkes, 2005). This technology has been used for many decades (Schoenheimer and Rittenberg, 1935). The infusion of stable isotopes (¹³C or ¹⁵N) as tracers combined with measurements of ¹³CO₂ or ¹⁵N in urinary urea or ammonia is a broadly used technique by which to explore the amino acid flux in metabolic pathways (Bier, 1997; Dietz et al., 1982). Extensive incorporation of ¹³C or ¹⁵N stable isotopes does not result in discernable health effects of the treated animals (Doherty and Beynon, 2006; Gregg et al., 1973).

Mass spectrometry (MS) is not inherently quantitative, and relative protein expression changes are instead most accurately measured by comparison of the natural form of a peptide with its stable isotope analog (Ong and Mann, 2005). In recent years, ¹⁵N labeling has been applied to microorganisms such as yeast (Oda et al., 1999; Pratt et al., 2002), *Caenorhabditis elegans*, and *Drosophila* (Krijgsveld et al., 2003). Even a rat has been partially (Wu et al., 2004) or completely ¹⁵N labeled (McClatchy et al., 2007). In addition, nonsaturated labeling of a chicken, by using the essential amino acid valine, allows for the MS-based analysis of protein turnover rates in vivo (Doherty et al., 2005).

Our laboratory has previously described stable isotope labeling by amino acids in cell culture (SILAC) (Mann, 2006; Ong et al., 2002), which has unique advantages for quantitative and functional proteomics because of its inherent accuracy of quantitation and the ease of interpretation of MS results (Blagoev et al., 2004; Kratchmarova et al., 2005). In a SILAC experiment, two cell populations are generated: one in a medium that contains the natural amino acid (i.e., ¹²C₆-lysine), and the other in a medium that contains the heavy isotope-substituted version (i.e., ¹³C₆-lysine). This allows for direct comparison of protein expression levels by mixing the nonlabeled "light" and the labeled "heavy" cell populations (Cox and Mann, 2007). Each peptide appears as a pair in MS analysis with a difference in mass of 6 Da, and the relative peak intensities reflect the abundance ratios. To date, SILAC labeling has been limited to cell culture or microorganisms. To extend this powerful technique to higher organisms, Oda and coworkers have SILAC labeled the Neuro 2A cell line to serve as an internal standard for quantitation of a subset of peptides of the mouse brain proteome (Ishihama et al., 2005).

In the present paper, we report the development of a mouse SILAC diet that leads to complete labeling of the F2 generation. We used in vivo SILAC quantitation to analyze newly synthesized proteins from plasma and tissue samples in vivo. Furthermore, we validated our in vivo quantitation system by comparing the proteomes from platelets, heart, and erythrocytes from $\beta 1$ integrin-, β -Parvin-, and Kindlin-3-deficient mice, respectively.

Integrins are heterodimeric transmembrane proteins, consist of α and β subunits, are ubiquitously expressed, and perform

cell-cell and cell-matrix adhesion functions. Association of the corresponding α and β subunits is required for their stability and transport to the plasma membrane, as single subunits are not stable and are rapidly degraded. Integrin-mediated cell adhesion triggers intracellular signaling pathways (outside-in signaling) that control migration, proliferation, survival, and differentiation of cells. Prior to ligand binding, integrins require an energy-dependent activation step, which is triggered within the cell (inside-out signaling) and is characterized by a profound conformational change in both integrin subunits. Although the mechanism(s) underlying integrin activation are far from understood, it is believed that the binding of the FERM-domain-containing adaptor proteins talin and Kindlin to the integrin β cytoplasmic domains represents the last step in the activation pathway (Calderwood, 2004; Moser et al., 2008).

Upon activation and ligand binding, integrins recruit and assemble a multiprotein complex at the site of cell adhesion that fulfills two major tasks: it connects the extracellular matrix with the actin cytoskeleton, and it alters the fluxes of many intracellular signaling pathways. A preformed complex consisting of the three proteins, ILK, PINCH, and Parvin, represents an important component of the integrin adhesion complex (Legate et al., 2006). Parvins comprise a family of three proteins, α -, β - and γ -Parvin, that directly bind to ILK, F-actin, and other actin-associated proteins, thereby linking the adhesion complex to the actin cytoskeleton and controlling actin dynamics.

Kindlins have recently been identified within the integrin-mediated cell adhesion complex and represent an additional family of ILK-binding proteins (Montanez et al., 2007). They consist of three members (Kindlin-1–3) and are named after the gene mutated in Kindler syndrome, an autosomal recessive skin blister disease in humans. Kindlin-3 expression is restricted to hematopoietic cells, and the highest levels are in megakaryocytes (Ussar et al., 2006). Inactivation of the Kindlin-3 gene in mice results in severe anemia, which is thought to be due to a bleeding defect caused by impaired activation of platelet integrins, defects in platelet aggregation, and thrombus formation (Moser et al., 2008).

To screen for potential defects in other cellular compartments of the hematopoietic system in Kindlin-3-deficient mice, we compared their proteome with those from control mice. During the course of these studies, we discovered a deficit of structural proteins in the plasma membrane of Kindlin-3-deficient erythrocytes, which contributes to the severe anemia seen in Kindlin-3-deficient mice.

RESULTS

A Heavy SILAC Diet Has No Influence on Weight Gain and Fertility

We prepared a SILAC diet by mixing $^{13}\text{C}_6$ -lysine or $^{12}\text{C}_6$ -lysine into a customized lysine-free mouse diet to a final concentration of 1% (Figure 1A) according to standard mouse nutritional requirements (Benevenga et al., 1995). The amino acid content was subsequently checked by hydrolysis and cation exchange chromatography (Figure S1 available online). We first tested whether the diet permits normal weight gain by feeding mice with a regular diet or the SILAC diet (with $^{12}\text{C}_6$ -lysine or

$^{13}\text{C}_6$ -lysine). During an observation period of 4 weeks, all animals showed the same food consumption and a similar increase in body weight of about 17% (Figures S2A and S2B), normal fertility, and motor activity irrespective of the diet consumed. Furthermore, we SILAC labeled mice over four generations (see below), indicating that the labeling is compatible with normal development and physiology. Thus, we conclude that SILAC labeling with a $^{13}\text{C}_6$ -substituted essential amino acid diet does not lead to obvious discernable health effects in mice (Figure 1B).

SILAC Incorporation Rates Differ in Blood, Liver, and Gut Epithelium

To track $^{13}\text{C}_6$ -lysine incorporation into the proteome over time, we sampled blood each week for 4 weeks. Serum proteins were separated on 1D gels in triplicate, in-gel digested, and analyzed by high-resolution MS. The average relative standard deviation of all quantified proteins was $\sim 20\%$ (Figure 1C), an accuracy similar to what was seen in previous SILAC quantitation experiments (Blagoev et al., 2004; Ong et al., 2003).

As an example of different incorporation levels, SILAC peptide pairs of three serum proteins and one red blood cell protein are shown in Figure 1C. For serum albumin, we observed a SILAC ratio of 1:3.2, indicating that at least 74% of the protein had been newly synthesized during the first week of feeding. Because proteins can be synthesized from dietary amino acids as well as from amino acids derived by protein catabolism, this value is a lower limit for the true turnover (Beynon and Pratt, 2005). After 4 weeks, the three serum proteins were labeled to 90%. In contrast, hemoglobin was only labeled to 57% after 4 weeks (Figure 1C), due to the 60-day half-life of mouse erythrocytes (Berlin et al., 1959). Additional profiles of blood proteins are listed in Table S1.

Next, we measured the labeling efficiencies of a number of organs after 4 weeks of feeding with the SILAC diet. Proteins from heart showed an average protein ratio of 1:4.4 (Figure 2A; Table S2), much lower than the serum proteins. Furthermore, the distribution of SILAC ratios was relatively broad, reflecting the different incorporation rates of individual cell types and the “contamination” of serum proteins in nonperfused samples. For example, serum albumin has a similarly high incorporation rate in blood (ratio 9) and heart (ratio 10) (Figures 1C and 2A). In contrast to heart tissue, in which most cells are quiescent, the intestinal epithelium regenerates within a few days (Radtke and Clevers, 2005). Disaggregating the epithelium from the digestive tube resulted in a more homogeneous cell pool consisting of only a few cell types. As a consequence, we observed a high SILAC ratio of $1:9.1 \pm 2.1$ reflecting a labeling efficiency of more than 90% (Figure 2B), which is fully consistent with the high proliferation rate of this tissue. For example, villin-1, a marker for epithelial cells from the digestive system, showed a SILAC ratio of 1:10.

Liver has a number of different physiological roles, including carrying out metabolic functions and producing major blood proteins. Accordingly, we observed a wide distribution of SILAC-incorporation ratios among liver proteins. Hepatocytes are the predominant liver cell type, and they are very rich in mitochondria. To demonstrate that in vivo SILAC ratios can be measured with subcellular resolution, we isolated mitochondria from liver

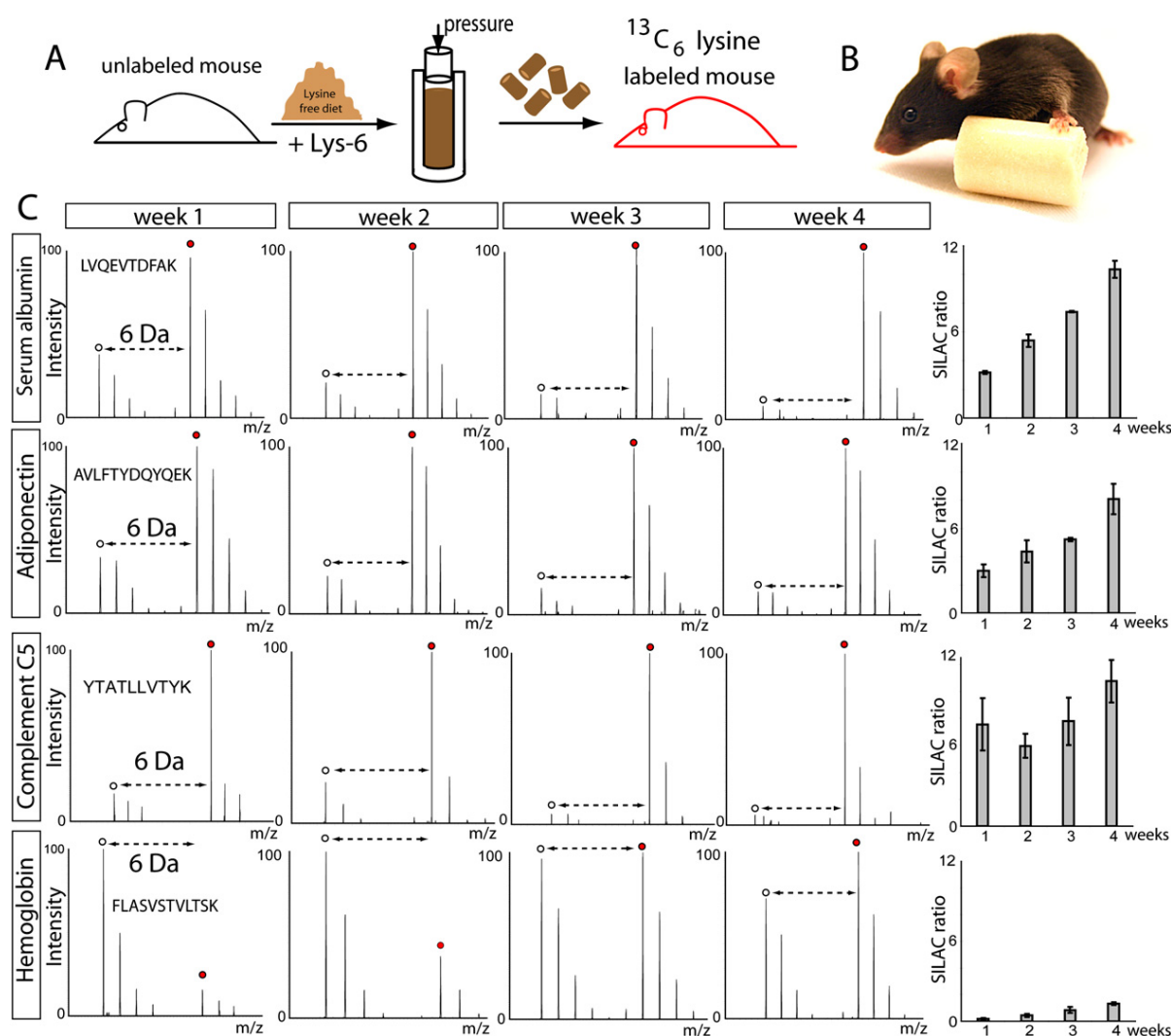


Figure 1. SILAC Labeling and Incorporation Rates of Blood Proteins

(A) Mice are SILAC labeled by being fed a pelleted, lysine-free diet supplemented with normal or heavy lysine.

(B) Mice on a SILAC diet cannot be visually distinguished from mice with a normal, commercial diet.

(C) Mass spectra showing SILAC pairs of a representative peptide for four blood proteins. The right-hand side shows lysine-6 incorporation over the course of 4 weeks as an average measurement of triplicates.

cells (Forner et al., 2006) and compared their labeling ratios to whole-cell lysates from the same sample (Figure 2C, black bars). Interestingly, proteins from mitochondria showed an average SILAC ratio of $1:8.6 \pm 2.4$. This shows that the incorporation rates of an organelle are more narrowly distributed and distinguishable from that of a whole tissue.

We next investigated several cell types of the hematopoietic system. Platelets are cell fragments that are constantly released by megakaryocytes into the blood stream. They have a half-life of $\sim 7\text{--}9$ days. We isolated platelets from a SILAC mouse after 4 weeks of labeling and measured incorporation levels of 86% from 241 quantified proteins (Figure 2D). In contrast, serum albumin, which was also measured within the platelet sample due to serum contamination, has a much higher incorporation level

compared to platelet proteins. Analysis of the red blood cell proteome revealed a significantly lower $^{13}\text{C}_6$ -lysine incorporation of 75% (Figure 2E). Thus, consideration of SILAC-incorporation rates could aid in the determination of the origin of the same proteins from different cellular pools via their different dynamic incorporation rates.

To combine SILAC-mouse analysis with cell sorting to obtain an accurately defined cell population, we separated CD45R-positive B lymphocytes from spleen by fluorescence-activated cell sorting (FACS) (Figures 2F and S3). An in-solution protein digest was performed from lysates of 1×10^6 spleen cells (Table S2F). The distribution of measured ratios was $1:5.4 \pm 1.3$, demonstrating that FACS-sorted populations of interest can readily be investigated in the SILAC mouse.

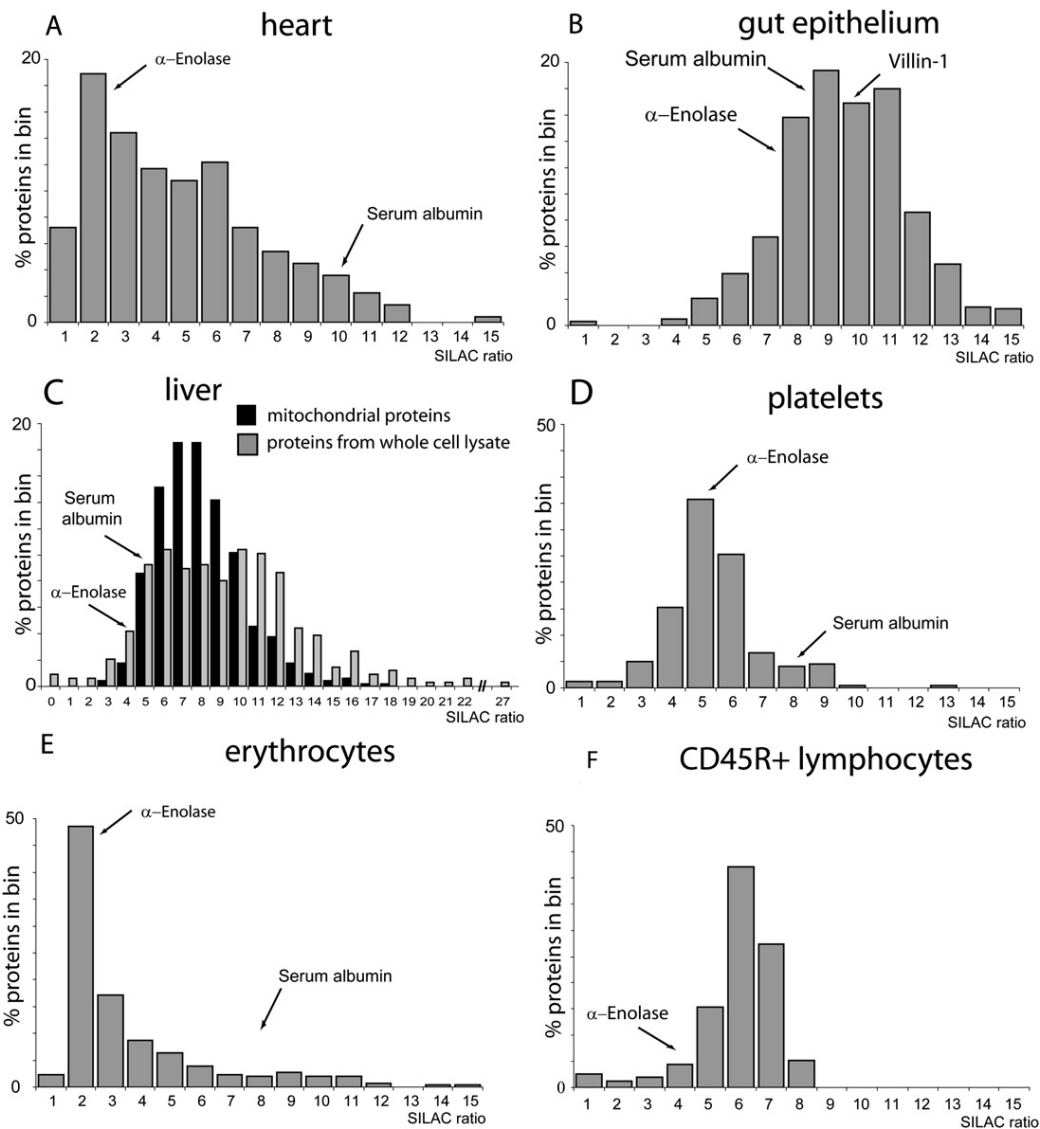


Figure 2. SILAC Label Incorporation into Different Cell Types and Tissues after 4 Weeks

(A–F) The panels show the relative number of proteins with the specified ratios for each proteome investigated. (A) Heart tissue. (B) Gut epithelium. (C) Incorporation into whole liver (gray bars) is compared with incorporation into liver mitochondria (black bars). (D) Platelets. (E) Erythrocytes. (F) CD45R-positive B lymphocytes from spleen.

Taken together, our results indicate that feeding mice with a SILAC diet is a suitable approach to label proteins *in vivo* and to follow their metabolic incorporation in any organ.

Complete SILAC-Based Labeling of F2 Mice

Although the label efficiency was relatively high in many tissues, we found that extending the labeling time did not lead to complete labeling. This is likely due to the recycling of internal amino acid sources (Doherty et al., 2005). Since labeling rates above 95% are required to perform comparative and quantitative proteomics by MS, we started feeding our mice over several generations with the heavy diet. Importantly, the consumption of the heavy diet did not affect litter size (Figure S2). The F1–F4 off-

spring developed normally, gained weight within the normal weight-gain chart (Figure S2), and showed normal mating behavior. Furthermore, newborn animals of the F1 generation were almost completely labeled, reaching ~93% in blood, brain, and liver (Figures 3 and S4). To obtain fully labeled animals to serve as internal standards and to investigate if SILAC labeling could be performed for many generations, we bred F2, F3, and F4 mice. These mice contained virtually no unlabeled peptides (Figures 3B, 3C, and 5A; Table S3).

Proteome of β 1 Integrin-Deficient Platelets

For validation of our *in vivo* quantitative proteomics approach, we analyzed and compared protein lysates from β 1 integrin-deficient

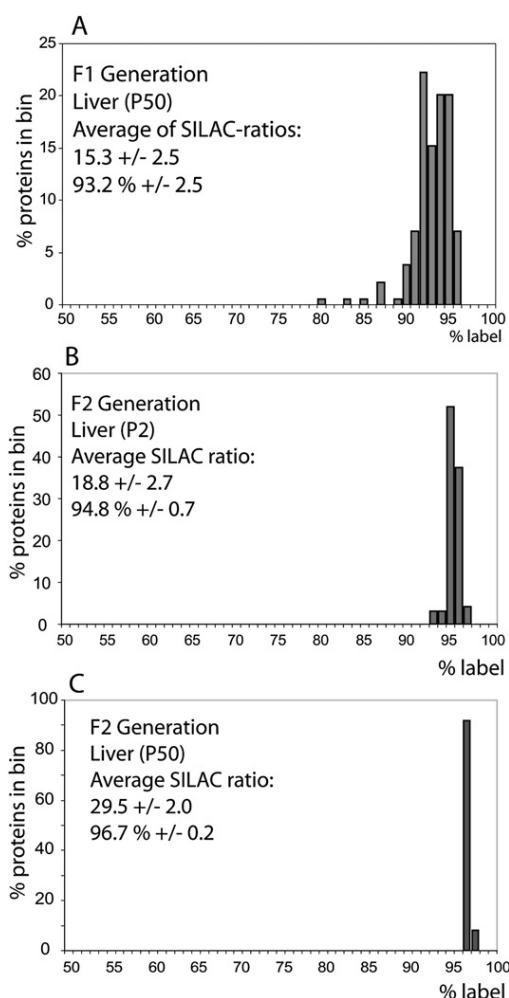


Figure 3. Complete Labeling of the F2 Generation

(A) Label efficiency of the liver of a 2-day-old mouse of the F1 generation. (B and C) Histograms of liver proteins with the specified percent incorporation at (B) P2 and at (C) P50 of the F2 generation. The averages of the SILAC ratios and the corresponding percent of the SILAC labeling are displayed in the histogram. The analysis encompasses ~100 proteins.

and control platelets (Nieswandt et al., 2001). We generated $\beta 1$ integrin-deficient platelets by intercrossing $\beta 1$ floxed mice ($\beta 1^{fl/fl}$) with a transgenic mouse expressing an Mx1 promoter-driven, interferon-inducible Cre (Mx1-Cre) (Brakebusch et al., 2000; Kuhn et al., 1995). We treated $\beta 1^{fl/fl}$; Mx1-Cre mice with synthetic double-stranded RNA (polyinosinic-polycytidylic acid, pl-pC), which triggers endogenous interferon production and subsequent Mx1-Cre activity. This leads to deletion of the $\beta 1$ integrin gene in all hematopoietic cells, including megakaryocytes. To monitor the knockout efficiency of $\beta 1$ integrin, we compared platelets from labeled wild-type animals with platelet populations from three groups of mice: (1) nonlabeled wild-type platelets; (2) platelets from nonlabeled, non-pl-pC-induced $\beta 1^{fl/fl}$; Mx1-Cre mice; and (3) platelets from nonlabeled, pl-pC-induced $\beta 1^{fl/fl}$; Mx1-Cre mice (Figure 4). All mice were backcrossed on a C57BL/6 background to reduce genetic variability.

We quantified ~645 proteins in these platelets, and, as expected, protein ratios of labeled and nonlabeled wild-type platelets were tightly distributed, with an overall ratio of 1:1. The quantitative MS analysis revealed complete loss of $\beta 1$ integrin in platelets from pl-pC-induced $\beta 1^{fl/fl}$; Mx1-Cre mice (Figure 4F). The proteins with the next highest ratios were the dimerization partners of the $\beta 1$ integrin subunit, strikingly confirming the sensitivity and reliability of our SILAC-mouse labeling system (Figure 4I). In a boxplot analysis, $\beta 1$, $\alpha 2$, and $\alpha 6$ integrins were all more than ten interquartile ranges away from the median (Figure S5A; Table S4). The complete loss of both α subunits can be explained by the formation of a stable integrin heterodimer during the synthesis and transport of the complexed integrin subunits to the plasma membrane. Without the correct β integrin subunit, the α subunit is rapidly degraded (Hynes, 2002). In contrast, the loss of $\beta 1$ integrin has no impact on the expression of other integrins, such as the major platelet integrin $\alpha IIb\beta 3$.

In addition, several other proteins in $\beta 1$ integrin-deficient platelets were outliers in the boxplot (Figure S5A; Table S4). However, a second independent experiment did not verify these proteins as being significantly downregulated. (Figure S5C). In contrast, the $\beta 1$ integrin dimerization partners $\alpha 2$ and $\alpha 6$ integrins were again strongly reduced (Figure S5).

Interestingly, the analysis of platelets from noninduced $\beta 1^{fl/fl}$; Mx1-Cre mice also revealed a slight downregulation of the $\beta 1$, $\alpha 2$, and $\alpha 6$ integrin levels compared to labeled wild-type platelets (Figure 4J). This effect is due to the natural, endogenous α/β interferon production in the bone marrow causing a low Mx1 promoter activity (Kuhn et al., 1995). The detection of this “leak” impressively underscores the sensitivity of our quantitative proteomics approach.

β -Parvin Deficiency in Heart Is Compensated by α -Parvin Induction

We next wanted to confirm the applicability of our in vivo SILAC approach to analyze the proteomes from knockout mice in a solid organ. To this end, we compared the proteomes from hearts of β -Parvin-deficient mice with those of control littermates. As a heavy standard, we used heart lysates from 2-week-old mice of the F4 generation, which showed an overall 97.7% incorporation of ^{13}C -lysine (Figure 5A). To test our quantitation system, we mixed “heavy” and “light” protein lysates from wild-type hearts in ratios of 1:1, 1:2, and 1:4. As shown in (Figure 5B), mixing of protein lysates from different heart samples gave rise to SILAC ratios that accurately reflected the lysate mixture.

β -Parvin represents the dominant Parvin isoform of the heart, since α -Parvin is only weakly present and γ -Parvin is absent from heart tissue. β -Parvin-deficient mice were generated by homologous recombination of a targeting vector in embryonic stem (ES) cells, which lacks exons 2 and 3 of the β -Parvin gene (I.T. and R.F., unpublished data). β -Parvin-deficient mice were viable and fertile and did not show any overt phenotype, indicating that β -Parvin is not essential for mouse development and organ formation. Mass spectrometric measurements of whole protein lysates from β -Parvin-deficient and control hearts of 2-week-old animals showed a complete absence of β -Parvin in knockout animals (Figures 5C and 5D). Out of 1205 proteins, only 4 proteins showed a two-fold decrease in their abundance compared to

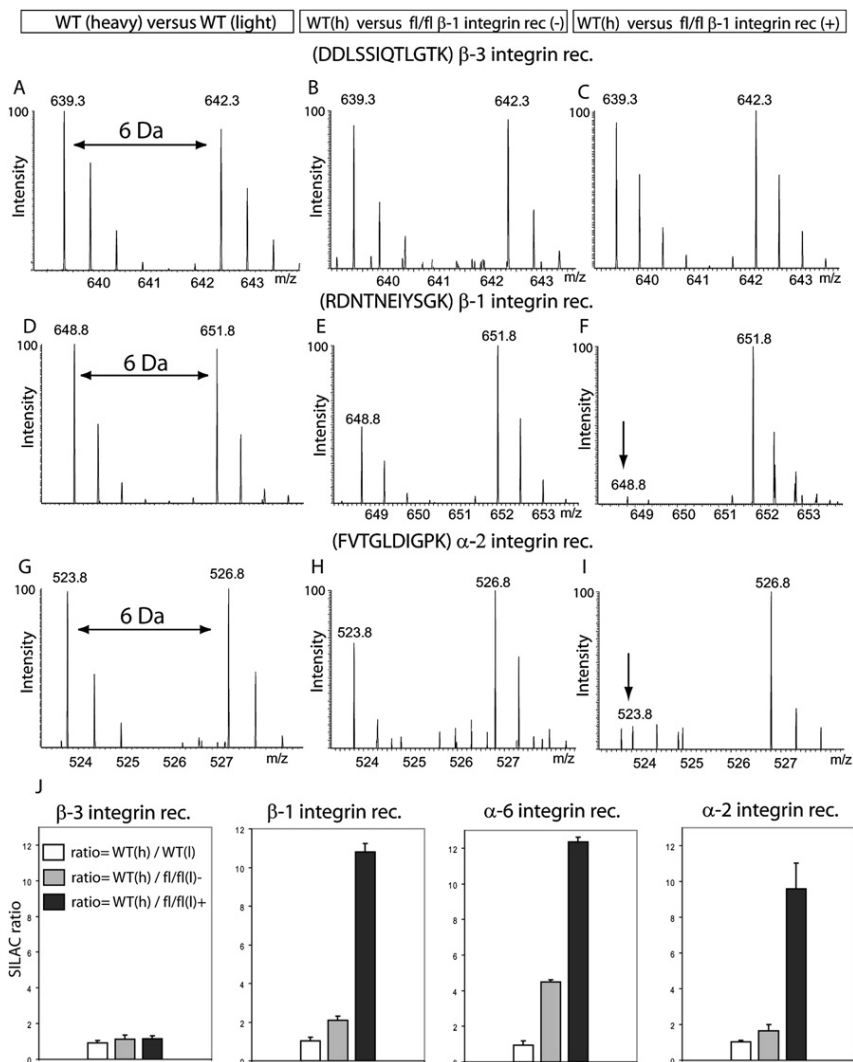


Figure 4. Analysis of β 1 Integrin Knockout Platelets

(A–J) (A, D, and G) Platelets from SILAC-labeled wild-type mice were mixed with platelets from a nonlabeled wild-type control mouse. Comparison of the wild-type SILAC mouse with (B, E, and H) noninduced β 1^{fl/fl}; Mx1-Cre mice and with (C, F, and I) pl-pC-induced β 1^{fl/fl}; Mx1-Cre mice. The slight decrease of β 1 integrin shown in (E) is due to Cre activity induced by low endogenous interferon expression. The arrows in (F) and (I) label the reduced peak intensity of β 1 and α 2 integrin, respectively. (J) Summary of quantified SILAC ratios for β 3, β 1, α 2, and α 6 integrin subunits. White bars represent the ratio between the labeled wild-type WT(h) animal and the nonlabeled wild-type animal, gray bars represent the SILAC ratio of WT(h) and noninduced β 1^{fl/fl}, and black bars represent the SILAC ratio between WT(h) and induced β 1^{fl/fl}; Mx1-Cre. The error bars show the variability of the measured ratios.

paired integrin trafficking in the absence of Kindlin-3 (Figure S6B).

We have previously reported that Kindlin-3 (also known as “unc-related protein 2”) is present in red blood cells (Pasini et al., 2006). This was confirmed by different SILAC-incorporation levels in platelets (incorporation rate of 1:6.0) compared to erythrocytes (incorporation rate of 1:2.1), measured after the initial 4-week labeling period (Figures 2, S7A, and S7B). Furthermore, Kindlin-3 gene activity in Ter119-positive Kindlin-3-heterozygous erythroblasts was further corroborated by measuring Kindlin-3 promoter-driven β -galactosidase reporter gene activity with FACS (Figure S7C).

To investigate whether loss of Kindlin-3 affects erythroid cells, we determined and quantitatively compared the proteomes from wild-type, Kindlin-3^{+/-}, and Kindlin-3^{-/-} erythrocytes (Figure 6; Table S7). MS confirmed a 50% reduction of Kindlin-3 in heterozygous and a complete absence of Kindlin-3 in Kindlin-3^{-/-} erythrocytes (Figure 6A). Out of 881 proteins identified in all 3 proteomes, more than 50 were two-fold increased in Kindlin-3^{-/-} erythrocytes, and only a few revealed a more than two-fold reduction. Interestingly, a large proportion of the upregulated proteins was annotated to be nuclear (Table S7).

Blood smears from Kindlin-3^{-/-} embryos and P3 animals showed a strong reduction of cells when compared to wild-type controls and, in concordance with this proteomic finding, many more nucleated erythroblasts (Figures 7B and 7C). In addition, the size and shape of Kindlin-3^{-/-} erythrocytes were markedly irregular.

Scanning electron microscopy showed abnormally shaped erythrocytes with striking membrane invaginations and protuberances (Figure 7D). Red blood cell membrane abnormalities

wild-type hearts (Table S5). Interestingly, lack of β -Parvin had no dramatic consequence on the level of ILK and PINCH-1, which are the two other components of the ILK/Pinch/Parvin complex. The two-fold increase of α -Parvin in β -Parvin-deficient hearts suggests that the absence of an obvious phenotype is due to compensatory upregulation of α -Parvin (Figure 5C).

Kindlin-3 Deficiency Disrupts the Red Blood Cell Membrane Skeleton

Kindlin-3-deficient mice die at birth and suffer from severe bleeding, anemia, and pale skin color (Figures 7A and 7B; Moser et al., 2008). To further validate the power of in vivo SILAC and to obtain novel insights into Kindlin-3 function, we performed quantitative proteomics of platelets and erythrocytes from Kindlin-3^{-/-} mice. Platelet analysis identified Kindlin-3 as the protein with the highest fold change of more than 1200 platelet proteins (Figure S6A; Table S6). Interestingly, the levels of integrin α IIb and β 3 subunits were normal, suggesting that the reduced surface levels found by FACS (Moser et al., 2008) were due to an im-

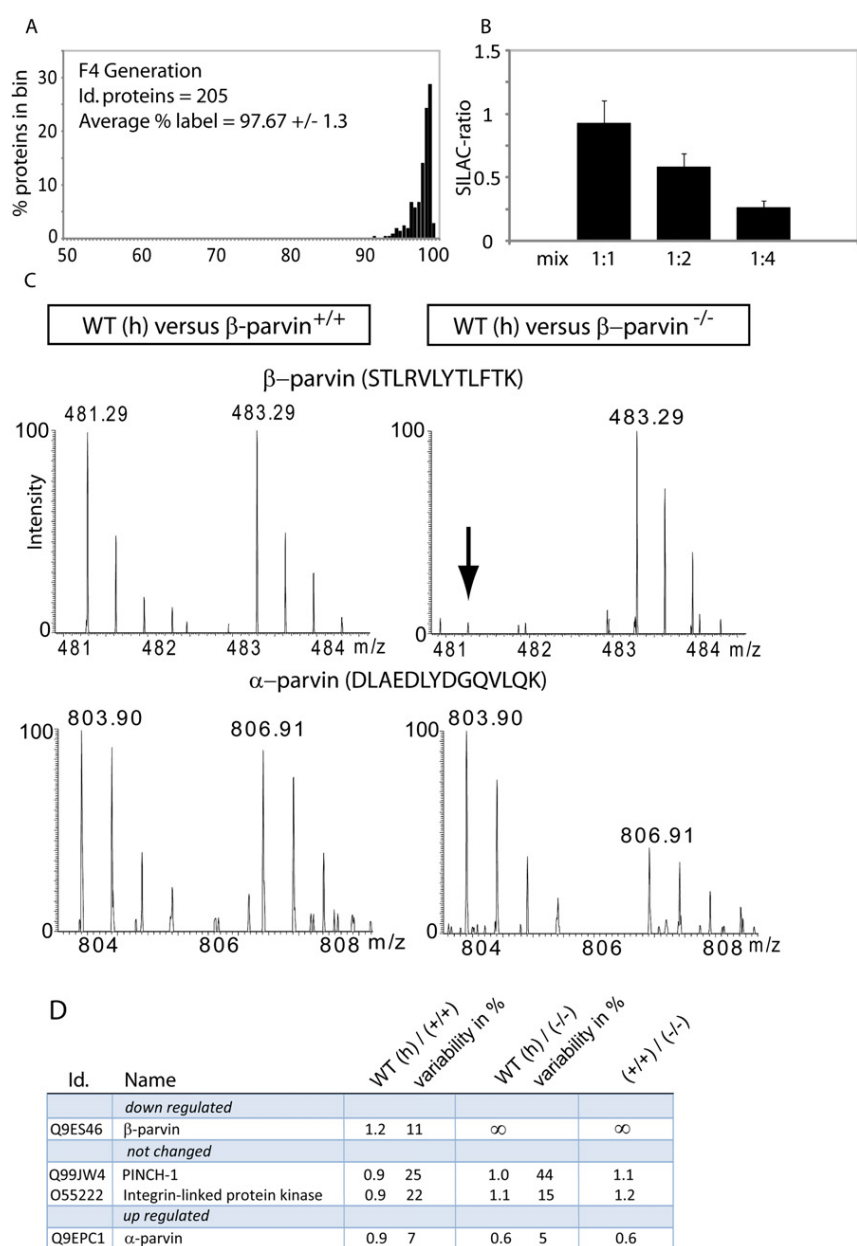


Figure 5. Analysis of Heart Tissue from β -Parvin Knockout Mice

(A) $^{13}\text{C}_6$ -Lysine incorporation of heart tissue from mice of the F4 generation shows a label efficiency of 97.7%.

(B) Heart tissue from labeled and nonlabeled animals was mixed 1:1, 1:2, and 1:4. The measured SILAC ratios after in-solution digestion were 0.93 ± 0.17 for the 1:1 mix, 0.58 ± 0.10 for the 1:2 mix, and 0.26 ± 0.05 for the 1:4 mix. Approximately 300 SILAC protein ratios were used for the quantification.

(C) Heart tissue from SILAC-labeled wild-type mice was mixed with nonlabeled β -Parvin (+/+) and β -Parvin (-/-) hearts. The arrow indicates the complete absence of β -Parvin.

(D) SILAC ratios of selected proteins.

and Kindlin-3^{-/-} mice and compared them to ghosts from SILAC-labeled control animals (Figure 7E). Quantitative SILAC-based analysis revealed an almost complete absence of ankyrin-1, band 4.1, adducin-2, and dematin (Figure 7F, right rows; Table S8), whereas other membrane-skeleton proteins, like α/β spectrin and band 3, were not changed.

Together, these findings show that Kindlin-3 is required for the assembly of a subset of proteins within the red blood cell membrane skeleton. Furthermore, the proteomic, morphological, and functional data provide a clear explanation for the anemia that leads to postnatal lethality.

DISCUSSION

Thus far, quantitative gene expression comparisons in higher organisms have been restricted to RNA analyses by gene chip approaches. These methods have many advantages: for example, ready accessibility and the fact that, in principle, almost all genes can be analyzed on one

chip. However, because of posttranscriptional regulation as well as regulated protein degradation, these data do not necessarily predict changes in protein levels within cells or tissues. Furthermore, there are specific cell populations, such as the platelets and erythrocytes investigated here, that are devoid of mRNA and are therefore out of reach for these techniques.

Here, we show that SILAC, a versatile and successful method for quantitative proteomics in cell culture-based systems or microorganisms, can be extended to mammalian model systems. Mice can be SILAC labeled without any obvious effect on growth, behavior, or fertility. SILAC food preparation is straightforward and not particularly expensive when considering other resources required for the generation and maintenance of

are often caused by mutations within membrane-skeleton proteins, and the absence of key components can have drastic consequences on the stability of the red cell membrane (Delaunay, 1995). To obtain an explanation for the structural defects, we quantitatively compared the membrane-skeleton proteins from total erythrocytes by using SILAC-based MS. The levels of the most prominent skeleton proteins (e.g., α/β spectrin, ankyrin, band 3, band 4.1, band 4.2, and actin) did not significantly differ between wild-type and Kindlin-3^{-/-} mice.

Next, we determined whether these proteins have formed a stable meshwork that is connected with the erythrocyte membrane. To address this question, we isolated the erythrocyte membranes (so called red blood cell "ghosts") from wild-type

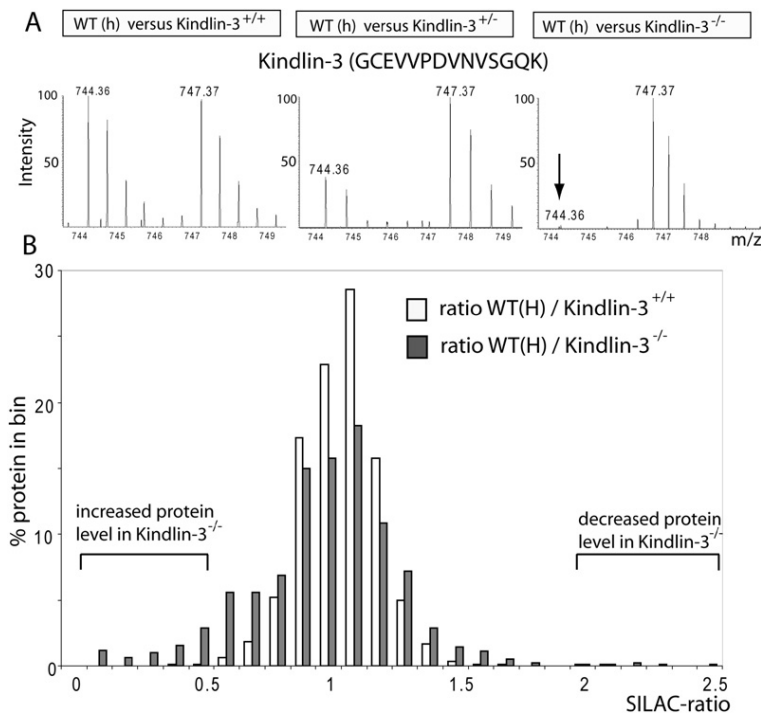


Figure 6. Quantitative Proteomics of Erythrocytes from Kindlin-3^{-/-} Mice

(A) Mass spectra of a Kindlin-3 peptide SILAC pair in Kindlin-3^{+/+}, Kindlin-3^{+/-}, and Kindlin-3^{-/-} erythrocytes.

(B) Histogram of SILAC ratios of wild-type (white bars) and Kindlin-3^{-/-} (gray bars) erythrocytes. The measured ratios were grouped into ratio bins, and the y axis shows the relative number of detected ratios per bin.

knockout animals. We chose ¹³C₆-lysine labeling, as lysine is not converted into other amino acids. This makes endoprotease Lys-C the preferred choice as the proteolytic enzyme. Another interesting enzyme for SILAC mice is Lys-N, which has recently been described as an efficient enzyme for proteomics and de novo peptide sequencing (Taouatas et al., 2008). Organs derived from SILAC mice can serve as standards for a large number of subsequent experiments, in which wild-type and knockout mice are compared. Importantly, cell types such as intestinal epithelium that are difficult to study ex vivo can be analyzed by the in vivo SILAC approach. Moreover, the SILAC mouse can serve as a reference model at any biological scale, from the whole organ through specific cell types down to intracellular compartments or single proteins of interest. As an example, we used SILAC mice to successfully study the mitochondrial proteome, which can be extended to investigations in relevant organs from metabolic or neurodegenerative disease models. In studies in which a large number of mice are required—such as in toxicology studies—labeled organ tissue could be stored and used as an internal standard for each measurement. A labeled SILAC-mouse liver, for example, yields sufficient internal standard for more than 1000 measurements. Although not shown here, phosphopeptides can also be enriched from SILAC mice and can serve as a standard for functional and time-resolved phosphoproteomics (Olsen et al., 2006).

We analyzed the proteomes of cells from three independent knockout mice. In all analyses, the complete absence of the targeted genes was immediately revealed by the SILAC technique. Furthermore, heterozygous Kindlin-3 animals present the expected two-fold reduction from wild-type levels, emphasizing the quantitative nature of our proteomic technology. This may be particularly useful in quantifying knockdown efficiencies in

transgenic RNAi mice. The sensitivity of the SILAC-based quantitation system became remarkably obvious by an observation from the β1 integrin inactivation in platelets. Deletion of the β1 integrin gene in hematopoietic cells is achieved by the induction of the Mx1-Cre transgene through the injection of pl-pC into β1 integrin floxed animals. Even without induction of Cre, the low expression levels of naturally expressed α/β interferon activated the Mx1 promoter and triggered β1 integrin deletion in a few cells. Even this slight difference in total β1 integrin expression proved sufficient for detection by the SILAC method.

Our proteomic data on platelets of β1 integrin mice showed that, although integrins control a number of different signaling pathways, the lack of the

β1 integrin has no consequences on the levels of other proteins in platelets, apart from its dimerization partners α2 and α6 integrins. This may be due to the fact that, in resting platelets, integrins are inactive and signaling into the cell is only induced upon stimulation via molecules like thrombin or collagen (Ruggeri, 2002). Further studies with the SILAC-mouse system could focus on activation of signaling cascades during platelet aggregation by using phosphoproteomics.

To test the SILAC-based analysis in a solid organ system, we compared the proteomes from heart of β-Parvin-deficient mice with control littermates. The complexity of a tissue, formed by different cell types, poses no limitation for the quantitative analysis by MS. The interpretation of results, however, is more challenging because changes in protein levels may result from non-cell-autonomous defects caused, for example, by altered cell-cell communication rather than cell-autonomous defects.

To study the molecular cause of the anemia observed in Kindlin-3 mutants, we analyzed the consequences of this deletion on the proteome of platelets and erythrocytes. Recently, we characterized Kindlin-3 as an essential factor for the activation of platelet integrins (Moser et al., 2008). Kindlin-3 directly binds to the cytoplasmic tails of both β1 and β3 integrin subunits. Its expression is restricted to cells of the hematopoietic system (Ussar et al., 2006). Our SILAC-based analysis of Kindlin-3-deficient erythrocytes revealed an increased amount of nuclear proteins, prompting us to investigate consequences of the knockout on this cell type. Consistent with the proteomic results, we found an increased number of nucleated erythroblasts in blood smears. Furthermore, Kindlin-3-deficient erythrocytes are irregular in size and shape. The structural defects of the red blood cell membrane skeleton suggested an additional function of Kindlin-3. With the help of the SILAC method, we quantitatively

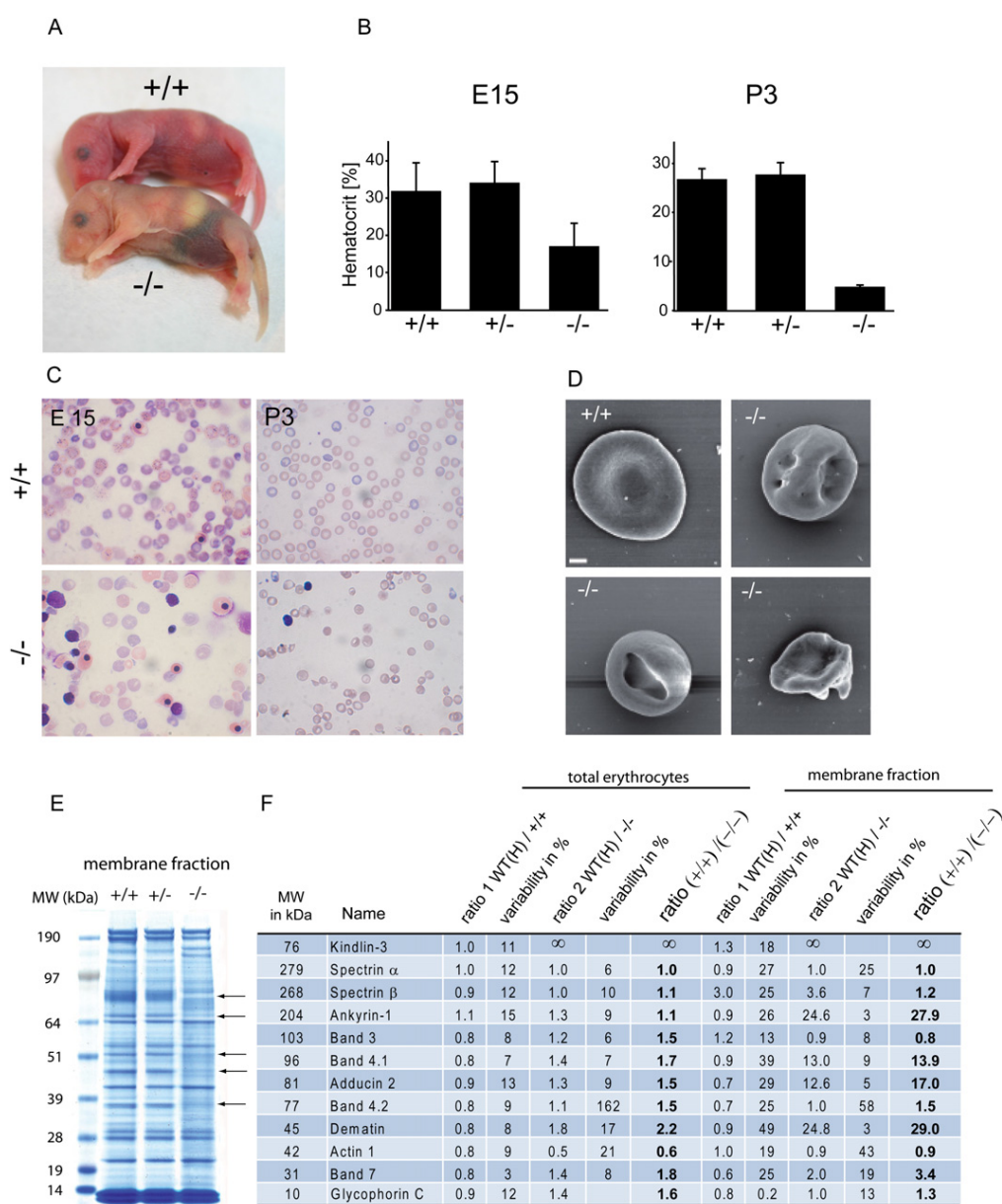


Figure 7. Kindlin-3-Deficient Erythrocytes Show Disrupted Membrane Skeletons

- (A) Kindlin-3 knockout mice are anemic.
 (B) Decreased hematocrit in Kindlin-3^{-/-} mutants at embryonic day 15 and P3.
 (C) Blood smears from E15 embryos and P3 wild-type and Kindlin-3^{-/-} mice reveal fewer erythrocytes and an increased number of nucleated erythroblasts.
 (D) Scanning electron microscopy of wild-type and Kindlin-3^{-/-} erythrocytes. The scale bar represents 1 μ m.
 (E) “Ghost” lysates from wild-type, heterozygous, and Kindlin-3^{-/-} mice were stained by Coomassie blue after SDS-PAGE. The arrows indicate the absence of proteins within the membrane-skeleton fraction of Kindlin-3^{-/-} erythrocytes.
 (F) SILAC-ratio comparison of total erythrocytes (left rows) and the membrane fraction (right row).

compared the membrane-skeleton proteins of control and Kindlin-3-deficient erythrocytes and revealed a critical role of Kindlin-3 in the formation or stabilization of this structure. The inner surface of the red blood cell membrane is laminated by a protein network that is linked to transmembrane proteins. In humans and mice, mutations in genes encoding ankyrin, band 3, spec-

trin, and protein 4.1 or protein 4.2 cause hereditary spherocytosis or poikilocytosis, often accompanied with hemolytic anemias (Delaunay, 1995; Peters et al., 1998; Rybicki et al., 1995; Shi et al., 1999; Southgate et al., 1996). The dramatic reduction of ankyrin-1, protein 4.1, and dematin in membrane preparations from Kindlin-3-deficient erythrocytes explains the severe

malformations. Thus, loss of Kindlin-3 affects erythropoiesis by disrupting the assembly of structural components within the red blood cell membrane skeleton.

In summary, a direct combination of the SILAC technology for quantitative proteomics with the large number of powerful mouse models generated by the community is now possible. We have demonstrated here how proteomics can be combined with several of the powerful technologies already used in this endeavor. We are confident that this technology will help to elucidate disease processes and guide novel intervention strategies.

Data Availability

Data used for quantitation accompany this article online.

EXPERIMENTAL PROCEDURES

Materials and Reagents

$^{13}\text{C}_6$ -Lysine (98 atom % ^{13}C) was purchased from Silantes, Martinsried, Germany. Chemicals for the “in-solution” and “in-gel” digests were purchased from Sigma-Aldrich, and LysC was obtained from WAKO. Wild-type mice were obtained from an in-house C57Bl/6 colony.

Knockout Mice

Transgenic mice expressing the Cre recombinase under the control of the Mx1 promoter (Kuhn et al., 1995) were mated with mice carrying a floxed $\beta 1$ integrin gene (Brakebusch et al., 2000). To ensure extensive downregulation of the $\beta 1$ integrin on platelets, pl-pC (250 μg per mouse) (Amersham) was injected intraperitoneally three times in a 2-day interval.

Kindlin-3-deficient mice were generated as described by Moser et al. (2008). A detailed description of the β -Parvin gene inactivation will be published elsewhere (I.T. and R.F., unpublished data).

Food Preparation, Weight Gain, and Food Consumption

A customized lysine-free mouse diet (Harlan-Teklad, TD.99386) was combined with the heavy $^{13}\text{C}_6$ -lysine and the natural isotope L-lysine (Sigma) to a final concentration of 1%. To obtain a homogenous distribution of the amino acid, the powder was vigorously mixed with a blender for 5 min. For the preparation of food pellets, ~10 g of the mixture was filled into an in-house-manufactured cylinder with an inner diameter of 1.5 cm and a length of 10 cm. Food was compressed with an exactly fitting pestle for 1 min. Pellets were taken out and dried overnight at room temperature. After drying, the pellets were cut into smaller pieces.

The lysine content was checked as described (Moore et al., 1958). Although the hydrolysis with subsequent chromatography does not allow for the exact determination of the amino acid contents, the supplemented lysine amount was comparable to that in the customized diet containing the natural lysine isotope.

For testing weight gain and food consumption, one group ($n = 3$ females) was fed with a regular mouse diet, one group ($n = 3$ females) was fed with the customized lysine-free diet supplemented with natural lysine (Sigma), and one animal was fed with the diet containing the heavy isotope for lysine. All animals were fed ad libitum and had access to water.

Food consumption was measured daily for 10 days during breeding and weaning periods (Figure S2). The label percentage was calculated as the mean of the heavy-labeled peptide signal divided by the sum of the light and heavy signals.

Sample Preparation

Blood Samples

Mice were anesthetized with isofluran, and 20 μl blood was taken from the retro-orbital plexus. Blood samples were incubated with heparin (20 U/ml), and, after centrifugation, the supernatant was frozen in liquid nitrogen and stored at -80°C .

Tissue Harvest

After sacrificing animals by cervical dislocation, tissues were dissected, washed in phosphate-buffered saline (PBS [pH 7.4]), and frozen in liquid nitrogen. For protein isolation, tissues were homogenized in a buffer containing 1% NP-40, 0.1% sodium deoxycholate, 150 mM NaCl, 1 mM EDTA, 50 mM Tris (pH 7.5), and protease inhibitors (Complete tablets, Roche). The lysates were centrifuged at $14,000 \times g$ to pellet cellular debris. A Bradford assay was performed to determine protein concentrations of the supernatants.

Mitochondria Isolation

Liver tissue was quickly washed in water, then washed three times in 250 mM sucrose, 10 mM Tris-HCl, 0.1 mM EGTA (pH 7.4) supplemented with protease inhibitors (Roche). Crude mitochondria were isolated as described previously (Forner et al., 2006) and were purified on a 30% Percoll density centrifugation gradient.

Platelets were isolated by differential centrifugation steps as described by Moebius et al. (2005).

Epithelial Cell Isolation from Gut

Small intestine was cut open and washed with PBS. The small intestine was transferred to dissociation buffer (130 mM NaCl, 10 mM EDTA, 10 mM HEPES [pH 7.4], 10% FCS, and 1 mM DTT) and was incubated for 45 min on a rotor at 37°C . The rest of the intestine was removed, and the epithelial clumps were collected by centrifugation at 800 rpm for 5 min and washed in PBS.

B Cell Isolation

For B cell isolation, spleen was cut into small fragments and digested with collagenase and DNase, followed by the addition of EDTA. Subsequently, cells were incubated with anti-CD45R, anti-CD3, and anti-CD49b (BD Pharmingen). B cells were selected as cells that stained positive for CD45R (B220) (Coffman, 1982) and negative for both anti-CD3 and anti-CD49b and were then sorted by using a FACS Aria system (Becton Dickinson).

Mass Spectrometry

For protein separation, samples were loaded on a NuPAGE 4%–12% Bis-Tris gel (Invitrogen). After staining of the gel with the Colloidal Blue Staining Kit (Invitrogen), evenly sized gel pieces were excised from the gel and processed for enhanced liquid chromatography-mass spectrometry (GelC-MS).

For blood analysis, Coomassie-stained gel lanes were cut into eight pieces. To determine incorporation ratios, we analyzed three gel pieces per lane from heart, gut epithelia, liver, red blood cell, and platelet samples.

The gel pieces were subjected to in-gel reduction and alkylation, followed by LysC digestion as previously described (Andersen et al., 2005; Shevchenko et al., 1996). Finally, peptides were extracted twice by adding an equal volume of 30% acetonitrile/0.3% trifluoroacetic acid (TFA) in water to digest the mixture, followed by a final extraction with 100% acetonitrile. Extracts were evaporated in a speedvac to remove acetonitrile and were subsequently acidified with 0.5% TFA. Samples were desalted and concentrated with StageTips and were resuspended in 5 μl of 0.5% acetic acid/1% TFA (Rappsilber et al., 2003). In-solution digestion of proteins was performed as described by Ong and Mann (2006).

Reverse-phase nano-LC-MS/MS was performed by using an Agilent 1100/1200 nanoflow LC system (Agilent Technologies) with a cooled, thermostated 96-well autosampler. The LC system was coupled to a 7-Tesla LTQ-FT or LTQ Orbitrap instrument (Thermo Fisher Scientific) equipped with a nano-electrospray source (Proxeon). Chromatographic separation of peptides was performed in a 10 cm long 8 μm tip opening/75 μm inner diameter capillary needle (Proxeon). The column was custom made with methanol slurry of reverse-phase ReproSil-Pur C18-AQ 3 μm resin (Dr. Maisch, GmbH). The LysC-digested peptide mixtures were autosampled at a flow rate of 0.5 $\mu\text{l}/\text{min}$ and then eluted with a linear gradient at a flow rate of 0.25 $\mu\text{l}/\text{min}$. The mass spectrometers were operated in the data-dependent mode to automatically measure MS and MS/MS. LTQ-FT full scan MS spectra (from m/z 300 to m/z 1600) were acquired with a resolution of $R = 100,000$ at m/z 400 (after accumulation to a target value of 3,000,000 in the linear ion trap). The five most intense ions were sequentially isolated and fragmented in the linear ion trap by using collisionally induced dissociation at a target value of 10,000 (Olsen et al., 2004).

Raw data files were converted to Mascot generic format files with in-house software (Raw2MSP), and Mascot (version 2.0) was used for a database search and protein identification. The following search

parameters were used in all MASCOT searches: LysC digest; no missed cleavage; carbamidomethylation of cysteine set as a fixed modification; and oxidation of methionines and L-lysine-6 allowed as variable modifications. The maximum allowed mass deviation for MS and MS/MS scans was 10 ppm and 0.5 Da, respectively. Only proteins that had at least two peptides with ion scores >20 were considered for identification and quantitation. MSQuant (Schulze and Mann, 2004) was used to verify and quantify the resulting SILAC-peptide pairs. All proteomic results were deposited in the publicly accessible MAPU database (Zhang et al., 2007). A target decoy database approach was used to identify false-positive peptides and to set threshold criteria such that <1% false positives were included in the peptide list (Tables S1 and S2, statistics sheet). After mass recalibration with MSQuant, the average absolute mass error of all peptides was better than 3 ppm.

Samples from all mouse mutants were analyzed by the in-house-developed software MaxQuant (Cox and Mann, 2007; Graumann et al., 2008). Briefly, MaxQuant performs a peak list, SILAC- and XIC-based quantitation, false-positive rates (Gingras et al., 2007), and peptide identification based on Mascot search results.

All data were searched against the International Protein Index sequence database (mouse IPI, version 3.24) (Kersey et al., 2004). Fold-change for ghost proteins was determined from the gel slice corresponding to the expected migration of the full-length protein.

Blood Cell Analyses

Hematocrit was measured from peripheral blood with a hematology analyzer (Nihon Kohden).

For "ghost" preparation, erythrocytes were washed twice in 0.9% NaCl, 10 mM sodium phosphate buffer (pH 7.0) before hypotonic lysis were performed in 0.25% NaCl, 10 mM sodium phosphate buffer (pH 7.0). Lysis was performed in several rounds in hypotonic buffer until the pellet became white.

Flow Cytometry

Flow cytometric lacZ staining of hematopoietic cells was performed on Ter119-positive bone marrow cells that have been incubated with the fluorescent β -galactosidase substrate FDG (fluorescein di- β -D-galactopyranoside) (Sigma) as described (Montanez et al., 2007). Flow cytometry was carried out on a Becton Dickinson FACSCalibur.

SUPPLEMENTAL DATA

Supplemental Data include seven figures and eight tables for protein identification and quantification and are available with this article online at <http://www.cell.com/cgi/content/full/134/2/353/DC1>.

ACKNOWLEDGMENTS

We thank other members of the department for proteomics and signal transduction and the Department of Molecular Medicine for sharing insights. Meredith O'Keeffe provided critical help in FACS sorting. We thank Gerhard Waner for imaging erythrocytes by scanning electron microscopy. This work was supported by a long-term European Molecular Biology Organization fellowship to M.K., by the 6th and 7th framework program of the European Union, by the Austrian Science Foundation (SFB021), and by the Max Planck Society.

Received: February 18, 2008

Revised: April 29, 2008

Accepted: May 20, 2008

Published: July 24, 2008

REFERENCES

Andersen, J.S., Lam, Y.W., Leung, A.K., Ong, S.E., Lyon, C.E., Lamond, A.I., and Mann, M. (2005). Nucleolar proteome dynamics. *Nature* 433, 77–83.

Benevenga, N.J., Calvert, C., Eckhart, C.D., Fahey, G.C., Greger, J.L., Keen, C.L., Knapka, J.J., Magalhaes, H., and Oftedal, O.T. (1995). Nutrient require-

ments of the mouse. In *Nutrient Requirements of Laboratory Animals*, J. Overton, ed. (Washington, D.C.: National Academy Press), pp. 192.

Berlin, N.I., Waldmann, T.A., and Weissman, S.M. (1959). Life span of red blood cell. *Physiol. Rev.* 39, 577–616.

Beynon, R.J., and Pratt, J.M. (2005). Metabolic labeling of proteins for proteomics. *Mol. Cell. Proteomics* 4, 857–872.

Bier, D.M. (1997). Stable isotopes in biosciences, their measurement and models for amino acid metabolism. *Eur. J. Pediatr.* 156 (Suppl 1), S2–S8.

Blagoev, B., Ong, S.E., Kratchmarova, I., and Mann, M. (2004). Temporal analysis of phosphotyrosine-dependent signaling networks by quantitative proteomics. *Nat. Biotechnol.* 22, 1139–1145.

Brakebusch, C., Grose, R., Quondamatteo, F., Ramirez, A., Jorcano, J.L., Pirro, A., Svensson, M., Herken, R., Sasaki, T., Timpl, R., et al. (2000). Skin and hair follicle integrity is crucially dependent on β 1 integrin expression on keratinocytes. *EMBO J.* 19, 3990–4003.

Calderwood, D.A. (2004). Integrin activation. *J. Cell Sci.* 117, 657–666.

Coffman, R.L. (1982). Surface antigen expression and immunoglobulin gene rearrangement during mouse pre-B cell development. *Immunol. Rev.* 69, 5–23.

Cox, J., and Mann, M. (2007). Is proteomics the new genomics? *Cell* 130, 395–398.

Delaunay, J. (1995). Genetic disorders of the red cell membranes. *FEBS Lett.* 369, 34–37.

Dietz, W.H., Jr., Wolfe, M.H., and Wolfe, R.R. (1982). A method for the rapid determination of protein turnover. *Metabolism* 31, 749–754.

Doherty, M.K., and Beynon, R.J. (2006). Protein turnover on the scale of the proteome. *Expert Rev. Proteomics* 3, 97–110.

Doherty, M.K., Whitehead, C., McCormack, H., Gaskell, S.J., and Beynon, R.J. (2005). Proteome dynamics in complex organisms: using stable isotopes to monitor individual protein turnover rates. *Proteomics* 5, 522–533.

Forner, F., Foster, L.J., Campanaro, S., Valle, G., and Mann, M. (2006). Quantitative proteomic comparison of rat mitochondria from muscle, heart, and liver. *Mol. Cell. Proteomics* 5, 608–619.

Gingras, A.C., Gstaiger, M., Raught, B., and Aebersold, R. (2007). Analysis of protein complexes using mass spectrometry. *Nat. Rev. Mol. Cell Biol.* 8, 645–654.

Graumann, J., Hubner, N.C., Kim, J.B., Ko, K., Moser, M., Kumar, C., Cox, J., Schoeler, H., and Mann, M. (2008). SILAC-labeling and proteome quantitation of mouse embryonic stem cells to a depth of 5111 proteins. *Mol. Cell. Proteomics* 7, 672–683. Published online November 28, 2007. 10.1074/mcp.M700460-MCP200.

Gregg, C.T., Hutson, J.Y., Prine, J.R., Ott, D.G., and Furchner, J.E. (1973). Substantial replacement of mammalian body carbon with carbon-13. *Life Sci.* 13, 775–782.

Hynes, R.O. (2002). Integrins: bidirectional, allosteric signaling machines. *Cell* 110, 673–687.

Ishihama, Y., Sato, T., Tabata, T., Miyamoto, N., Sagane, K., Nagasu, T., and Oda, Y. (2005). Quantitative mouse brain proteomics using culture-derived isotope tags as internal standards. *Nat. Biotechnol.* 23, 617–621.

Kersey, P.J., Duarte, J., Williams, A., Karavidopoulou, Y., Birney, E., and Apweiler, R. (2004). The International Protein Index: an integrated database for proteomics experiments. *Proteomics* 4, 1985–1988.

Kratchmarova, I., Blagoev, B., Haack-Sorensen, M., Kassem, M., and Mann, M. (2005). Mechanism of divergent growth factor effects in mesenchymal stem cell differentiation. *Science* 308, 1472–1477.

Krijgsveld, J., Ketting, R.F., Mahmoudi, T., Johansen, J., Artal-Sanz, M., Verrijzer, C.P., Plasterk, R.H., and Heck, A.J. (2003). Metabolic labeling of *C. elegans* and *D. melanogaster* for quantitative proteomics. *Nat. Biotechnol.* 21, 927–931.

Kuhn, R., Schwenk, F., Aguet, M., and Rajewsky, K. (1995). Inducible gene targeting in mice. *Science* 269, 1427–1429.

Legate, K.R., Montanez, E., Kudlacek, O., and Fassler, R. (2006). ILK, PINCH and parvin: the tIPP of integrin signalling. *Nat. Rev. Mol. Cell Biol.* 7, 20–31.

- Mann, M. (2006). Functional and quantitative proteomics using SILAC. *Nat. Rev. Mol. Cell Biol.* 7, 952–958.
- McClatchy, D.B., Dong, M.Q., Wu, C.C., Venable, J.D., and Yates, J.R., 3rd. (2007). ¹⁵N metabolic labeling of mammalian tissue with slow protein turnover. *J. Proteome Res.* 6, 2005–2010.
- Moebius, J., Zahedi, R.P., Lewandrowski, U., Berger, C., Walter, U., and Sickmann, A. (2005). The human platelet membrane proteome reveals several new potential membrane proteins. *Mol. Cell. Proteomics* 4, 1754–1761.
- Montanez, E., Piwko-Czuchra, A., Bauer, M., Li, S., Yurchenco, P., and Fassler, R. (2007). Analysis of integrin functions in peri-implantation embryos, hematopoietic system, and skin. *Methods Enzymol.* 426, 239–289.
- Moore, S., Spackman, D.H., and Stein, W.H. (1958). Automatic recording apparatus for use in the chromatography of amino acids. *Fed. Proc.* 17, 1107–1115.
- Moser, M., Nieswandt, B., Ussar, S., Pozgajova, M., and Fässler, R. (2008). Kindlin-3 is essential for integrin activation and platelet aggregation. *Nat. Med.* 14, 325–330. Published online February 17, 2008. 10.1038/nm1722.
- Nieswandt, B., Brakebusch, C., Bergmeier, W., Schulte, V., Bouvard, D., Mokhtari-Nejad, R., Lindhout, T., Heemskerk, J.W., Zirngibl, H., and Fassler, R. (2001). Glycoprotein VI but not $\alpha 2\beta 1$ integrin is essential for platelet interaction with collagen. *EMBO J.* 20, 2120–2130.
- Oda, Y., Huang, K., Cross, F.R., Cowburn, D., and Chait, B.T. (1999). Accurate quantitation of protein expression and site-specific phosphorylation. *Proc. Natl. Acad. Sci. USA* 96, 6591–6596.
- Olsen, J.V., Ong, S.E., and Mann, M. (2004). Trypsin cleaves exclusively C-terminal to arginine and lysine residues. *Mol. Cell. Proteomics* 3, 608–614.
- Olsen, J.V., Blagoev, B., Gnäd, F., Macek, B., Kumar, C., Mortensen, P., and Mann, M. (2006). Global, in vivo, and site-specific phosphorylation dynamics in signaling networks. *Cell* 127, 635–648.
- Ong, S.E., and Mann, M. (2005). Mass spectrometry-based proteomics turns quantitative. *Nat. Chem. Biol.* 1, 252–262.
- Ong, S.E., and Mann, M. (2006). A practical recipe for stable isotope labeling by amino acids in cell culture (SILAC). *Nat. Protoc.* 1, 2650–2660.
- Ong, S.E., Blagoev, B., Kratchmarova, I., Kristensen, D.B., Steen, H., Pandey, A., and Mann, M. (2002). Stable isotope labeling by amino acids in cell culture, SILAC, as a simple and accurate approach to expression proteomics. *Mol. Cell. Proteomics* 1, 376–386.
- Ong, S.E., Kratchmarova, I., and Mann, M. (2003). Properties of ¹³C-substituted arginine in stable isotope labeling by amino acids in cell culture (SILAC). *J. Proteome Res.* 2, 173–181.
- Pasini, E.M., Kirkegaard, M., Mortensen, P., Lutz, H.U., Thomas, A.W., and Mann, M. (2006). In-depth analysis of the membrane and cytosolic proteome of red blood cells. *Blood* 108, 791–801.
- Peters, L.L., Weier, H.U., Walensky, L.D., Snyder, S.H., Parra, M., Mohandas, N., and Conboy, J.G. (1998). Four paralogous protein 4.1 genes map to distinct chromosomes in mouse and human. *Genomics* 54, 348–350.
- Pratt, J.M., Robertson, D.H., Gaskell, S.J., Riba-Garcia, I., Hubbard, S.J., Sidhu, K., Oliver, S.G., Butler, P., Hayes, A., Petty, J., et al. (2002). Stable isotope labelling in vivo as an aid to protein identification in peptide mass fingerprinting. *Proteomics* 2, 157–163.
- Radtke, F., and Clevers, H. (2005). Self-renewal and cancer of the gut: two sides of a coin. *Science* 307, 1904–1909.
- Rappsilber, J., Ishihama, Y., and Mann, M. (2003). Stop and go extraction tips for matrix-assisted laser desorption/ionization, nanoelectrospray, and LC/MS sample pretreatment in proteomics. *Anal. Chem.* 75, 663–670.
- Ruggeri, Z.M. (2002). Platelets in atherothrombosis. *Nat. Med.* 8, 1227–1234.
- Rybicki, A.C., Musto, S., and Schwartz, R.S. (1995). Decreased content of protein 4.2 in ankyrin-deficient normoblastosis (nb/nb) mouse red blood cells: evidence for ankyrin enhancement of protein 4.2 membrane binding. *Blood* 86, 3583–3589.
- Schoenheimer, R., and Rittenberg, D. (1935). Deuterium as an indicator in the study of intermediary metabolism. *Science* 82, 156–157.
- Schulze, W.X., and Mann, M. (2004). A novel proteomic screen for peptide-protein interactions. *J. Biol. Chem.* 279, 10756–10764.
- Shevchenko, A., Wilm, M., Vorm, O., and Mann, M. (1996). Mass spectrometric sequencing of proteins silver-stained polyacrylamide gels. *Anal. Chem.* 68, 850–858.
- Shi, Z.T., Afzal, V., Collier, B., Patel, D., Chasis, J.A., Parra, M., Lee, G., Paszty, C., Stevens, M., Walensky, L., et al. (1999). Protein 4.1R-deficient mice are viable but have erythroid membrane skeleton abnormalities. *J. Clin. Invest.* 103, 331–340.
- Southgate, C.D., Chishti, A.H., Mitchell, B., Yi, S.J., and Palek, J. (1996). Targeted disruption of the murine erythroid band 3 gene results in spherocytosis and severe haemolytic anaemia despite a normal membrane skeleton. *Nat. Genet.* 14, 227–230.
- Taouatas, N., Drugan, M.M., Heck, A.J., and Mohammed, S. (2008). Straightforward ladder sequencing of peptides using a Lys-N metalloendopeptidase. *Nat. Methods* 5, 405–407. Published online April 20, 2008. 10.1038/nmeth.1204.
- Ussar, S., Wang, H.V., Linder, S., Fassler, R., and Moser, M. (2006). The Kindlins: subcellular localization and expression during murine development. *Exp. Cell Res.* 312, 3142–3151.
- Wolfe, R.R., and Chinkes, D.L. (2005). *Isotope tracers in metabolic research* (New Jersey: Wiley-LISS).
- Wu, C.C., MacCoss, M.J., Howell, K.E., Matthews, D.E., and Yates, J.R., 3rd. (2004). Metabolic labeling of mammalian organisms with stable isotopes for quantitative proteomic analysis. *Anal. Chem.* 76, 4951–4959.
- Zhang, Y., Zhang, Y., Adachi, J., Olsen, J.V., Shi, R., de Souza, G., Pasini, E., Foster, L.J., Macek, B., Zougman, A., et al. (2007). MAPU: Max-Planck Unified database of organellar, cellular, tissue and body fluid proteomes. *Nucleic Acids Res.* 35, D771–D779.

Paper VI

Leukocyte Adhesion Deficiency-III (LAD-III) is caused by mutations in the adhesion protein Kindlin-3

*Lena Svensson¹, *Kimberley Howarth², Alison McDowall¹, Irene Patzak¹, Rachel Evans¹, Siegfried Ussar³, Ayse Metin⁴, Mike Fried⁵, Ian Tomlinson² and Nancy Hogg¹

*These two authors contributed equally to this study

¹Leukocyte Adhesion Laboratory and ²Molecular and Population Genetics Laboratory, Cancer Research UK London Research Institute, London, UK; ³Dept of Molecular Medicine, Max Planck Inst. of Biochemistry, Martinsried, Germany; ⁴Division of Immunology, Diskapi Children's Hospital, Ankara, Turkey; ⁵UCSF Cancer Research Institute, San Francisco, USA.

Correspondence: Dr N Hogg,
CR UK London Research Institute,
44 Lincoln's Inn Fields,
London WC2A 3PX

Email: nancy.hogg@cancer.org.uk

Phone: 44-207-269-3255

Fax: 44-207-269-3093

Running title:

Mutation in Kindlin-3, not CalDAG-GEF1, is responsible for LAD-III

Abstract

Integrins on leukocytes become active following "inside out" signalling through other membrane receptors. This signalling is faulty in the Leukocyte Adhesion Deficiency (LAD)-III disorder. LAD-III in two Turkish patients has been attributed to a C>A base change postulated to alter splicing of the *CalDAG-GEF1* gene. Here we describe two further Turkish LAD-III patients containing the same mutation, but show that it is not responsible for the LAD-III disorder. We identify two independent inactivating mutations in the *Kindlin-3* gene as the cause of LAD-III in Maltese and Turkish patients. The Kindlins bind to the integrin β subunit and cooperate with the protein talin to induce an increase in

integrin affinity. The mutations both cause decreased Kindlin-3 mRNA levels. Importantly, the transfection of the patients' lymphocytes with the wild-type Kindlin-3 cDNA, but not wild-type CalDAG-GEF1 cDNA, reverses the LAD-III defect that prevents integrin-mediated adhesion and migration.

Integrins are the major adhesion receptors of hematopoietically-derived cells. The ability of leukocytes to use the integrins LFA-1 and $\alpha 4\beta 1$ to migrate across vessels and into tissues is critical for a successful immune response^{1,2}. The integrins on circulating leukocytes and platelets bind poorly to their ligands, but adopt an active conformation following signals delivered through other membrane receptors, termed "inside-out" signalling³. The inside-out signalling pathway(s) leads to the activation of integrins defined by increased affinity for ligand⁴. A critical step in this process consists of talin binding to the β integrin cytoplasmic tail causing $\alpha\beta$ tail separation and a conformational change resulting in high affinity integrin^{5,6}.

The functional importance of integrins has been highlighted by Leukocyte Adhesion Deficiency-1 (LAD-1) patients who characteristically have mutations in the $\beta 2$ subunit of the leukocyte integrins^{7,8}. This results in the failure of $\beta 2$ integrins, LFA-1, Mac-1 and p150,95, to be expressed on leukocytes leading to recurrent bacterial infections. The platelet integrin $\alpha IIb\beta 3$ initiates the process of blood clotting through binding to fibrinogen. Mutation in either the α or β subunit of $\alpha IIb\beta 3$ causes the bleeding disorder termed Glanzmann thrombasthenia (GT).

An additional group of patients, termed LAD-1/variant⁹ or LAD-III¹⁰, display symptoms of both LAD-1 and GT. Unlike these two disorders, the

haematopoietically-derived cells of LAD-III patients express $\beta 1$, $\beta 2$ and $\beta 3$ integrin subsets at normal levels, but the integrins fail to function because of defective “inside out” signalling. Thirteen LAD-III patients have been reported so far^{9,11-14}. They vary chiefly in the timing at which problems with particular integrin subsets are observed.

Deficiency in Rap1 activity has been reported in two LAD-III patients and such a decrease could be caused by a defective RapGEF¹⁵. CalDAG-GEF1 is a RapGEF that is activated through binding of DAG and Ca^{2+} ^{16,17}. The *CalDAG-GEF1* gene, located at human chromosome 11q13.1, specifies two proteins as a result of alternative splicing. One protein has 609 residues and is expressed in the cytosol and a second (termed RasGRP2) has 671 residues, contains an additional 62 amino acid N terminal sequence and is membrane localized due to myristoylation and/or palmitoylation¹⁸. *CalDAG-GEF1*^{-/-} mice mimic the LAD-III phenotype in that they display GT-like bleeding problems¹⁹ and defective function of neutrophil $\beta 1$ and $\beta 2$ integrins²⁰. Mutations in *CalDAG-GEF1* leading to a LAD-III-like disorder are also found in three dog breeds²¹. Recently a C>A base change in a putative splice acceptor site of the *CalDAG-GEF1* gene (exon 15 of the smaller form and exon 16 of the larger form) has been described in two patients²². This mutation is reported to cause a splicing problem leading to a loss of *CalDAG-GEF1* mRNA and has been suggested to be responsible for the human LAD-III disorder.

Kindlin-3(URP2, MIG-2B) is an adhesion plaque protein that is highly expressed by all white blood cells²³ and is also located on chromosome 11q13.1. Recently *Kindlin-3*^{-/-} mice have been characterized and found to have a GT-like phenotype²⁴ and leukocytes with integrin activation problems

(Markus Moser and Reinhard Fässler, personal communication). Kindlin-3 is highly homologous to Kindlin-1/URP1, expressed in epithelial cells and also to the widely expressed Kindlin-2/Mig-2²³. Kindler syndrome is a human disease characterized by skin blistering that is caused by various loss-of-function mutations in Kindlin-1 leading to integrin dysfunction^{25,26}.

The Kindlins have a FERM (protein4.1/ezrin/radixin/moesin) domain with F1, F2 and F3 subdomains^{27,28} that is most homologous to the FERM domain of talin⁶. It is the F3 subdomain of talin that binds to the integrin β subunit cytoplasmic tail causing integrin activation^{5,29} and it is to the membrane proximal NPXY motif that it binds^{6,29}. A hallmark of the Kindlins is the interruption of the F2 subdomain by a pleckstrin homology (PH) domain. Kindlin-3 and Kindlin-2 both bind to the β subunit at the second membrane distal NPXY motif and, importantly, the integrin activation-inducing activity of talin is enhanced by integrin-bound Kindlins^{24,30,31}.

We describe a new LAD-III patient and analyse both *CalDAG-GEF1* and *Kindlin-3* genes in this patient and in two previously reported LAD-III patients and their relatives. Our two patients of Turkish origin display the previously described C>A change in the *CalDAG-GEF1* gene²², but this mutation is not found in a third patient of Maltese origin. We show in this study that the LAD-III disorder is caused by two disabling mutations in the *Kindlin-3* gene. Transfection of a wild-type Kindlin-3 cDNA, but not a wild-type CalDAG-GEF1 cDNA, in the B cells of our three patients overcomes the LAD-III adhesion/migration defect.

Results

Characterization of a new LAD-III patient

Maltese patient 1¹² and Turkish patient 2 (Family 5 in¹⁴) have been defined previously as LAD-III patients (**Fig. 1a**). We here characterize a new LAD-III patient of Turkish origin (family 3). The expression of integrins LFA-1 (α L and β 2 subunits) and α 4 β 1 (α 4 and β 1 subunits), that are the major functional integrins on T cells, were comparable between the LAD-III patient, normal control T cells (**Fig. 1b**) and both parents (data not shown). Analysis of the same two integrin classes on neutrophils and EBV-transformed B cells also revealed normal levels of expression (data not shown). However, when adhesion to LFA-1 ligand ICAM-1 and α 4 β 1/ α 5 β 1 ligand fibronectin was stimulated by means of inside-out signaling that leads to integrin activation (phorbol ester, PdBu; Ca^{2+} mobiliser thapsigargin; or mAb crosslinking of the T cell receptor/CD3 complex)¹², the T cells of the patient failed to firmly adhere (**Fig. 1c**). In contrast, the T cells of the patient's mother and father behaved similarly to unrelated normal T cells. This finding is reinforced by the observation that the parent's T cells attached and spread on ICAM-1 in a typical LFA-1-dependent manner, in contrast to the patient's cells that were unable to spread (**Fig. 1d**). Thus the patient from family 3 exhibits the hallmarks typical of the LAD-III disorder.

Assessment of the CalDAG-GEF1 mutation

Based on the likelihood that LAD-III in our Turkish and Maltese pedigrees was a recessive condition caused by mutations inherited from a common ancestor(s), we used homozygosity mapping to indicate that the most

likely location of the gene responsible for the LAD-III disorder was a region between 60.6Mb and 65.3Mb on chromosome 11 (**Fig. 2a**). The *CaIDAG-GEF1* gene (chr11:64.25-64.27Mb) lies on the distal boundary of the region. Sequence analysis of the region specifying the putative splice acceptor site of exon 16 of the larger form (*RasGRP2*) of the *CaIDAG-GEF1* gene revealed that the patients of Turkish families 2 and 3 were homozygous for the C>A base change described by Pasvolsky and colleagues²²(**Fig. 2b, Supplementary Fig. 1 online**). The parents of these patients were heterozygous, whereas the sister of patient 2 was homozygous for the normal C allele. In contrast, the C>A change was not present in the Maltese patient or her relatives (family 1). Furthermore sequencing of all 18 exons and all the intron/exon boundaries of the *CaIDAG-GEF1* gene for the 3 patients and their relatives yielded no further unexpected nucleotide changes (data not shown but available on request).

The C>A mutation was reported to prevent correct splicing of the *CaIDAG-GEF1* transcript (exon 15 to exon 16), resulting in unstable *CaIDAG-GEF1* mRNA²². We performed Taqman analysis on mRNA from the EBV-transformed B cells of the three families and compared them to two normal EBV transformed B cell lines. All patients and their parents produced *CaIDAG-GEF1* mRNA and the levels were within the range of the two normal control cell lines (**Fig. 2c**). When the mRNA from the larger alternatively spliced form of *CaIDAG-GEF1* (*RasGRP2*) mRNA was specifically analyzed, the patients' levels were observed to be similar to those of their parents and the normal controls (**Supplementary Fig. 2 online**). We also investigated the levels of *CaIDAG-GEF1* protein by Western blot analysis. All LAD-III patients expressed

CalDAG-GEF1 proteins that were indistinguishable in both size and quantity from the proteins present in the parent and control samples (**Fig. 2d**).

The effect of wild-type CalDAG-GEF1 on the migration of the LAD-III leukocytes

Despite not affecting protein and mRNA sizes or levels, it was possible that the C>A change affected the function of CalDAG-GEF1. Thus we tested whether the EBV-transformed B cells were able to undergo LFA-1-mediated adhesion/migration on ICAM-1. The parents' cells migrated without added stimulant, whereas the LAD-III patients' cells were unable to migrate on ICAM-1 (**Fig. 3a**). $\alpha4\beta1/\alpha5\beta1$ -mediated migration on fibronectin showed the same difference (data not shown). The same patterns were also observed in adhesion assays on ICAM-1 and fibronectin (data not shown).

We next investigated whether transfection of the patients' B cells with wild-type CalDAG-GEF1 cDNA would overcome the migration defect of the LAD-III cells. We used a human CalDAG-GEF1 (RasGRP2) cDNA construct that included the N-terminal myristoylation domain involved in membrane localization¹⁸. There was no observed effect of the transfected wild-type CalDAG-GEF1 cDNA on the migration of the LAD-III patients' B cells (**Fig. 3b**) or on their individual cell tracking patterns (data not shown). A similar negative result was obtained by transfecting cDNA constructs of both human and murine cytosolic CalDAG-GEF1 cDNAs (data not shown). We next used interference reflection microscopy (IRM) to investigate in more detail the effect of CalDAG-GEF1 on the LFA-1 adhesions made by migrating cells. The parent's cells showed a pattern of close contact with ICAM-1, whereas the

LAD-III patient's cells were only lightly attached (**Fig. 3c**). Quantification of the areas of attachment indicating the extent of integrin-mediated adhesiveness showed that the CalDAG-GEF1-transfected LAD-III cells were similar to control LAD-III cells. The conclusion of these experiments was that expression of wild-type CalDAG-GEF1, specifying either the membrane or cytosolic form, failed to repair the adhesion/migration defect caused by the LAD-III disorder.

LAD-III patients have mutations in Kindlin-3

Since the *Kindlin-3* gene (*FERMT*, chr11:63.73-63.76Mb) lies within our minimal region mapped for the LAD-III disorder (**Fig. 2a**), *Kindlin-3*^{-/-} mice suffer from a GT-like disorder²⁴ and leukocytes express high levels of Kindlin-3²³, we screened it for germline mutations in our three LAD-III patients and their immediate families. We found that the two LAD-III cases of Turkish origin (families 2 and 3) were homozygous for a C>T nonsense mutation (R509X) at nucleotide 1525 in exon 12 that changes a CGA codon to a TGA stop codon (**Fig. 4a**). The parents were heterozygous for this change and the healthy sister of family 2 was homozygous for the wild-type allele. The C>T base change generating the termination codon in exon 12 lies within the amino acid sequence coding for the C-terminal half of the FERM F2 domain and could thus be expected to have impact on the integrin binding F3 subdomain (**Fig. 4c**).

In contrast to the Turkish families, all members of the Maltese kindred (family 1) were homozygous for the wild-type C allele at nucleotide 1525. However further screening revealed a different homozygous mutation in the *Kindlin-3* gene in the affected Maltese child. The Maltese mutation was an A>G

change at the splice acceptor site of exon 14 (**Fig. 4b**). The three other unaffected Maltese family members were heterozygous for this change, whereas the Turkish patients and their relatives were all homozygous for the wild-type A allele at this splice acceptor site. This splicing mutation, which affects the correct joining of Kindlin-3 exon 13 to exon 14, would also prevent the generation of an intact FERM F3 subdomain (**Fig. 4c**). Thus this mutation would also be predicted to have implications for the binding of Kindlin-3 to integrin.

Effect of mutations on Kindlin-3 mRNA levels

We next investigated the effect that these mutations had on Kindlin-3 mRNA production. mRNA levels were assessed by qRT-PCR for two regions of the Kindlin-3 mRNA. One probe covered the sequence spanning exons 6 and 7 and a second probe covered the region spanning exons 13 and 14. This latter probe would measure the integrity of the mRNA in the neighbourhood of the exon 14 splice acceptor site mutation detected in the Maltese patient. The patients' parents mRNA levels, assessed with both sets of probes, were similar to normal controls (**Fig. 5a**).

The two Turkish LAD-III patients expressed substantially reduced levels of mRNA for both the region spanning exons 6 and 7 as well as the region spanning exons 13 and 14 (**Fig. 5a**). Therefore the mutation specifying the termination codon at nucleotide 1525 in exon 12 in the Turkish patients results in a decrease in the mRNA levels specifying sequences both upstream and downstream of the mutation. This indicates that the C>T mutation in exon 12 affects the stability of the Kindlin-3 mRNA.

The Maltese patient expressed mRNA spanning exons 6 and 7 at somewhat reduced levels, but no mRNA was detected spanning exons 13 and 14 (see asterisk) (**Fig. 5a**). The lack of detection of mRNA species spanning exon 13 and 14 in the Maltese patient strongly suggests that the intronic A>G base change results in the disabling of the exon 14 splice acceptor site.

It was possible to detect some low level Kindlin-3 transcripts from the exon 13 region in the Maltese patient. DNA sequence analysis of the PCR products generated only unique sequence for exon 13, but not for the sequence following this exon (**Fig 5b**). In this region, instead of unique exon 14 sequence, as found for the parent (WT), sequence analysis revealed a number of low level aberrant splice products. These results are consistent with the mutation in the exon 14 splice acceptor site in the Maltese patient causing inhibition of the normal splicing connecting exon 13 and exon 14. Thus the mutation of the *Kindlin-3* gene in the Maltese LAD-III patient is particularly informative in terms of the function of Kindlin-3 protein in that mRNA specifically coding for the Kindlin-3 FERM F3 domain that is involved in binding to integrins is absent.

Wild-type Kindlin-3 expression repairs the LAD-III lesion in adhesion and migration

The role of Kindlin-3 in activation of murine integrins and their adhesion-related functions has been demonstrated²⁴. However there has been no comparable study of human Kindlin-3 and it was essential to test whether the defects in adhesion and migration displayed by the LAD-III patients' cells could be repaired by the expression of wild-type Kindlin-3. We therefore transfected

EBV-transformed B cells of the three LAD-III patients with the previously described cDNA specifying murine GFP-Kindlin-3²³ that is able to reverse the integrin activation defect in Kindlin-3^{-/-} cells (Markus Moser, personal communication). The LFA-1 adhesions made by our LAD-III patients B cells with and without expression of murine GFP-Kindlin-3 were compared with their parent's cells using IRM. As in Fig. 3c, the LAD-III cells made poor contacts compared with the parent's cells (**Fig. 6a**). Importantly, however, expression of the murine GFP-Kindlin-3 cDNA in the LAD-III B cells increased adhesion to ICAM-1. Both IRM images and quantification of the areas of attachment showed that the Kindlin-3-transfected cells made adhesions equalling those made by the parents' cells.

To show further that expression of wild-type Kindlin-3 was able to overcome the LAD-III phenotype, we tested the same cells for their ability to undergo LFA-1-mediated migration on ICAM-1-coated surfaces. LAD-III cells from all three families expressing GFP-Kindlin-3 migrated on ICAM-1 similarly to the control transfected parents' cells, whereas this was not the case for the GFP-transfected LAD-III cells (**Fig. 6b, Supplementary Videos online**). The LAD-III B cells, expressing wild-type Kindlin-3, not only had a similar speed of migration as the parent's cells, but also an identical pattern of random motility (**Fig. 6c**).

Discussion

A key feature that distinguishes LAD-III or LAD-1/variant patients from those with other integrin deficiency syndromes is the normal expression but lack of function of the β 1, β 2 and β 3 integrins expressed by their leukocyte and

platelets. This failure to function leads to immune deficiency and bleeding problems as described previously³². The nature of the disabling mutation(s) has been a focus of interest for more than a decade since the first reports of these patients^{9,11-13}.

The RapGEF, CalDAG-GEF1, is a good candidate for the LAD-III gene. It lies within a region of significant homology between LAD-III patients on chromosome 11q13.1 and the deletion of the *CalDAG-GEF1* gene in mice^{19,20} and mutation of CalDAG-GEF1 in dogs²¹ causes a LAD-III-like disorder. Pasvolsky *et al* postulated that a C>A change in a putative splice acceptor site upstream of exon 16 of the *CalDAG-GEF1* gene results in low mRNA levels and is the causative mutation responsible for the LAD-III disorder. The observation that a C>A change was detected in both alleles of our two Turkish LAD-III patients and also in the two Turkish patients described by Pasvolsky and colleagues²², but not in our Maltese patient, suggests that this mutation is exclusive to the LAD-III patients of Turkish origin. Significantly, in our Turkish patients, in contrast to those described by Pasvolsky *et al*, the presence of the C>A change has no impact on CalDAG-GEF1 mRNA or protein levels as they are within the range found in the patients' parents and normal controls. Furthermore, in an experiment not done by Pasvolsky and colleagues, we find that exogenous expression of the wild type *CalDAG-GEF1* gene in all three patients' cells is unable to reverse the LAD-III adhesion/migration defect. These data strongly argue that mutation in the *CalDAG-GEF1* gene is not the cause of human LAD-III, at least in the patients described here.

Furthermore knock down of CalDAG-GEF1 expression in human T cells affects LFA-1-mediated adhesion to ICAM-1, but not $\alpha 4\beta 1$ adhesion to VCAM-

1 that is PKC-dependent³³. These CalDAG-GEF1 and PKC pathways also operate synergistically in the activation of platelet $\alpha\text{II}\beta\text{3}$ ³⁴. Thus the characteristics of CalDAG-GEF1 function do not conform to the hallmark of the LAD-III disorder in which the activity of β1 , β2 and β3 integrin subsets are substantially compromised in leukocytes and platelets.

However the association of the C>A change in CalDAG-GEF1 with LAD-III suggests a Turkish founder effect maintained through consanguineous marriage. The implication is that there is strong linkage disequilibrium between the *CalDAG-GEF1* gene and the gene responsible for the LAD-III syndrome.

Kindlin-3 had recently become a prime candidate for LAD-III because the gene is located 0.5 Mb away from CalDAG-GEF1 at chromosome 11q13.1 in the region of shared haplotypes in our LAD-III kindred and also because *Kindlin-3*^{-/-} mice have recently been characterized and found to display a GT-like phenotype²⁴. We describe two independent disabling mutations in the *Kindlin-3* gene and show that the LAD-III phenotype can be repaired by expression of wild-type Kindlin-3.

We define in both Turkish patients a single homozygous mutation in exon 12 leading to a stop codon that destabilises Kindlin-3 mRNA. In the Maltese patient, there is a second independent inactivating mutation within the splice acceptor site associated with exon 14 of Kindlin-3 which leads to an absence of mRNA for exons 13/14. This is particularly informative in terms of the LAD-III disorder as the FERM F3 subdomain of murine Kindlin-3 has been identified to have integrin β subunit binding activity²⁴ and it is this region that is encoded by exons 13/14 of human Kindlin-3. As the LAD-III phenotype is repaired by expression of murine Kindlin-3 in the patients' B cells, it is of

interest that there is 100% amino acid identity between the Kindlin-3 mouse and human F3 subdomains (data not shown).

Finally the implication is that the binding of Kindlin-3 is a critical component of the sequence of events leading to integrin activation. Kindlin-2 and Kindlin-3 are both reported to bind to $\beta 1$ and $\beta 3$ cytoplasmic tails at the membrane distal NPXY motif^{24,30,31}. This binding enhances talin binding at the membrane proximal NPXY site and causes a subsequent increase in integrin affinity. Further detail of the relationship between Kindlin-3 and talin binding to the β subunit and the identification of any other interaction partners remains to be discovered. Our findings here suggest that Kindlin-3 binds not only to human $\beta 1$ and $\beta 3$, but also to $\beta 2$ integrins and that binding to all three integrin subtypes is instrumental in the generation and/or maintenance of integrin activity in leukocytes and platelets.

Fourteen LAD-III patients have so far been reported of which the majority are of Turkish origin^{9,11-14}. The LAD-III patients exhibit very similar symptoms, but the timing of the observed integrin subset defects can vary. This might be explained by the nature of the Kindlin-3 mutations. Alternatively, although we found that mutation in CalDAG-GEF1 did not explain the LAD-III disorder in our patients, it remains possible that either CalDAG-GEF1, or another molecule involved in the pathway to integrin activation that includes Kindlin-3, might be responsible for a subset of other LAD-III patients. However our demonstration that expression of wild-type Kindlin-3 can overcome the LAD-III defects in these patients by generating integrin adhesive contacts and integrin-mediated migration of LAD-III lymphocytes provides strong biological

evidence to support the assignment of Kindlin-3 as the source of disrupting mutations associated with the LAD-III phenotype.

Methods

Patients

All affected children in the three families suffered from cerebral haemorrhages at birth. All displayed an increased leukocyte blood count characteristic of LAD-III patients whose leukocytes have difficulty leaving the circulation leading to recurrent infections during early life. Family 1: The patient was born of non-consanguineous Maltese parents and has been characterized previously as a LAD-III¹². Family 2: The patient is a 4 yr old Turkish boy whose parents are first cousins. He has mental and motor retardation because of neonatal intracranial haemorrhages that occurred at birth. He has previously been identified as a LAD-III (Family 5¹⁴). Family 3: We describe this Turkish LAD-III patient for the first time. Consanguinity is present as the mother and father are the grandchildren of sisters. There have been 2 sibling deaths with a history of delayed cord separation, hematuria, melena, petechias and severe infection. This female patient (<1 yr old), first presented early in life with anemia, thrombocytopenia and leukocytosis ($35-100 \times 10^9$ cells/L; neutrophilia and lymphocytosis in equal proportions). All features have persisted necessitating repeated erythrocyte transfusions. The subject had a clinical phenotype suggestive of the severe form of LAD-1: septicemia, axillary ulceration without pus collection, diffuse cellulitis on the right arm, delayed cord separation (surgical separation at day 20). Platelet aggregation tests showed abnormality similar to GT.

Antibodies and other reagents

The use of mAbs 38 (α L, CD11a), TS1/18 (β 2, CD18), HP2/1 (α 4, CD49d) and (β 1, CD29) have been previously reported^{12,35}. Other Abs used were rabbit polyclonal anti-CalDAG-GEF1 #3752, a gift from Drs Ann Graybiel and Jill Crittenden; DM 1A anti- α -tubulin (Sigma-Aldrich, Dorset, UK). Full length ICAM-1Fc protein was prepared as previously¹².

The human cytosolic Myc-CalDAG-GEF1 and membrane localised CalDAG-GEF1 (RasGRP2-FLAG) cDNAs were gifts from Dr John Hancock¹⁸ and the murine cytosolic CalDAG-GEF1-FLAG cDNA, a gift from Drs Ann Graybiel and Jill Crittenden. The murine pEGFP-Kindlin-3 DNA construct has been described previously²³.

Cells and cell transfections

T lymphocytes were prepared and expanded in culture as previously described¹². Epstein-Barr virus transformed (EBV-transformed) B lymphoblastoid cells were derived from peripheral blood mononuclear cells of patients, their relatives and non-related controls (BS, POS) by Research Cell Services, Cancer Research UK using standard procedures. All cells were maintained in RPMI-1640 with 10% FCS.

To transfect the cDNA constructs, EBV-transformed B cells were washed in OptiMEM+GlutaMAX (Invitrogen, Paisley, UK) and electroporation was performed using 2×10^7 cells with 10 μ g per reaction of CalDAG-GEF1 or Kindlin-3 cDNA constructs or 5 μ g of pEGFP-N1 (BD Biosciences, Oxford, UK) using a Gene Pulser with Capacitance Extender (Bio-Rad UK, Hemel

Hemstead, UK) set at 960 μ FD and 260 mV. The DNA-transfected cells were maintained in RPMI 1640/10% FCS up to 24 hours. The efficiency of the transfection was evaluated by flow cytometry and the GFP positive cells were sorted using a MoFlo Cell Sorter (Beckman Coulter, CA) before use in migration assays. The level of cDNA construct expression was quantified by Western blotting.

Sequencing the *CalDAG-GEF1* and *Kindlin-3* genes

Genomic DNA from all patients, relatives and non-related controls was analysed for sequence alterations in all exons and intron-exon boundaries of the *CalDAG-GEF-1* and *Kindlin-3* genes by direct DNA sequencing in both orientations. Details and PCR conditions are available from the authors.

Taqman Assays

The human *CalDAG-GEF-1* and *Kindlin-3* mRNA levels were quantified using TaqMan technology. Briefly RNA was extracted from leukocytes using GenElute™ Mammalian Total RNA Miniprep Kit (Sigma-Aldrich). RNA was reverse-transcribed using the AffinityScript™ QPCR cDNA Synthesis Kit (Agilent Tech. UK Ltd., Cheshire, UK), and purified using the QIAquick PCR Purification Kit (Qiagen Ltd Sussex, UK). A total of 40 ng of cDNA per reaction was amplified using TaqMan Gene assays: for *CalDaG-GEF1*(*RasGRP2*), Hs00183378_m1 (exons 8-9), Hs01057123_m1 (exons 2-3); for *Kindlin-3*, Hs00258828_m1 (exons 13-14) and Hs01075695_m1 (exons 6-7); and controls Hs99999905_m1 (*GAPDH*) and Hs00202782_m1 (*SF3B1*).

The samples were analyzed on the ABI 7900HT Sequence Detection System instrument. Each sample was run in quadruplicate and expressed as a function of threshold cycle (Ct). The Ct values for reactions amplifying CalDAG-GEF-1 were corrected by the Ct value for SF3B1 or GAPDH to give Δ Ct. The difference in Δ Ct values between test and control cDNA samples allowed the relative expression of the gene to be quantified as follows: $2^{-(\Delta$ Ct test - Δ Ct SF3B1/GAPDH) - (\DeltaCt control - Δ Ct SF3B1/GAPDH)} (Applied Biosystems, Cheshire, UK).

Flow cytometry

Leukocytes (5×10^5) were incubated for 20 min at 4°C in 50 μ l of PBS/0.2% BSA containing primary mAb at optimal dilution as described previously¹². Bound mAb was detected by incubation with FITC-conjugated goat anti-mouse IgG (Sigma) for 20 min at 4°C and analysed by a FACS Calibur flow cytometer (BD Biosciences, CA).

Cell attachment assays

Flat-bottom Immulon-1 96 well plates were coated with 100 μ l ICAM-1Fc (3 μ g/ml) or fibronectin (10 μ g/ml) in PBS overnight at 4°C and blocked with 2.5 % BSA. Cells were labelled with 2.5 μ M 2',7'-bis-(carboxyethyl)-5(6')-carboxyfluorescein (BCECF; Merck Chemicals, Nottingham, UK.) then washed into HBSS/20 mM HEPES and plated at 2×10^5 cells per well (samples in triplicate). The cells were treated as indicated and incubated at 37°C for 30 mins. Non-adherent cells were removed by gentle washing and adhesion quantified using a Cytofluor multiwell plate reader (PerSeptive Biosystems, Hertford, UK).

Video microscopy

Either 35 mm glass bottom microwell dishes (MatTek Corp. MA) or ibiTreat μ -Slides VI (ibidi, Thistle Scientific, Glasgow, UK) were coated overnight with 3 μ g/ml ICAM-1Fc then blocked with BSA. Lymphocytes (4×10^5 /ml in HBSS/20 mM HEPES buffer) were allowed to settle for 10 min at 37°C, then non-attached cells removed with gentle washing. Images were taken with a Nikon Diaphot 300 microscope, using a 20x or 63x lens and AQM²⁰⁰¹ Kinetic Acquisition Manager software (Kinetic Imaging Ltd., UK). Cells were tracked at 15 sec intervals using Motion Analysis software (Kinetic Imaging Ltd.) and the data analyzed using a Mathematica notebook (Wolfram Research Inc., USA) developed by Daniel Zicha (Cancer Research UK). Statistical analysis was carried out using the Anova test.

Interference Reflection Microscopy (IRM)

EBV-transformed B cells were plated on ibiTreat μ -Slides coated with 3 μ g/ml ICAM-1. Images of close substrate contact of the migrating cells were acquired between 10-30 mins of attachment to ICAM-1 using a Zeiss Axiovert 100M Inverted confocal microscope with a 63x NA1.4 Plan-Apochromat oil immersion objective lens. For evaluation of adhesion status, the area of contact was measured using MetaMorph Offline 7.1 (n=35 cells per sample type).

Acknowledgements

We are greatly indebted to Dr Reinhard Fässler, Max Planck Institute of Biochemistry, Martinsried, Germany for helpful discussion, Drs Jill Crittenden, Ann Graybiel MIT, Boston, USA and Denisa Wagner, Harvard Medical School, Boston, USA for CalDAG-GEF-1 antibodies and cDNA constructs and helpful discussion and Dr John Hancock, U of Queensland Medical School, Brisbane, Australia for CalDAG-GEF-1 constructs. We are also grateful to Darren Harvey, CR UK LRI for generation of the EBV transformed cell lines. LS was supported by a Marie Curie Individual Fellowship.

References

1. von Andrian, U.H. & Mempel, T.R. Homing and cellular traffic in lymph nodes. *Nat Rev Immunol* **3**, 867-78 (2003).
2. Hogg, N., Laschinger, M., Giles, K. & McDowall, A. T-cell integrins: more than just sticking points. *J Cell Sci* **116**, 4695-705 (2003).
3. Kellermann, S.A., Dell, C.L., Hunt, S.W., 3rd & Shimizu, Y. Genetic analysis of integrin activation in T lymphocytes. *Immunol Rev* **186**, 172-88 (2002).
4. Kinashi, T. Intracellular signalling controlling integrin activation in lymphocytes. *Nat Rev Immunol* **5**, 546-59 (2005).
5. Calderwood, D.A. et al. The phosphotyrosine binding-like domain of talin activates integrins. *J Biol Chem* **277**, 21749-58 (2002).
6. Garcia-Alvarez, B. et al. Structural determinants of integrin recognition by talin. *Mol Cell* **11**, 49-58 (2003).
7. Anderson, D.C. & Springer, T.A. Leukocyte adhesion deficiency: an inherited defect in the Mac-1, LFA-1, and p150,95 glycoproteins. *Annu Rev Med* **38**, 175-94 (1987).
8. Hogg, N. & Bates, P.A. Genetic analysis of integrin function in man: LAD-1 and other syndromes. *Matrix Biol* **19**, 211-22 (2000).
9. Kuijpers, T.W. et al. Leukocyte adhesion deficiency type 1 (LAD-1)/variant. A novel immunodeficiency syndrome characterized by dysfunctional beta2 integrins. *J Clin Invest* **100**, 1725-33 (1997).
10. Etzioni, A. & Alon, R. Leukocyte adhesion deficiency III: a group of integrin activation defects in hematopoietic lineage cells. *Curr Opin Allergy Clin Immunol* **4**, 485-90 (2004).
11. Harris, E.S. et al. A novel syndrome of variant leukocyte adhesion deficiency involving defects in adhesion mediated by beta1 and beta2 integrins. *Blood* **97**, 767-76 (2001).
12. McDowall, A. et al. A novel form of integrin dysfunction involving beta1, beta2, and beta3 integrins. *J Clin Invest* **111**, 51-60 (2003).
13. Alon, R. et al. A novel genetic leukocyte adhesion deficiency in subsecond triggering of integrin avidity by endothelial chemokines results in impaired

- leukocyte arrest on vascular endothelium under shear flow. *Blood* **101**, 4437-45 (2003).
14. Kuijpers, T.W. et al. Natural history and early diagnosis of LAD-1/variant syndrome. *Blood* **109**, 3529-37 (2007).
 15. Kinashi, T. et al. LAD-III, a leukocyte adhesion deficiency syndrome associated with defective Rap1 activation and impaired stabilization of integrin bonds. *Blood* **103**, 1033-6 (2004).
 16. Springett, G.M., Kawasaki, H. & Spriggs, D.R. Non-kinase second-messenger signaling: new pathways with new promise. *Bioessays* **26**, 730-8 (2004).
 17. Stone, J.C. Regulation of Ras in lymphocytes: get a GRP. *Biochem Soc Trans* **34**, 858-61 (2006).
 18. Clyde-Smith, J. et al. Characterization of RasGRP2, a plasma membrane-targeted, dual specificity Ras/Rap exchange factor. *J Biol Chem* **275**, 32260-7 (2000).
 19. Crittenden, J.R. et al. CalDAG-GEFI integrates signaling for platelet aggregation and thrombus formation. *Nat Med* **10**, 982-6 (2004).
 20. Bergmeier, W. et al. Mice lacking the signaling molecule CalDAG-GEFI represent a model for leukocyte adhesion deficiency type III. *J Clin Invest* **117**, 1699-707 (2007).
 21. Boudreaux, M.K., Catalfamo, J.L. & Klok, M. Calcium-diacylglycerol guanine nucleotide exchange factor I gene mutations associated with loss of function in canine platelets. *Transl Res* **150**, 81-92 (2007).
 22. Pasvolsky, R. et al. A LAD-III syndrome is associated with defective expression of the Rap-1 activator CalDAG-GEFI in lymphocytes, neutrophils, and platelets. *J Exp Med* **204**, 1571-82 (2007).
 23. Ussar, S., Wang, H.V., Linder, S., Fassler, R. & Moser, M. The Kindlins: subcellular localization and expression during murine development. *Exp Cell Res* **312**, 3142-51 (2006).
 24. Moser, M., Nieswandt, B., Ussar, S., Pozgajova, M. & Fassler, R. Kindlin-3 is essential for integrin activation and platelet aggregation. *Nat Med* **14**, 325-30 (2008).
 25. Siegel, D.H. et al. Loss of kindlin-1, a human homolog of the *Caenorhabditis elegans* actin-extracellular-matrix linker protein UNC-112, causes Kindler syndrome. *Am J Hum Genet* **73**, 174-87 (2003).
 26. Jobard, F. et al. Identification of mutations in a new gene encoding a FERM family protein with a pleckstrin homology domain in Kindler syndrome. *Hum Mol Genet* **12**, 925-35 (2003).
 27. Weinstein, E.J. et al. URP1: a member of a novel family of PH and FERM domain-containing membrane-associated proteins is significantly over-expressed in lung and colon carcinomas. *Biochim Biophys Acta* **1637**, 207-16 (2003).
 28. Kloeker, S. et al. The Kindler syndrome protein is regulated by transforming growth factor-beta and involved in integrin-mediated adhesion. *J Biol Chem* **279**, 6824-33 (2004).
 29. Campbell, I.D. & Ginsberg, M.H. The talin-tail interaction places integrin activation on FERM ground. *Trends Biochem Sci* **29**, 429-35 (2004).
 30. Montanez, E. et al. Kindlin-2 controls bidirectional signaling of integrins. *Genes Dev* **22**, 1325-30 (2008).
 31. Ma, Y.Q., Qin, J., Wu, C. & Plow, E.F. Kindlin-2 (Mig-2): a co-activator of beta3 integrins. *J Cell Biol* **181**, 439-46 (2008).

32. Alon, R. & Etzioni, A. LAD-III, a novel group of leukocyte integrin activation deficiencies. *Trends Immunol* **24**, 561-6 (2003).
33. Ghandour, H., Cullere, X., Alvarez, A., Luscinikas, F.W. & Mayadas, T.N. Essential role for Rap1 GTPase and its guanine exchange factor CalDAG-GEFI in LFA-1 but not VLA-4 integrin mediated human T-cell adhesion. *Blood* **110**, 3682-90 (2007).
34. Cifuni, S.M., Wagner, D.D. & Bergmeier, W. CalDAG-GEFI and protein kinase C represent alternative pathways leading to activation of integrin α IIb β 3 in platelets. *Blood* **112**, 1696-703 (2008).
35. Smith, A. et al. A talin-dependent LFA-1 focal zone is formed by rapidly migrating T lymphocytes. *J Cell Biol* **170**, 141-51 (2005).

Figure legends

Figure 1. LAD-III patient genealogy and characterization of a new LAD-III patient. **a.** The family pedigrees of the three LAD-III patients and their families are shown. Families 1(Maltese) and 2(Turkish) have been reported previously^{12,14}; the parents in family 3 are the grandchildren of Turkish sisters. A double line indicates the level of known consanguinity. A forward line in the patient generation indicates that the individual is deceased; **b.** FACS analysis showing the expression levels of the integrin subunits $\alpha 4$, $\beta 1$, αL and $\beta 2$ are equivalent between family 3 LAD-III patient and control T lymphoblasts (control cells -grey fill; patient cells -dark line; representative mAb negative control-dashed line); **c.** Adhesion of family 3 T lymphoblasts to LFA-1 ligand ICAM-1 and $\alpha 4\beta 1/\alpha 5\beta 1$ ligand fibronectin following “inside out” signalling mediated by phorbol ester (PdBu), Ca^{2+} mobiliser thapsigargin (Thaps); or CD3 mAb crosslinking of the T cell receptor/CD3 complex (CD3XL) (n=2). **d.** Images of T lymphoblast adhesion to ICAM-1. The family 3 parent’s cells spread as expected, whereas the family 3 patient’s cells were lightly attached and failed to spread. Scale bar=10 μm .

Figure 2. Mutation in the *Ca/DAG-GEF1* gene and lack of effect on mRNA and protein levels. **a.** Homozygosity mapping. The display from the program <http://uk-lif-lbio02.crnet.org/~cazier01/> indicates the largest shared region of homozygosity (chr 11: 60.6Mb to 65.3Mb Mb) present in affected individuals (purple bars) and absent in unaffected family members from the three kindreds. Data is from Affymetrix 500K SNP arrays with a mis-call tolerance of 1%. There were no areas in the whole genome other than at centromere

regions with larger than 1Mb homozygosity in all three patients. In the absence of knowledge of allele frequencies in the almost certainly inbred populations under study, this relatively simple display method does not take SNP information content into account and hence centromeric regions (red) with low homozygosity are often shown falsely, as here, as being identical by descent.

b. Alignment of the DNA sequence surrounding the C>A base change (**bold**) in the *Ca/DAG-GEF1* gene of the LAD-III patients and their relatives (reference). The original data is shown in **Supplementary Figure 1**. (reference genomic data from [http://genome.ucsc.edu/\(chr11:64,250,959-64,269,504\)](http://genome.ucsc.edu/(chr11:64,250,959-64,269,504))).

c. Quantification of CalDAG-GEF1 mRNA levels by qRT-PCR analysis of patients (P) and their relatives (M=mother; F=father) compared to two normal control EBV transformed cell lines. A 1.5 fold difference from the controls (set at 1.0) was considered significant (dotted line) (n=2-4 for each family); **d.** CalDAG-GEF1 protein levels were similar between patients (P), relatives (M=mother, F=father) and control (C) as assessed by Western blotting (n=2).

Figure 3. Migration characteristics and IRM images of LAD-III B cells adhered to ICAM-1 and expressing CalDAG-GEF1. **a.** Parents' cells randomly migrate on ICAM-1, whereas the LAD-III patients' cells are lightly attached but do not migrate (representative experiment of n=3); **b.** LAD-III cells transfected with the wild type CalDAG-GEF1 or pEGFP-N1 (GFP) cDNA constructs compared with the migration of the pEGFP-N1-transfected parents' cells. The CalDAG-GEF1 construct was without effect on migration (n=4 independent experiments for each family); **c.** DIC and IRM images of the family 3 LAD-III B cells transfected as in **b.** The mother's (Parent) cells form LFA-1

adhesions, but the LAD-III patient's cells expressing CalDAG-GEF-1 are indistinguishable from the patient's control cells expressing GFP (n=2) Scale bar=10 μ m; Lower figure: quantification of the area of close contact for n=35 cells.

Figure 4. Mutations in the *Kindlin-3* gene. **a.** The DNA sequence around the location of the C>T base change in exon 12 of the *Kindlin-3* (*FERMT*) gene in the Turkish (mutated) and Maltese families (reference <http://genome.ucsc.edu/chr11:63,730,782-63,747,930>); C or T at this position indicated in bold; C/T denotes heterozygosity. The C>T mutation generates a TGA stop codon causing truncation of the Kindlin-3 protein and also affects Kindlin-3 mRNA stability. Below: the traces of the DNA sequence analysis around the mutation site in exon 12 for wild type (WT), a heterozygote Turkish parent (Het) and a homozygous mutant Turkish LAD-III patient (LAD-III). Y indicates the presence of a pyrimidine (both C and T). **b.** The DNA sequence around the location of the A>G base change in the *Kindlin-3* exon 14 splice acceptor site in the Maltese (mutated) and Turkish families is shown; A or G at this position indicated in bold; A/G denotes heterozygosity. This mutation leads to a splicing defect affecting the joining of exons 13 and 14 of the *Kindlin-3* mRNA. Below: the traces of the DNA sequence analysis around the mutation site in splice acceptor site of exon 14 for the wild type (WT) the heterozygote Maltese parents (Het) and the homozygous mutant Maltese LAD-III patient (LAD-III); R indicates the presence of a purine (both A and G). More extensive original data for (a) and (b) is shown in **Supplementary Figure 3**. **c.** Diagrammatic representation of human *Kindlin-3* protein with its PH and FERM domains. The

location of the exons encoding the different regions of the Kindlin-3 protein is shown. The position of the two LAD-III mutations, one in exon 12 and the other affecting the join of exons 13 and 14 of the Kindlin-3 gene detailed above in (a) and (b), are shown by red asterisks.

Figure 5. Analysis of Kindlin-3 mRNA in LAD-III patients and their relatives

a. Quantification of Kindlin-3 mRNA levels by qRT-PCR analysis of patients (P) and their relatives (M=mother; F=father; S=sister) compared to two control EBV transformed cell lines. A 1.5 fold difference from the controls (set at 1.0) was considered significant (dotted line) (n=2 for each family); **b.** Effect of splice acceptor site mutation in the Maltese patient on Kindlin-3 mRNA at the exon13/14 junction. The ReverseTranscribed-PCR product encompassing the mRNA sequence specifying the end of exon 13 and the start of exon 14 is compared between parent (WT) and the Maltese LAD-III patient (LAD-III). The unique DNA sequence specifying the end of exon 13 (last 7 bp) and the start of exon 14 (25 bp) is shown for WT. For the Maltese LAD-III patient, only the last 7 bases of exon 13 are detectable which is consistent with an exon 14 splice acceptor mutation.

Figure 6. Adhesion and migration characteristics of EBV-transformed B cells expressing wild-type Kindlin-3. **a.** DIC and IRM images of the LAD-III B cells transfected with either pEGFP or Kindlin-3 cDNAs and compared with a parent's B cells transfected with pEGFP. Expression of Kindlin-3 induces the patient's cells to form LFA-1 adhesions similar to the parent's cells (n=2).

Images are accompanied by quantification of the area of close contact for n=35 cells. Scale bar=10 μm ; **b.** Parents' cells randomly migrate on ICAM-1, whereas the LAD-III patients' cells are lightly attached but do not migrate; The LAD-III cells were transfected with the wild type Kindlin-3 cDNA or pEGFP constructs and compared with the migration of the pEGFP-transfected parents' cells. Expression of the Kindlin-3 construct increased the migration of the LAD-III cells to that of the parent's cells (representative experiment of n=3 for each family). **c.** The cell tracking results from an individual experiment with family 2 LAD-III patient and father transfected as in **b.**

Figure 1

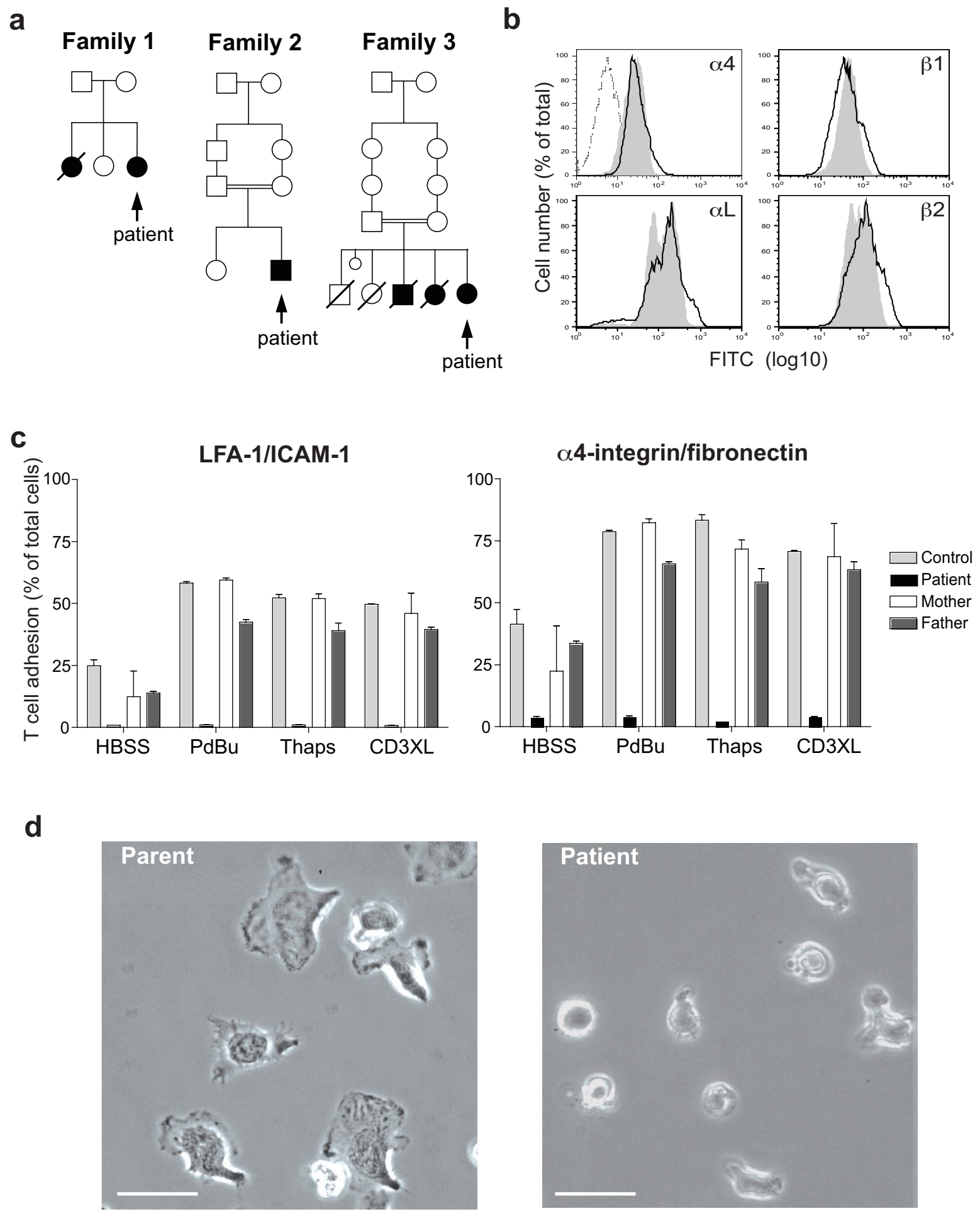
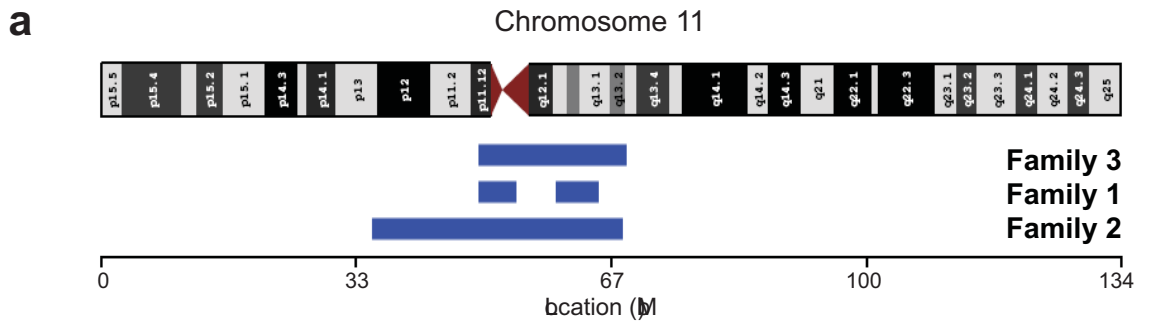


Figure 2



b

CalDAG-GEF1 Splice acceptor site Exon 15/16

Genomic	TGCTCC CCC	CAG CCTGC GAG TA
Family1 Patient	TGCTCC CCC	CAG CCTGC GAG TA
Family1 Mther	TGCTCC CCC	CAG CCTGC GAG TA
Family1 Father	TGCTCC CCC	CAG CCTGC GAG TA
Family1 Bng	TGCTCC CCC	CAG CCTGC GAG TA
Family2 Patient	TGCTCC CCC	AAG CCTGC GAG TA
Family2 Mther	TGCTCC CCC	C/AAG CCTGC GAG TA
Family2 Father	TGCTCC CCC	C/AAG CCTGC GAG TA
Family2 Bng	TGCTCC CCC	CAG CCTGC GAG TA
Family3 Patient	TGCTCC CCC	AAG CCTGC GAG TA
Family3 Mther	TGCTCC CCC	C/AAG CCTGC GAG TA
Family3 Father	TGCTCC CCC	C/AAG CCTGC GAG TA

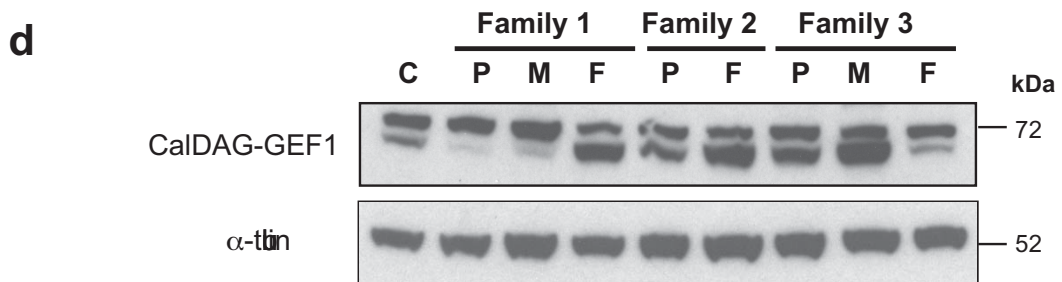
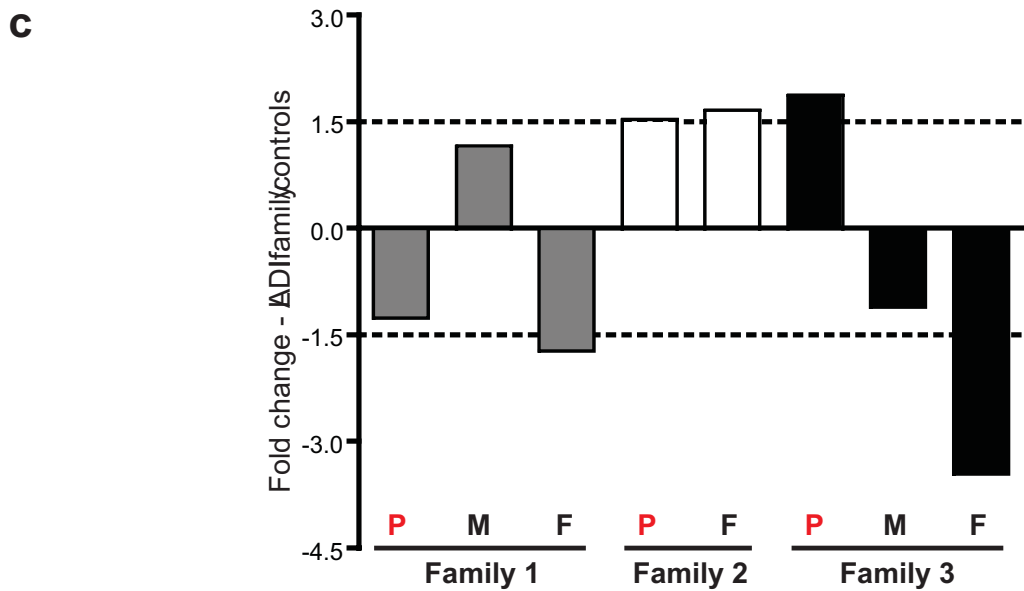


Figure 3

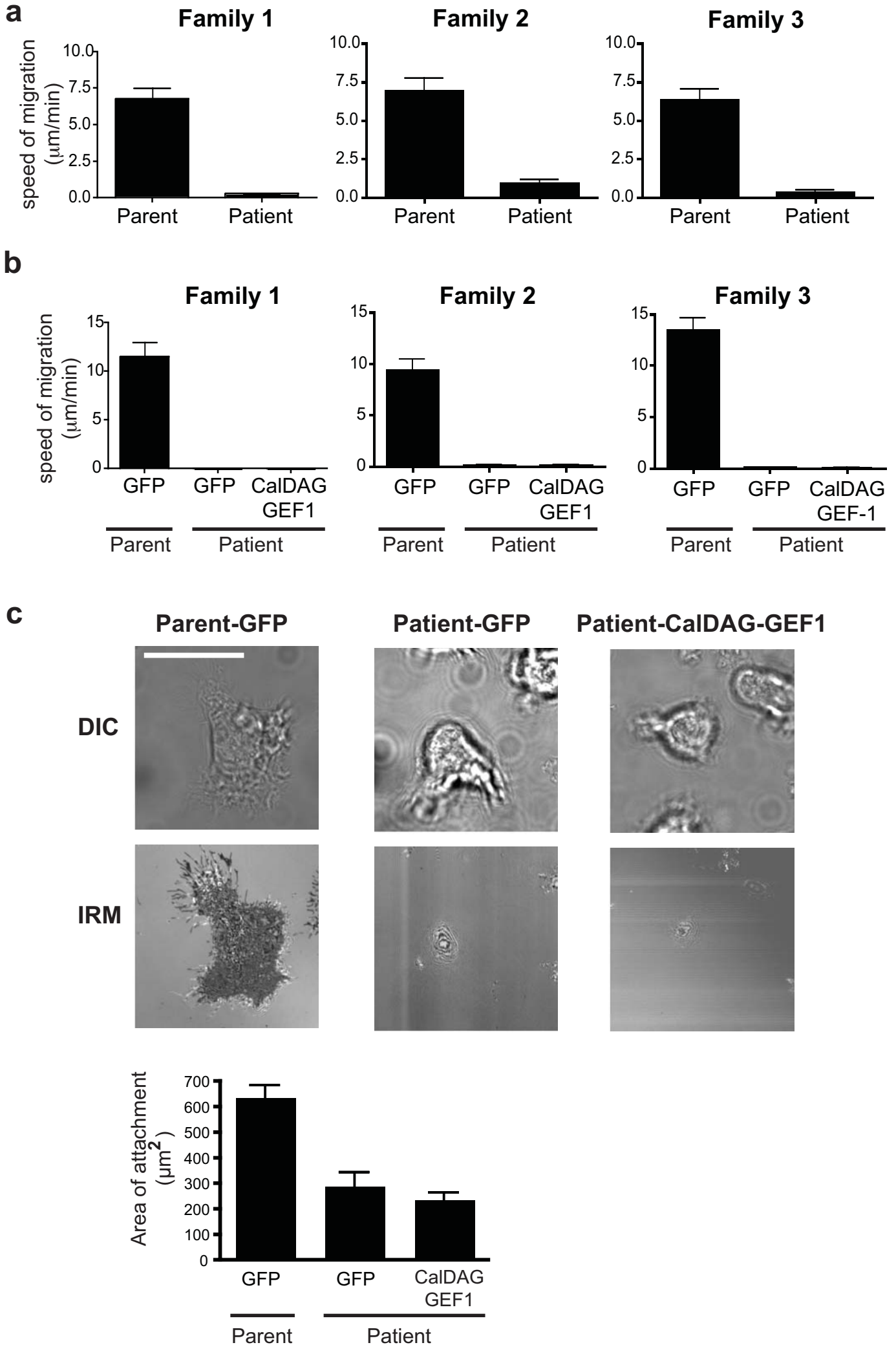
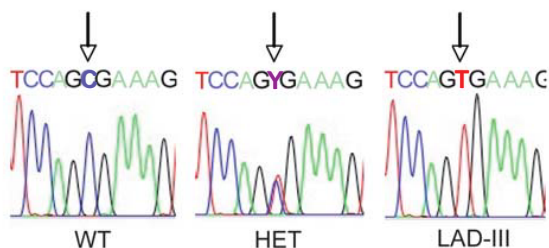


Figure 4

a

Kindlin-3 Exon 12 Mutation

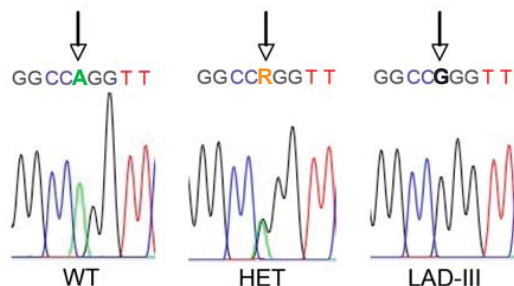
Genomic	CGT TTC CAG CGA AAG TTC AAG
Family 1 Patient	CGT TTC CAG CGA AAG TTC AAG
Family 1 Mother	CGT TTC CAG CGA AAG TTC AAG
Family 1 Father	CGT TTC CAG CGA AAG TTC AAG
Family 1 Sibling	CGT TTC CAG CGA AAG TTC AAG
Family 2 Patient	CGT TTC CAG TGA AAG TTC AAG
Family 2 Mother	CGT TTC CAG C/TGA AAG TTC AAG
Family 2 Father	CGT TTC CAG C/TGA AAG TTC AAG
Family 2 Sibling	CGT TTC CAG CGA AAG TTC AAG
Family 3 Patient	CGT TTC CAG TGA AAG TTC AAG
Family 3 Mother	CGT TTC CAG C/TGA AAG TTC AAG
Family 3 Father	CGT TTC CAG C/TGA AAG TTC AAG



b

Kindlin-3 Splice acceptor site Exon 13/14

	← Intron	Exon 14 →
Genomic	CCT GGG GGC CAG	G TTC AAG GGC
Family 1 Patient	CCT GGG GGC CGG	G TTC AAG GGC
Family 1 Mother	CCT GGG GGC CA/GG	G TTC AAG GGC
Family 1 Father	CCT GGG GGC CA/GG	G TTC AAG GGC
Family 1 Sibling	CCT GGG GGC CA/GG	G TTC AAG GGC
Family 2 Patient	CCT GGG GGC CAG	G TTC AAG GGC
Family 2 Mother	CCT GGG GGC CAG	G TTC AAG GGC
Family 2 Father	CCT GGG GGC CAG	G TTC AAG GGC
Family 2 Sibling	CCT GGG GGC CAG	G TTC AAG GGC
Family 3 Patient	CCT GGG GGC CAG	G TTC AAG GGC
Family 3 Mother	CCT GGG GGC CAG	G TTC AAG GGC
Family 3 Father	CCT GGG GGC CAG	G TTC AAG GGC



c

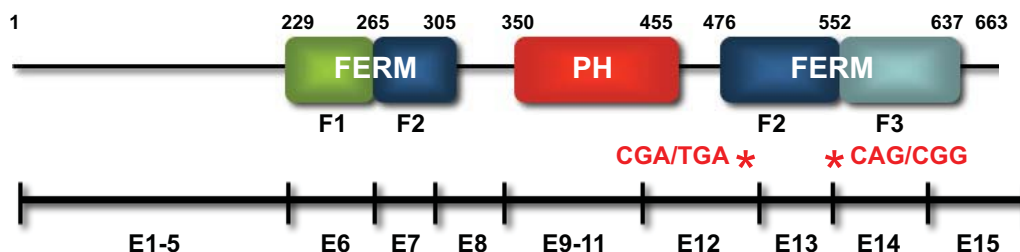
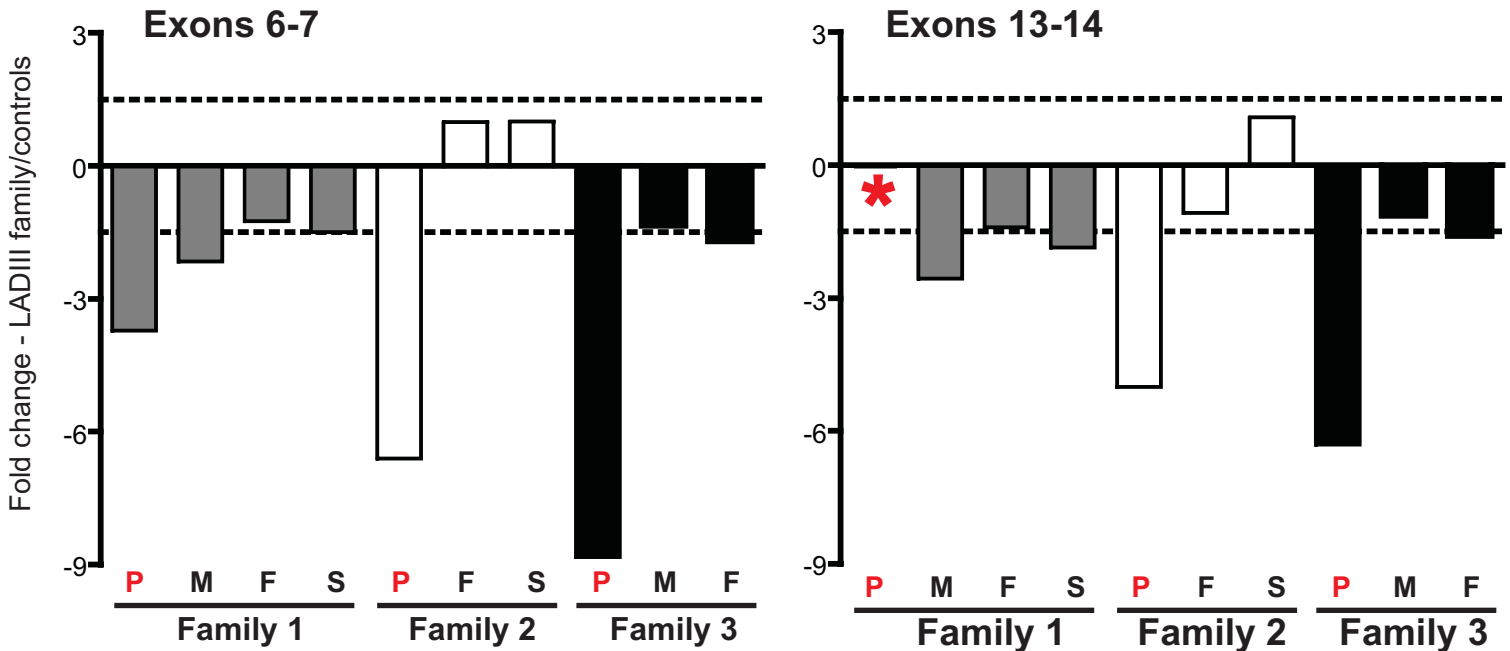


Figure 5

a



b

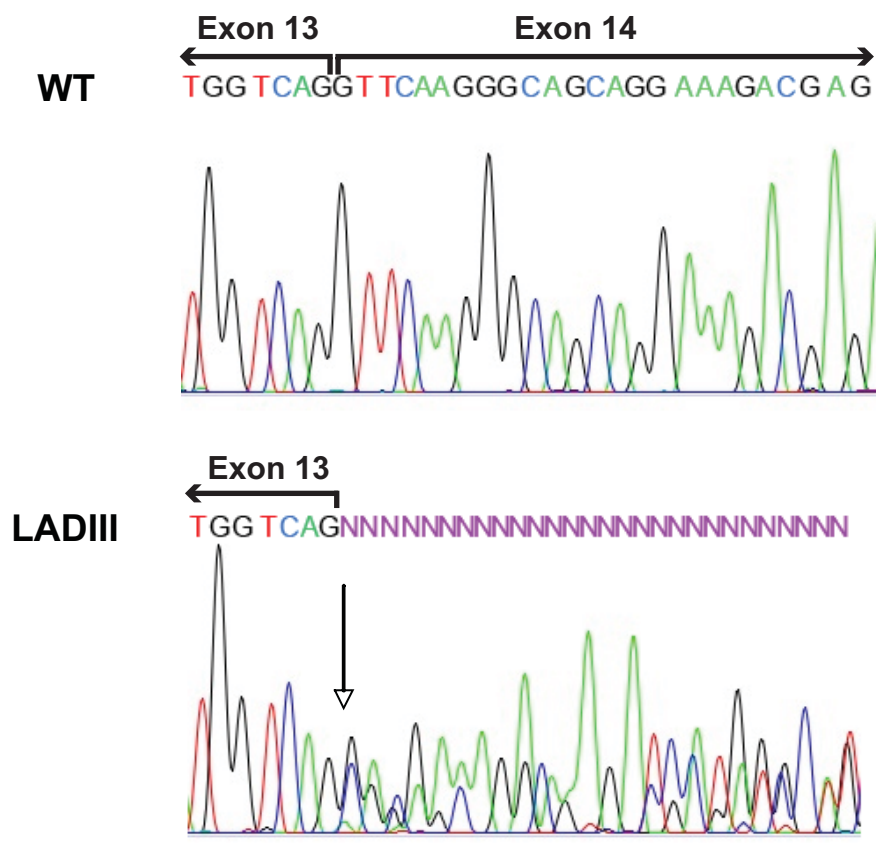
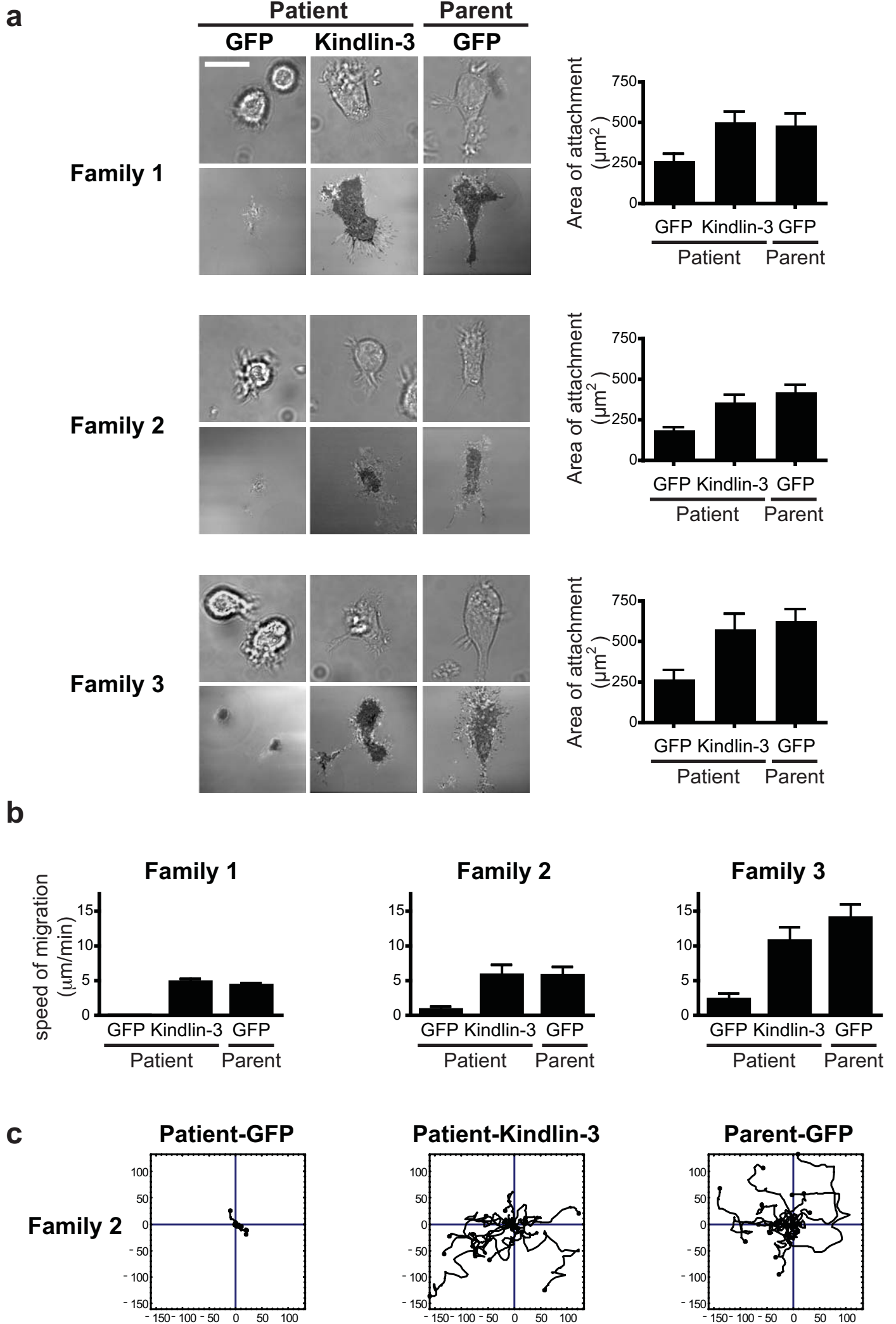


Figure 6

On line Supplementary Data

Figure 1 The sequence of the genomic DNA surrounding the C/A base change in CalDAG-GEF-1 (see arrow) is shown for all LAD-III patients and their relatives.

Figure 2 Measurement of mRNA levels of the longer CalDAG-GEF1 isoform (671 amino acids) by quantitative PCR using Taqman Gene Expression Assay Hs01057123_m1 (CalDAG-GEF1 exons 2-3). The results are expressed as fold difference of patients (P) and relatives (M = mother, F = father, S = sibling) compared with two control EBV transformed B cell lines.

Figure 3 The sequence of the genomic DNA surrounding the Kindlin-3 base changes in exon 12 and splice acceptor site associated with exon 14 is shown for all LAD-III patients and their relatives.

Video 1 GFP-expressing LAD-III B cells (Turkish family 3) migrating on ICAM-1. These cells have dynamic membranes but are not motile. Each frame=1/10 sec representing 15 sec real time.

Video 2 CalDAG-GEF-1 expressing LAD-III B cells (Turkish family 3) migrating on ICAM-1. These cells have dynamic membranes, are not motile and resemble the cells expressing only GFP (video 1). Each frame=1/10 sec representing 15 sec real time.

Video 3 Kindlin-3- expressing LAD-III B cells (Turkish family 3) migrating on ICAM-1. Expression of Kindlin-3 renders these cells motile almost to the same extent as the parent's cells in Video 4. Each frame=1/10 sec representing 15 sec real time.

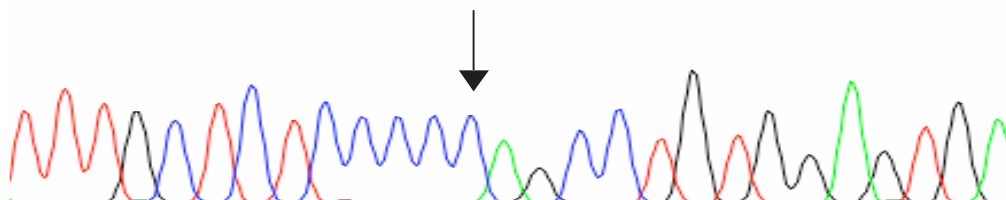
Video 4 GFP-expressing B cells of the mother of family 3 migrating on ICAM-1. Each frame=1/10 sec representing 15 sec real time.

Suppl. Fig. 1 – CalDAG-GEF1

Family 1

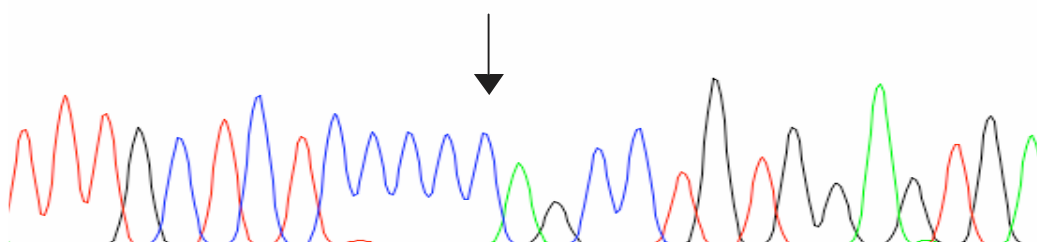
Patient

T T T G C ²⁰⁰ T C T C C C C C C A G ²¹⁰ C C T G T G G A G T G A ²²⁰



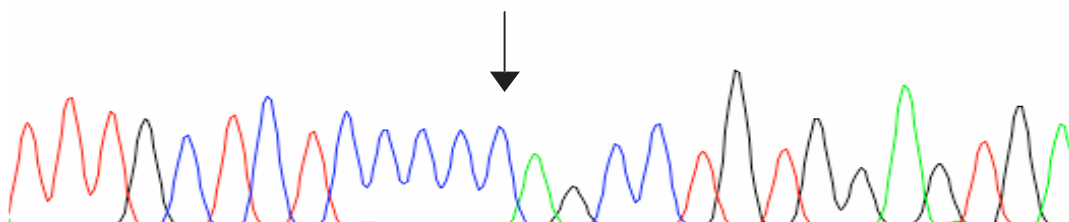
Mother

T T T G C ¹⁹⁰ T C T C C C C C C A G ²⁰⁰ C C T G T G G A G T G A ²¹⁰



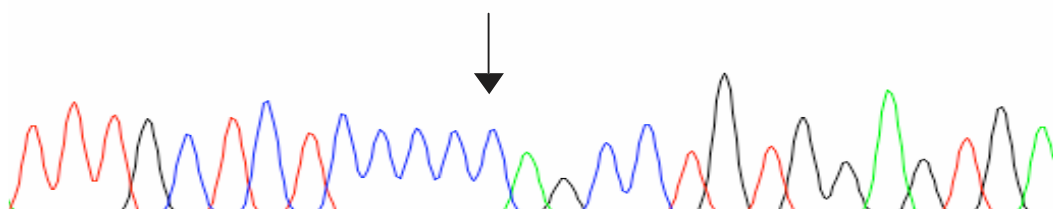
Father

T T T G C ¹⁹⁰ T C T C C C C C C A G ²⁰⁰ C C T G T G G A G T G A ²¹⁰



Sibling

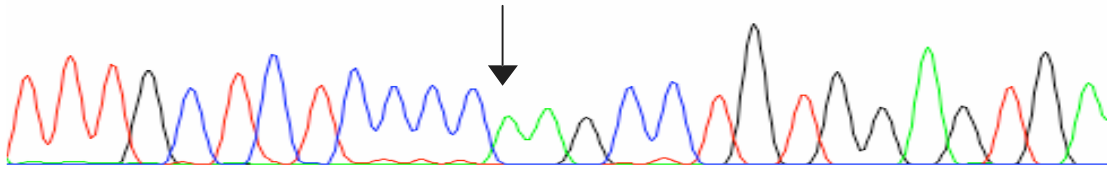
T T T G C ¹⁹⁰ T C T C C C C C C A G ²⁰⁰ C C T G T G G A G T G A ²¹⁰



Family 2

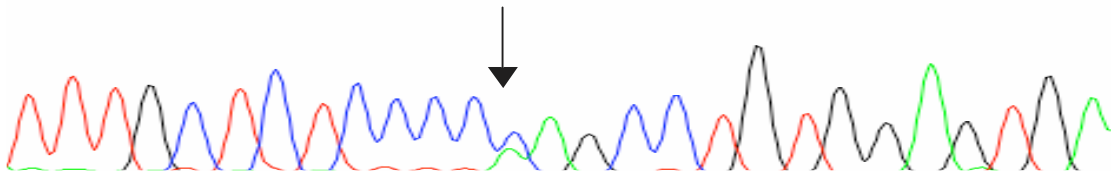
Patient

180 T T T G C T C T C C C C C A A G C C T G T G 200 G A G T G A



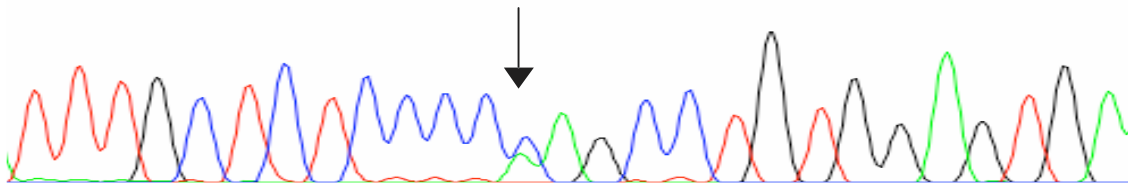
Mother

190 T T T G C T C T C C C C C A G C C T G T G G A G T G A 210



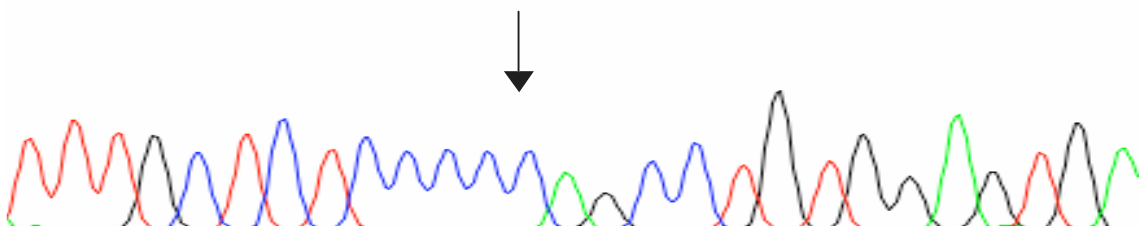
Father

190 T T T G C T C T C C C C C A G C C T G T G G A G T G A 210



Sibling

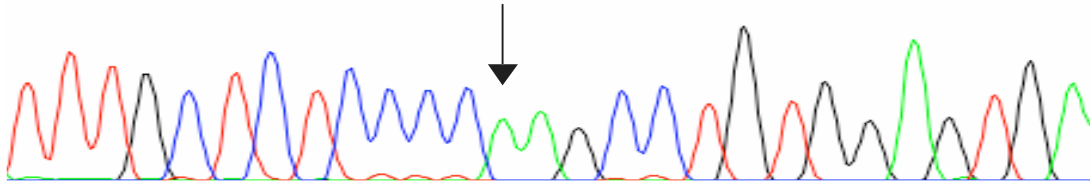
190 T T T G C T C T C C C C C A G C C T G T G G A G T G A 210



Family 3

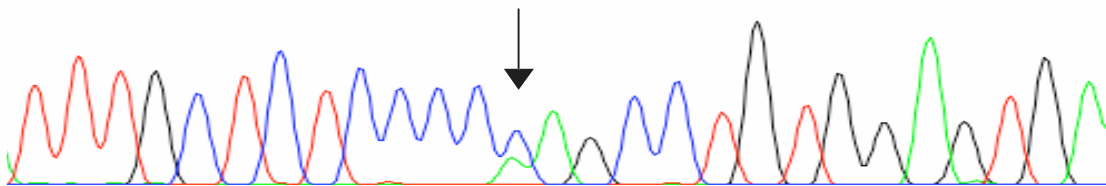
Patient

T T T G C T C T C C C C A A G C C T G T G G A G T G A



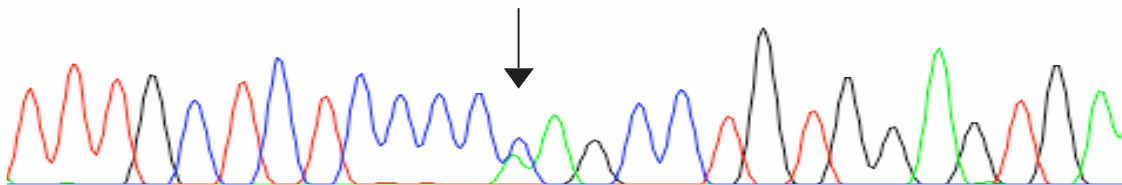
Mother

T T T G C T C T C C C C A G C C T G T G G A G T G A

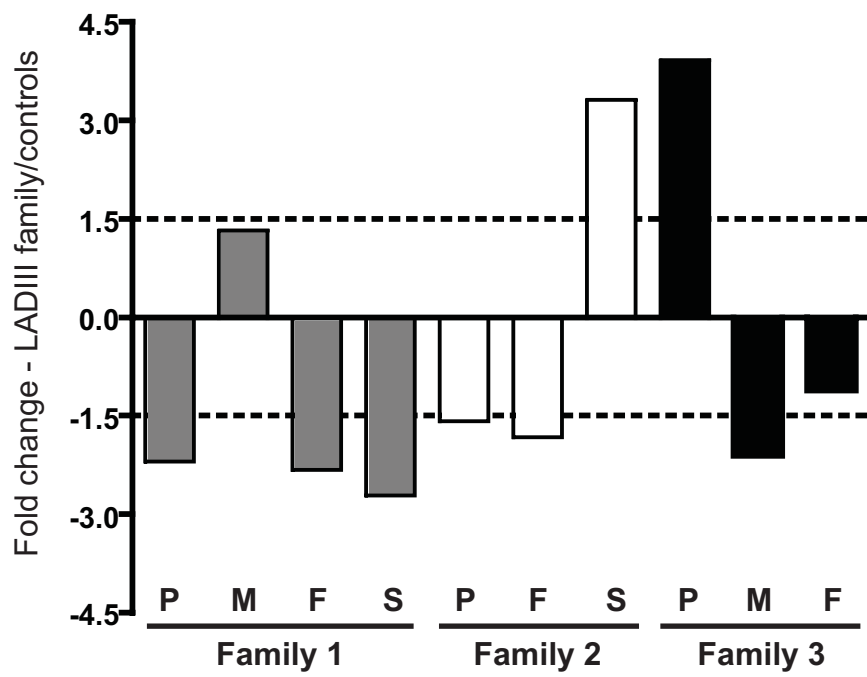


Father

T T T G C T C T C C C C N A G C C T G T G G A G T G A



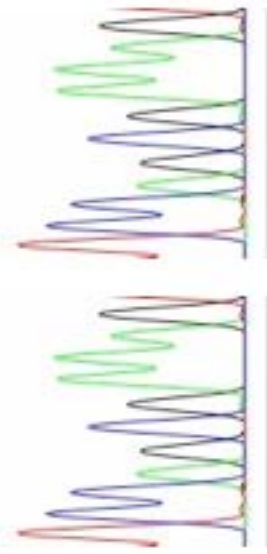
Suppl. Fig. 2



Suppl. Fig. 3

Kindlin-3: sequence surrounding the C>T mutation (exon 12)

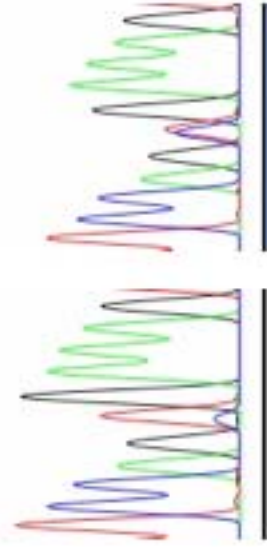
TCCAGCGAAAG' TCCAGCGAAAG'



Family 1 Patient

Family 1 Mother

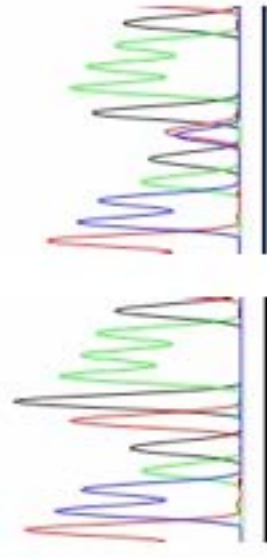
TCCAGTGAAAG' TCCAGTGAAAG'



Family 2 Patient

Family 2 Mother

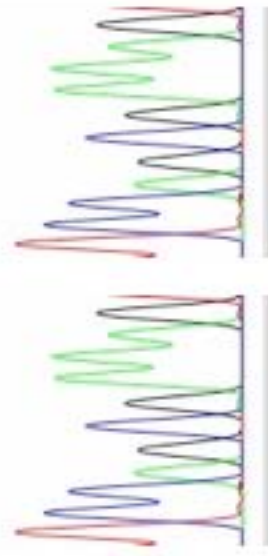
TCCAGTGAAAG' TCCAGTGAAAG'



Family 3 Patient

Family 3 Mother

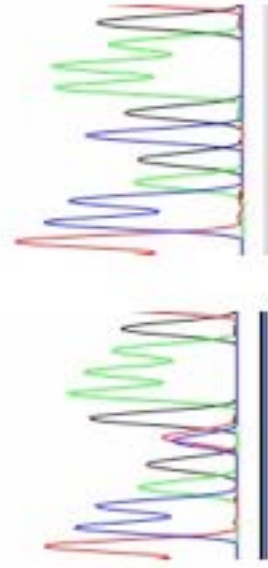
TCCAGCGAAAG' TCCAGCGAAAG'



Family 2 Father

Family 1 Sibling

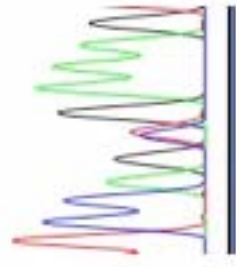
TCCAGTGAAAG' TCCAGCGAAAG'



Family 2 Father

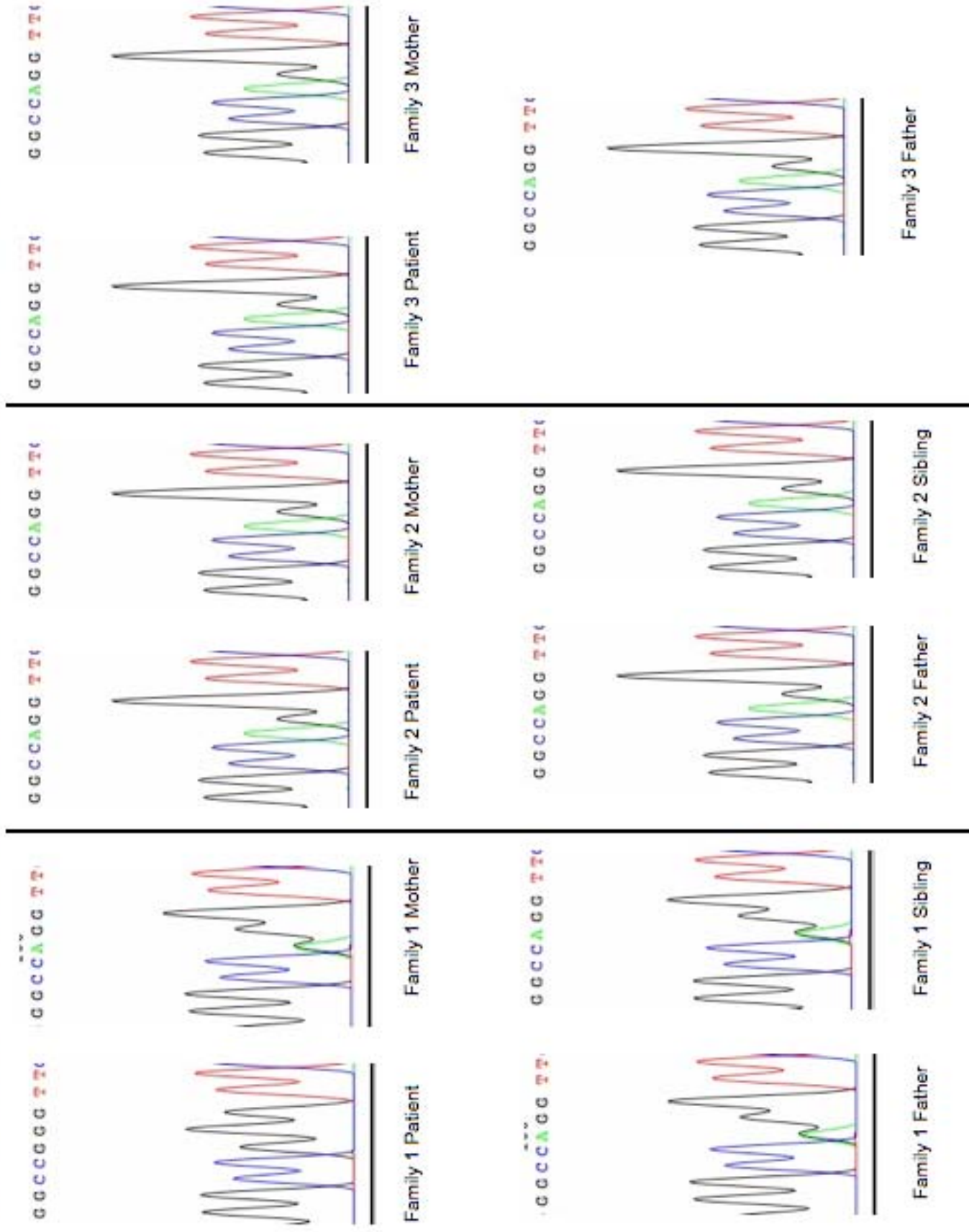
Family 2 Sibling

TCCAGTGAAAG'



Family 2 Father

Kindlin-3: sequence surrounding the splice acceptor site A>G mutation (exon 14)



Paper VII

Loss of Kindlin-1 causes skin atrophy and lethal neonatal ulcerative colitis

Siegfried Ussar¹, Markus Moser¹, Moritz Widmaier¹, Emanuel Rognoni¹, Christian Harrer^{1,2}, Orsolya Genzel-Boroviczeny², Reinhard Fässler¹

¹Department of Molecular Medicine, Max-Planck Institute of Biochemistry, Am Klopferspitz 18, 82152 Martinsried, Germany; ²Division of Neonatology, Perinatal Center, Children's Hospital Ludwig-Maximilians-University Munich, Munich, Germany

Kindler Syndrome (KS), characterized by transient skin blistering followed by abnormal pigmentation, skin atrophy and skin cancer, is caused by mutations in the FERMT1 gene. Although a few KS patients have been reported to also develop ulcerative colitis (UC), a causal link to the FERMT1 gene mutation is unknown. The FERMT1 gene product belongs to a family of focal adhesion proteins (Kindlin-1, -2, -3) that bind several β integrin cytoplasmic domains. We show here that deleting Kindlin-1 in mice gives rise to skin atrophy and a lethal UC. The UC is triggered by defective intestinal epithelial cell integrin activation leading to detachment of this barrier followed by a destructive inflammatory response. The UC is not primarily dependent on an abnormal immune reaction. Thus, we describe the first genetic cause of UC, which is initiated by compromised epithelial cell adhesion.

Introduction

Kindler Syndrome (KS) is a rare, recessive genodermatosis caused by mutations in the FERMT1 gene (C20ORF42/KIND1) [1,2]. KS patients suffer from varying skin abnormalities that occur at distinct phases of their life [3]. Skin blisters develop and disappear after birth, followed by skin atrophy, pigmentation defects and finally skin cancer. The severity of the individual symptoms varies extensively among individual patients. FERMT1 mutations are distributed along the entire gene and can give rise to different truncated Kindlin-1 proteins [4]. Interestingly, the different courses of the KS cannot be linked to mutations within specific regions of the FERMT1 gene [3] suggesting that additional environmental and/or genetic factors contribute to the disease course.

Kindlin-1 belongs to a novel family of cytoplasmic adaptor proteins consisting of three members (Kindlin-1-3) [5]. Kindlins are composed of a central FERM (band 4.1, ezrin, radixin, moesin) domain, which is disrupted by a pleckstrin homology (PH) domain. They localize to cell-matrix adhesion sites (also called focal adhesions, FAs) where they regulate integrin function. In line with the role of Kindlins in integrin function, keratinocytes from KS patients and Kindlin-1-depleted keratinocytes display impaired cell adhesion and delayed cell spreading [6,7]. The mechanism how Kindlin-1 regulates integrin function is not understood and controversial. Kindlin-2 and Kindlin-3 were shown to bind to the membrane distal NxxY motif of $\beta 1$ and $\beta 3$ integrin cytoplasmic domains. This binding, in concert with talin recruitment to the membrane proximal NPxY motif, leads to the activation (inside-out signaling) of $\beta 1$ and $\beta 3$ class integrins enabling them to bind to their ligand. Following ligand binding, Kindlin-2 and Kindlin-3 stay in matrix adhesion sites where they link the ECM to the actin cytoskeleton by recruiting ILK and Migfillin to FAs (outside-in signaling). Consistent with this adaptor function of Kindlin-1, keratinocytes from KS patients and keratinocytes depleted of Kindlin-1 display impaired cell adhesion and delayed cell spreading [6,7]. Importantly, however, Kindlin-1 was reported to have different properties than Kindlin-2 and -3, since it was shown to bind like talin to the proximal NPxY motif of $\beta 1$ integrin tails [6],

The Kindlins have a specific expression pattern. Kindlin-1 is expressed in epithelial cells, while Kindlin-2 is expressed ubiquitously. They are both found at integrin adhesion sites and/or cadherin-based cell-cell junctions. Kindlin-3 is exclusively

expressed in hematopoietic cells, where it controls a variety of functions ranging from integrin signaling in platelets [8] to stabilizing the membrane cytoskeleton in mature erythrocytes [9].

Although the FERMT1 gene is expressed in epithelial cells of almost all tissues and organs [5], only abnormalities of the skin and the oral mucosa are associated with the disorder. Recently it has been reported, however, that some KS patients also develop ulcerative colitis (UC) [4,10,11], which together with Crohn's disease belongs to idiopathic inflammatory bowel disease.

UC usually occurs in the second or third decade of life, although the incidence in pediatric patients is steadily rising [12,13]. UC is restricted to the colon and is characterized by superficial ulcerations of the mucosa. It is currently believed that the mucosal ulcerations are triggered by the release of a complex mixture of inflammatory mediators leading to severe inflammation and subsequent epithelial cell destruction [12]. In line with this paradigm a large number of murine colitis models occur when the innate or adaptive immune response is altered [12]. Genetic linkage analysis in man led to the identification of several susceptibility loci [14,15]. Importantly, however, there is still no genetic mutation assigned to the disease etiology. In line with the UC disease course most of the KS patients develop their first UC symptoms in adulthood. Interestingly, however, one of them suffered from a severe neonatal form of UC and was diagnosed with a null mutation in the FERMT1 gene after developing trauma-induced skin blistering later in life [10]. Since only a few KS patients were reported to develop intestinal symptoms, it is currently debated whether UC development is directly linked to FERMT1 gene mutations or secondarily caused by a microbial infection or an abnormal inflammatory response.

In this study we directly investigated the role of Kindlin-1 *in vivo* by generating mice carrying a constitutive null mutation in the Kindlin-1 gene. We demonstrate that Kindlin-1 deficient mice develop skin atrophy and a lethal UC, which results in early postnatal lethality. The UC is caused by defective intestinal epithelial integrin activation, which leads to severe epithelial detachment followed by a severe inflammatory reaction.

Results

Loss of Kindlin-1 leads to lethal ulcerative colitis

To unravel the consequences of loss of Kindlin-1 *in vivo*, we established a mouse strain with a disrupted *Fermt1* gene, leading to a complete loss of Kindlin-1 mRNA and protein (Figure 1A-C). Heterozygous Kindlin-1 mice (Kindlin-1^{+/-}) had no phenotype and were fertile. Kindlin-1-deficient mice (Kindlin-1^{-/-}) were born with a normal Mendelian ratio (29.6% +/+; 44.1% +/-; 26.3% -/-; n = 203 at P21) and appeared normal at birth. Two days postnatal (P2), all Kindlin-1^{-/-} mice analyzed so far were dehydrated (Figure 1D), failed to thrive (Figure 1E) and died between P3-P5 (Figure 1E). Blood glucose and triglyceride levels of Kindlin-1^{-/-} mice were normal suggesting a normal absorption of nutrients in the small intestine (Supplementary Figure 1). Their urine showed an increased osmolarity further pointing to severe dehydration (Figure 1F).

The skin was assessed to determine whether skin abnormalities caused the perinatal lethality. Although Kindlin-1^{-/-} mice showed features of KS like skin atrophy and reduced keratinocyte proliferation (Figure 2A and B), adhesion of basal keratinocytes to the basement membrane (BM) was unaltered (Figure 2A and Supplementary Figure 2). Histology of backskin sections from different developmental stages revealed normal keratinocyte differentiation (Supplementary Figure 3), normal development of the epidermal barrier (Supplementary Figure 4A and Figure 2C and D), and comparable epidermal thickness at E18.5 and P0. In line with the progressing proliferation defect a reduction of the epidermal thickness was first observed at P1 (Supplementary Figure 4B). Interestingly despite the mild *in vivo* phenotype, Kindlin-1^{-/-} keratinocytes displayed severe adhesion and spreading defects in culture (Supplementary Figure 5A and B) further indicating that Kindlin-1^{-/-} keratinocytes from mouse and man display similar defects [7].

These results indicated that another defect is responsible for their perinatal lethality. When the stomach and the intestine of Kindlin-1^{-/-} mice were examined, they were swollen and filled with gas (Figure 3A) suggesting severe intestinal dysfunction might be the cause of death. At P2, the terminal ileum and colon were shortened and swollen and strictures were evident in the distal colon, which are signs of acute inflammation (Figure 3B). By P3, when the majority of mutant mice were dying, most of the colonic epithelium detached (Figure 3C), became apoptotic (Supplementary

Figure 6) and was replaced by granulation tissue enriched with macrophage, granulocyte and T cell infiltrates (Figure 3D). The shortened colon was neither a consequence of increased apoptosis, which was only seen in detached epithelium, nor a result of reduced intestinal epithelial cell (IEC) proliferation (Supplementary Figure 6).

The epithelial detachment and severe inflammation extended into the ileum (Figure 3C). In contrast, the proximal small intestine (duodenum and jejunum) had no evidence of IEC detachment or inflammation (Figure 4). The phenotype of Kindlin-1^{-/-} mice for the most part phenocopied the intestinal disease observed in the patient with a complete loss of Kindlin-1, who developed severe neonatal UC prior to skin blistering becoming apparent [10].

Kindlin-1 is required for intestinal epithelial cell adhesion

To define the cell type affected by loss of Kindlin-1 we localized Kindlin-1 in the normal intestine by immunostaining. Similar to the situation in man [4], Kindlin-1 is present throughout the cytoplasm of IECs of the colon and at the basolateral sites of both IECs of the colon (Figure 5A) and the small intestine (Figure 5B). The anti-Kindlin-1 polyclonal antibody produced some weak unspecific background signals in the intestinal mesenchyme of wild type and Kindlin-1^{-/-} mice (Figure 5B). Kindlin-2 was exclusively found in cell-cell contacts and did not change its distribution in the absence of Kindlin-1 (Figure 5C and D). Focal adhesion (FA) components such as Talin and Migfilin as well as F-actin were expressed normally in Kindlin-1^{-/-} colonic epithelium that was still adhering to the BM (Figure 5C and data not shown).

Next we determined the time point when mutant mice began developing intestinal abnormalities. At E18.5 the ileum and colon of Kindlin-1^{-/-} mice were histologically normal and electron microscopy revealed an intact epithelium and basement membrane (BM) (Figure 6A). Shortly after birth (P0), wild-type and Kindlin-1^{-/-} mice began to suckle and accumulated milk in their stomachs. Within 5-7 hours nursed Kindlin-1^{-/-} mice contained colostrum in the intestinal lumen and displayed extensive epithelial cell detachment (Figure 6B) but no infiltrating immune cells (Figure 6B and C) in the distal colon. No epithelial detachment occurred when Kindlin-1^{-/-} mice were delivered by Caesarean section and incubated in a heated and humidified chamber for up to 7 hours (Figure 6B) indicating that mechanical stress applied by stool caused IEC detachment. However, intestinal inflammation occurred over time in fed

mice (Figure 6D) with all the signs of a classical UC [16] including a significantly increased expression of the proinflammatory cytokines TNF- α and IL-6 and a reduction in goblet cell mucins (Figure 6D and E.). Although inflammation extended into the ileum at P3 (Figure 6B and C), the epithelial cells of the ileum were never detached suggesting that Kindlin-1^{-/-} mice develop a so-called backwash ileitis caused by stool “washed back” from the colon into the ileum [13]. These analyses revealed that the epithelial detachment begins at P0 in the distal parts of the colon and subsequently expands proximally.

Kindlin-1 controls activation of integrins

An important question is how Kindlin-1 deficiency leads to detachment of intestinal epithelial cells. One potential explanation could be loss of support by a disrupted BM as reported for skin of KS patients [1,2,3]. Moreover, it is known that BM digestion and epithelial detachment in inflammatory bowel disease (IBD) can be triggered via the secretion of MMPs by epithelial and/or infiltrating immune cells [17]. This possibility could be excluded, since Kindlin-1^{-/-} mice at P1 showed a continuous BM with all major components present, both in areas of the colon where IECs were still adherent as well as in areas where IECs were detached (Figure 7A). Interestingly, also the skin of Kindlin-1^{-/-} mice showed a normal BM distribution by immunostaining (Supplementary Figure 2).

An alternative explanation for the IEC detachment could be a dysfunction of integrins, similar to that reported for Kindlin-3-deficient platelets [8] and Kindlin-2-deficient primitive endoderm [18]. The normal distribution of β 1 integrin (Figure 7B) and the comparable levels of β 1 and α v integrins (Figure 7C and D and data not shown) excluded a defect in expression and/or translocation of integrins to the plasma membrane. Flow cytometry of primary IECs with the monoclonal antibody 9EG7, which recognizes an activation-associated epitope on the β 1 integrin subunit, showed significantly reduced binding (Figure 8A) suggesting that loss of Kindlin-1 decreases activation (inside-out signaling) of β 1 integrins. Primary keratinocytes from Kindlin-1^{-/-} mice also showed normal localization (Supplementary Figure 7A) and surface expression of β 1 integrins (Supplementary Figure 7B). Interestingly, 9EG7 staining revealed reduced, although not statistically significant, activation of β 1 integrins (Supplementary Figure 7C).

Since it is difficult to culture and maintain primary murine IECs, we depleted Kindlin-1 in a human colon carcinoma cell line (HT-29) using RNAi (HT-29siKind1; Figure 8B) to show that integrin-mediated cell adhesion and shear stress induced detachment were also perturbed in a colon cell line. HT-29siKind1 cells were unable to adhere to fibronectin, showed strongly reduced adhesion to Laminin-332 and Collagen IV (Figure 8C) and easily detached from FN upon exposure to low as well as high shear stress (Supplementary Figure 8). The remaining adhesion to Laminin-332 and Collagen IV is likely mediated by other Laminin- and Collagen-binding receptors on colonic epithelial cells such as $\alpha6\beta4$ integrins and discoidin domain receptors [19,20], which are both known to function independent of Laminin and Collagen binding $\beta1$ integrins [21].

These findings indicate that (i) loss of Kindlin-1 impairs integrin activation, which compromises adhesion of colonic epithelial cells and finally leads to inflammation and UC, that (ii) Kindlin-2 cannot rescue Kindlin-1 loss in colonic epithelial cells, and that (iii) the residual adhesion to Laminin and Collagen supports the *in vivo* observation that shear is required to detach IECs Collagen IV-containing BMs *in vivo*.

It has been reported that Kindlin-1 associates with the membrane proximal NPxY motif of $\beta1$ and $\beta3$ integrins [6]. This observation, however, is in contrast with observations made with Kindlin-2 and -3, both of which bind the membrane distal NxxY motifs of $\beta1$ and $\beta3$ integrins to trigger their activation [8,18,22]. To explore the mechanism whereby Kindlin-1 induces integrin activation, we performed pull down experiments with recombinant GST-tagged cytoplasmic β integrin tails in IEC and keratinocyte lysates. The results confirmed that Kindlin-1 associated with the cytoplasmic domains of $\beta1$ and $\beta3$ (Figure 8D). Since substitutions of the tyrosine residues in the proximal NPxY motifs with alanine ($\beta1Y788A$; $\beta3Y747A$) allowed Kindlin-1 binding, while tyrosine to alanine substitutions in the distal NxxY motif of $\beta1$ and $\beta3$ integrin tails ($\beta1Y800A$; $\beta3Y759A$) abolished Kindlin-1 binding, we conclude that the binding and functional properties are conserved among all Kindlins. This was further confirmed with direct binding assays, which showed that the recombinant His-tagged C-terminal FERM domain of Kindlin-1 (aa 471-677) containing the phosphotyrosine binding (PTB) motif bound GST-tagged $\beta1$ but not the Y800A mutated $\beta1$ integrin cytoplasmic tail (Figure 8E).

It is well established that Talin can induce activation of integrins, and for a long time it was believed that it is sufficient for the execution of this task. This important function

of Talin was discovered by overexpressing Talin or its FERM domain in CHO cells. This resulted in shifting the inactive conformation of the platelet integrin $\alpha\text{IIb}\beta\text{3}$ [23] to a high affinity state as demonstrated by increased binding of the PAC1 antibody recognizing activation associated epitopes on $\alpha\text{IIb}\beta\text{3}$ integrin. In contrast to Talin, overexpression of Kindlin-1 failed to trigger activation of $\alpha\text{IIb}\beta\text{3}$ integrin in CHO cells. Interestingly, as described for Kindlin-2 [18,22], overexpression of both the Talin FERM domain and Kindlin-1 doubled PAC1 binding when compared with cells expressing only the Talin FERM domain (Figure 8F). The synergism between Talin and Kindlin-1 depends on a Kindlin-1 and β integrin tail interaction, as a PTB mutant of Kindlin-1 (QW611/612AA) failed to bind β integrin tails (Figure 8G) and the synergistic effect with Talin was lost. These findings suggest that Kindlin-1 is not sufficient for integrin activation but is required for inducing Talin-mediated integrin activation. This notion was confirmed with CHO cells, in which endogenous Kindlin-2 levels were depleted by RNAi (Figure 8H). Furthermore, overexpressing Talin failed to induce integrin activation in these cells, but re-expression of Kindlin-1 restored this function (Figure 8I).

These findings show (i) that Kindlin-1 and -2 require Talin for integrin activation, (ii) that Talin requires Kindlins for integrin activation, and (iii) that Kindlin-1 and Kindlin-2 have redundant functions *in vitro* as both Kindlin-1 and -2 are recruited to FAs where they exert identical functions on integrin cytoplasmic tails. However, *in vivo* this is not the case as Kindlin-2 is recruited to cell-cell contacts in IECs and apparently does not compensate Kindlin-1 loss.

Discussion

In the present study we show that a null mutation in the *Fermt1* gene gives rise to skin atrophy and an acute and fulminant, neonatal UC. We demonstrate that, unlike other forms of UC, the primary defect is a loss of the intestinal epithelial barrier that secondarily leads to inflammatory cell infiltrates and the development of all classical characteristics of UC. Furthermore, we show that loss of the intestinal epithelial barrier is caused by a severe adhesion defect of intestinal epithelial cells to the underlying BM, which in turn is caused by the inability of integrins to become activated and to bind BM components. It is possible that in addition to defective integrin activation and epithelial detachment, Kindlin-1 exerts other yet unidentified functions that contribute to the phenotype in *Kindlin-1^{-/-}* mice. To our knowledge, the *Kindlin-1*-deficient mice represent the first animal model for UC caused by a single non embryonic lethal gene mutation.

Kindler syndrome (KS) is thought to be primarily a skin disease with a disease course that is characterized by epidermal atrophy and followed by epidermal blistering, pigmentation defects and skin cancer. The complex disease syndrome is difficult to diagnose at the disease onset due to similarities with other forms of skin blistering diseases (also called epidermolysis bullosa; EB) that are caused by mutations in keratin and BM genes [24]. EB patients are not prone to UC, although they can develop gastrointestinal symptoms that are, however, restricted to the esophagus and rectum, as both organs have a similar BM composition and keratin expression pattern as epidermal keratinocytes [11]. Recent case reports showed that KS may involve more organs than only the skin, as several KS patients also suffer from intestinal symptoms. One patient with a severe form of KS developed a severe postnatal UC. Interestingly, this patient was diagnosed with a null mutation in the *FERMT1* gene after developing trauma-induced skin blistering later in life [10]. In line with this severe UC case of KS, we found that the null mutation of the *Fermt1* gene in mice also leads to a dramatic and lethal UC very shortly after birth. Lethality is usually not seen in KS patients, which is most likely due to the immaturity of the murine intestine at birth, making it more vulnerable to injury [25].

The UC of *Kindlin-1*-deficient mice is characterized by flat and superficial ulcerations in the colon, as the epithelium detaches from an intact BM. The defects begin in the rectum and extend along the entire colon finally leading to a severe pancolitis. The

ulcerations and epithelial cell detachments are restricted to the colon, although the ileum shows signs of a secondary inflammation at later stages of the disease. *In vitro* studies with primary IECs from Kindlin-1^{-/-} mice and Kindlin-1-depleted HT-29 cells showed that the cell detachment is caused by impaired activation of integrins leading to weak adhesion of IECs to the underlying BM. The conclusion that UC is triggered by IEC detachment rather than by a primary inflammatory defect in Kindlin-1 deficient mice is based on the observation that epithelial cell detachment always occurred prior to immune cell infiltration. We would therefore, argue that the detachment of IECs resembles an intestinal wound, which secondarily triggers a strong wound healing response leading to immune cell infiltrates and release of a cytokine storm. In line with this hypothesis, epithelial cell detachment, induction of UC and inflammatory reactions can be completely prevented when Kindlin-1 pups are delivered by Caesarian section and subsequently incubated in a humidified and temperature controlled chamber. Mechanical stress applied by the colostrum is likely inducing the detachment of the weakly adhering epithelial cells in the colon. The vast majority of mouse models reported to develop colitis so far have an abnormal immune system [12,26]. This fact as well as the identification of several susceptibility loci in human patients [14,15] led to the conclusion that defects in the immune system are of central importance for UC development. Severe adhesion defects of IECs leading to a massive wound response represent a novel and alternative etiology for UC development.

Although adhesion is severely compromised in the colon of Kindlin-1-deficient mice, like KS patients they are born without skin blisters. This is in line with KS patients, who are also born without skin blisters even when they are delivered by the vaginal route but develop blisters postnatally at trauma prone sites. Interestingly, Kindlin-1 deficient mice did not show defective adhesion of basal keratinocytes to the BM even after application of mild mechanical stress. The different severity of the adhesion defect in skin and colon could be reflected by the functional properties of the distinct set of integrins expressed in the two organs and the absence of classical hemidesmosomes in intestinal epithelial cells [27].

Another pronounced skin defect in Kindlin-1-deficient mice as well as KS patients is skin atrophy, which seems to be due to reduced proliferation of interfollicular keratinocytes. This finding raises several questions; first, regarding the mechanism

underlying the molecular control of cell proliferation by Kindlin-1. The mechanism is unknown and could result from a diminished cross talk between integrin and growth factor signaling. Second, it is also unclear how a molecular player that supports proliferation is giving rise to cancer at a later stage. It is possible that the localization of Kindlins in different cellular compartments, i.e. cell-matrix adhesion sites, cell-cell adhesion sites and in certain instances in the nucleus, equips them with different functions that become evident at different time points in life.

Kindlin-1 and -2 are co-expressed in epidermal cells as well as epithelial cells of the colon. Interestingly, we found that Kindlin-2 cannot compensate Kindlin-1 function *in vivo*, neither in the colon nor in skin. Since Kindlin-2 is recruited to cell-cell adhesions in both mutant cell types and does not translocate to integrin adhesion sites in mutant intestinal and epidermal epithelial cells, it is unable to compensate for the loss of Kindlin-1, although both Kindlins are capable of performing the same tasks at the integrin tails *ex vivo* and *in vitro* [27]. Hence, a therapeutic strategy to reroute some of the Kindlin-2 from cell-cell to the integrin adhesion sites may represent a promising approach to prevent ulceration in KS patients with severe UC.

Materials & Methods

Mouse strains

The Kindlin-1^{-/-} mice were obtained by replacing the ATG-containing exon 2 with a neomycin resistance cassette (detailed information on the cloning of the targeting construct can be obtained from Faessler@biochem.mpg.de). The construct was electroporated into R1 embryonic stem (ES) cells (passage 15) and homologous recombination was verified with Southern blots. Genomic DNA was digested with EcoRV, blotted and then hybridized with a 5' probe or digested with BglII, blotted and hybridized with a 3' probe (Figure 1A). Targeted ES cells were injected into blastocysts and transferred into foster mice. Mice were housed in a special pathogen free mouse facility. All animal experiments have been approved by the local authorities.

Histology, Immunohistochemistry and Immunofluorescence stainings

For H&E stainings intestinal segments were either PFA fixed and embedded in paraffin, or frozen on dry-ice in cryo-matrix (Thermo). Immunohistochemistry of paraffin embedded sections was carried out as previously described [5]. Sections of 8µm thickness were prepared and stained following routine protocols. Cryo sections were fixed in 4% PFA/PBS except for the Kindlin-1 staining where sections were fixed with 1:1 methanol/acetone at -20°C. Subsequently tissue sections were blocked with 3% BSA/PBS, incubated with primary antibodies in a humidity chamber over night at 4°C, with fluorescently labeled secondary antibodies for 1h at RT and finally mounted in Elvanol. Pictures were taken with a Leica DMIRE2 confocal microscope with a 100x or 63x NA 1.4 oil objective.

GST-pull downs

Recombinant GST-β1, β1Y788A, β1Y800A, β3, β3Y747A, β3Y759A cytoplasmic tails were expressed and purified from *E.coli* under non denaturing conditions. 5µg of recombinant tails were incubated with 500µg IEC lysate (in 50mM Tris pH 7.4, 150mM NaCl, 1mM EDTA, 1% Triton-X-100) overnight. GST-constructs were precipitated with glutathione beads (Novagen). Subsequent western blots were probed for Kindlin-1 and GST.

Antibodies

A polyclonal peptide antibody against Kindlin-1 was raised against the peptide YFKNKELEQGEPIEK as previously described [5].

The following antibodies were used at the given concentration indicated for western blot (W), immunoprecipitation (IP), immunofluorescence (IF), immunohistochemistry (IHC): Kindlin-1 (W: 1:5000, IF cells: 1:200, IF tissue: 1:1000), Kindlin-2 (W: 1:1000, IF cells 1:200, IF tissue: 1:200), E-cadherin (Zymed, W: 1:5000), Migfilin (W: 1:5000, IF cells 1:100, IF tissue: 1:100), GAPDH (Chemicon; W: 1:10000), phalloidin Tritc (Sigma; IF cells: 1:800, IF tissue: 1:800), Mac-1 (EuroBioscience; IF tissue: 1:100), GR-1 (eBioscience; IF tissue: 1:100), Th1.2 (PharMingen; IF tissue: 1:100), GST (Novagen; W: 1:10000), His (CellSignaling; W: 1:1000), PAC1 (BD; FACS: 1:100), α 6 integrin (PharMingen; IF tissue: 1:100), CollagenIV (a gift from Dr. Rupert Timpl; IF tissue: 1:100), Laminin-332 (a gift from Dr. Monique Aumelley; IF tissue: 1:200), Perlecan (a gift from Dr. Rupert Timpl; IF tissue: 1:100), β 1 integrin (Chemicon; WB: 1:3000, IF tissue: 1:600), 9EG7 (PharMingen; FACS: 1:100), EGFP (Abcam; WB: 1:10000), β 1 integrin (PharMingen; FACS: 1:200), α v integrin (PharMingen; FACS: 1:200). Keratin10 (Covance; IHC: 1:600), Keratin14 (Covance; IHC: 1:600), Loricrin (Covance; IHC: 1:500) Ki67 (Dianova; IHC: 1:50), cCaspase3 (CellSignaling, IHC: 1:100).

Caesarean section

Pregnant mice were sacrificed by cervical dislocation when embryos were at E18.5-E19 of gestation. The uterus was removed and cut open. Embryos were taken out and the umbilical cord was cut. Mice were subsequently dried and kept in an incubator at 37°C and high humidity.

Real Time PCR

Total RNA from whole colons was extracted with a PureLink Micro to Midi RNA extraction kit (Invitrogen) following the manufacturers instructions. cDNA was prepared using the iScript cDNA Synthesis Kit (Biorad). Real Time PCR using a Sybr Green ready mix (Biorad) was performed in an iCycler (Biorad). Each sample was measured in triplicates and values were normalized to GAPDH. Following primers

were used; TNF α fwd: AAAATTCGAGTGACAAGCCTGTAGC, TNF α rev: GTGGGTGAGGAGCACGTAG. IL-6 fwd: CTATACCACTTCACAAGTCGGAGG IL-6 rev: TGCACAACCTCTTTTCTCATTTC. RT-PCR for Kindlin-1 and GAPDH was performed as previously described [5].

Isolation of IECs

Neonatal mouse intestine was removed and flushed with 1ml PBS. The intestine was longitudinally cut open, rinsed with PBS and incubated for 40 min. in IEC isolation buffer (130mM NaCl, 10mM EDTA, 10mM Hepes pH 7.4, 10% FCS and 1mM DTT) at 37°C on a rotor. The epithelium was shaken off and pelleted by centrifugation at 2000rpm for 5 min. For WB analysis cells were washed once with PBS and subsequently lysed. For flow cytometry cells were washed once with PBS and trypsinized with 2x trypsin (GIBCO) for 10 min. at 37°C. Trypsin was inactivated with DMEM containing 10%FCS. A single cell suspension was prepared by passing cells through a cell strainer (BD).

Isolation of keratinocytes

Primary keratinocytes were isolated from P3 mice as described previously [28]. Cells were cultured on a mixture of Coll (Cohesion) and 10 μ g/ml FN (Invitrogen) coated plastic dishes in keratinocyte growth medium containing 8% chelated FCS (Invitrogen) and 45 μ M Ca $^{2+}$.

Flow cytometry

IEC's and keratinocytes were stained with 9EG7 antibody in Tris buffered saline [29]. For the PAC1 binding assay CHO cells were stained for 40 minutes at RT as described previously [23]. Cells were gated for viability by excluding propidium iodide-positive cells. CHO cells transfected with EGFP-tagged constructs were additionally gated for highly EGFP-positive cells. Measurements were performed with a FACS Calibur (BD) and data evaluation was done with FlowJo software.

Constructs

The EGFP-Kindlin-1 expression plasmid was previously described [5]. The cDNA encoding His-Kindin-1 C-terminus (aa 471-677) was amplified by PCR and cloned into the pQE-70 vector (Qiagen). The Kindlin-1 PTB mutation QW611/612AA was

introduced with a site directed mutagenesis kit (Stratagene) following the manufacturers recommendations. All EGFP constructs were cloned into the pEGFP-C1 vector (Clontech) and subsequently sequenced. EGFP-Talin head was previously described [8].

Cell culture

CHO and HT-29 cells were maintained in DMEM containing penicillin/streptomycin, non-essential amino-acids and 10% or 20% FCS, respectively (GIBCO). Cells were transfected with 2µg of each DNA in six well plates using Lipofectamine 2000 following the manufacturers' instructions (Invitrogen).

RNAi

To deplete Kindlin-1 constitutively from HT-29 cells, an shDNA corresponding to the cDNA sequence GTAAGTCCTGGTTTATACA of hKindlin-1 and a control cDNA with the sequence AGCAGTGCATGTATGCTTC were cloned into the pSuperRetro vector (OligoEngine). Viral particles were prepared as described previously [30]. HT-29 cells were infected and subsequently selected with 2mg/l puromycin. Transient knockdown of Kindlin-2 from CHO cells was achieved by transfection of the siRNAs; Kind2_1: GCCUCAAGCUCUUCUUGAUdTdT and Kind2_2: CUCUGGACGGGAUAAGGAUdTdT, and a control siRNA (purchased from Sigma) using Lipofectamine 2000 (Invitrogen), following the manufacturers instructions. Cells were harvested and assayed 24 hours after transfection.

Adhesion assay

The adhesion assays were performed as previously described [29], using 40000 cells per well in serum free DMEM (HT-29) or MEM (primary keratinocytes).

Osmolarity

Osmolarity was measured from 50µl urine using an Osmomat 030 from Gonotec.

X-gal barrier assay

Embryonic skin barrier formation was determined as previously described [31].

Shear stress assay

Slides with a 1 μ diameter (ibidi BioDiagnostics) were coated overnight with 5 μ g/ml fibronectin and then blocked with 1% BSA. 100.000 cells were seeded onto the slides and incubated for 2.5 hours in a cell culture incubator. Cells were subsequently exposed to increasing amounts of shear force in two minute intervals (as indicated in the Supplementary Figure 8) and pictures were taken every second.

Co-Immunoprecipitation

CHO cells were transiently transfected with the indicated EGFP constructs. Approximately 1mg of protein lysate was immunoprecipitated using the μ MACS Epitope Tag Protein Isolation Kit for EGFP tags (Miltenyi Biotec) following the manufacturers instructions.

Electron microscopy

Electron microscopy was performed as previously described [29].

Statistical analysis

Analyses were performed with GraphPad Prism. If not mentioned otherwise in the figure legends, Gaussian distribution of datasets was determined by a D'Agostino & Pearson omnibus normality test. If samples were not Gaussian distributed a Mann-Whitney test was performed. Gaussian distributed samples were either compared with a one way ANOVA and a Tukey's multiple comparison post test or an unpaired two-tailed t-test.

Acknowledgements

We would like to thank Wilhelm Bloch for electron microscopy, Reinhart Kluge for blood parameter measurements, Klaus-Peter Janssen for IL-6 and TNF α primers, Julia Schlehe, Sara Wickström, Mercedes Costell, Ralph Boettcher, Anika Lange, Ambra Pozzi and Roy Zent for critical reading of the manuscript and Simone Bach and Melanie Ried for excellent technical assistance. This work was supported by the BMBF, the Austrian Science Foundation (SFB021) and the Max Planck Society.

References

1. Siegel DH, Ashton GH, Penagos HG, Lee JV, Feiler HS, et al. (2003) Loss of kindlin-1, a human homolog of the *Caenorhabditis elegans* actin-extracellular-matrix linker protein UNC-112, causes Kindler syndrome. *Am J Hum Genet* 73: 174-187.
2. Jobard F, Bouadjar B, Caux F, Hadj-Rabia S, Has C, et al. (2003) Identification of mutations in a new gene encoding a FERM family protein with a pleckstrin homology domain in Kindler syndrome. *Hum Mol Genet* 12: 925-935.
3. Lai-Cheong JE, Liu L, Sethuraman G, Kumar R, Sharma VK, et al. (2007) Five new homozygous mutations in the *KIND1* gene in Kindler syndrome. *J Invest Dermatol* 127: 2268-2270.
4. Kern J, Herz C, Haan E, Moore D, Nottelmann S, et al. (2007) Chronic colitis due to an epithelial barrier defect: the role of kindlin-1 isoforms. *J Pathol*.
5. Ussar S, Wang HV, Linder S, Fassler R, Moser M (2006) The Kindlins: subcellular localization and expression during murine development. *Exp Cell Res* 312: 3142-3151.
6. Kloeker S, Major MB, Calderwood DA, Ginsberg MH, Jones DA, et al. (2004) The Kindler syndrome protein is regulated by transforming growth factor-beta and involved in integrin-mediated adhesion. *J Biol Chem* 279: 6824-6833.
7. Herz C, Aumailley M, Schulte C, Schlotzer-Schrehardt U, Bruckner-Tuderman L, et al. (2006) Kindlin-1 is a phosphoprotein involved in regulation of polarity, proliferation, and motility of epidermal keratinocytes. *J Biol Chem* 281: 36082-36090.
8. Moser M, Nieswandt B, Ussar S, Pozgajova M, Fassler R (2008) Kindlin-3 is essential for integrin activation and platelet aggregation. *Nat Med*.
9. Krueger M, Moser M, Ussar S, Thievensen I, Lubert C, et al. (in-press) SILAC-mouse for quantitative proteomics uncovers Kindlin-3 as an essential factor for red blood cell function. *Cell*.
10. Sadler E, Klausegger A, Muss W, Deinsberger U, Pohla-Gubo G, et al. (2006) Novel *KIND1* gene mutation in Kindler syndrome with severe gastrointestinal tract involvement. *Arch Dermatol* 142: 1619-1624.
11. Freeman EB, Kogelmeier J, Martinez AE, Mellerio JE, Haynes L, et al. (2008) Gastrointestinal complications of epidermolysis bullosa in children. *Br J Dermatol*.
12. Xavier RJ, Podolsky DK (2007) Unravelling the pathogenesis of inflammatory bowel disease. *Nature* 448: 427-434.
13. Podolsky DK (2002) Inflammatory bowel disease. *N Engl J Med* 347: 417-429.
14. Fisher SA, Tremelling M, Anderson CA, Gwilliam R, Bumpstead S, et al. (2008) Genetic determinants of ulcerative colitis include the *ECM1* locus and five loci implicated in Crohn's disease. *Nat Genet*.
15. Franke A, Balschun T, Karlsen TH, Hedderich J, May S, et al. (2008) Replication of signals from recent studies of Crohn's disease identifies previously unknown disease loci for ulcerative colitis. *Nat Genet*.
16. Mudter J, Neurath MF (2007) Il-6 signaling in inflammatory bowel disease: pathophysiological role and clinical relevance. *Inflamm Bowel Dis* 13: 1016-1023.
17. Medina C, Radomski MW (2006) Role of matrix metalloproteinases in intestinal inflammation. *J Pharmacol Exp Ther* 318: 933-938.
18. Montanez E, Ussar S, Schifferer M, Bosl M, Zent R, et al. (2008) Kindlin-2 controls bidirectional signaling of integrins. *Genes Dev* 22: 1325-1330.
19. Vogel W, Gish GD, Alves F, Pawson T (1997) The discoidin domain receptor tyrosine kinases are activated by collagen. *Mol Cell* 1: 13-23.

20. Alves F, Vogel W, Mossie K, Millauer B, Hofler H, et al. (1995) Distinct structural characteristics of discoidin I subfamily receptor tyrosine kinases and complementary expression in human cancer. *Oncogene* 10: 609-618.
21. Vogel W, Brakebusch C, Fassler R, Alves F, Ruggiero F, et al. (2000) Discoidin domain receptor 1 is activated independently of beta(1) integrin. *J Biol Chem* 275: 5779-5784.
22. Ma YQ, Qin J, Wu C, Plow EF (2008) Kindlin-2 (Mig-2): a co-activator of beta3 integrins. *J Cell Biol* 181: 439-446.
23. O'Toole TE, Katagiri Y, Faull RJ, Peter K, Tamura R, et al. (1994) Integrin cytoplasmic domains mediate inside-out signal transduction. *J Cell Biol* 124: 1047-1059.
24. Aumailley M, Has C, Tunggal L, Bruckner-Tuderman L (2006) Molecular basis of inherited skin-blistering disorders, and therapeutic implications. *Expert Rev Mol Med* 8: 1-21.
25. Hauck AL, Swanson KS, Kenis PJ, Leckband DE, Gaskins HR, et al. (2005) Twists and turns in the development and maintenance of the mammalian small intestine epithelium. *Birth Defects Res C Embryo Today* 75: 58-71.
26. Kang SS, Bloom SM, Norian LA, Geske MJ, Flavell RA, et al. (2008) An antibiotic-responsive mouse model of fulminant ulcerative colitis. *PLoS Med* 5: e41.
27. Fontao L, Stutzmann J, Gendry P, Launay JF (1999) Regulation of the type II hemidesmosomal plaque assembly in intestinal epithelial cells. *Exp Cell Res* 250: 298-312.
28. Romero MR, Carroll JM, Watt FM (1999) Analysis of cultured keratinocytes from a transgenic mouse model of psoriasis: effects of suprabasal integrin expression on keratinocyte adhesion, proliferation and terminal differentiation. *Exp Dermatol* 8: 53-67.
29. Czuchra A, Meyer H, Legate KR, Brakebusch C, Fassler R (2006) Genetic analysis of beta1 integrin "activation motifs" in mice. *J Cell Biol* 174: 889-899.
30. Massoumi R, Chmielarska K, Hennecke K, Pfeifer A, Fassler R (2006) Cyld inhibits tumor cell proliferation by blocking Bcl-3-dependent NF-kappaB signaling. *Cell* 125: 665-677.
31. Patel S, Xi ZF, Seo EY, McGaughey D, Segre JA (2006) Klf4 and corticosteroids activate an overlapping set of transcriptional targets to accelerate in utero epidermal barrier acquisition. *Proc Natl Acad Sci U S A* 103: 18668-18673.

Figure legends

Figure 1. Loss of Kindlin-1 results in early postnatal lethality

(A) The *Fermt1* gene was disrupted by replacing the ATG start codon containing exon 2 with a neomycin resistance cassette. (B) Kindlin-1 mRNA levels were determined by PCR from cDNAs derived from P3 kidneys. (C) Loss of Kindlin-1 protein was confirmed by western blotting in colonic IEC lysates. (D) Pictures from newborn (P0) and two day old mice (P2). Scale bars represent 5mm. (E) Weight curve of Kindlin-1^{-/-} (n=8) and control littermates (+/+; n=8; +/-; n=9) where a † indicates when mice died. *** indicates a P-value <0.0001. (F) Osmolarity of P2 Kindlin-1^{-/-} and control (+/+) urine (n=3 per genotype). Error bars show standard deviations. *** indicates a P-value <0.0001.

Figure 2. Atrophy and reduced proliferation in Kindlin-1^{-/-} skin

(A) H&E stainings from P3 backskin show severe epidermal atrophy in Kindlin-1^{-/-} mice. The BM is indicated by a dashed line and separates the epidermis (e) from the dermis (d). sc: stratum corneum. Scale bar indicates 50µm. (B) Percentage of Ki67-positive interfollicular keratinocytes at different ages. *, p<0.05; **, p<0.02 (n=7 per genotype). Error bars show standard errors of the mean. (C) Kindlin-2 (red; co-stained with α6 integrin (α6-int) in green) and E-cadherin (green, co-stained with Collagen IV in red) staining of P3 backskin sections. Nuclei are shown in blue. Scale bar indicates 10µm. (D) FITC-Lucifer yellow stain of P3 backskin overlaid with DIC. Lack of lucifer yellow dye penetration shows normal skin barrier in Kindlin-1^{-/-} mice. Scale bar indicates 50µm.

Figure 3. Severe inflammation and epithelial detachment in Kindlin-1^{-/-} colon

(A) Opened abdomen with intestine from P2 mice. Arrowheads indicate air in the stomach and small intestine of Kindlin-1^{-/-} mice. bl; bladder. Scale bar represents 5mm. (B) Whole gut preparations from P2 mice. Scale bar represents 5mm. Arrowhead indicates a stricture in the distal colon. The caecum is highlighted with a red circle and the colon is marked with a green line. (C) H&E staining of P3 colon and ileum. Kindlin-1^{-/-} mice show complete absence of colonic epithelium (e), exposure of the submucosa to the intestinal lumen (lu) and severe inflammation in colon and ileum. Scale bar represents 50µm. (D) Macrophage and granulocyte infiltrations in P3

colon shown with Mac-1 staining in green. T-cell infiltrates in P3 colon shown with Thy1.2 staining in green. Fibronectin (FN) is stained in red. Scale bar represents 50µm.

Figure 4. Normal duodenum and jejunum in Kindlin-1^{-/-} mice

H&E stainings of P1 (A) and P3 (B) duodenal and jejunal sections reveal a normal histology of the Kindlin-1^{-/-} small intestine. Scale bar represents 50µm.

Figure 5. Kindlin-1 localization in mouse intestine

(A) Immunofluorescence staining of Kindlin-1 in neonatal colon. Arrows indicate BM. (B) Immunofluorescence staining of P1 ileum for Kindlin-1. Arrows indicate the BM. (C) Immunofluorescence staining of P1 colon for Kindlin-2, Migfilin, F-actin (red), α6 integrin (α6-int; green) and Laminin-332 (LN332; green). (D) Immunofluorescence staining of Kindlin-2 (green) and E-cadherin (E-cad; red). All scale bars represent 10µm.

Figure 6. Progressive ulcerative colitis in Kindlin-1^{-/-} mice

(A) Normal morphology of IECs and BM at E18.5. Shown are H&E stainings of the ileum and colon and electron microscopy pictures at 12000x magnification from the colon. The boxed enlargement shows the BM, e: epithelium. Arrows point to the BM. (B) Colonic IEC (e) detachment at P0 but not in mice delivered by Caesarean section (CS) and kept unfed for 7 hours. (C) IEC detachment but no macrophage and granulocyte infiltrations at P0 (Mac-1 and GR-1 in green; perlecan indicating BM in red). Arrows indicate IEC detachment. (D) Immune cell infiltrations in the lumen of the colon and floating epithelial sheets (e) in the colonic lumen at P1. PAS staining shows reduced goblet cell mucins in Kindlin-1^{-/-} colonic epithelium. Scale bars in A, B and D represent 50µm and in C 10µm. (E) Median of Real Time PCR results from whole colon mRNA at E18.5 (n=2 per genotype) and P1 (n=5 per genotype) for TNF-α and IL-6. Error bars show range. The P value was determined using a Mann-Whitney test.

Figure 7. Normal BM composition and integrin localization in P1 colon

(A) Electron micrograph at 12000x magnification shows detachment of IECs from the BM at P1. Arrows point to the BM. The boxed enlargement shows the BM, e:

epithelium. Cryo-sections from the colon of P1 Kindlin-1^{+/+} and Kindlin-1^{-/-} mice stained for Collagen IV (ColIV), Laminin-332 (LN332) and Perlecan. The staining of them shows a normal distribution and localization in Kindlin-1^{-/-} colon. Scale bar represents 10 μ m. (B) β 1 integrin staining of P1 colon. Arrows indicate the BM. Scale bar represents 10 μ m. (C) Western blot from IECs for β 1 integrin. (D) β 1 and α v integrin FACS profile on primary IECs.

Figure 8. Kindlin-1 association with β integrins is required for talin-mediated integrin activation

(A) Kindlin-1 IECs display significantly reduced 9EG7 binding (active β 1 integrin). The 9EG7 binding was quantified by subtracting background (BG) values from mean fluorescence intensity (MFI) values and normalized to total β 1 integrin expression (n=8 mice per genotype). Error bars show standard deviations. (B) Western blot from HT-29 cells expressing a control siRNA or an siRNA directed against hKindlin-1 (siKind1). (C) Adhesion assay of control and Kindlin-1-depleted HT-29 cells on the indicated substrates (n=5). Shown are mean values, error bars show standard errors of the mean (***) p<0.001) Col IV, Collagen IV; FN, fibronectin; LN332, Laminin-332; PLL, Poly-L lysine. (D) Kindlin-1 pull-down from IEC lysates using GST-tagged cytoplasmic β integrin tails. (E) Direct interaction of Kindlin-1 with β 1 integrin cytoplasmic tails. His-tagged Kindlin-1 C-terminus was co-precipitated with GST-tagged β 1 integrin cytoplasmic tails, but not with GST alone or an Y800A mutant form of β 1 integrin. (F) Quantification of α IIb β 3 integrin activation, as measured by activation specific antibody PAC1 in CHO cells using flow cytometry (n=9). Shown are mean values, error bars show standard deviations. *, p<0.05; ***, p<0.0001 (G) Pull-down with GST-tagged cytoplasmic β 3 integrin tail from CHO cells transiently transfected with the indicated EGFP-constructs. (H) Western blot of CHO cells 24 hours after transfection with the indicated siRNAs. (I) Quantification of α IIb β 3 integrin activation in CHO cells transfected with the indicated cDNA constructs and/or siRNAs (n=8). Shown are mean values, error bars show standard deviations.

Supplementary Figure 1: Normal Triglyceride and Glucose levels in the blood of P3 Kindlin-1^{-/-} mice

Triglyceride (n=7 per genotype) and glucose (n=5 per genotype) measurement from total blood at P3 are statistically insignificant in Kindlin-1^{-/-} mice. Shown are mean values, error bars show standard deviations.

Supplementary Figure 2: Normal BM composition and deposition in P3 Kindlin-1^{-/-} backskin

P3 backskin of wild type and Kindlin-1^{-/-} mice was stained for the BM components Laminin-332 (LN332), Collagen IV (ColIV) and Fibronectin (FN; red) and co-stained with α 6 or β 4 integrin marking (green) the basal site of basal keratinocytes. The stainings reveal no differences in BM deposition and composition or α 6 and or β 4 integrin localization between control and Kindlin-1^{-/-} littermates. Scale bar indicates 30 μ m.

Supplementary Figure 3: Normal skin differentiation

P3 backskin of control and Kindlin-1^{-/-} mice was stained for epidermal differentiation markers Keratin14, Keratin10 and Loricrin (red) and co-stained with α 6 integrin (green) to mark basal keratinocytes. The stainings show no difference in the differentiation pattern of Kindlin-1^{-/-} keratinocytes. Scale bar indicates 10 μ m.

Supplementary Figure 4: Normal skin development

(A) Normal X-Gal staining in E17 Kindlin-1^{-/-} embryos indicating normal barrier formation during development. Scale bars indicate 5mm. (B) H&E staining of back skin from control and Kindlin-1^{-/-} littermates of different age. In Kindlin-1^{-/-} mice the epidermal (e) thickness at E18.5 and P0 is normal but clear epidermal atrophy is seen at P1. Scale bar indicates 50 μ m. (d): dermis.

Supplementary Figure 5: Altered adhesion and spreading by Kindlin-1^{-/-} keratinocytes

(A) Adhesion assay of control and Kindlin-1^{-/-} keratinocytes on Col IV, Collagen IV; FN, fibronectin; LN332, Laminin-332; PLL, Poly-L lysine (n=3). Shown are mean values, error bars show SEM (* p<0.05). (B) Cell area measured upon spreading on 5 μ g/ml fibronectin at the indicated time-points using MetaMorph software (n=30 cells per genotype from 3 independent experiments). Shown are mean values, error bars show SD (***) p<0.0001)

Supplementary Figure 6: Normal IEC proliferation but detachment induced apoptosis

P1 colons from wild type and Kindlin-1^{-/-} mice were DAB stained for cleaved Caspases-3 to determine apoptosis and Ki67 for proliferating IECs. Apoptosis occurs in detached epithelium of Kindlin-1^{-/-} mice. In areas of still adhering epithelium the number of proliferating IECs is similar between wild type and Kindlin-1^{-/-} mice. Scale bar indicates 50µm.

Supplementary Figure 7: β1 integrin activation in Kindlin-1^{-/-} keratinocytes

(A) Immunofluorescence staining for β1 integrin (green) and Laminin-332 (red) from P3 backskin shows normal localization of β1 integrin in Kindlin-1^{-/-} backskin. (B) Representative β1 integrin FACS profile of freshly isolated control (blue) and Kindlin-1^{-/-} keratinocytes (red) shows unaltered β1 integrin expression on basal keratinocytes. (C) 9EG7 FACS of freshly isolated P2 keratinocytes shows no significant reduction in β1 integrin activation (n=4).

Supplementary Figure 8: Shear induced detachment of Kindlin-1 depleted HT-29 cells

Control and Kindlin-1 depleted HT-29 (siKind1) cells were plated on fibronectin-coated flow chamber slides and exposed to increasing shear forces as indicated in the Figure. Control cells did not detach from the matrix while Kindlin-1 depleted cells were unable to resist even low shear rates. Scale bar indicates 50µm.

Figure 1 Ussar et al.

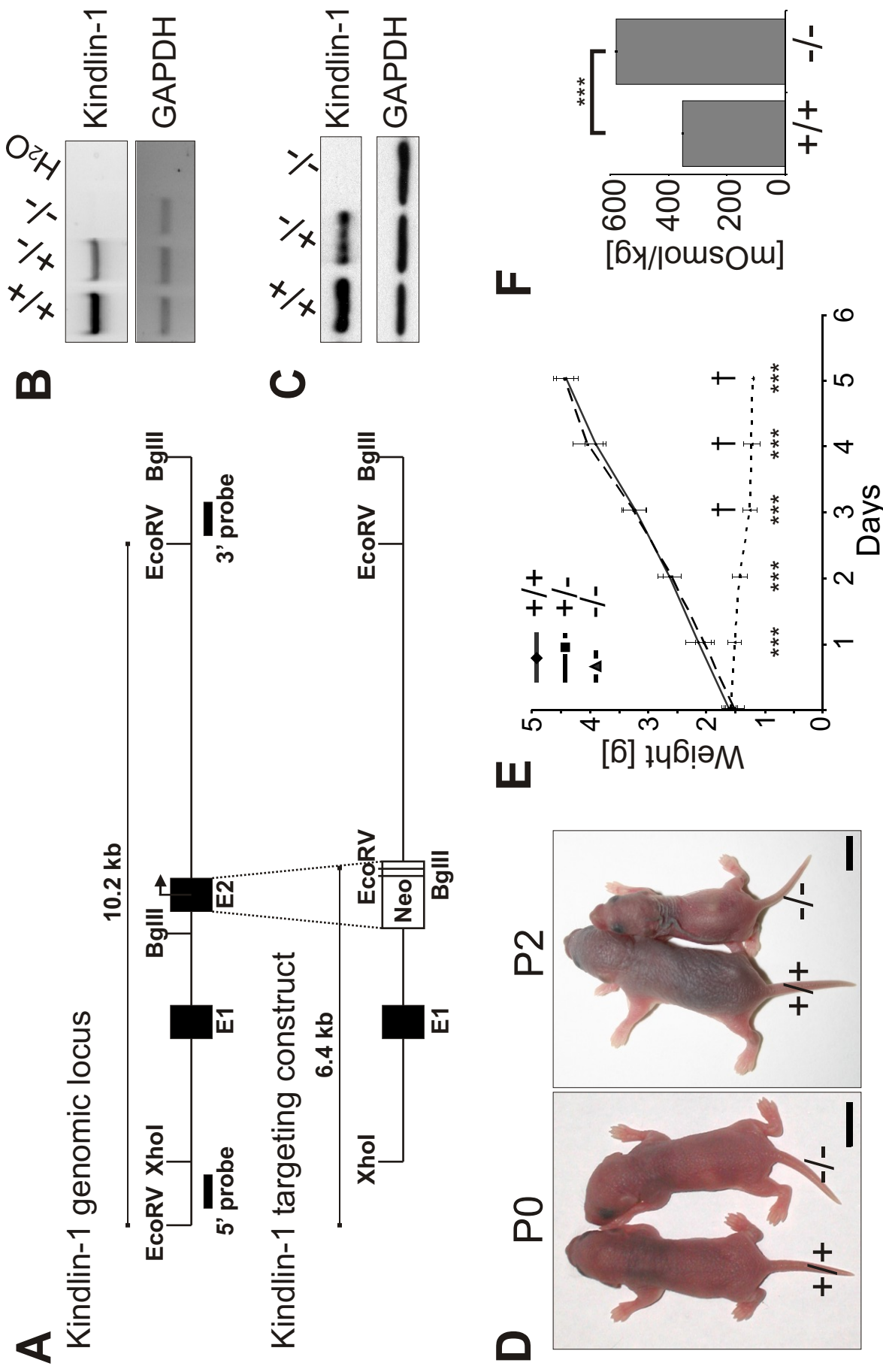


Figure 2 Ussar et al.

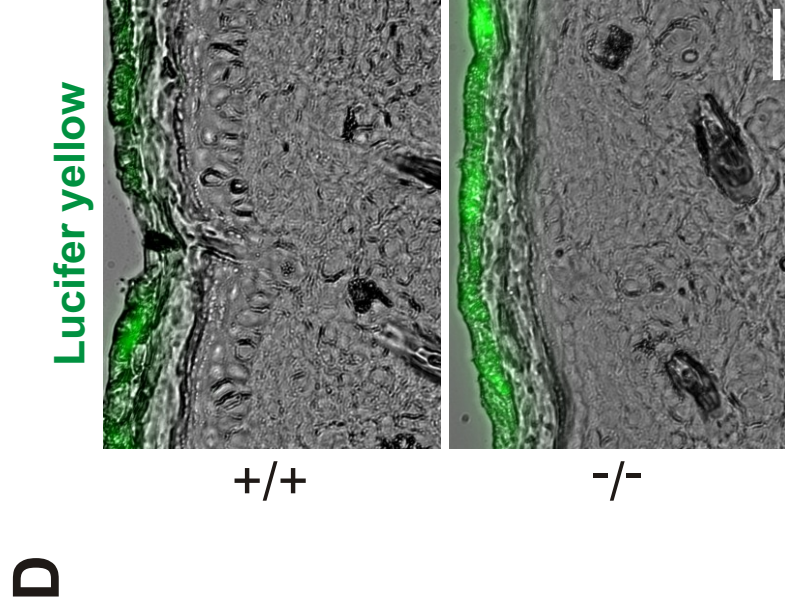
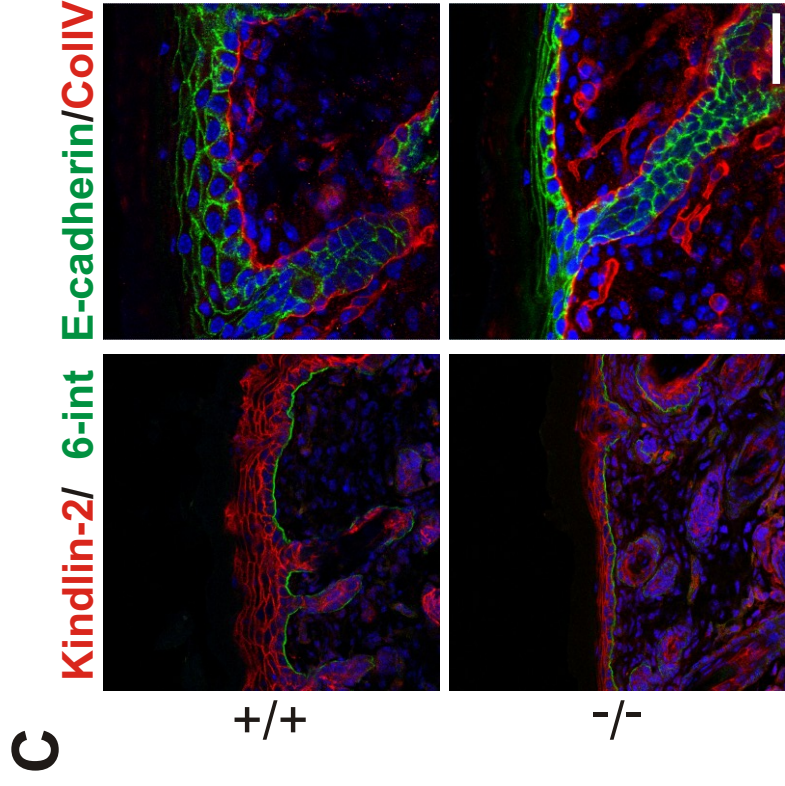
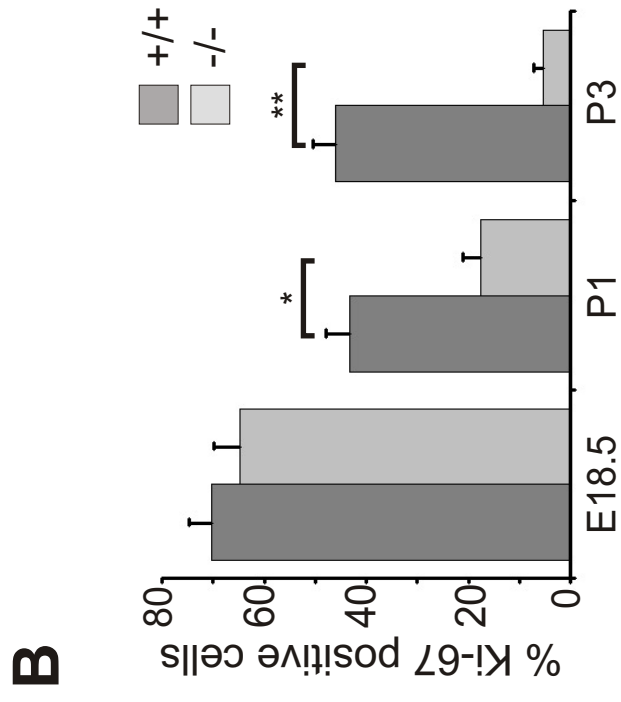
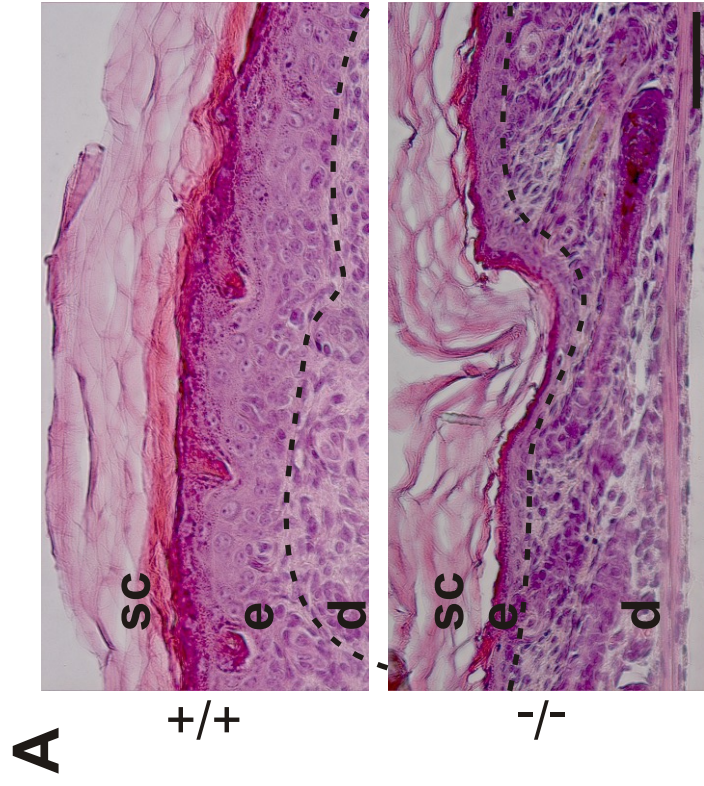


Figure 3 Ussar et al.

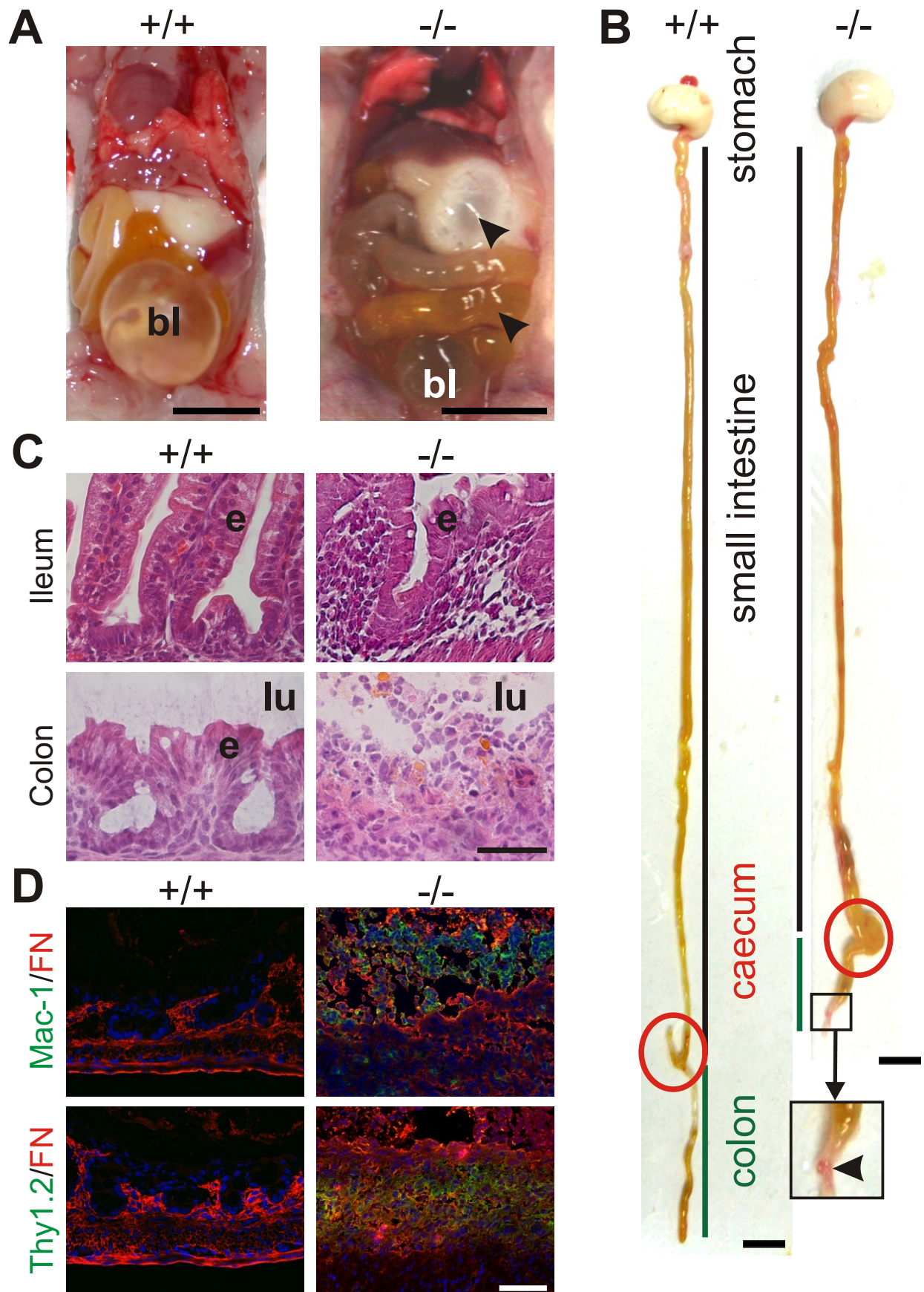


Figure 4 Ussar et al.

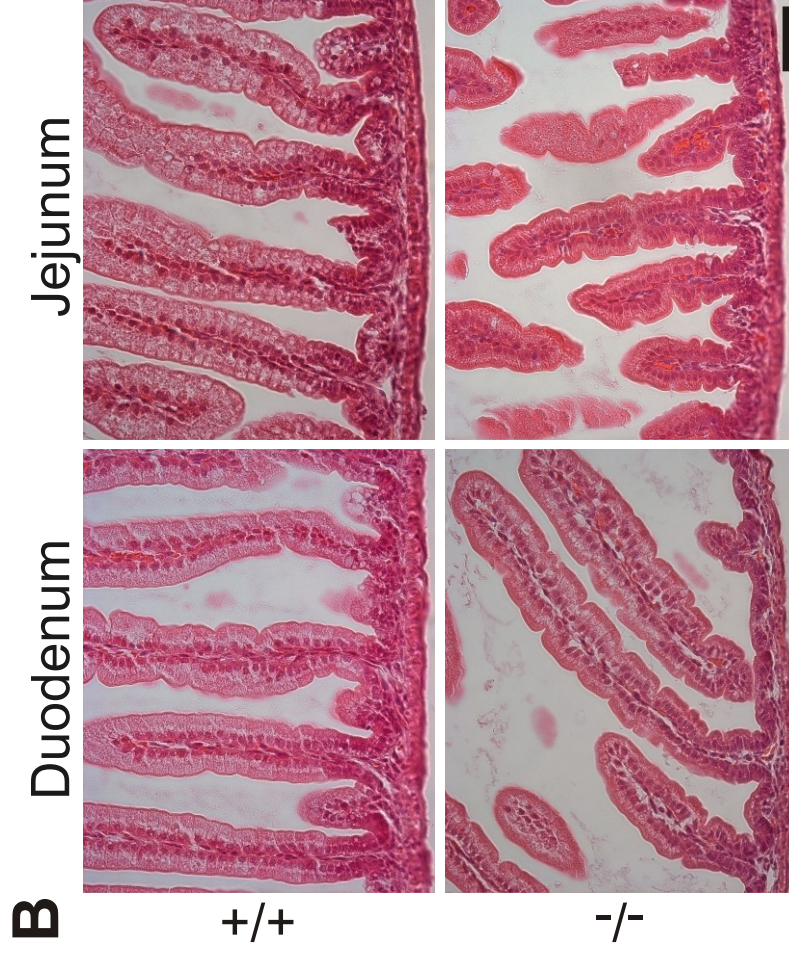
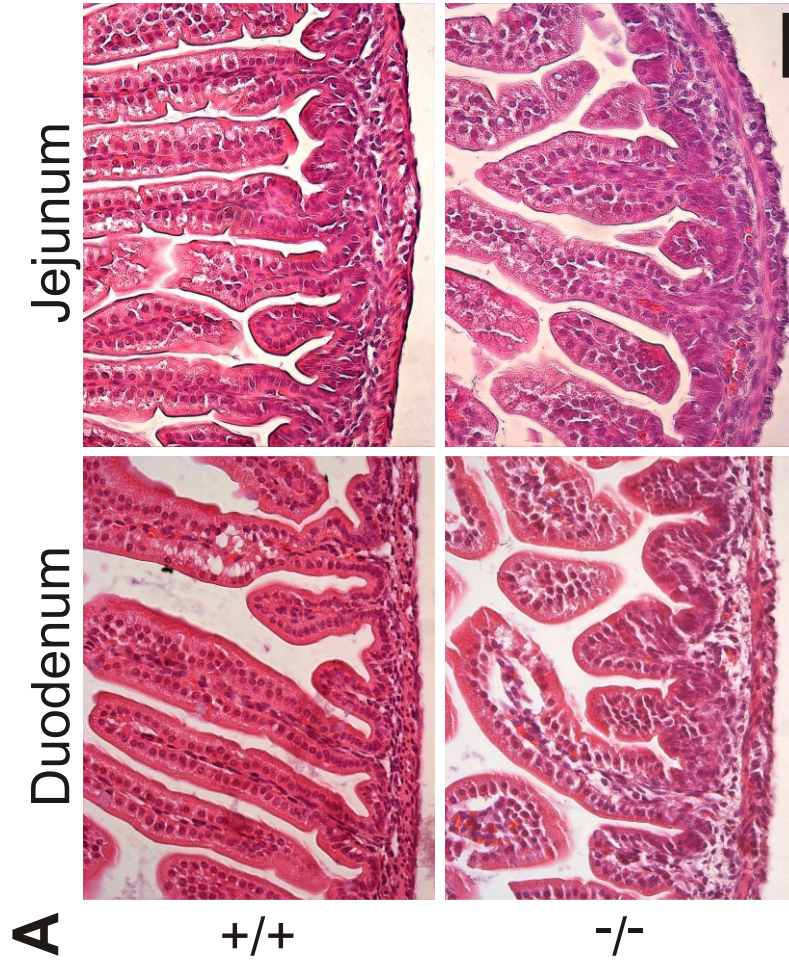


Figure 5 Ussar et al.

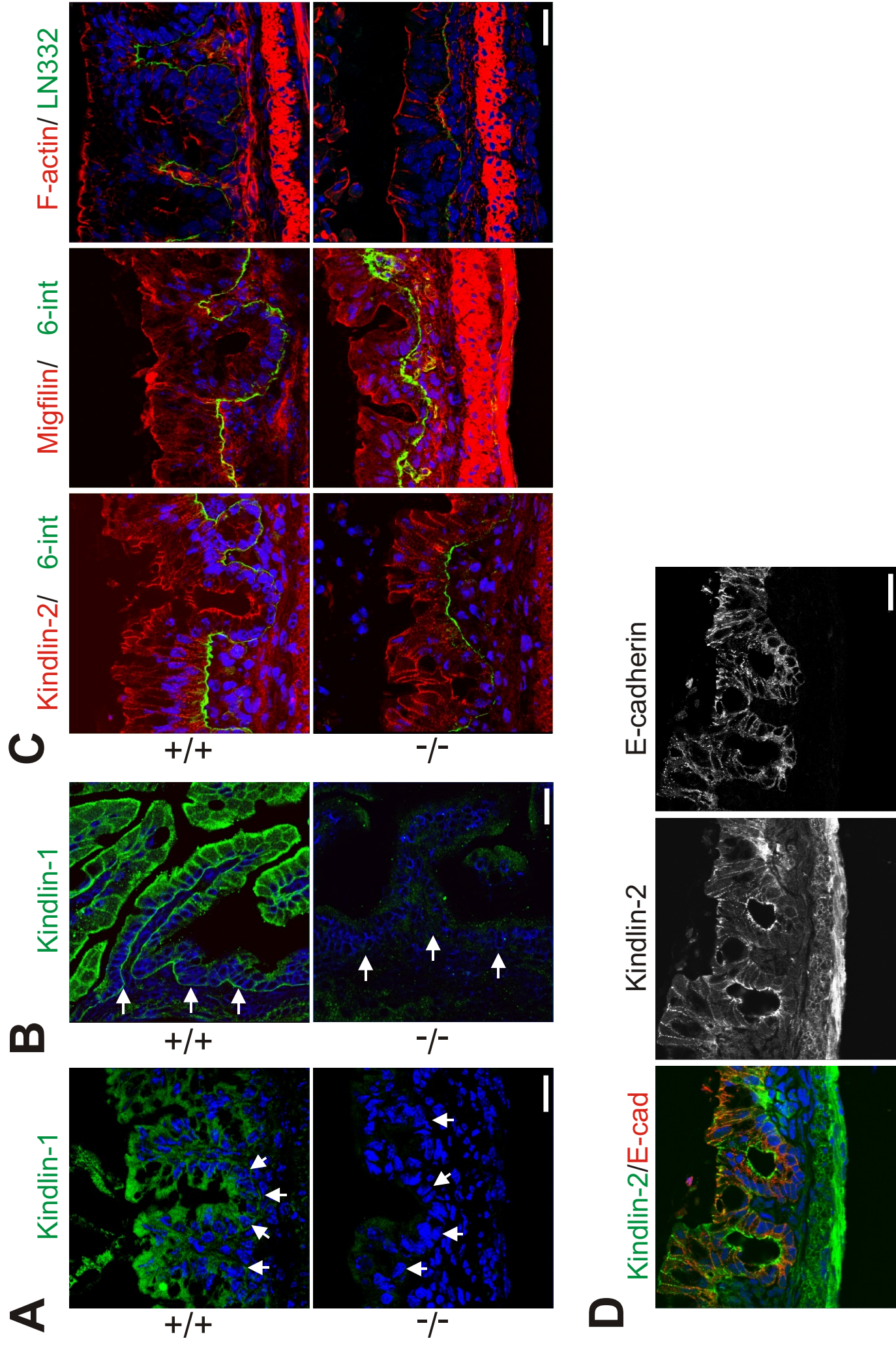


Figure 6 Ussar et al.

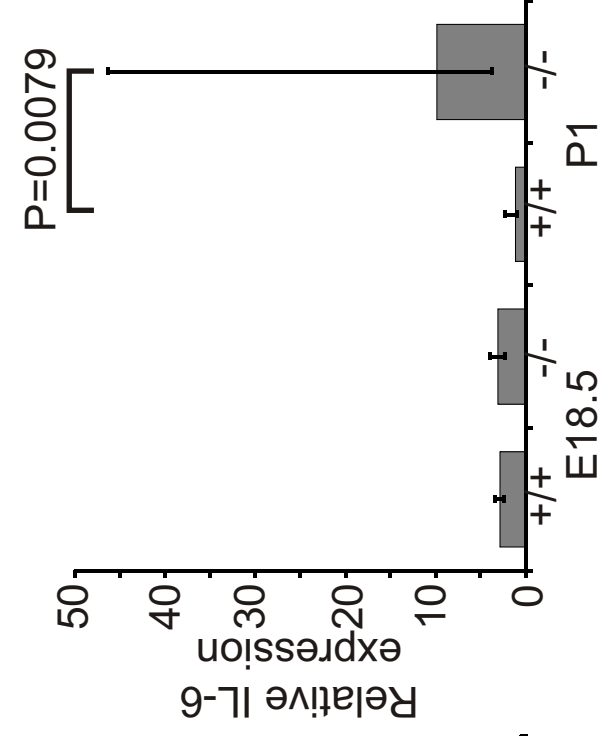
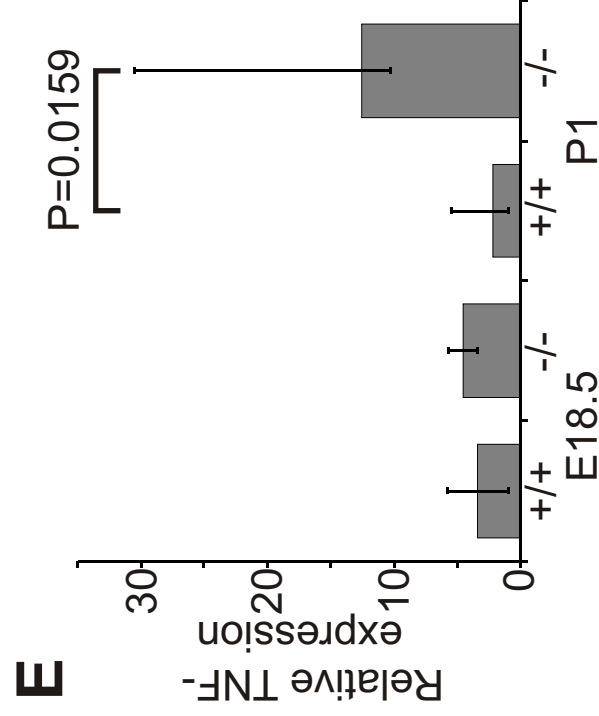
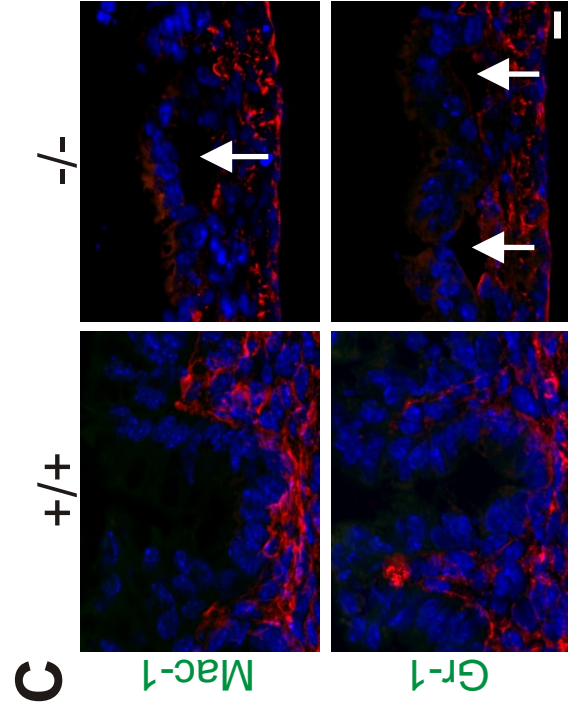
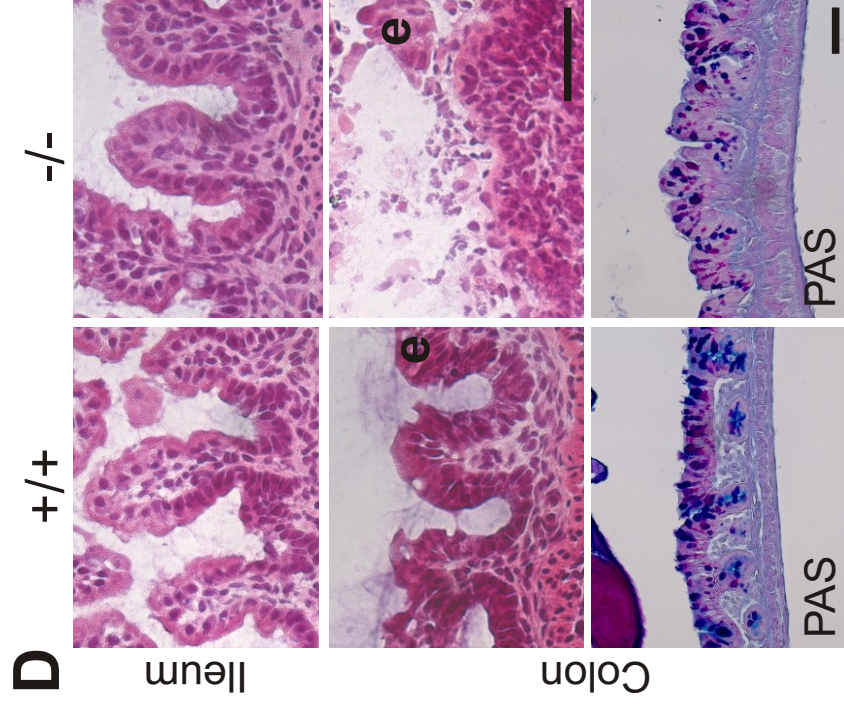
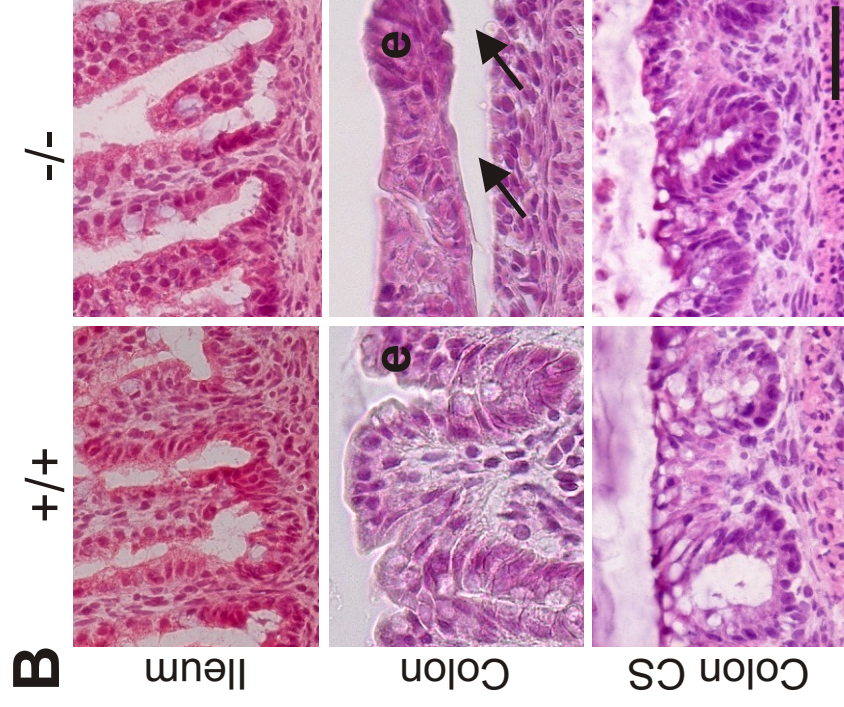
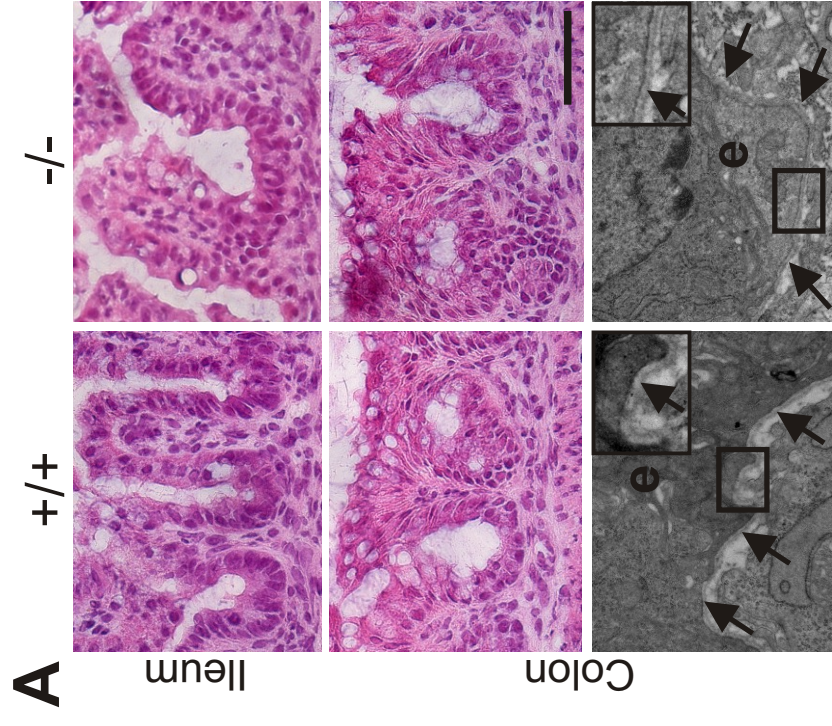


Figure 7 Ussar et al.

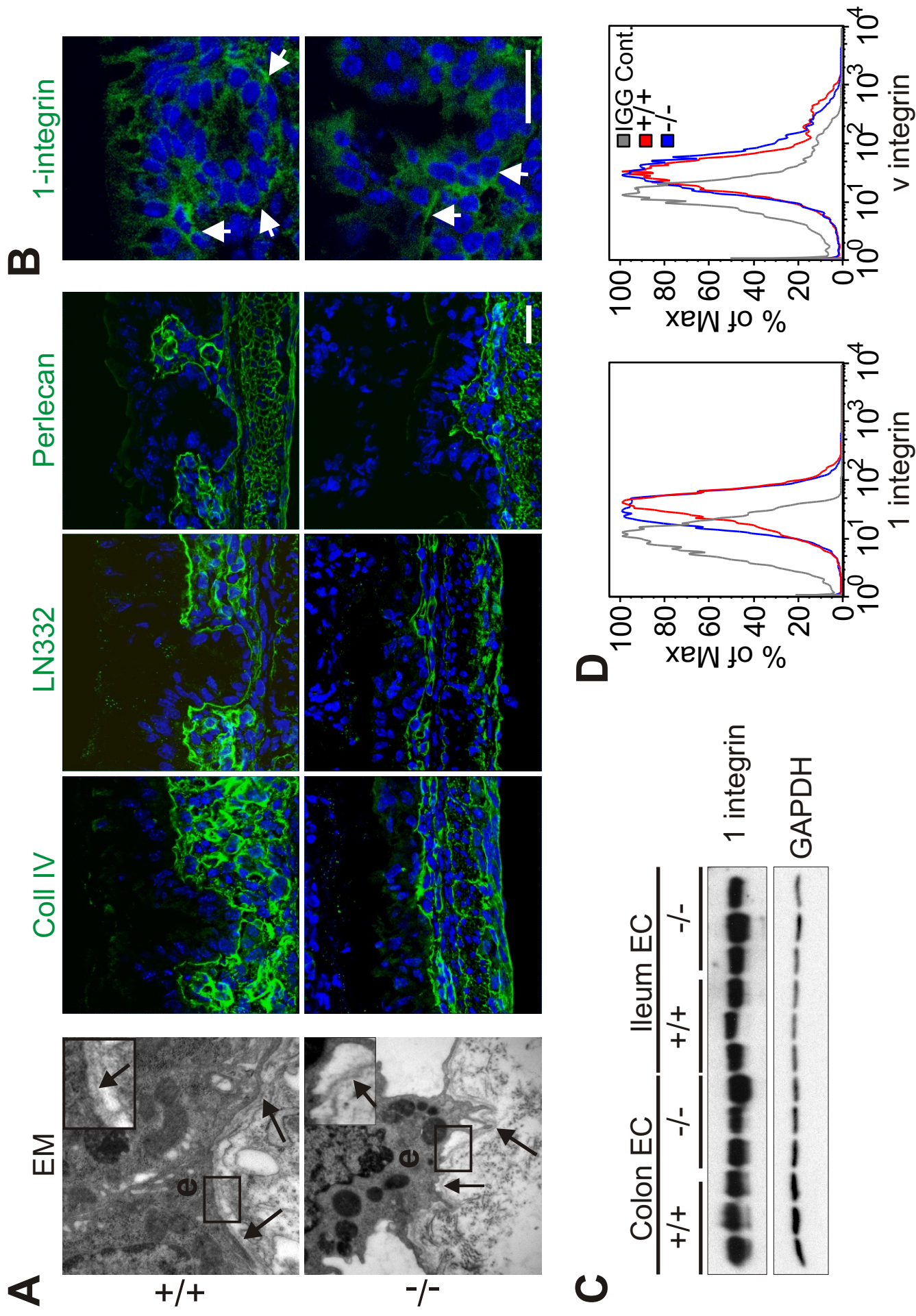
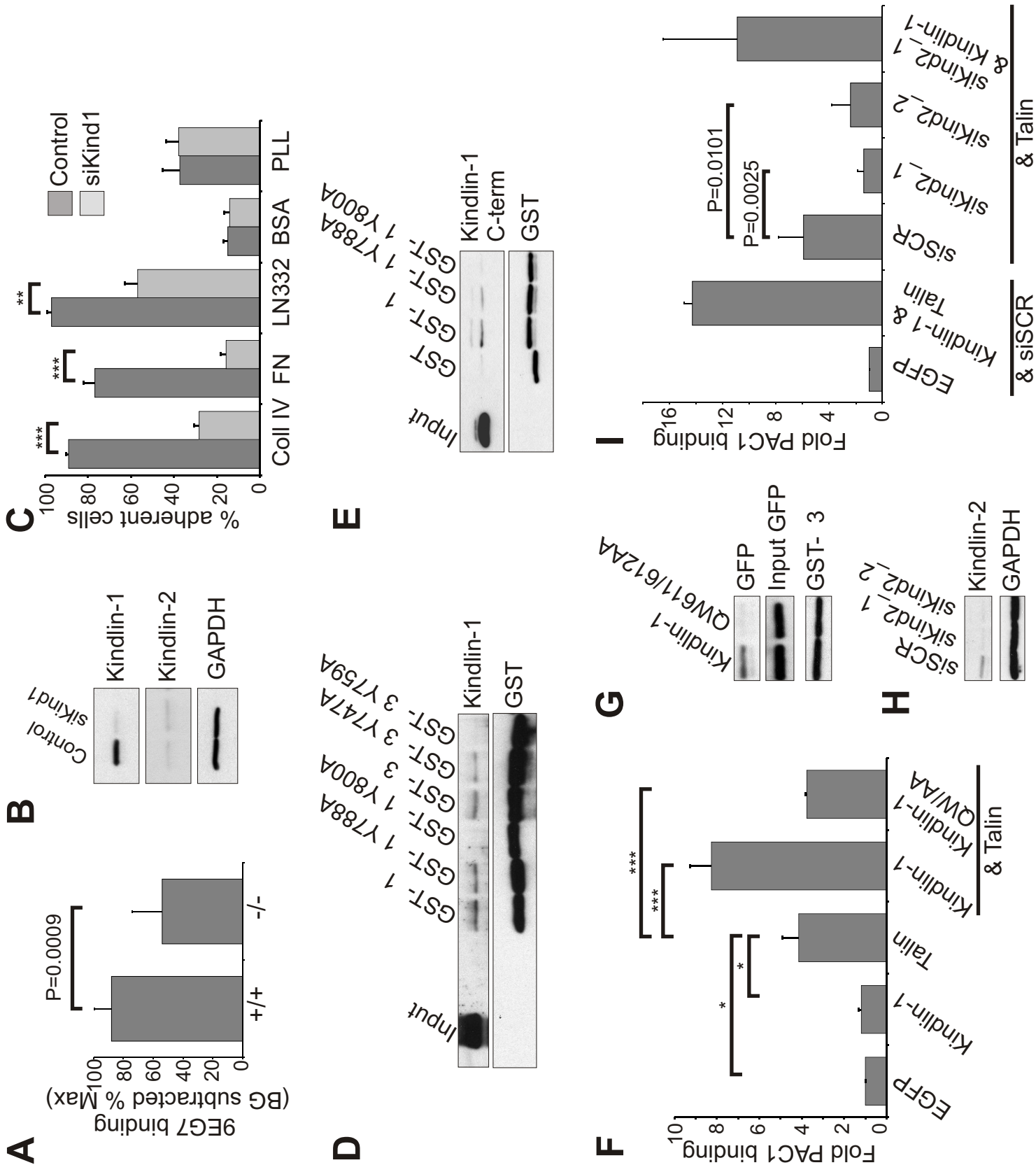
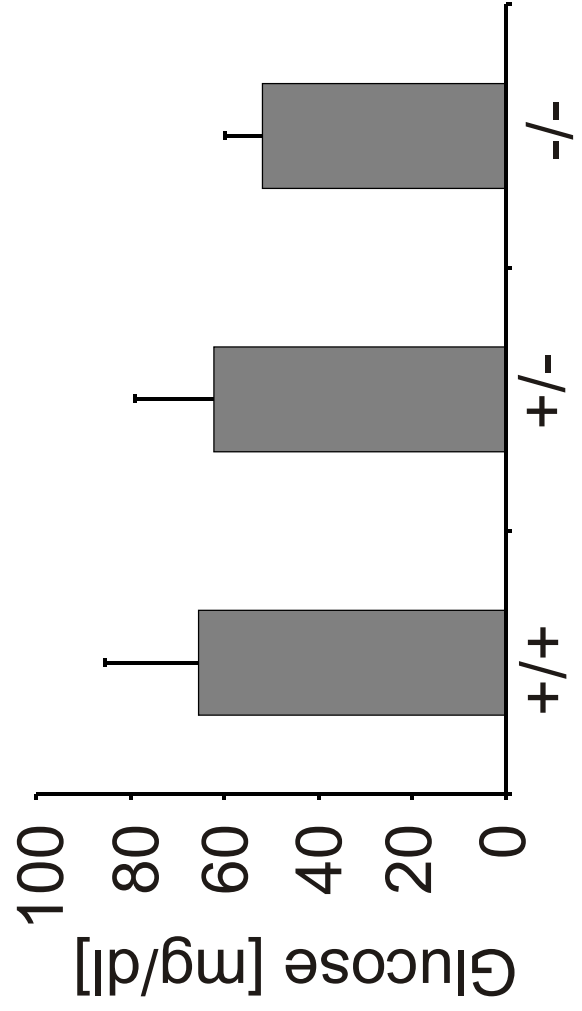
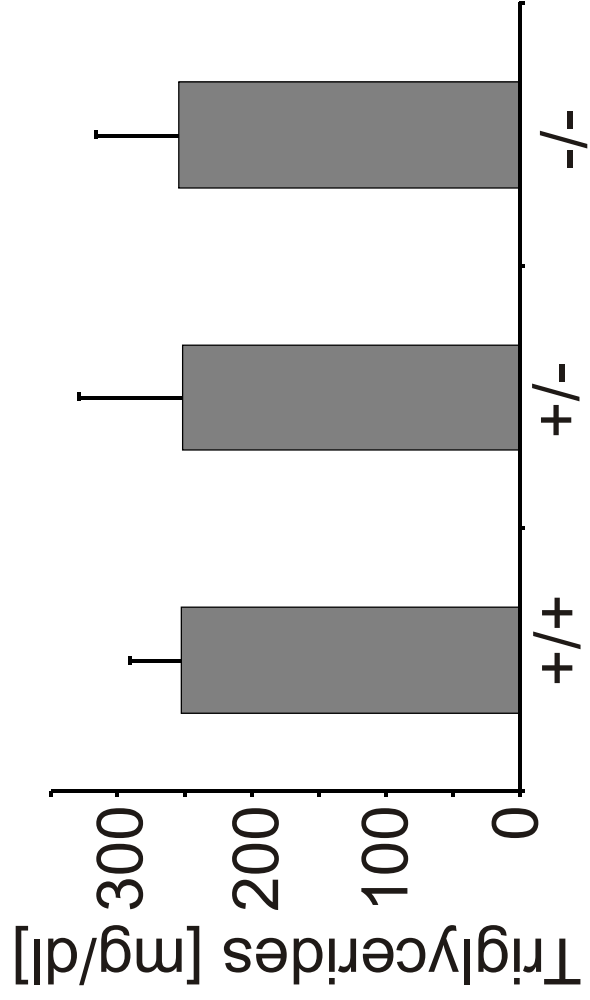


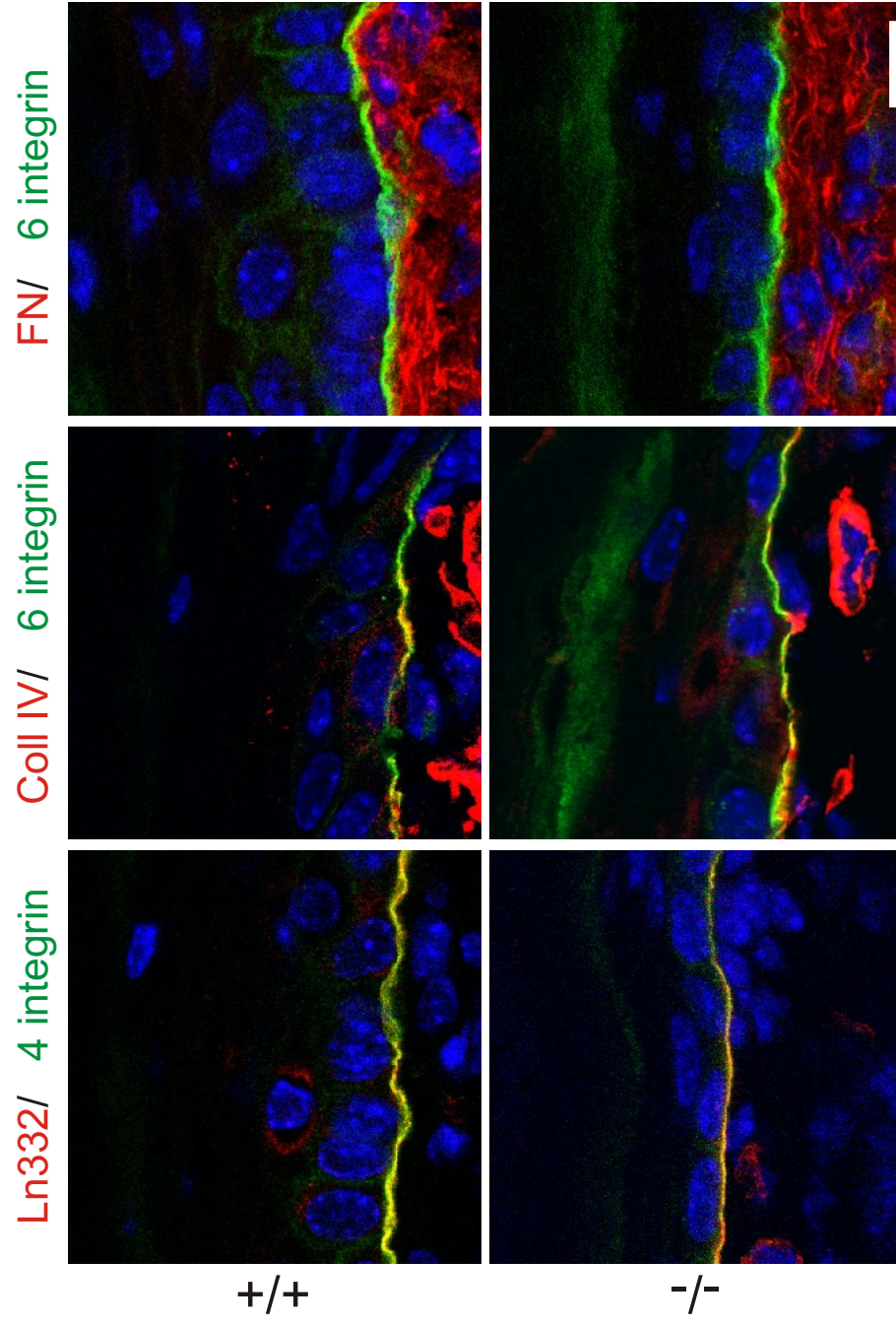
Figure 8 Ussar et al.



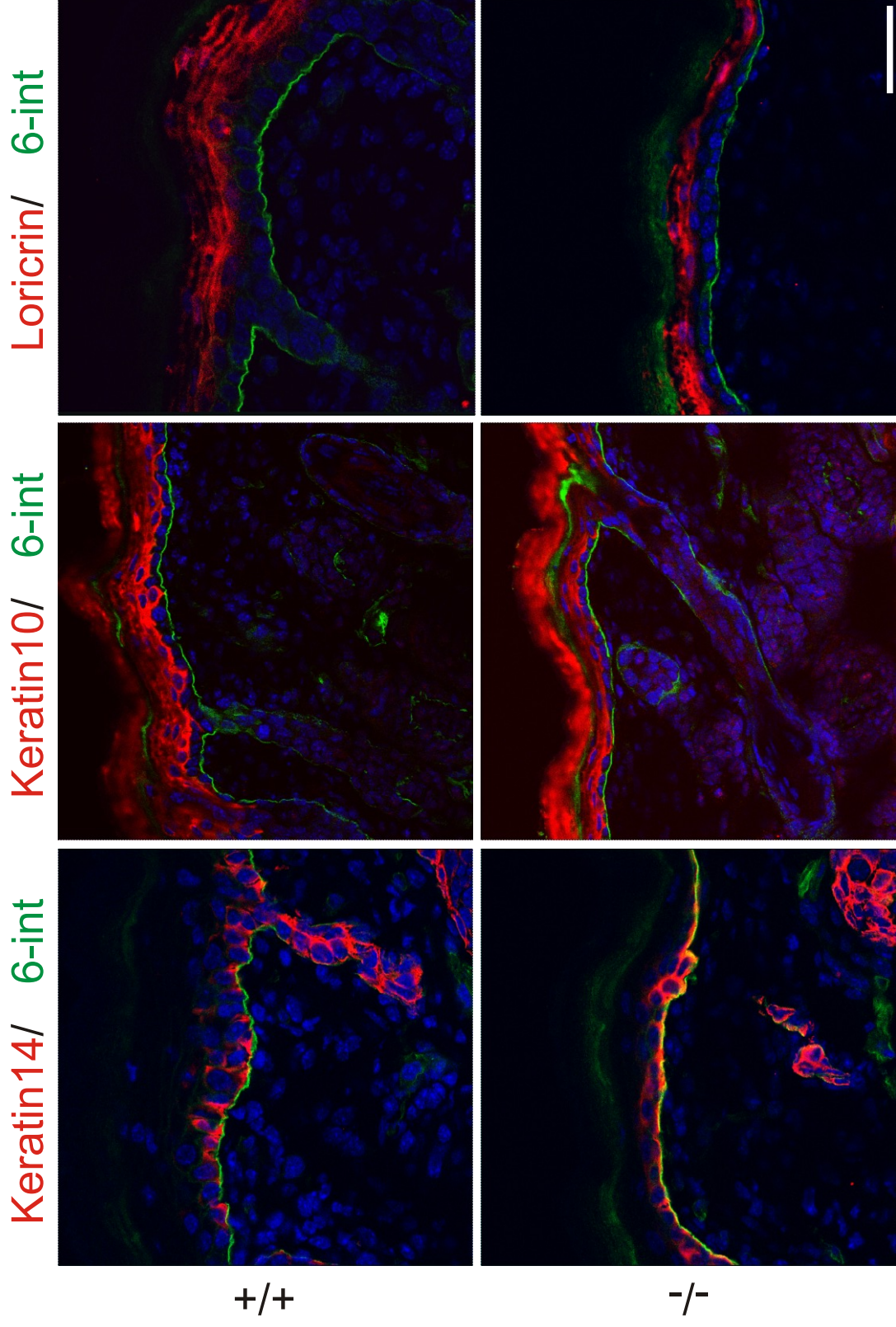
Supplementary Figure 1



Supplementary Figure 2

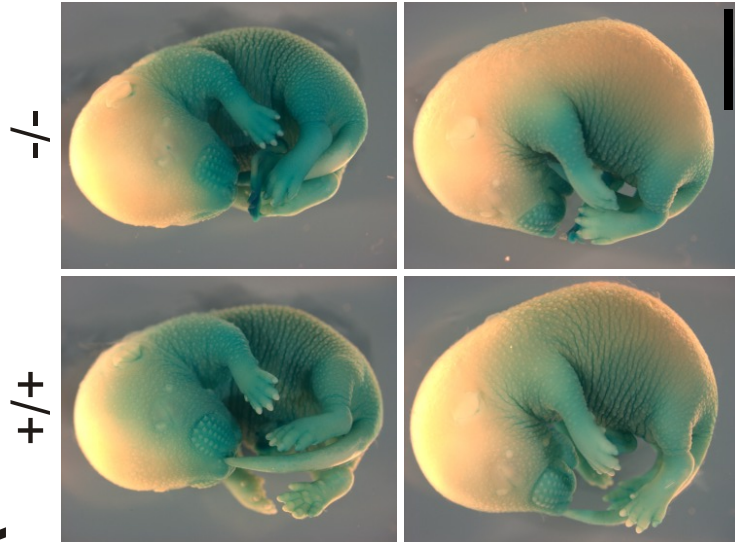


Supplementary Figure 3

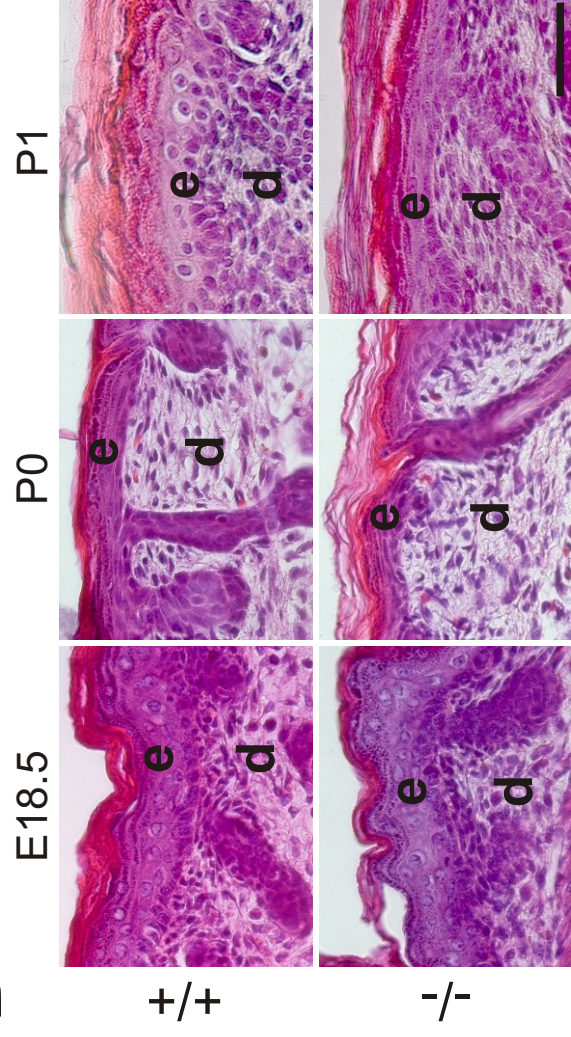


Supplementary Figure 4

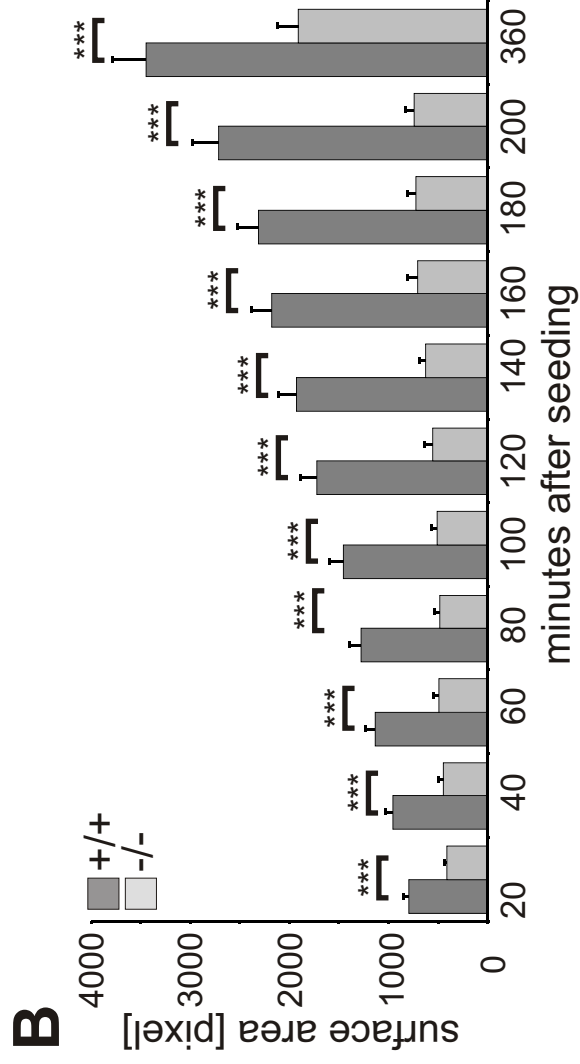
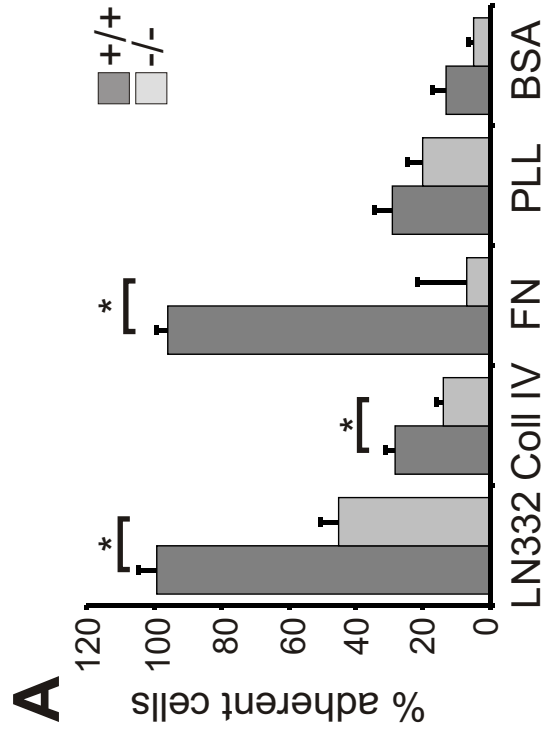
A



B

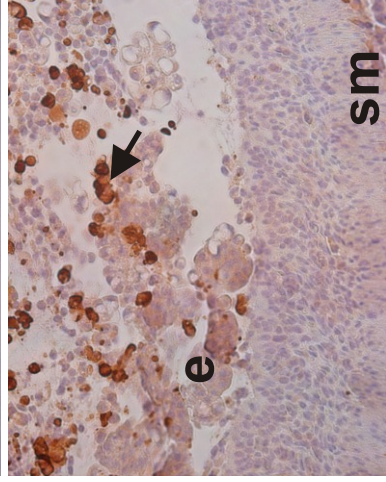
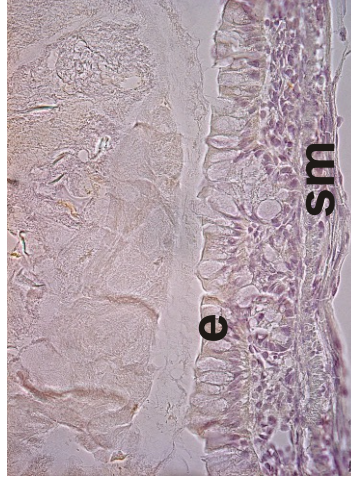
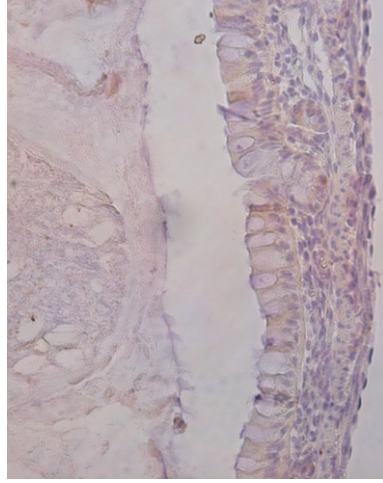


Supplementary Figure 5

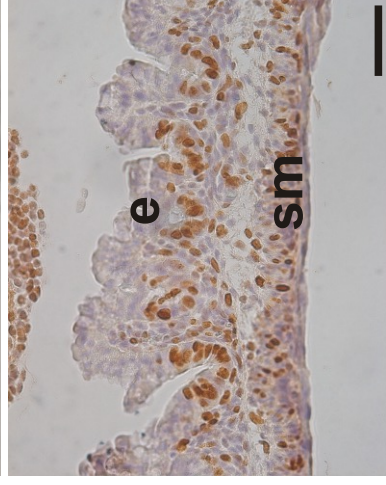
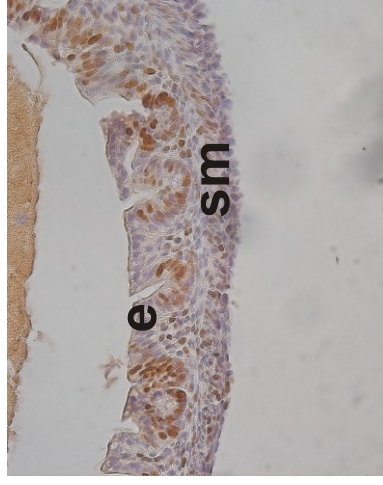


Supplementary Figure 6

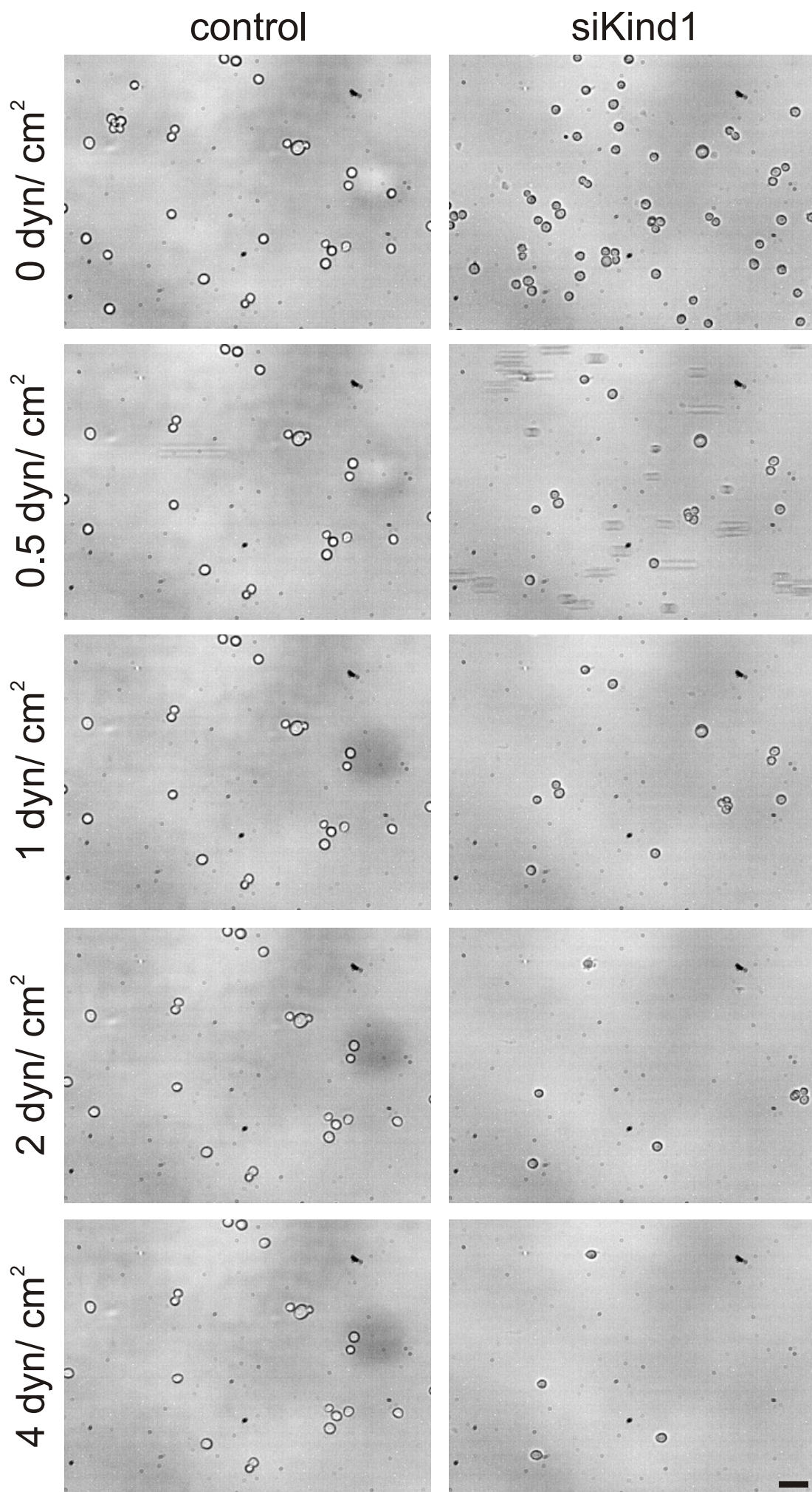
cleaved Caspase 3



Ki67



Supplementary Figure 8



Paper VIII

Colocalization of Kindlin-1, Kindlin-2, and Migfilin at Keratinocyte Focal Adhesion and Relevance to the Pathophysiology of Kindler Syndrome

JE Lai-Cheong^{1,2}, S Ussar³, K Arita¹, IR Hart² and JA McGrath¹

Kindler syndrome (KS) results from pathogenic loss-of-function mutations in the *KIND1* gene, which encodes kindlin-1, a focal adhesion and actin cytoskeleton-related protein. How and why abnormalities in kindlin-1 disrupt keratinocyte cell biology in KS, however, is not yet known. In this study, we identified two previously unreported binding proteins of kindlin-1: kindlin-2 and migfilin. Co-immunoprecipitation and confocal microscopy studies show that these three proteins bind to each other and colocalize at focal adhesion in HaCaT cells and normal human keratinocytes. Moreover, loss-of-function mutations in *KIND1* result in marked variability in kindlin-1 immunolabeling in KS skin, which is mirrored by similar changes in kindlin-2 and migfilin immunoreactivity. Kindlin-1, however, may function independently of kindlin-2 and migfilin, as loss of kindlin-1 expression in HaCaT keratinocytes by RNA interference and in KS keratinocytes does not affect *KIND2* or *FBLIM1* (migfilin) gene expression or kindlin-2 and migfilin protein localization. In addition to identifying protein-binding partners for kindlin-1, this study also highlights that *KIND1* gene expression and kindlin-1 protein labeling are not always reduced in KS, findings that are relevant to the accurate laboratory diagnosis of this genodermatosis by skin immunohistochemistry.

Journal of Investigative Dermatology advance online publication, 5 June 2008; doi:10.1038/jid.2008.58

INTRODUCTION

Kindler syndrome (KS; OMIM173650) is a rare autosomal recessive genodermatosis characterized by blistering in trauma-prone sites, photosensitivity, poikiloderma, and mucosal erosions and strictures (Kindler, 1954). The gene responsible for KS, *KIND1*, was identified in 2003 (Jobard *et al.*, 2003; Siegel *et al.*, 2003) and, to date, 32 different pathogenic *KIND1* mutations have been documented (see Lai-Cheong *et al.*, 2007 for mutation summary and Arita *et al.*, 2007; Mansur *et al.*, 2007 for additional recent mutations). The *KIND1* gene encodes a 677 amino-acid protein, kindlin-1, which is expressed mainly in basal keratinocytes, colon, kidney, and placenta (Siegel *et al.*, 2003). Kindlin-1 has been shown to associate with vinculin in the epithelial cell line PtK2 transiently transfected with EGFP-kindlin-1 and, to some extent, with filamentous actin (Siegel *et al.*, 2003). Kindlin-1 forms complexes with β 1- and

β 3-integrin cytoplasmic tails (Kloeker *et al.*, 2004), and a reduction in kindlin-1 expression by RNA interference (RNAi) in HaCaT cells results in decreased cell spreading (Kloeker *et al.*, 2004).

Kindlin-1 forms part of a family of kindlin proteins that includes two other members: kindlin-2 and kindlin-3 (Siegel *et al.*, 2003). Kindlin-2 (also known as mitogen inducible gene-2; Mig2) associates with actin stress fibers and thus is a component of cell-extracellular matrix adhesion structures (Tu *et al.*, 2003). RNAi studies, resulting in the knockdown of kindlin-2 expression in HeLa cells, have shown that kindlin-2 is required for the control of cell spreading, probably via integrin-linked kinase (Tu *et al.*, 2003). Kindlin-2 has also been demonstrated to associate with and recruit migfilin at cell-matrix adhesions (Tu *et al.*, 2003). Kindlin-3 is expressed in pulmonary and hematopoietic tissues but, thus far, has no known binding partners (Ussar *et al.*, 2006). Migfilin is a novel LIM-containing protein that localizes to cell-matrix adhesions and associates with actin via its N-terminal domain while interacting with kindlin-2 through its C-terminal domain (Tu *et al.*, 2003). Like kindlin-2, migfilin is critical for the control of cell shape (Tu *et al.*, 2003) and has been shown to bind to filamin and vasodilator-stimulated phosphoprotein (Zhang *et al.*, 2006).

In this study, we have identified two key binding partners of kindlin-1, namely kindlin-2 and migfilin, and demonstrate both their tissue and cellular distribution. Furthermore, we have shown that not every patient with KS with pathogenic

¹Genetic Skin Disease Group, St John's Institute of Dermatology, Division of Genetics and Molecular Medicine, King's College London, London, UK;

²Tumour Biology Centre, Institute of Cancer, Bart's and The London School of Medicine and Dentistry, London, UK and ³Max-Planck Institute of Biochemistry, Martinsried, Germany

Correspondence: Dr John McGrath, Genetic Skin Disease Group, St John's Institute of Dermatology, 9th Floor Tower Wing, Guy's Hospital, London SE1 9RT, UK. E-mail: john.mcgrath@kcl.ac.uk

Abbreviations: KS, Kindler syndrome; NHK, normal human keratinocytes; RNAi, RNA interference; siRNA, small interfering RNA

Received 18 July 2007; revised 2 January 2008; accepted 27 January 2008

KIND1 mutations has reduced immunolabeling for kindlin-1, with some individuals having normal levels of kindlin-1 expression and yet suffering from KS. These observations provide further insight into the role of kindlin-1 in pathophysiology of KS.

RESULTS

Clinical features of KS patients

The clinical features of the 13 patients with KS assessed in this study are summarized in Table 1. All these individuals have previously determined loss-of-function mutations on both *KIND1* alleles.

Immunoblotting reveals expression of kindlin-1, kindlin-2, and migfilin in HaCaT cells, normal human keratinocytes (NHK), and KS keratinocytes

Western blotting showed that kindlin-1, kindlin-2, and migfilin were expressed in both HaCaT cells, a spontaneously immortalized human keratinocyte cell line (Boukamp *et al.*,

1988), and in NHK. Discrete bands of ~77 kDa were noted for both kindlin-1 (Figure 1a, lanes H and NHK) and kindlin-2 (Figure 1b, lanes H and NHK) and an ~50 kDa band was detected for migfilin (Figure 1c, lanes H and NHK) in HaCaT and NHK lysates. Additionally, in HaCaT lysate, there was an ~74 kDa band that may correspond to the dephosphorylated form of the kindlin-1 protein (Herz *et al.*, 2006). In KS keratinocyte lysate, there was loss of the ~77 kDa band, a finding that confirmed the specificity of this kindlin-1 protein band (Figure 1a, lane KS). In the same KS lysate, however, a different ~65 kDa protein band was observed. Although the nature of this band is currently unknown, it may correspond to a truncated or alternatively spliced form of the protein.

Co-immunoprecipitation studies identify kindlin-1, kindlin-2, and migfilin as potential biochemical partners

We focused on kindlin-2 and migfilin as potential kindlin-1-binding partners, as they have previously been shown to be components of cell-matrix adhesions as well as being

Table 1. Summary of ethnicity, clinical features, *KIND1* mutations, and skin immunostaining patterns for anti-kindlin-1, anti-kindlin-2, and anti-migfilin antibodies in 13 patients with KS

Patient	<i>KIND1</i> mutations	Blistering	Skin atrophy	Poikiloderma	Photosensitivity	Gingival inflammation	Urethral stenosis	Immunolabeling			Reference
								Kindlin-1	Kindlin-2	Migfilin	
Indian	p.C468X/ p.C468X	Y	Y	Y	Y	Y	Y	±	++	–	Sethuraman <i>et al.</i> , 2005
Indian	p.E516X/ p.E516X	Y	Y	Y	N	Y	N	±	++	–	Lai-Cheong <i>et al.</i> , 2007
Omani	p.R271X/ p.R271X	Y	Y	Y	Y	N	Y	+	+	–	Siegel <i>et al.</i> , 2003
Omani	p.W616X/ p.W616X	Y	Y	Y	Y	N	Y	+	+	+	Ashton <i>et al.</i> , 2004
Omani	p.W616X/ p.W616X	Y	Y	Y	Y	N	Y	+	++	+	Ashton <i>et al.</i> , 2004
Brazilian	c.676insC/ c.676insC	Y	Y	Y	Y	Y	Y	+	++	±	Martignago <i>et al.</i> , 2007
US Caucasian	p.R271X/ c.1755delT	Y	Y	Y	NK	Y	Y	+	++	–	Siegel <i>et al.</i> , 2003
US Caucasian	p.E304X/ c.1188insT	Y	Y	Y	Y	NK	Y	+++	+++	+++	Ashton <i>et al.</i> , 2004
US Caucasian	p.E304X/ c.1161delA	Y	Y	Y	Y	Y	Y	+++	++	++	Ashton <i>et al.</i> , 2004
UK Caucasian	p.E304X/ c.1909delA	Y	Y	Y	N	Y	Y	++	+++	+++	Ashton <i>et al.</i> , 2004
UK Caucasian	p.R288X/ p.R288X	Y	Y	Y	Y	NK	Y	+++	+++	+++	Siegel <i>et al.</i> , 2003
UK Caucasian	p.E304X/ p.L302X	Y	Y	Y	N	Y	N	+++	+++	+++	Ashton <i>et al.</i> , 2004
Italian	IVS7-1G>A/ IVS7-1G>A	Y	Y	Y	Y	Y	Y	+++	+++	+++	Ashton <i>et al.</i> , 2004
NHS	WT/WT	N	N	N	N	N	N	+++	+++	+++	

N, no; NK, not known; NHS, normal human skin; Y, yes; WT, wild type. ++++, bright immunostaining; ++, slight reduction in immunoreactivity; +, marked reduction in immunostaining; ±, barely detectable immunolabeling; –, complete absence of labeling.

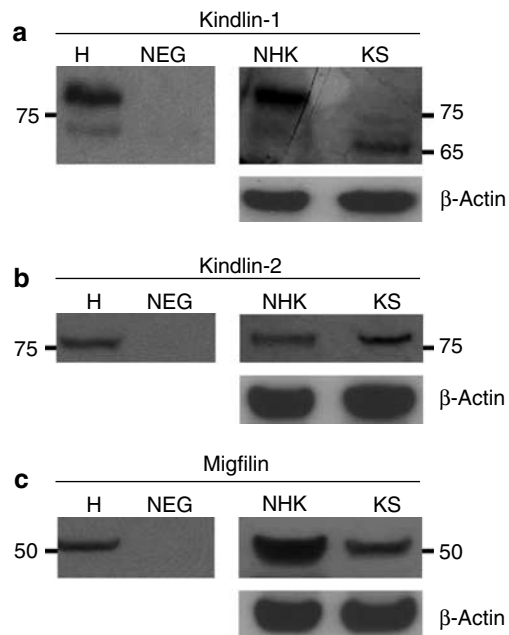


Figure 1. Immunoblotting shows different expression patterns of kindlin-1 (but not kindlin-2 or migfilin) in KS or control keratinocytes. Immunoblotting shows (a) ~77 and ~74 kDa protein bands matching the molecular weight of kindlin-1 and its dephosphorylated form in HaCaT cell lysate (lane H). The same ~77 kDa band was present in lane NHK but absent in lane KS. In addition, an ~65 kDa band was seen in lane KS. (b) In lanes H, NHK, and KS, an ~77 kDa band corresponding to the molecular weight of kindlin-2 was seen. (c) An ~50 kDa band that equates to the expected molecular weight of migfilin was observed in lanes H, NHK, and KS. H, HaCaT cell lysate; NEG, negative control; NHK, normal human keratinocytes; KS, Kindler syndrome.

biochemically related to each other (Tu *et al.*, 2003; Wu 2005). To determine whether these three proteins are biochemical partners, co-immunoprecipitation was performed on HaCaT cell lysates, which were precipitated separately with anti-kindlin-1, anti-kindlin-2, and anti-migfilin antibodies. When anti-kindlin-1 antibody was used to probe the blot, an ~77 kDa band was detected not only for kindlin-1 but also for kindlin-2 and migfilin (Figure 2a). Similar patterns of reactivity were observed when anti-kindlin-2 antibody was used to probe the blot (Figure 2b). In both blots, there were protein bands at ~50 and ~25 kDa corresponding to the molecular weight of heavy- and light-chain immunoglobulins, respectively. Western blotting of the same immunoprecipitates using a rabbit polyclonal anti-collagen VII antibody as an irrelevant antibody control showed the absence of protein bands at ~77 kDa but the continued presence of bands corresponding to the heavy- and light-chain immunoglobulins, respectively (Figure 2c).

Confocal microscopy studies show that kindlin-1, kindlin-2, and migfilin colocalize at focal contacts in NHK and HaCaT cells

To determine whether kindlin-1 colocalizes with its two biochemical partners, confocal microscopy studies were performed on NHK individually labeled with anti-kindlin-1, anti-kindlin-2, or anti-migfilin antibody. Focal adhesions were revealed by double-staining the cells with anti-vinculin

antibody. In NHK, kindlin-1 showed diffuse cytoplasmic expression and punctate nuclear localization and colocalized with vinculin (Figure 3a). In addition, kindlin-2 and migfilin were expressed in the cytoplasm as well as at focal adhesions (Figures 3b and c). The independent colocalization of kindlin-1, kindlin-2, and migfilin with vinculin suggests that all three proteins may colocalize with each other. To assess this, confocal microscopy imaging was performed on HaCaT cells co-transfected with EGFP-kindlin-1 (Figure 4a) and FLAG-migfilin (Figure 4b) and then immunostained with anti-kindlin-2 antibody (Figure 4c). The merged image showed that the three proteins colocalized at focal adhesions (Figure 4d).

Confocal microscopy studies on primary KS keratinocytes show loss of kindlin-1 expression at focal adhesions but presence of kindlin-2 and migfilin

To explore the pathophysiological role of kindlin-1 and its two potential binding partners in KS, confocal microscopy analysis was performed on primary KS keratinocytes (harboring compound heterozygous *KIND1* mutations, p.E304X/p.L302X) immunolabeled separately with anti-kindlin-1, anti-kindlin-2, and anti-migfilin antibodies. In these KS keratinocytes, kindlin-1 no longer colocalized with vinculin at focal adhesions despite cytoplasmic expression being present. However, nuclear localization of kindlin-1 was still present in these cells (Figure 3d). In contrast, kindlin-2 and migfilin still colocalized with vinculin at focal adhesion (Figures 3e and f).

Knockdown of kindlin-1 by RNAi does not alter expression of kindlin-2 or migfilin in HaCaT cells

To understand the consequences of loss of kindlin-1 expression on kindlin-2 and migfilin, an RNAi study was performed in HaCaT cells using kindlin-1 (k) and scrambled control (s) small interfering RNAs (siRNAs) at a concentration of 100 nM. A gradual reduction in kindlin-1 expression was observed from day 2 post-transfection to almost complete knockdown at day 8 (Figure 5a). However, the reduction of kindlin-1 did not alter the expression of kindlin-2 (Figure 5b). An increase in migfilin expression was noted from day 6 post-transfection in both the scrambled and kindlin-1-transfected HaCaT cells, as well as in the oligofectamine-transfected cells (Figure 5c). This was confirmed by optical densitometry analysis using ImageJ software (<http://rsb.info.nih.gov/ij/>), which showed up to a fourfold increase in migfilin compared with day 2 transfected cells (data not shown). The increase in migfilin expression occurred in both the scrambled control and kindlin-1-transfected cells, suggesting therefore that it is not a consequence of kindlin-1 knockdown.

Kindlin-2 and migfilin localization is unchanged following kindlin-1 siRNA transfection of HaCaT keratinocytes

Confocal microscopy studies performed on kindlin-1 siRNA-treated HaCaT keratinocytes showed loss of kindlin-1 localization at focal adhesions (Figure 6a, arrows). However, diffuse cytoplasmic staining of kindlin-1 was still seen. In contrast, kindlin-2 and migfilin still colocalized at focal adhesions (Figures 6b and c). In the scrambled control siRNA-treated

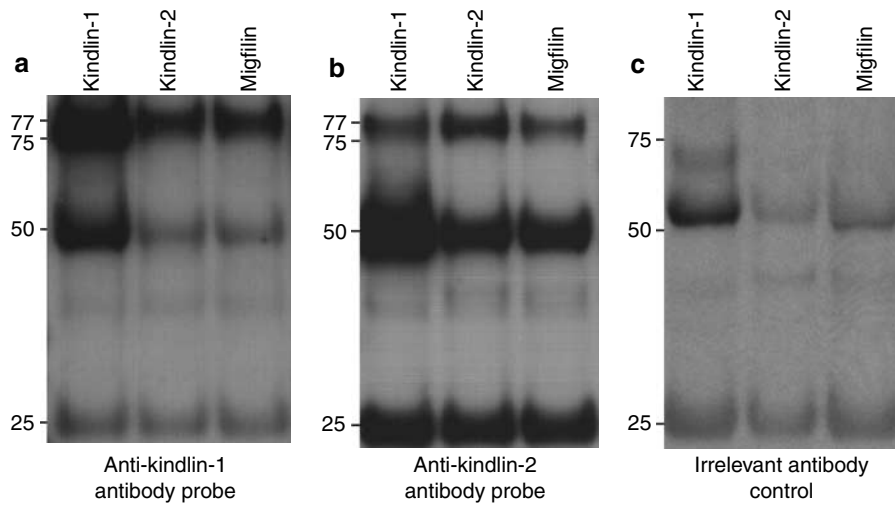


Figure 2. Co-immunoprecipitation studies show that kindlin-1, kindlin-2, and migfilin can bind to each other. (a) Western blotting on the immunoprecipitates using anti-kindlin-1 antibody shows ~77 kDa bands in all three lanes, indicating that kindlin-1 forms a complex with kindlin-2 and migfilin. (b) Similarly, western blotting using anti-kindlin-2 antibody reveals ~77 kDa bands in all three lanes, indicating that kindlin-2 associates with kindlin-1 and migfilin. (c) Immunoblotting performed using rabbit polyclonal anti-collagen VII IgG antibody as irrelevant antibody control shows absence of the ~77 kDa protein band but persistence of the ~50 and ~25 kDa bands.

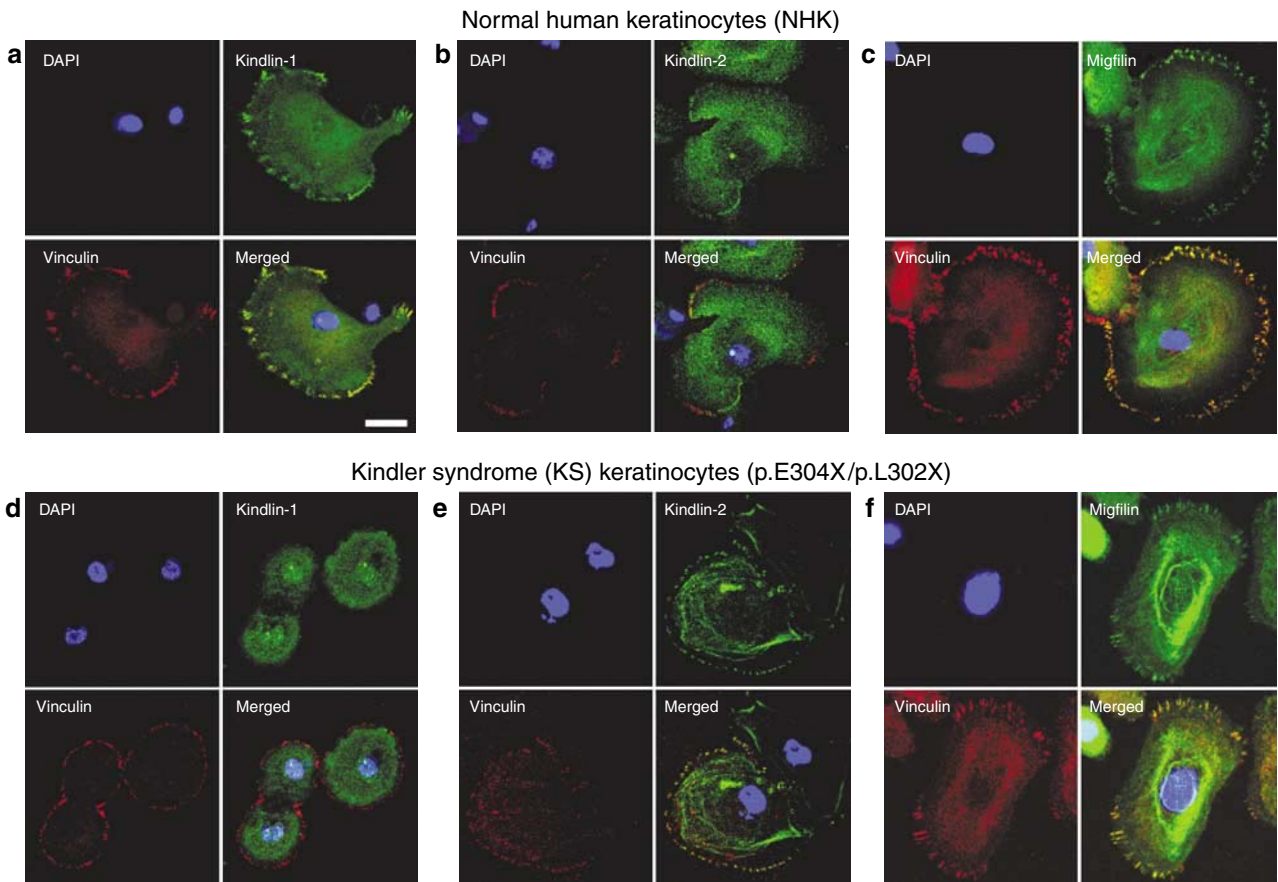


Figure 3. Confocal microscopy studies show different kindlin-1 localization but preserved kindlin-2 and migfilin localization in NHK and KS keratinocytes, respectively. (a) In NHK, kindlin-1 was expressed both in the cytoplasm and near the cell periphery and colocalized with vinculin at focal adhesions. Similarly, both (b) kindlin-2 and (c) migfilin showed cytoplasmic and peripheral distribution and colocalized with vinculin. (d) In KS keratinocytes, there was cytoplasmic localization of kindlin-1 but kindlin-1 expression at focal adhesions was absent, as evidenced by the lack of colocalization with vinculin. In contrast, (e) kindlin-2 and (f) migfilin subcellular localization was not affected. Bar = 20 μm.

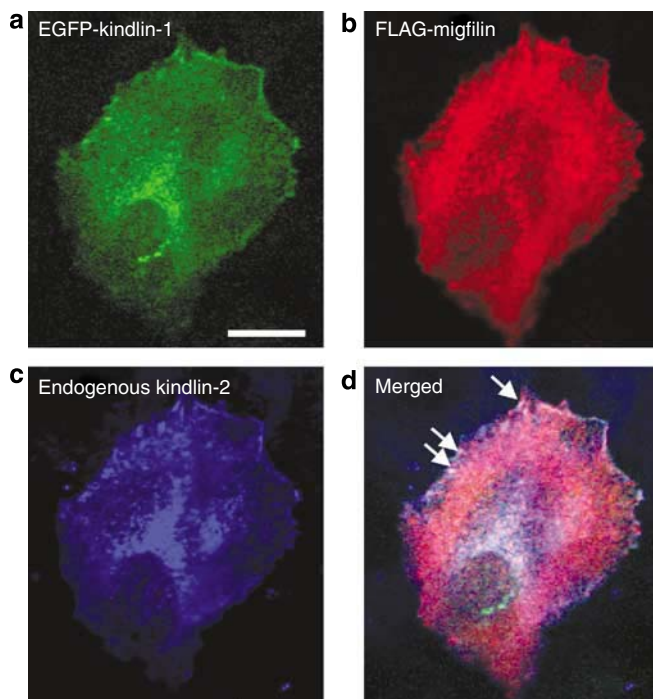


Figure 4. Confocal microscopy shows that kindlin-1, kindlin-2, and migfilin all colocalize at focal adhesions. (a) Kindlin-1 localizes to the ends of actin stress fibers and also demonstrates a perinuclear distribution. (b) Migfilin is distributed both in the cytoplasm and at the cell periphery. (c) Endogenous kindlin-2 also localizes to the ends of actin stress fibers. (d) Merged confocal image shows colocalization of kindlin-1, kindlin-2, and migfilin at focal adhesions as shown by the white staining at the cell periphery (arrows). Bar = 20 μ m.

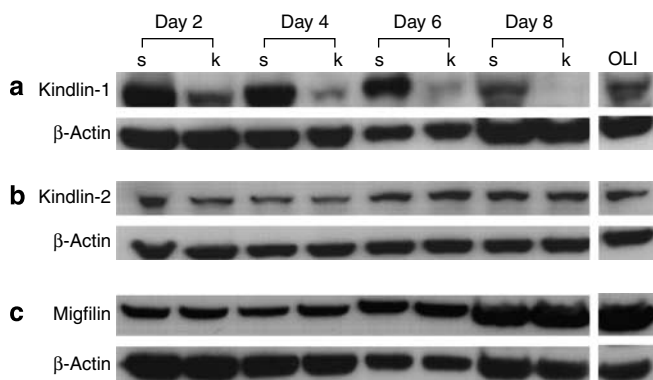


Figure 5. Kindlin-2 and migfilin expression is not altered after RNAi-mediated knockdown of kindlin-1 in HaCaT cells. (a) Gradual reduction of kindlin-1 expression was noted from day 2 post-transfection. (b) Expression of kindlin-2 does not seem to be altered by kindlin-1 knockdown. (c) However, there was an increase in migfilin expression from day 6 post-transfection in the scrambled control and kindlin-1-transfected HaCaT cells. Oligoectamine-only (OLI)-treated HaCaT keratinocytes lysate was used as control and showed no reduction in kindlin-1 expression. In contrast, no reduction in kindlin-1 expression was seen when the cells were treated with scrambled siRNA.

cells, colocalization of kindlin-1, kindlin-2, and migfilin with vinculin at focal adhesions was still present, with no change in the protein distribution or appearances of focal adhesions (Figures 6d–f).

Immunofluorescence microscopy shows highly variable kindlin-1 immunostaining in KS patients with pathogenic *KIND1* mutations

To determine the tissue distribution of kindlin-1, immunofluorescence microscopy labeling was performed in both normal and KS frozen skin sections. In normal skin sections immunolabeled with anti-kindlin-1 antibody, there was bright staining near the cell periphery in the basal keratinocytes (arrows) as well as less intense labeling throughout the epidermis (Figure 7a). Frozen skin sections from 13 patients with KS with pathogenic *KIND1* mutations were immunolabeled for kindlin-1. A surprising finding was that not every patient showed reduced or absent anti-kindlin-1 immunostaining. In fact, kindlin-1 labeling was markedly reduced in seven patients (Figure 7b) and was normal or only slightly reduced in six patients with KS (Figure 7c). The immunofluorescence microscopy data are summarized in Table 1.

Immunolabeling for kindlin-2 and migfilin in KS skin mirrors the variable kindlin-1 immunostaining patterns

Immunostaining with anti-kindlin-2 antibody on frozen normal skin sections showed pan-epidermal membranous labeling but with no staining along the lower pole of basal keratinocytes in contact with the basement membrane (Figure 7d). Anti-migfilin antibody labeling on frozen normal skin sections showed basal epidermal staining near the cell periphery with sparing of the rest of the epidermis (Figure 7g). Of note, there was a reduction of immunolabeling for kindlin-2 (Figure 7e) and also migfilin (Figure 7h) in the seven patients with KS with reduced anti-kindlin-1 labeling. However, in the six patients in whom kindlin-1 labeling was normal or slightly reduced, kindlin-2 and migfilin immunostaining was of normal or near-normal intensity (Figures 7f and i). Table 1 provides a summary of the immunolabeling data.

Semi-quantitative reverse transcriptase PCR (RT-PCR) shows variable reduction in *KIND1* mRNA expression but normal *KIND2* and *FBLIM1* (migfilin) mRNA levels

To begin to understand why some patients with KS have reduced or almost normal anti-kindlin-1 immunostaining patterns, we assessed *KIND1* mRNA expression in four patients with KS, all of whom had pathogenic *KIND1* mutations determined in their genomic DNA. RT-PCR was performed using cDNA synthesized from skin samples from three patients with reduced or absent anti-kindlin-1 immunolabeling and one patient with near-normal immunostaining, respectively. The three patients harboring the following homozygous nonsense mutations p.E516X/p.E516X, p.W616X/p.W616X, and p.R271X/p.R271X all had reduced anti-kindlin-1 immunolabeling and were found to have correspondingly decreased expression of full-length *KIND1* mRNA (Figure 8a, lanes 4–6). The reduction in *KIND1* mRNA in these cases is consistent with nonsense-mediated RNA decay (Nagy and Maquat, 1998; Frischmeyer and Dietz, 1999; Holbrook *et al.*, 2004; Maquat 2004), notwithstanding that the mutation p.W616X occurs close to the 3' end of the penultimate *KIND1* exon (exon 14). Whole skin cDNA was

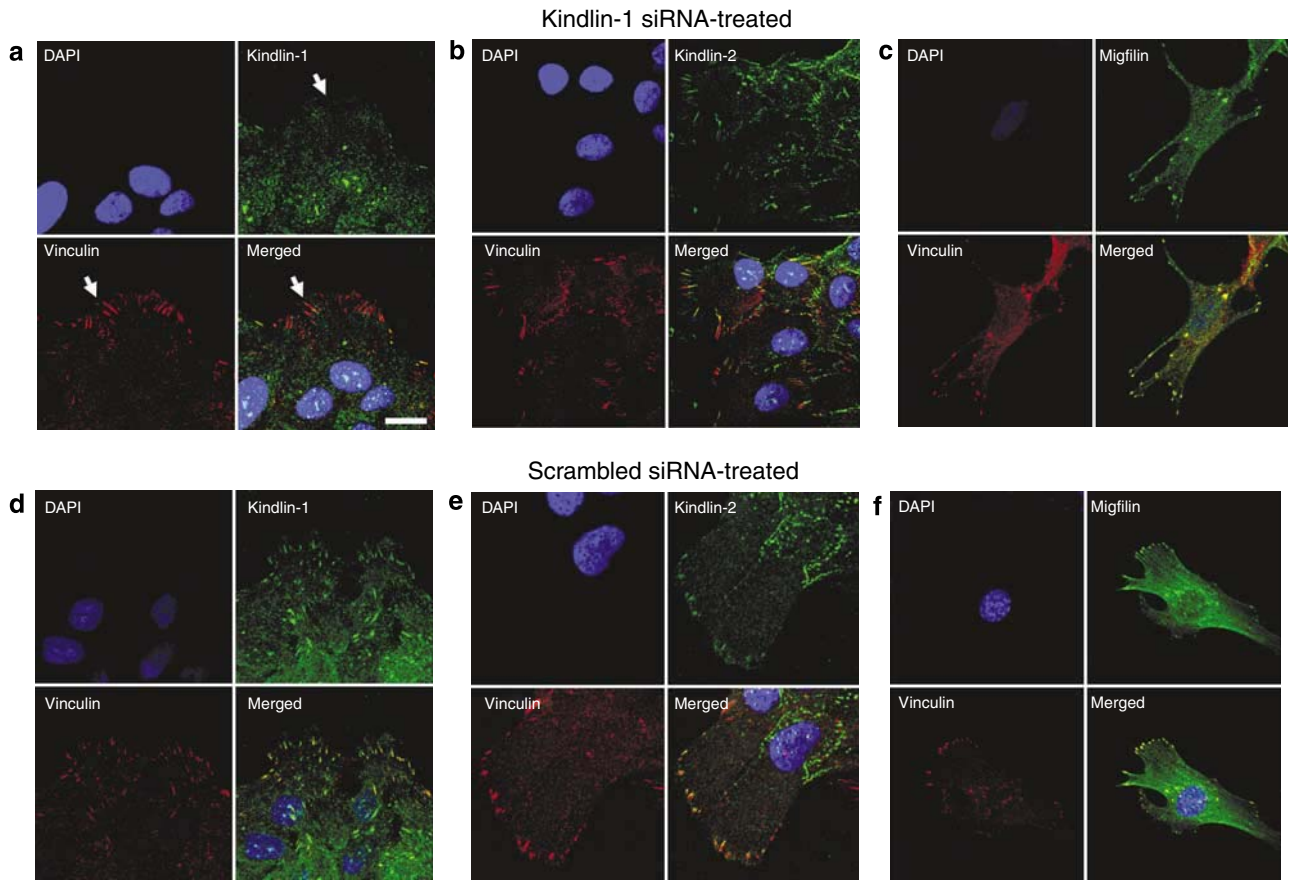


Figure 6. Kindlin-2 and migfilin localization remains unchanged in kindlin-1 siRNA-transfected HaCaT keratinocytes. (a) In HaCaT keratinocytes transfected with kindlin-1 siRNA, there was no localization of kindlin-1 at focal adhesions (arrows). However, (b) kindlin-2 and (c) migfilin still colocalized with vinculin at focal adhesions. In contrast, in the scrambled control-transfected HaCaT cells, there was no change in (d) kindlin-1, (e) kindlin-2, and (f) migfilin subcellular localization. Bar = 20 μ m.

available only from one patient with normal kindlin-1 immunostaining (harboring the compound heterozygous mutations p.E304X/c.1909delA) who was subsequently found to have normal expression of *KIND1* mRNA (Figure 8, lane 7). However, all four patients had normal levels of *KIND2* and *FBLIM1* (migfilin) mRNA levels compared with normal controls (Figures 8b and c) despite the individuals in lanes 4–6 showing reduced kindlin-2 and migfilin labeling on skin sections (cf. Figure 7e and h).

DISCUSSION

In this study, we have identified kindlin-2 and migfilin as two novel biochemical partners of kindlin-1 by co-immunoprecipitation supported by confocal microscopy imaging on NHK, KS keratinocytes, as well as on transfected HaCaT cells. Previous studies have established the colocalization of kindlin-1 with other focal adhesion proteins such as paxillin in various cell types including mouse embryonic fibroblasts (Ussar *et al.*, 2006) and the epithelial cell line Ptk2 (Siegel *et al.*, 2003). However, our confocal microscopy studies provide novel *in vitro* data regarding the localization of kindlin-1, kindlin-2, and migfilin in both NHK and KS keratinocytes. Additionally, we have shown that loss of

kindlin-1 in both KS keratinocytes and kindlin-1 siRNA-transfected HaCaT cells does not seem to alter the expression or localization of either kindlin-2 or migfilin at focal adhesions.

Our study also identifies a potential pitfall in using immunofluorescence microscopy to assist the clinical diagnosis of KS. Previously, our group has reported the usefulness of immunofluorescence microscopy on frozen skin sections in making a rapid diagnosis of KS (Ashton *et al.*, 2004; Fassihi *et al.*, 2005; Burch *et al.*, 2006; Arita *et al.*, 2007). Although it remains an invaluable tool, immunostaining of a larger number of cases now highlights that some patients with KS, with loss-of-function *KIND1* mutations confirmed by gene sequencing, have almost normal anti-kindlin-1 immunostaining. Thus, positive anti-kindlin-1 immunolabeling does not rule out a diagnosis of KS, and therefore *KIND1* gene sequencing remains the gold standard in diagnosing this condition. An explanation for the positive anti-kindlin-1 antibody labeling may be gleaned from immunoblotting data comparing kindlin-1 expression in NHK and KS lysates (obtained from an individual with KS harboring compound heterozygous *KIND1* mutations, p.E304X/p.L302X). In this individual, positive anti-kindlin-1 skin immunolabeling was observed, which may reflect the presence of the ~65 kDa

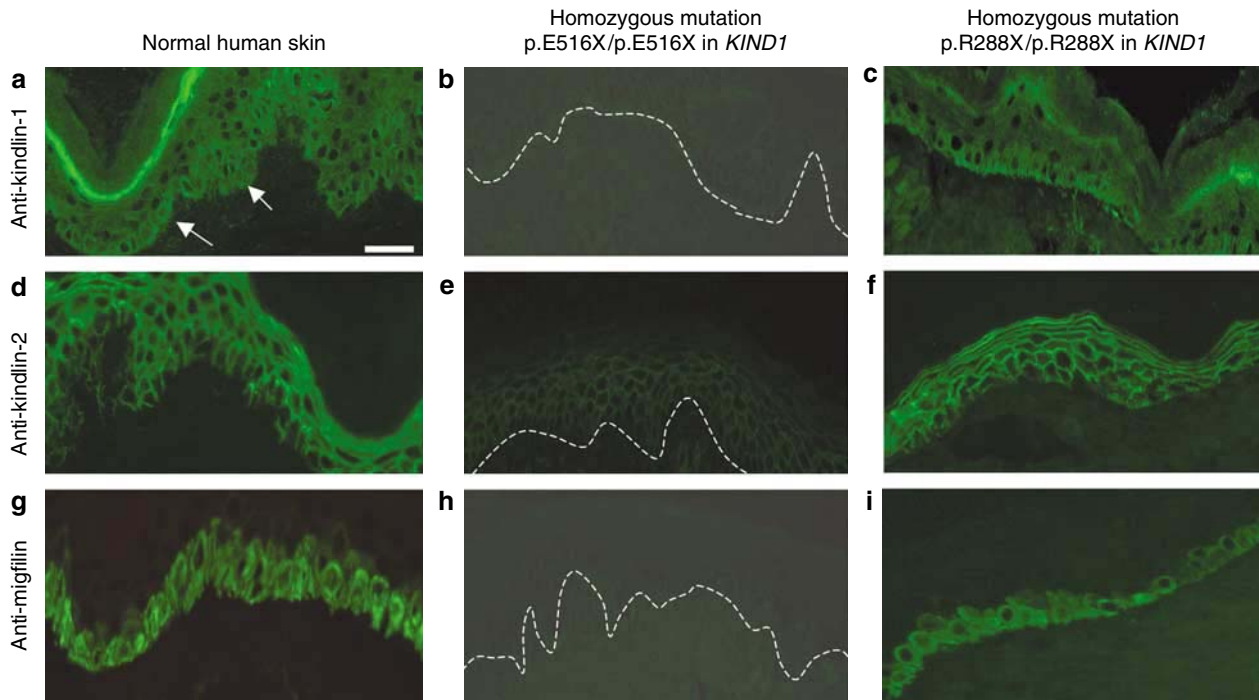


Figure 7. Immunofluorescence microscopy shows two patterns of labeling for kindlin-1, kindlin-2, and migfilin in KS skin. (a) Immunolabeling with anti-kindlin-1 antibody on normal skin sections shows bright epidermal staining predominantly at the cell periphery (but also in the cytoplasm) mostly within the basal keratinocyte layer (arrows) but with less intense pan-epidermal labeling. (b) In the KS patient with the homozygous nonsense mutation p.E516X/p.E516X there is barely detectable staining for kindlin-1. (c) In contrast, in the KS patient with the homozygous mutation p.R288X/p.R288X there is similar kindlin-1 immunolabeling intensity to control skin (cf. Figure 7a). (d) Anti-kindlin-2 immunostaining of normal skin sections shows pan-epidermal membranous labeling with the absence of staining being noted along the lower pole of basal keratinocytes. (e) Marked reduction in anti-kindlin-2 antibody immunoreactivity is seen in the patient's skin harboring the homozygous nonsense mutation p.E516X/p.E516X. (f) Kindlin-2 antibody labeling in the patient with the homozygous nonsense mutation p.R288X/p.R288X is similar to that in normal skin. (g) Anti-migfilin staining of normal skin sections shows membranous and cytoplasmic labeling of the basal keratinocytes. (h) Anti-migfilin antibody labeling in the patient with homozygous nonsense mutation p.E516X/p.E516X shows barely detectable labeling. (i) Anti-migfilin antibody labeling in the patient with the homozygous nonsense mutation p.R288X/p.R288X is similar to that in normal skin. White dashed lines indicate the position of the dermal-epidermal junction in (b), (e), and (h). Bar = 50 μm.

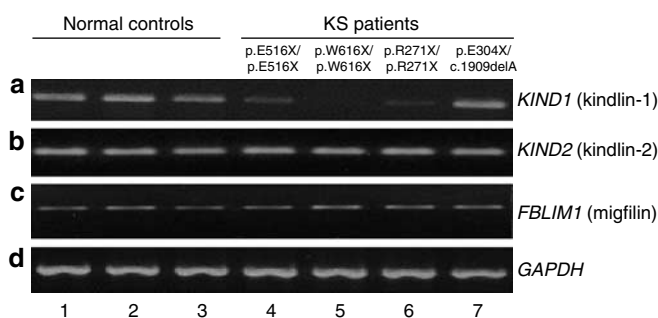


Figure 8. Semi-quantitative RT-PCR shows correlation between *KIND1* mRNA expression and the corresponding kindlin-1 labeling patterns. (a) Compared with the three normal controls (lanes 1–3), patients with reduced anti-kindlin-1 immunostaining (lanes 4–6) had variably reduced *KIND1* mRNA levels, whereas the patient with normal immunolabeling of anti-kindlin-1 (lane 7) had a normal or near-normal level of *KIND1* mRNA. (b) Patients with reduced kindlin-2 labeling (lanes 4–6), however, had no reduction in *KIND2* mRNA expression compared with normal controls (lanes 1–3) or the patient with normal kindlin-2 immunostaining (lane 7). (c) Similarly, there was no difference in *FBLIM1* mRNA expression in any of the patients compared with normal controls. (d) *GAPDH* mRNA expression was used as loading control in these experiments.

protein band detected by immunoblotting. Although the nature of this band is currently unknown, it could correspond to either a smaller kindlin-1 isoform or a truncated form of the protein, or it could represent nonspecific antibody binding.

The immunofluorescence data also raise several key points. First, there does not appear to be any clear correlation between the site or nature of the mutations, immunostaining patterns, and specific clinical features of the disease. For instance, the patients with the homozygous nonsense mutations p.R271X/p.R271X and p.R288X/p.R288X might be predicted to have similar immunostaining patterns, but our results suggest otherwise. Secondly, the seven patients with reduced or absent anti-kindlin-1 immunostaining had similar clinical features to those with positive immunolabeling, observations which suggest that the low levels of kindlin-1 expression or normally expressed but defective kindlin-1 protein are insufficient to maintain normal skin integrity and homeostasis. Thirdly, it appears that patients of Caucasian background have more positive anti-kindlin-1 immunostaining compared with other affected individuals (for example, from the Middle East, South America, or Asia), suggesting that the diverse ethnic, geographical, and environmental

backgrounds of the cases studied may also have an impact on phenotype and expression of kindlin-1. Fourthly, although skin immunolabeling reveals a mirror effect for kindlin-1, kindlin-2, and migfilin immunolabeling (that is, a reduction of kindlin-1 labeling is paralleled by a decrease in both kindlin-2 and migfilin labeling), kindlin-2 or migfilin expression and localization were still demonstrated by immunoblotting and confocal microscopy, respectively.

KIND1 mRNA expression was variably reduced in the three patients with reduced anti-kindlin-1 labeling. However, the individual harboring the compound heterozygous mutations p.E304X/c.1909delA (normal anti-kindlin-1 labeling) had near-normal *KIND1* mRNA expression. In this case, we anticipated *KIND1* mRNA expression to be ~50% of normal, as the mutation c.1909delA occurs in the last exon of *KIND1* and is therefore unlikely to be affected by nonsense-mediated mRNA decay. However, *KIND1* mRNA levels were normal, suggesting that the other mutation p.E304X in exon 7 also does not seem to affect the stability of *KIND1* mRNA. No evidence for alternative splicing of *KIND1* was detected in this individual, and thus an adequate explanation for the near-normal mRNA levels is lacking.

The identification of kindlin-2 and migfilin as binding partners of kindlin-1 provides new insight into the pathophysiology of KS. First, it is evident that not all cases of KS harbor pathogenic mutations in *KIND1*—perhaps ~25% of cases may result from mutations in other, as yet unidentified, candidate genes (JAM, unpublished data). It is therefore plausible that some individuals with KS or a KS-like genodermatosis might have underlying pathogenic mutations in *KIND2* or *FBLIM1*. Secondly, the biochemical association of these proteins provides new information regarding the role of focal adhesion proteins in the pathogenesis of skin disease and helps us understand further the pathophysiology of KS.

MATERIALS AND METHODS

Antibodies

A rabbit polyclonal anti-kindlin-1 antibody that recognizes the last 277 amino-acid residues of kindlin-1 was kindly supplied by Dr Mary Beckerle (Salt Lake City, OH). Rabbit polyclonal anti-kindlin-2 and anti-migfilin antibodies were supplied by Reinhard Fässler (Max Planck Institute of Biochemistry, Martinsried, Germany). Alexa Fluor 488 goat anti-rabbit IgG secondary antibody (Invitrogen, Eugene, OR) was used for immunofluorescence labeling on skin sections. For cell immunofluorescence staining, mouse monoclonal anti-vinculin (Sigma-Aldrich, St Louis, MO) and anti-FLAG M2 antibodies (Sigma-Aldrich) were used. Alexa Fluor 546 goat anti-mouse IgG and Alexa Fluor 647 goat anti-rabbit IgG secondary antibodies (Invitrogen), both highly cross-adsorbed, were used in cell immunofluorescence microscopy.

Skin biopsies

Skin biopsies were taken for immunofluorescence microscopy studies, tissue culture, and nucleic acid extraction after written, informed consent was obtained from each patient, in accordance with the Ethics Committee approval from the Guy's and St Thomas' Hospital. The study was conducted according to the Declaration of Helsinki principles.

Western blotting

Keratinocytes were lysed with NuPage LDS sample buffer (Invitrogen, Carlsbad, CA) and 10% 2-mercaptoethanol (Sigma-Aldrich). The lysates were then loaded and run on NuPage 4–12% bis-Tris gels (Invitrogen) at 150 V for 1.5 hours. The proteins were then transferred onto Hybond-ECL nitrocellulose membranes (Amersham Biosciences, Little Chalfont, UK) and blocked in 5% skimmed milk in 0.1% Tween-20 (Sigma-Aldrich) and Tris-buffered saline. The membranes were then probed with anti-kindlin-1, anti-kindlin-2, and anti-migfilin antibodies overnight at 4°C. Mouse monoclonal anti-β actin (Sigma-Aldrich) was used as loading control. Anti-rabbit horseradish peroxidase-conjugated IgG antibody was used as secondary antibody. Visualization of protein bands was done with ECL western blotting detection reagents (Amersham Biosciences).

Co-immunoprecipitation

For co-immunoprecipitation, confluent HaCaT cell culture in 75 cm² flask was lysed with 500 μl of Ripa (Radioimmunoprecipitation assay) lysis buffer (Upstate Cell Signaling Solutions, Charlottesville, VA) containing 5 μl of 100 mM protease inhibitor cocktail set (Merck Bioscience, Nottingham, UK) and 5 μl of 100 mM sodium orthovanadate at 4°C for 5 minutes. Following centrifugation, the supernatant was precleared with Trueblot anti-rabbit Ig immunoprecipitation beads (Insight Biotechnology Ltd, Middlesex, UK) for 30 minutes at 4°C. The beads were then removed by centrifugation and the supernatant was mixed separately with anti-kindlin-1, anti-kindlin-2, and anti-migfilin antibodies for 1 hour at 4°C. Subsequently, Trueblot anti-rabbit Ig immunoprecipitation beads were added to the immunoprecipitates and incubated on ice for a further hour. The beads were then collected by centrifugation and washed three times with Ripa buffer before proceeding with western blotting. Rabbit Trueblot HRP-conjugated anti-rabbit IgG was used as secondary antibody (Insight Biotechnology Ltd). Visualization of protein bands was achieved with ECL western Blotting detection reagents.

Plasmid transfection of HaCaT cells

EGFP-kindlin-1, EGFP-kindlin-2, and FLAG-migfilin were supplied by Professor Reinhard Fässler. EGFP-kindlin-1 and EGFP-kindlin-2 were cloned as described previously (Ussar *et al.*, 2006). HaCaT keratinocytes, at a seeding density of 2×10^5 cells per well on 13 mm diameter coverslips in a 6-well plate, were transfected with EGFP-kindlin-1 and FLAG-migfilin. Briefly, 1 μg of each plasmid was mixed with 500 μl of Optimem (Gibco, Paisley, UK) and incubated for 5 minutes at room temperature. A volume of 5 μl of oligofectamine (Invitrogen) was added to 500 μl optimem and the mixture was incubated for 5 minutes at room temperature. The two solutions were then mixed, incubated for a further 20 minutes at room temperature before being added to the HaCaT keratinocytes, and incubated at 37°C for 4 hours.

Cell immunofluorescence microscopy

For immunofluorescence, the fixed cells (fixation achieved using either 4% formaldehyde for 10 minutes at room temperature or an equal mixture of methanol/acetone for 10 minutes at –20°C) were blocked with 10% goat serum (Sigma-Aldrich) and 0.3% BSA in phosphate-buffered saline by incubation with primary antibody. Secondary antibody incubation was performed for 1 hour at room

temperature. The coverslips containing the fixed immunolabeled cells were mounted with Prolong Gold AntiFade Reagent (Invitrogen) onto Superfrost Plus slides (VWR) and analyzed with a Zeiss Axioplan 2 Imaging confocal microscopy system.

RNA interference

Kindlin-1 expression was knocked down by RNAi using kindlin-1 siRNA (Dharmacon/Perbio, Cramlington, UK) as described previously (Kloeker *et al.*, 2004). Preparation of the transfectants involved incubating each siRNA with OptiMax for 5 minutes at room temperature before adding the mixture to an oligofectamine/OptiMax solution. The cells were incubated for 4 hours with this transfection mixture.

Immunofluorescence microscopy

Five-micrometer-thick frozen skin sections were cut from skin biopsies obtained from 13 patients with KS in whom loss-of-function mutations in *KIND1* had been determined. The sections were blocked with 10% goat serum for 30 minutes followed by incubation with the primary antibody for 30 minutes at 37°C. Secondary antibody incubation was performed for 30 minutes at 37°C. Following phosphate-buffered saline wash, the sections were air-dried and mounted with Vectashield Hard Set with DAPI (Vector Laboratories, Peterborough, UK) and viewed under a fluorescent microscope.

Extraction of total RNA from skin biopsies and cDNA synthesis

Skin biopsies were taken from patients with KS harboring the mutations p.E516X/p.E516X, p.W616X/p.W616X, p.R271X/p.R271X, and p.E304X/c.1909delA, and stored in RNeasy Lysis Buffer (Qiagen, Crawley, UK) before processing. Total RNA was extracted from each skin biopsy using the RNeasy Fibrous Tissue Mini Kit (Qiagen). First-strand cDNA synthesis was performed with 2 µg of total RNA using SuperScript II Reverse Transcriptase (Invitrogen).

Semi-quantitative PCR analysis

First-strand cDNA was amplified by PCR in a reaction volume consisting of 2 µl of 2.5 mM dNTP, 2 µl forward and reverse primers, 1 µl of cDNA, 10.375 µl water, 0.125 µl of *Taq* polymerase, 5 µl Q buffer, and 2.5 µl of 10 × buffer. All PCR reagents were purchased from Qiagen. Details of *KIND1*, *KIND2*, and *FBLIM1* cDNA primers are as follows: *KIND1* forward cDNA primer: 5'-TCAAACAGTGGATGTAACACTGG-3'; *KIND1* reverse cDNA primer: 5'-TACATGCTGGCACGTTAGG-3'; *KIND2* forward cDNA primer: 5'-GAACAAGCAGATAACAGC-3'; *KIND2* reverse cDNA primer: 5'-CGGTGACCATTTGATTTCCC-3'; *FBLIM1* forward cDNA primer: 5'-AAAATCGAATGCATGGGAAG-3'; *FBLIM1* reverse cDNA primer: 5'-GCAGGTTA GGAAGGGAAACC-3'. All the primer pairs were designed to amplify a region in the 3' UTR of each gene and were purchased from MWG (Ebersberg, Germany). To ensure equal loading, a housekeeping gene (*GAPDH*) was simultaneously amplified. The PCR products were assessed on a 2% agarose gel.

HaCaT culture

The HaCaT cell line was grown to 70–80% confluence in DMEM (Invitrogen) and 10% fetal bovine serum (Invitrogen).

Primary keratinocyte culture

Skin biopsies were incubated overnight at 4°C with dispase I (dilution 34 U in 20 ml phosphate-buffered saline) (Roche Applied

Science, Burgess Hill, UK). The detached epidermal sheet was then incubated with a 0.05% trypsin/EDTA solution (Invitrogen) for 15 minutes at 37°C. The solution was subsequently filtered through a 100 µm cell strainer (VWR International, Lutterworth, UK) and the released keratinocytes were centrifuged at 1200 r.p.m. for 5 minutes. The cell pellet was resuspended in Epilife Basal Medium (Cascade Biologics, Mansfield, UK) supplemented with Epilife Defined Growth Supplement and Gentamicin/Amphotericin B (Cascade Biologics) and plated in T25 flasks previously treated with Coating Matrix (Cascade Biologics).

CONFLICT OF INTEREST

The authors state no conflict of interest.

ACKNOWLEDGMENTS

J.L.-C. is supported by a Wellcome Trust Research Training Fellowship. Additional funding support from the Barbara Ward Childrens' Foundation and the Dystrophic Epidermolysis Bullosa Research Association (DeBRA, UK) is gratefully acknowledged.

REFERENCES

- Arita K, Wessagowit V, Inamadar AC, Palit A, Fassihi H, Lai-Cheong JE *et al.* (2007) Unusual molecular findings in Kindler syndrome. *Br J Dermatol* 157:1252–6
- Ashton GH, McLean WH, South AP, Oyama N, Smith FJ, Al-Suwaid R *et al.* (2004) Recurrent mutations in kindlin-1, a novel keratinocyte focal contact protein, in the autosomal recessive skin fragility and photosensitivity disorder, Kindler syndrome. *J Invest Dermatol* 122:78–83
- Boukamp P, Petrussevska RT, Breitkreutz D, Hornung J, Markham A, Fusenig NE (1988) Normal keratinization in a spontaneously immortalized aneuploid human keratinocyte cell line. *J Cell Biol* 106:761–71
- Burch JM, Fassihi H, Jones CA, Mengshol SC, Fitzpatrick JE, McGrath JA (2006) Kindler syndrome: a new mutation and new diagnostic possibilities. *Arch Dermatol* 142:620–4
- Fassihi H, Wessagowit V, Jones C, Dopping-Hepenstal P, Denyer J, Mellerio JE *et al.* (2005) Neonatal diagnosis of Kindler syndrome. *J Dermatol Sci* 39:183–5
- Frischmeyer PA, Dietz HC (1999) Nonsense-mediated mRNA decay in health and disease. *Hum Mol Genet* 8:1893–900
- Herz C, Aumailley M, Schulte C, Schlötzer-Schrehardt U, Bruckner-Tuderman L, Has C (2006) Kindlin-1 is a phosphoprotein involved in regulation of polarity, proliferation, and motility of epidermal keratinocytes. *J Biol Chem* 281:36082–90
- Holbrook JA, Neu-Yilik G, Hentze MW, Kulozik AE (2004) Nonsense-mediated decay approaches the clinic. *Nat Genet* 36:801–8
- Jobard F, Bouadjar B, Caux F, Hadj-Rabia S, Has C, Matsuda F *et al.* (2003) Identification of mutations in a new gene encoding a FERM family protein with a pleckstrin homology domain in Kindler syndrome. *Hum Mol Genet* 12:925–35
- Kindler T (1954) Congenital poikiloderma with traumatic bulla formation and progressive cutaneous atrophy. *Br J Dermatol* 66:104–11
- Kloeker S, Major MB, Calderwood DA, Ginsberg MH, Jones DA, Beckerle MC (2004) The Kindler syndrome protein is regulated by transforming growth factor-beta and involved in integrin-mediated adhesion. *J Biol Chem* 279:6824–33
- Lai-Cheong JE, Liu L, Sethuraman G, Kumar R, Sharma VK, Reddy SR *et al.* (2007) Five new homozygous mutations in the *KIND1* gene in Kindler syndrome. *J Invest Dermatol* 127:2268–70
- Mansur AT, Elcioglu NH, Aydingöz IE, Akkaya AD, Serdar ZA, Herz C *et al.* (2007) Novel and recurrent *KIND1* mutations in two patients with Kindler syndrome and severe mucosal involvement. *Acta Derm Venereol* 87:563–5

- Maquat LE (2004) Nonsense-mediated mRNA decay: splicing, translation and mRNP dynamics. *Nat Rev Mol Cell Biol* 5:89-99
- Martignago BC, Lai-Cheong JE, Liu L, McGrath JA, Cestari TF (2007) Recurrent KIND1 (C20orf42) gene mutation, c.676insC, in a Brazilian pedigree with Kindler syndrome. *Br J Dermatol* 157:1281-4
- Nagy E, Maquat LE (1998) A rule for termination-codon position within introns containing genes: when nonsense affects RNA abundance. *Trends Biochem Sci* 23:198-9
- Sethuraman G, Fassihi H, Ashton GH, Bansal A, Kabra M, Sharma VK et al. (2005) An Indian child with Kindler syndrome resulting from a new homozygous nonsense mutation (C468X) in the KIND1 gene. *Clin Exp Dermatol* 30:286-8
- Siegel DH, Ashton GH, Penagos HG, Lee JV, Feiler HS, Wilhelmsen KC et al. (2003) Loss of kindlin-1, a human homolog of the *Caenorhabditis elegans* actin-extracellular-matrix linker protein UNC-112, causes Kindler syndrome. *Am J Hum Genet* 73:174-87
- Tu Y, Wu S, Shi X, Chen K, Wu C (2003) Migfilin and Mig-2 link focal adhesions to filamin and the actin cytoskeleton and function in cell shape modulation. *Cell* 113:37-47
- Ussar S, Wang HV, Linder S, Fässler R, Moser M (2006) The Kindlins: subcellular localization and expression during murine development. *Exp Cell Res* 312:3142-51
- Wu C (2005) Migfilin and its binding partners: from cell biology to human diseases. *J Cell Sci* 118:659-64
- Zhang Y, Tu Y, Gkretsi V, Wu C (2006) Migfilin interacts with vasodilator-stimulated phosphoprotein (VASP) and regulates VASP localization to cell-matrix adhesions and migration. *J Biol Chem* 281:12397-407

Paper IX

C-terminally truncated kindlin-1 leads to abnormal adhesion and migration of keratinocytes

C. Has,* R.J. Ludwig,† C. Herz,*‡ J.S. Kern,*‡ S. Ussar,§ F.R. Ochsendorf,¶ R. Kaufmann,¶ H. Schumann,* J. Kohlhase** and L. Bruckner-Tuderman*

*Department of Dermatology, University Medical Center Freiburg, Hauptstr. 7, 79104 Freiburg, Germany

†Department of Dermatology, University Schleswig-Holstein, Campus Lübeck, Lübeck, Germany

‡Faculty of Biology, University of Freiburg, Freiburg, Germany

§Department of Molecular Medicine, Max-Planck-Institute of Biochemistry, Martinsried, Germany

¶Department of Dermatology, University of Frankfurt, Frankfurt, Germany

**Center for Human Genetics, Freiburg, Germany

Summary

Correspondence

Leena Bruckner-Tuderman.

E-mail: bruckner-tuderman@uniklinik-freiburg.de

Accepted for publication

1 April 2008

Keywords

ainhum, blister, Kindler syndrome, kindlin-1, splice site mutation

Conflicts of interest

None declared.

DOI 10.1111/j.1365-2133.2008.08760.x

Background The Kindler syndrome (KS) protein kindlin-1 is a member of a protein complex that links cortical actin to integrins on the surface of basal keratinocytes. Loss of kindlin-1 leads to abnormalities of cell adhesion and motility, and to skin blistering and progressive poikiloderma as clinical symptoms.

Objectives Here we investigated a severely affected patient, disclosed the mutation that caused the disease and delineated its biological consequences.

Methods Mutation screening of the kindlin-1 gene, *KIND1* (now called *FERMT1*), was performed with polymerase chain reaction (PCR) amplification of all exons and sequencing. Mutated kindlin-1 was characterized by reverse transcriptase (RT)-PCR and immunoblotting, and genotype–phenotype correlations were analysed using immunohistochemical staining of skin biopsies and keratinocytes from the patient's skin. Cell adhesion and motility were assessed with functional tests.

Results We disclosed a splice site mutation in the first position of intron 13 of the *FERMT1* gene, which caused skipping of exon 13. The short transcript partially escaped nonsense-mediated mRNA decay and was translated into a truncated protein.

Conclusion A C-terminally truncated kindlin-1 in keratinocytes could not function correctly even if it were expressed.

Kindler syndrome (KS; OMIM 173650) is a rare heritable skin disorder with an intriguing complex phenotype, which is not well understood. The disease begins with congenital skin blistering and photosensitivity, which improve with age, and continues with progressive generalized poikiloderma.¹ Additional clinical features include chronic gingival erosions, oesophageal and gastrointestinal involvement and an increased risk of mucocutaneous malignancy. The disorder results from recessive loss-of-function mutations of the *FERMT1* gene that encodes the protein kindlin-1, a component of focal adhesions in epithelial cells.^{2,3} In vitro, loss of kindlin-1 function is associated with abnormal cell shape, reduced cell adhesion, proliferation and perturbed directed motility, presumably through a role in integrin-associated signalling platforms.^{4,5}

Despite rapid advances in discerning the genetic basis of KS,^{6–8} the pathogenetic chain from molecular defects to the functional tissue deficiencies in KS is not well understood. In this study we describe the biological consequences of a *FERMT1* splice site mutation, which leads to reduced expression of truncated kindlin-1.

Material and methods

Patient

The clinical diagnosis of KS in the patient was based on physical examination and personal history. Two skin biopsies were obtained and processed for histopathological analysis, immunohistochemistry and cell culture. A blood sample in EDTA was obtained from the patient after informed consent and with approval by the ethics committee of the University of Freiburg.

FERMT1 mutation detection and reverse transcriptase-polymerase chain reaction

Genomic DNA extracted from peripheral lymphocytes was used for polymerase chain reaction (PCR) amplification of the entire coding region and exon–intron boundaries of the *FERMT1* gene, and sequencing, as described.⁹

Total RNA was extracted from subconfluent normal human keratinocytes (NHK) and primary KS keratinocytes and reverse

transcribed as reported.⁴ For amplification of the *FERMT1* cDNA, the following primers were used: KSex6F: 5'-ttggtagactctcaccg-3' and KSex9R: 5'-gagattatctgcaagtttaggg-3'; KSex12F: 5'-ctcaggtgcttccagtctc-3' and KSex14R: 5'-cgg-tggctgcatcaattta-3'. As a control, primers for glyceraldehyde-3-phosphate dehydrogenase (BD Bioscience, Heidelberg, Germany) were used.

Morphological analyses

Dermatohistopathology, immunohistochemistry and indirect immunofluorescence (IIF) staining were performed with standard techniques.⁴ The following primary antibodies were used: collagen XVII,¹⁰ Ki67, pankeratin (both from Dako, Hamburg, Germany), filaggrin (Novocastra, Newcastle, U.K.), BM165 to human laminin $\alpha 3$ chain (Dr P. Rouselle, Lyon, France) and LH 7.2 to the NC1-domain of collagen VII (Sigma, Taufenkirchen, Germany). The secondary antibodies were labelled with FITC or rhodamine antimouse or antirabbit IgG, or the AEC system (Dako). The signals were visualized with immunofluorescence (Zeiss Axio Imager; Carl Zeiss, Jena, Germany) or light microscopy. We used DAPI as a nuclear stain and haematoxylin as a counterstain.

Cell culture and functional assays

Primary keratinocytes were isolated from KS and control skin and grown in serum-free keratinocyte growth medium.⁴ The morphology and shape of the cells were observed with an Olympus CKX41 microscope (Olympus, Hamburg, Germany) and recorded with a digital camera. Cell adhesion and *in vitro* wound healing assays were performed in triplicate as described.⁴ Because of the low proliferation rate of primary keratinocytes,⁴ no mitomycin C was added to the culture medium in *in vitro* wound healing assays.

Protein extraction and immunoblotting

Cultured cells were lysed as reported.⁴ Equal amounts of protein were separated by 10% SDS-PAGE and transferred to nitrocellulose. The blots were blocked with either 10% defatted milk or 3% bovine serum albumin in 0.01% Tween TBS and incubated with two different affinity purified antibodies

to epitopes within the N-terminal part of kindlin-1 (KS4⁴ and S. Ussar, unpublished data) and with β -tubulin antibodies (Sigma) and processed as reported.⁴

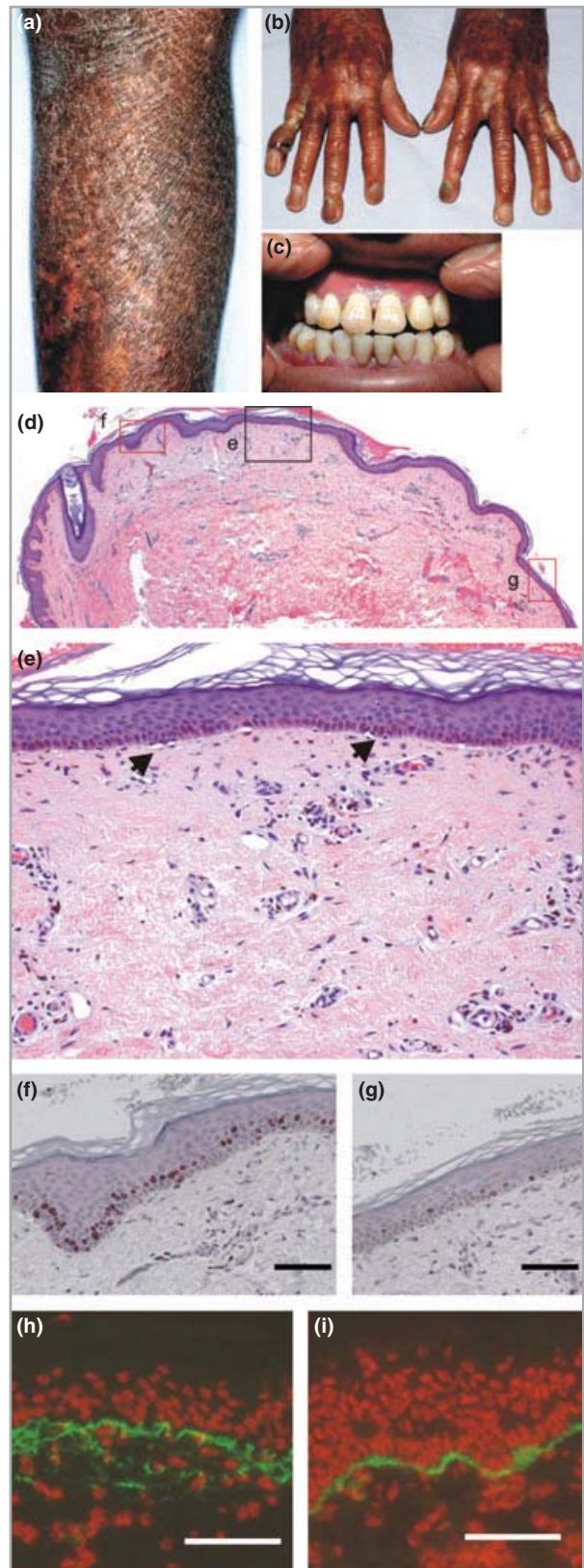


Fig 1. Clinical presentation and morphological analysis of the patient's skin. (a) Extensive poikiloderma and dry skin. (b) Skin atrophy on the dorsal aspects of the hands, flexion contractures and pseudoainhum. (c) Periodontitis with erosions and whitish deposits, teeth enamel defects. (d) Dermatohistopathology of a skin biopsy. The frames indicate the areas shown in panels (e)–(g). (e) Micro-blisters are indicated by arrows. (f, g) Staining of the patient's skin with the proliferation marker Ki67. (h, i) Indirect immunofluorescence staining with antibodies to collagen VII (green) in the patient's (h) and control skin (i). Nuclei are shown in red. Bars for (f)–(i) = 50 μ m.

Results

The 27-year-old patient of Somalian origin was the only affected member of his family. He spent the first 20 years of life in his homeland and the clinical diagnosis of KS was not established until 3 years ago. Since early childhood he suffered from skin blistering after mechanical trauma or sun exposure. With advancing age, generalized skin dryness and focally hypopigmented areas developed, and the clinical presentation became reminiscent of a mild ichthyosis (Fig. 1a). The skin of the hands became especially atrophic and sclerotic, which led to flexion contractures. Within the last year, pseudoainhum of several fingers developed causing functional deficiency and

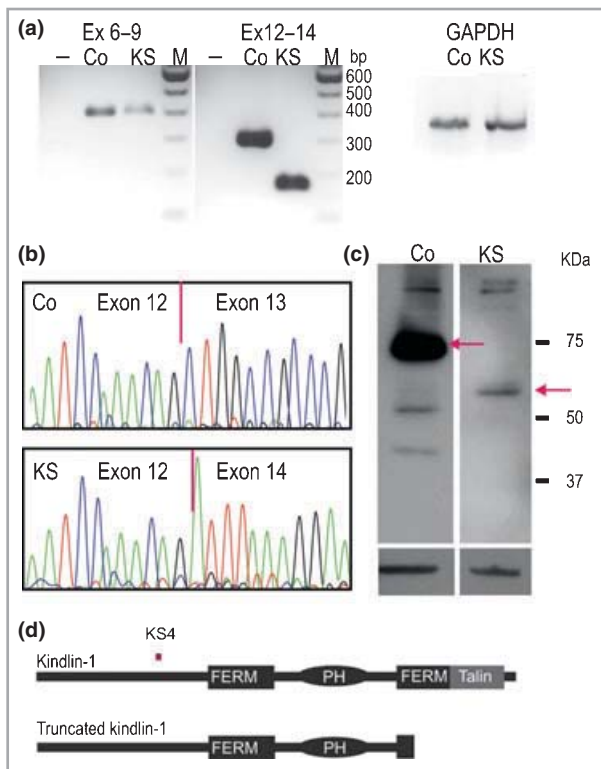


Fig 2. Expression of kindlin-1 in the patient's skin and keratinocytes. (a) Reverse transcriptase-polymerase chain reaction (RT-PCR) with total RNA from control (Co) and patient (KS) keratinocytes with primers for *FERMT1* Ex6-9 and Ex12-14, and glyceraldehyde-3-phosphate dehydrogenase (GAPDH). In the patient's sample a 125 bp shorter, abnormally spliced transcript was identified with primers spanning exons 12-14; -, negative controls without DNA; M, 100 bp DNA ladder. (b) Direct sequencing of the RT-PCR products spanning exons 12-14 revealed the normal transcript in the control, and skipping of exon 13 in the patient. (c) Western blot analysis of control (Co) and patient (KS) keratinocyte lysates with a kindlin-1 antibody (upper panels). In the control the full-length kindlin-1 and in the patient truncated kindlin-1 of approximately 60 kDa are indicated by arrows. β -Tubulin is shown as a loading control (lower panels). (d) In the upper panel, the domain-structure of normal kindlin-1 is shown. The sequence recognized by the domain-specific antibody KS4 is depicted in pink. In the lower panel, the truncated kindlin-1 identified in the KS patient's keratinocytes is shown.

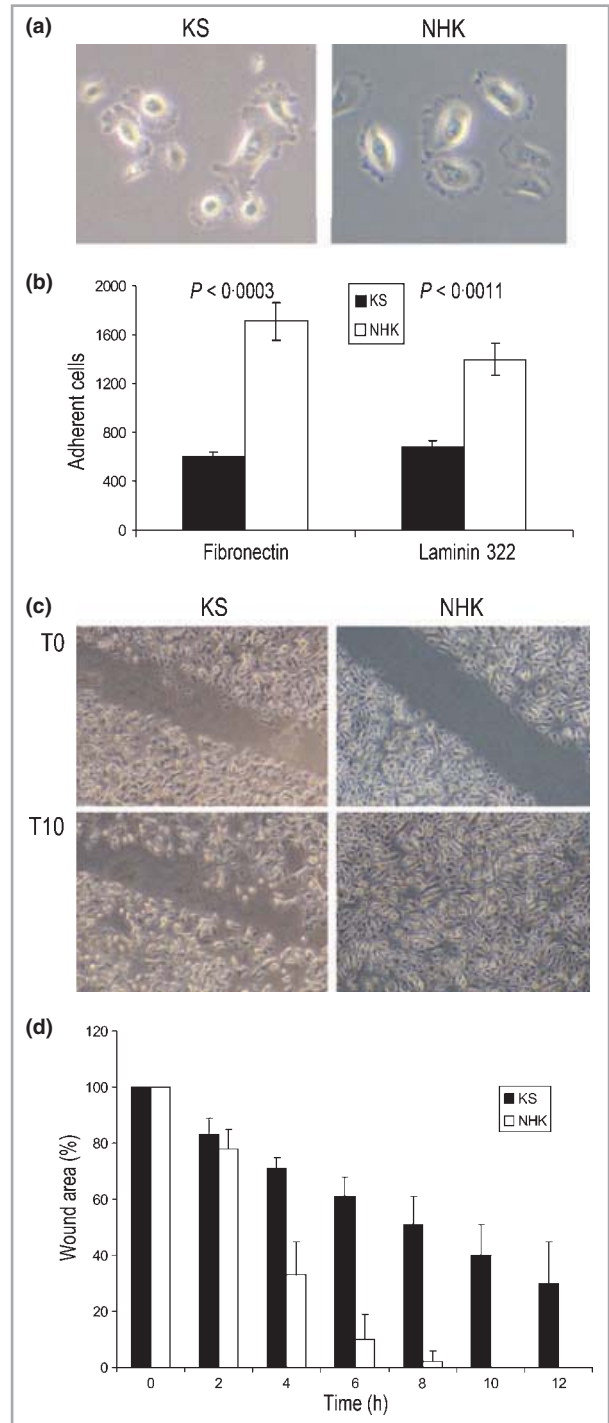


Fig 3. Functional analysis of Kindler Syndrome (KS) keratinocytes. (a) Normal human keratinocytes (NHK) spread and had one broad lamellipodium, whereas KS keratinocytes remained round or exhibited multipolar morphology with multiple leading edges. (b) Adhesion of KS keratinocytes was clearly reduced, as compared to NHK. (c) Phase contrast microscopy pictures of the *in vitro* wound closure assays performed with KS cells and NHK. The upper panels represent the time point 0, and the lower panels represent the time point 10 h. (d) The corresponding graphs showing the percentage of wound closure in time. Black columns represent KS cells, while NHK are represented by white columns.

pain (Fig. 1b). The patient complained about pain and bleeding of the gums during eating and brushing of the teeth (Fig. 1c), difficulties in swallowing solid foods, diarrhoea alternating with constipation, and anal bleeding.

Histopathology of a skin biopsy revealed long stretches of flattened epidermis, orthohyperkeratosis, microblistering at the dermal–epidermal junction and pigmentary incontinence (Fig. 1d,e). Staining with the proliferation marker Ki67 demonstrated a patchy pattern in the epidermis, with a significantly reduced number of positive cells in the flattened epidermis and a high number of positive cells in nonatrophic areas (Fig. 1f,g). Because some of the clinical features were suggestive of an ichthyosis, filaggrin staining was performed; it showed a normal staining pattern (not shown). IIF staining with antibodies to collagen VII (Fig. 1h,i), collagen XVII and laminin 332 (not shown) revealed a fragmented and branched basement membrane zone. Keratin-positive cell bodies were occasionally present in the upper dermis (not shown).

Mutation screening disclosed a homozygous *FERMT1* mutation of the first position in intron 13, c.1718 + 1G > A. In order to analyse the biological consequences of the mutation, keratinocytes were cultured from the patient's skin for RT-PCR and protein analysis (Fig. 2). RT-PCR with primers spanning *FERMT1* exons 6–9 revealed reduced levels of the *FERMT1* mRNA in KS cells (Fig. 2a). The aberrant transcript obtained with primers for exon 12–14 resulted from skipping of exon 13 (Fig. 2b), and led to a frameshift and a premature termination codon at the second position of the abnormal sequence. This transcript, predicted to generate a truncated kindlin-1 polypeptide of about 60 kDa, which lacks 145 amino acids in the carboxyterminus (Fig. 2d), was identified by immunoblotting with antibodies to kindlin-1 in the KS cells (Fig. 2c).

In vitro assays were used to investigate the functional properties of KS keratinocytes. The patient's cells did not form colonies resembling NHK and exhibited aberrant morphology (Fig. 3a). In the first passage, 44% of KS keratinocytes remained round and had not spread, and 42% of the cells exhibited multipolar morphology and multiple leading edges. Adhesion of KS keratinocytes was clearly reduced, to fibronectin by 66% ($P < 0.0003$) and to laminin 332 by 50% ($P < 0.001$) in comparison with NHK (Fig. 3b). The directed migration of cells was analysed by *in vitro* wound closure assays. KS cells demonstrated undirected migratory behaviour as they had not filled the wounded area after 12 h, while NHK closed the wounds within 8–10 h (Fig. 3c,d). The proliferation of KS cells was drastically reduced; the doubling time was 7 days, while for NHK it was 3 days (not shown).

Discussion

So far, very little is known about the molecular basis of the clinical and biological KS phenotypes and their heterogeneity. Our patient had several noteworthy clinical features, including scleroatrophy of the hands, pseudoainhum, and ichthyosiform scaling, and seems to be very severely affected as compared

with other individuals with similar mutations.^{7,9,11} A 30-year-old Indian male patient, homozygous for the same mutation, was described to be relatively mildly affected.⁷ A mutation of the neighbouring nucleotide, c.1718 + 2T > C was reported in a male newborn with blistering and dry, scaly skin.¹¹ Yet another mutation, IVS13–1G > A, led to aberrant splicing of exon 14 and to typical KS symptoms.¹¹ It is likely that in our patient environmental factors played a major role, i.e. life in Somalia, lack of systematic UV protection and medical care up to young adulthood aggravated the clinical picture.

The 31 *FERMT1* mutations described to date are predicted to result in complete loss of kindlin-1 and its functions.^{6–8} The fact that the present mutation in intron 13 lies close to the 3' end of the *FERMT1* gene with 15 exons is likely to render the nonsense-mediated RNA decay mechanisms partly inactive.¹² The amount of *FERMT1* mRNA was reduced to about a half. The resulting truncated kindlin-1 polypeptide lacking the FERM subdomain containing the talin homology region seemed to be sensitive to proteolytic degradation, as the intensity of the immunoblot band was about 5% of the control. Compared to NHK, the adhesion and proliferation of KS keratinocytes were significantly reduced to levels similar to those we described for kindlin-1-negative cells.⁴ Also KS cells had abnormal morphology, and were not able to migrate in a directed manner similarly to kindlin-1-null cells,⁴ suggesting that kindlin-1 functions require the C-terminal domains. The most likely explanation is that in the present case, both the reduced amount and the truncation played a role. The deleted 145 amino acid stretch of kindlin-1, which contains the talin homology region, is functionally important. The talin-FERM domain mediates β integrin–talin binding.¹³ In the case of kindlin-2 and -3, experimental data demonstrated that the talin homology domain contained the β integrin-binding site.^{14,15} Therefore, we hypothesize that the truncated kindlin-1 molecule lacking the talin homology domain cannot interact with $\beta 1$ integrin, which abrogates pivotal functions of the integrin adhesion-signalling complex.

Acknowledgments

The authors thank Margit Schubert, Vera Morand and Gabriele Grüninger for expert technical assistance. This work was supported in part by a grant from the Research Commission of the Medical Faculty of the University of Freiburg and the ROSA Skin Research Award to C.H., and by the Network Epidermolysis bullosa grant from the Federal Ministry for Education and Research (BMBF) to L.B.T.

References

- 1 Has C, Bruckner-Tuderman L. Molecular and diagnostic aspects of genetic skin fragility. *J Dermatol Sci* 2006; **44**:129–44.
- 2 Jobard F, Bouadjar B, Caux F *et al.* Identification of mutations in a new gene encoding a FERM family protein with a pleckstrin homology domain in Kindler syndrome. *Hum Mol Genet* 2003; **12**:925–35.

- 3 Siegel DH, Ashton GH, Penagos HG *et al.* Loss of kindlin-1, a human homolog of the *Caenorhabditis elegans* actin-extracellular-matrix linker protein UNC-112, causes Kindler syndrome. *Am J Hum Genet* 2003; **73**:174–87.
- 4 Herz C, Aumailley M, Schulte C *et al.* Kindlin-1 is a phosphoprotein involved in regulation of polarity, proliferation, and motility of epidermal keratinocytes. *J Biol Chem* 2006; **281**:36082–90.
- 5 Kloeker S, Major MB, Calderwood DA *et al.* The Kindler syndrome protein is regulated by transforming growth factor-beta and involved in integrin-mediated adhesion. *J Biol Chem* 2004; **279**:6824–33.
- 6 Arita K, Wessagowit V, Inamadar AC *et al.* Unusual molecular findings in Kindler syndrome. *Br J Dermatol* 2007; **157**:1252–6.
- 7 Lai-Cheong JE, Liu L, Sethuraman G *et al.* Five new homozygous mutations in the *KIND1* gene in Kindler syndrome. *J Invest Dermatol* 2007; **127**:2268–70.
- 8 Mansur AT, Elcioglu NH, Aydingoz IE *et al.* Novel and recurrent *KIND1* mutations in two patients with Kindler syndrome and severe mucosal involvement. *Acta Derm Venereol* 2007; **87**:563–5.
- 9 Has C, Wessagowit V, Pascucci M *et al.* Molecular basis of Kindler syndrome in Italy: novel and recurrent Alu/Alu recombination, splice site, nonsense, and frameshift mutations in the *KIND1* gene. *J Invest Dermatol* 2006; **126**:1776–83.
- 10 Schacke H, Schumann H, Hammami-Hauasli N *et al.* Two forms of collagen XVII in keratinocytes. A full-length transmembrane protein and a soluble ectodomain. *J Biol Chem* 1998; **273**:25937–43.
- 11 Fassihi H, Wessagowit V, Jones C *et al.* Neonatal diagnosis of Kindler syndrome. *J Dermatol Sci* 2005; **39**:183–5.
- 12 Isken O, Maquat LE. Quality control of eukaryotic mRNA: safeguarding cells from abnormal mRNA function. *Genes Dev* 2007; **21**:1833–56.
- 13 Calderwood DA. Integrin activation. *J Cell Sci* 2004; **117**:657–66.
- 14 Shi X, Ma YQ, Tu Y *et al.* The MIG-2/integrin interaction strengthens cell-matrix adhesion and modulates cell motility. *J Biol Chem* 2007; **282**:20455–66.
- 15 Moser M, Nieswandt B, Ussar S *et al.* Kindlin-3 is essential for integrin activation and platelet aggregation. *Nat Med* 2008; **14**:325–30.